Divergent regulation of zinc metallopeptidases by shear stress in macrovascular endothelial cells via an NADPH oxidase - superoxide pathway

A dissertation submitted for the degree of Ph.D by

Anthony F. Guinan, B.Sc

Under the supervision of Dr. Philip M. Cummins

September 2011

Faculty of Science and Health, School of Biotechnology,
Dublin City University, Dublin 9, Ireland

Declaration:

I hereby certify that this material, which I now submit for assessment on the programme of study leading to the award of Doctor of Philosophy is entirely my own work, that I have exercised reasonable care to ensure that the work is original, and does not to the best of my knowledge breach any law of copyright, and has not been taken from the work of others save and to the extent that such work has been cited and acknowledged within the text of my work.

Signature: _____

Student I.D: 52727358

Date: _____

Acknowledgements

Firstly I would like to thank Phil for having faith, confidence and patience with me over the course of my PhD. None of this would have been possible without all of his guidance, constant support and a lot of red pens. I also want to express my gratitude to Ronan who was always forthcoming with ideas and solutions to problems throughout my time in the lab. I am sure ye are devastated that I am done, but I am confident that ye will struggle on without me.

I would also like to thank the previous members of both the EBG and IBG. From Maria, who showed me the ropes when I started in the lab, to Tony, Andrew, Mishan and Paul who were always good for a few pranks, pints and a bit of science information too. I can't forget the new members of both labs Fiona, Keith, Brian, Ciaran and Shan. From the invention of street tennis, lunch time BBQs, the erection of XB11a and the long list of many more things that made every day in the lab an experience and a joy to work in, I thank all of ye. Go Bears!!

I would also like to say a special thanks to all my friends who were there for constant meetings for 'tea' and a talk about anything but science. And to everyone in the judo club, for all the anger management sessions.

Next I want to thank my family. There are a lot of us and I think I have called on all of ye at some stage over the last few years. I doubt many landladies get thanked at the start of a thesis, but in this case she will. Thank you Helena for having the foresight to buy an apartment close to DCU, it turned out to be very useful. PJ, the co-founder of Saints and Scholars Brewing Company, you had to put up with me all during my PhD and worst of all through me writing it up and you still managed not to kill me, so thanks for that I do appreciate it.

Susan, I suppose you have earned a mention too. Since I have met you, you have been a great support. You are like an encyclopaedia of scientific knowledge that I have been able to call upon. Thank you for all you help and companionship over the past few years and especially for all the help, and distractions when I needed them most, when I was writing up.

Finally and most importantly I want to thank my mammy and daddy. If it wasn't for everything that ye did for me I wouldn't have had the opportunities I have had in my life. Ye have constantly supported me in everything I have done and never said that there was anything that I couldn't do. It was daddy who taught me about stickability and gave me a good mantra to live life by 'If it is to be it's up to me'. I am very lucky to be part of such a supportive family and I hope that I have made ye proud.

Introduction: The hemodynamic environment of blood vessels is a crucial feature of endothelium-mediated vasoregulation. Flow-associated laminar shear stress (LSS) imparts an atheroprotective stimulus on the vascular endothelium, causing realignment of endothelial cells in the direction of flow and strengthening of intercellular tight junction barriers. Conversely, disturbed shear stress (DSS), a contributing factor to vascular diseases such as atherosclerosis and coronary artery disease, prevents cellular realignment and causes barrier weakening. Equally crucial to endothelium-mediated vasoregulation are vasoactive peptidases. Evidence is emerging to show that peptidase expression and activity within the vasculature is regulated in a highly coordinated manner by vessel hemodynamic forces (Fitzpatrick, et al. 2009). Indeed, this phenomenon likely has significant consequences for the *net balance* of pressor versus depressor peptides within the endothelium, subsequently leading to downstream effects on vessel wall tone and remodeling events. Of particular importance are the 'thermolysin-like' family of zinc metallopeptidases belonging to the Clan MA (Barrett, Rawlings and O'Brien 2001), which hydrolyse peptide hormone substrates of less than 40 amino acids, and which are known to contain a single copy shear stress response element (-GAGACC-) within their promoter regions. *In the current study it is therefore hypothesised that, in view of their opposing physiological actions in vivo, shear stress can modulate vascular endothelial expression of neprilysin (NEP, EC3.4.24.11) and thimet oligopeptidase (TOP, EC3.4.24.15) in an inverse manner, with functional consequences for endothelial homeostasis.*

Results: Exposure of cultured bovine/human aortic endothelial cells (BAECs/HAECs) to LSS of varying magnitude and duration (0-10 dynes/cm^2, 0-48 hrs) resulted in dose- and time-dependent modulation of NEP (down-regulation) and TOP (up-regulation) expression as monitored via qPCR, immunocytochemistry, and Western blotting. Using a luciferase reporter vector (pGL3-TOP, full-length promoter -901/+120), LSS was also found to substantially increase TOP promoter activity. By contrast, DSS had opposite effects to LSS on the expression of NEP (up-regulation) and TOP (down-regulation). We subsequently employed pharmacological antioxidants (*N*-acetyl-L-cysteine), inhibitors (Rac1/NSC23766, NADPH oxidase/apocynin) and siRNAs (p47Phox) in shearing experiments to confirm a pivotal role for NADPH oxidase-mediated superoxide production in the LSS mechanotransduction of these reciprocal events. Finally, using a TOP siRNA, an investigation of how LSS-induced TOP up-regulation impacts on endothelial functions (i.e. proliferation and bradykinin hydrolysis) was carried out, and points to functional consequence between these events under shear.

Conclusions: This study indicates that the expression of NEP and TOP, zinc metallopeptidases of high physiological relevance to the endothelium, are regulated in an opposing manner by shear stress, with potential consequences for endothelial function and flow-dependent vascular pathologies.

Table of contents

List of figures

List of tables

Abbreviations

aa	amino acid
Aβ	Amyoid-β
AC	Adenylate cyclase
ACE	Angiotensin converting enzyme
ADAM	Advanced detection and accurate measurement
ANP	Atrial natriuretic peptide
Ang I	Angiotensin I
Ang II	Angiotensin II
Ang (1-7)	Angiotensin (1-7)
ATP	Adenosine diphosphate
BAEC	Bovine aortic endothelial cell
BBB	Blood brain barrier
BCA	*Bicinchoninic* acid
BK	Bradykinin
BNP	Brain natriuretic peptide
BSA	Bovine serum albumin
BH_4	Tetrahydrobiopterin
CaM	Calmodulin
CCK	Cholecystokinin
cDNA	Complementary DNA
CFDA-SE	Carboxyfluorescein diacetate succinimidyl ester

CFSE	Carboxyfluorescein succinimidyl ester
CHD	Coronary heart disease
Cl^-	Chloride
CNP	C-type natriuretic peptide
CO_2	Carbon dioxide
CPN	Carboxypeptidase N
CVD	Cardiovascular disease
dH_2O	Distilled water
DNA	Deoxyribonucleic acid
dNTP	Deoxyribonucleotide
DMSO	Dimethylsulphoxide
DSS	Disturbed shear stress
EC	Endothelial cell
ECE	Endothelin converting enzyme
ECL	Enhanced chemiluminescence
ECM	Extracellular matrix
EDRF	Endothelium derived relaxing factor
EDTA	Ethylenediaminetetraacetic acid
EG	Endothelial glycocalyx
ELISA	Enzyme-linked immunosorbent assay
eNOS	Endothelial nitric oxide synthase
ER	Endoplasmic reticulum
ERK	Extracellular-signal-regulated kinases

ERM	Ezrin Radixin Moesin
ET	Endothelin
EU	European Union
FAK	Focal adhesion kinase
FBS	Fetal bovine serum
GAPDH	Glyceraldehyde 3-phosphate dehydrogenase
GDP	Guanosine diphosphate
GFP	Green *fluorescent protein*
GnRH	Gonadotropin-releasing hormone
GPCR	G-protein coupled receptor
GPI	Glycosylphosphatidylinositol
GTP	Guanosine triphosphate
H_2O	Water
H_2O_2	Hydrogen peroxide
HAEC	Human aortic endothelial cell
HRP	Horseradish peroxidase
IC	Immunocytochemistry
iNOS	Inducible nitric oxide synthase
KD	Kallidin
Kir	Inward rectifying potassium
LB	Lysogeny broth
LOX	Lysyl oxidase
LSS	Laminar shear stress

MAP	Mitogen-activated protein
MHC	Major histocompatibility complex
MIQE	Minimum information for publication of quantitative real-time PCR experiments
Mn-SOD	Mitochondrial SOD
mRNA	Messenger ribonucleic acid
mtNOS	Mitochondrial nitric oxide synthase
NAC	N-Acetyl –L-Cysteine
NADPH	Nicotinamide adenine dinucleotide phosphate
NEP	Neprilysin
nNOS	Neuronal-type nitric oxide synthase
NO	Nitric oxide
NOS	Nitric oxide synthase
NYP	Neuropeptide Y
O_2^-	Superoxide anion
$^{\bullet}OH$	Hydroxyl radical
$ONOO^-$	Peroxynitrite
OSS	Oscillatory shear stress
PAGE	Polyacrylamide gel electrophoresis
PBS	Phosphate buffer saline
PCR	Polymerase chain reaction
PECAM-1	Platelet endothelial cell adhesion molecule-1
PGI_2	Prostaglandin I_2

pH	Power of the hydrogen ion
PI	Propidium iodide
PI3K	Phosphoinositide 3-kinase
PKC	Protein kinase C
PLC	Phospholipase C
qPCR	Quantative real time polymerase chain reaction
RAS	Renin angiotensin system
RIPA	*Radioimmunoprecipitation* assay
RNA	Ribonucleic acid
ROS	Reactive oxygen species
ROX	6-carboxyl-X-rhodamine
RTK	Receptor tyrosine kinase
RT-PCR	Reverse transcription polymerase chain reaction
sACE	Somatic ACE
SDS	Sodium dodecyl sulphate
siRNA	Small interfering RNA
SOD	Superoxide dismutase
SMC	Smooth muscle cell
SSRE	Shear stress response element
tACE	Testicular ACE
TAP	Transporter associated with antigen processing
TBS	Tris buffered saline
TEMED	Tetramethylethylenediamine

TMB	Tetramethylbenzidine
TOP	Thimet oligopeptidase
UV	Ultraviolet
VE-cadherin	Vascular endothelial cadherin
VEGF	Vascular endothelial growth factor
VEGFR2	Vascular endothelial growth factor receptor 2
vWF	Von Willebrand Factor
XO	Xanthine oxidase

Units

Å	Ångström
aa	Amino acids
bp	Base pairs
cm	Centimeters
g	Grams
hrs	Hours
KB	Kilo base pair
kDa	Kilo daltons
kg	Kilogram
L	Litre
M	Molar
mg	Miligrams
min	Minute
ml	Millilitre
mm	Millimetre
mM	Millimolar
ng	Nanogram
nm	Nanometer
N/m^2	Newton meter squared
^{o}	Degree celsius
Pa	Pascal

rpm	Revolution per minute
sec	Seconds
U	Enzyme units
μg	Microgram
μl	Microlitre
μm	Micrometre
μM	Micromolar
V	Volts
v/v	Volume per volume
w/v	Weight per volume
yr	Year

Publications

Peer-reviewed journals

Tobin NP, Henehan GT, Murphy RP, Atherton JC, **Guinan AF**, Kerrigan S, Cox D, Cahill PA, Cummins PM. *Helicobacter pylori*-induced inhibition of endothelial cell functions: a role for VacA-dependent nitric oxide reduction. American Journal of Physiology Heart Circulatory Physiology 2008; 295:H1403-H1413.

Fitzpatrick PA, **Guinan AF**, Walsh TG, Murphy RP, Killeen MT, Tobin NP, Pierotti AR, Cummins PM. Down-regulation of neprilysin expression in vascular endothelial cells by laminar shear stress involves NADPH oxidase-dependent ROS production. International Journal of Biochemistry and Cell Biology 2009; 41:2287-2294.

Walsh TG, Murphy RP, Fitzpatrick P, Rochfort KD, **Guinan AF**, Murphy A, Cummins PM. Stabilization of Brain Microvascular Endothelial Barrier Function by Shear Stress Involves VE-Cadherin Signaling Leading to Modulation of pTyr-Occludin Levels. Journal of Cellular Physiology 2011, 226(11), pp 3053-3063.

Anthony F. Guinan, Paul A. Fitzpatrick, Ronan P. Murphy, Andrew Murphy, Tony G. Walsh, Adrian R. Pierotti, and Philip M. Cummins. Thimet oligopeptidase (EP24.15) expression in vascular endothelial cells is up-regulated by laminar shear stress in a redox-dependent manner. In preparation.

Posters/Abstracts

Anthony F. Guinan, Paul A. Fitzpatrick, Tony G. Walsh, Ronan P. Murphy, Adrian R. Pierotti, and Philip M. Cummins. Shear Stress Regulates Neprilysin Expression in Vascular Endothelial Cells via a Reactive Oxygen Species-Dependent Pathway. *North American Vascular Biology Organization (NAVBO) Workshop: Biology of Signaling in the Cardiovascular System 2008;* Hyannis MA, USA.

Anthony F. Guinan, Paul A. Fitzpatrick, Tony G. Walsh, Ronan P. Murphy, Adrian R. Pierotti, and Philip M. Cummins. Shear Stress Regulates Neprilysin Expression in Vascular Endothelial Cells via a Reactive Oxygen Species-Dependent Pathway. *School of Biotechnology: Research Day 2009*, Dublin City University.

Walsh T.G, **Guinan A.F**, Rochfort K.D, Cummins P.M: Stabilization of brain microvascular endothelial barrier function by shear stress involves a signaling pathway linking adherens and tight junctions via Rac1. *University Hospital Zurich, 13th International Symposium of the Blood Brain Barrier 2010;* Zurich, Switzerland.

Fiona Martin, **Anthony F. Guinan**, Andrew Murphy, Ronan P Murphy, and Philip M Cummins. Cyclic strain induced thrombomodulin release: putative role in macrovascular endothelial injury. *(Bio)pharmaceutical & Pharmacological Sciences research day 2011, Dublin City University.*

Guinan A.F, Murphy A, Murphy RP, and Cummins PM. Shear-Dependent Regulation of Endothelial TOP and NEP: Mechanotransduction and Functional

Consequences. *School of Biotechnology: Research Day 2011*, Dublin City University.

Guinan A.F, Murphy A, Murphy RP, and Cummins PM. Shear-Dependent Regulation of Endothelial TOP and NEP: Mechanotransduction and Functional Consequences. *Sigma-Aldrich Functional Genomics European Seminar Tour 2011*, Dublin City University.

Oral presentations

Regulation of Endothelial Metallopeptidases by Blood Flow-Associated Shear Stress: Roles for NADPH Oxidase and Superoxide. *School of Biotechnology: Research Day 2010*, Dublin City University.

The effect of shear stress on vascular endothelial cells. *School of Health and Human Performance: School seminar 2011*, Dublin City University.

Chapter 1:

Introduction

The following section gives an overview of the vascular system, with particular focus on endothelial cells, their role in vascular haemostasis and the consequences if they become dysfunctional. The ability of endothelial cells to sense and respond to changes in blood flow is essential for both vasoregulation and arterial wall remodelling, while abnormalities in endothelial responsiveness to flow play an important role in the development of atherosclerosis. Endothelial cell membranes contain mechanosensors which are responsible for the transduction of physical forces into biochemical signals. A tight regulation of the signalling pathways activated as a result of mechanosensing is critical to vascular health, as these pathways control the regulation of vasoactive peptides, including zinc metallopeptidases. The production of reactive oxygen species, especially superoxide, is a crucial step in the divergent regulation of shear sensitive genes. The functional aspects of the regulation and dysregulation of these essential signalling molecules will also be discussed in greater detail below.

1.1 The vascular system

The human heart starts to beat around 22 days after conception and on average beats 100,000 times in one day, or 35 million times in a year. During an average lifetime, the human heart will beat more than 2.5 billion times. The human body contains 5.6 litres of blood, which circulates through the body three times every minute. In one day, blood travels a total of 19,000 km through the cardiovascular system; that's roughly the distance between Ireland and New Zealand.

1.1.1 Cardiovascular disease

Cardiovascular disease (CVD) is a general diagnostic term characterised by dysfunction of the heart or circulatory system. This broad ranging condition

includes diseases such as arteriosclerosis, coronary artery disease, heart failure, hypertension and congenital heart disease.

Cardiovascular disease is the leading cause of death in the western world today. Figures from the Irish Heart Foundation state that approximately 10,000 Irish people die each year from CVD - including coronary heart disease (CHD), stroke and other circulatory diseases. This is the most common cause of death in Ireland, accounting for 36% of all deaths. The largest number of these deaths relates to CHD, mainly heart attack, at 5,000 people. Twenty two percent of premature deaths (under age 65) are from CVD.

In Ireland mortality rates from CVD increased up to the 1970s when they peaked at 54% of all deaths in 1974. Since then the trend has been moving towards a reduction in mortalities from 13,241 in 1998, to 9,662 in 2006. However, these figures relate only to CVD-related deaths and do not include patients who presented with symptoms and were treated successfully. In 2009, Ireland's mortality rate from CHD was similar to the European Union (EU) average for both men and women. With respect to stroke mortality in Ireland, men and women had among the lowest rates in the EuroHeart countries, with French women being the only EuroHeart country with lower stroke mortality rates than Ireland.

Figures from the Central Statistics Office show that before 2004, Ireland was still above average for premature deaths from CVD for the EU member countries, with available figures showing that Ireland had 52 premature deaths per 100,000 in comparison with the (pre-2004) EU average of 42. However, with the inclusion of the Eastern European accession states, the average EU figure for the equivalent period rises to 101 premature deaths per 100,000.

In Europe each year CVD causes over 4.3 million deaths, of which over 2.0 million deaths occur in the EU. This accounts for almost half of all deaths in Europe (48%) and in the EU (42%). CVD is the main cause of death in women in all the countries of Europe and is the main cause of death in men in all countries except France, the Netherlands and Spain.

Overall CVD is estimated to cost the EU economy €192 billion a year. Approximately 57% of this is due to health care costs, 21% is due to productivity losses and 22% is due to informal care of people with CVD. In 2008, the direct health care fee alone costs each resident of the EU €231 (Allender, et al. 2008).

A report from the American Heart Association states that 1 in 3 Americans has some form of CVD and since 1900 CVD has been the number one killer in the United States every year except 1918, during the Spanish flu epidemic. Nearly 2,500 Americans die of CVD each day, which is an average of one person every 35 seconds. The direct and indirect cost of CVD for 2006 in the United States was $403.1 billion (Leal, et al. 2006). The World Health Organisation estimates that 16.7 million people around the world die from the disease annually, which is 29% of all deaths worldwide per year, with a projected increase of this figure to 40% of all deaths by 2020.

There are nine easily measurable and potentially modifiable risk factors that account for over 90% of the initial acute myocardial infarction. These nine factors are cigarette smoking, abnormal blood lipid levels, hypertension, diabetes, abnormal obesity, a lack of physical activity, low daily fruit and vegetable consumption, alcohol over-consumption and psychosocial index.

Other uncontrollable factors that place subjects into a risk category for developing CVD are age, gender, family history and ethnicity. The above risk factors play a critical role in initiating or exacerbating the effects of CVD. These risk factors have been extensively studied and links proven with respect to CVD and the endothelium, through studies on atherosclerosis, stroke or the regulation of blood flow-associated hemodynamic forces and blood pressure.

1.1.2 The vasculature

The vasculature is made up of both the microvasculature and the macrovasculature. The microvasculature is the portion of the circulatory system composed of the smallest vessels, such as capillaries, arterioles and venules. The

macrovasculature is the portion of the vasculature containing large vessels; those with an internal diameter of greater than 100 microns (arteries and veins).

All of the blood vessels of the microvasculature and macrovasculature, except for capillaries, share a common three layered structure (Figure 1.1). These three layers are the: (i) tunica adventitia; (ii) tunica media and; (iii) tunica intima.

(i) Tunica adventitia

The tunica adventitia is the outer-most layer covering of the blood vessel. It consists of elastic and collagen fibres. A network of elastic fibres separates the tunica adventitia from the tunica media. The external adventitia contains numerous nerves and, especially in larger vessels, tiny blood vessels that supply the tissues of the vessel wall. These small vessels that supply blood to the tissues of the vessel are called vasa vasorum, or "vessels to the vessels". In addition to the important role of supplying the vessel wall with nerves and self-vessels, the tunica adventitia also helps anchor the vessels to surrounding tissues.

(ii) Tunica media

The tunica media is a muscular and connective tissue layer that is composed of a relatively thick layer of smooth muscle cells (SMCs) and large amounts of elastic fibres. The smooth muscle cells are spindle shaped and take up a circular arrangement around the vessel, perpendicular to the direction of flow. This regulates the diameter of the lumen and, as a direct result, regulates the blood pressure in the vessel.

(iii) Tunica intima

The tunica intima forms the inner lining of the blood vessel and is in direct contact with the blood as it flows through the lumen of the vessel. It consists of the endothelium and a basement membrane. The basement membrane provides a physical support base for the endothelium. Its framework of collagen fibres gives the basal lamina significant tensile strength, while also providing resilience for pulsatile stretch and recoil. The basement membrane is also involved in regulating molecular movement between the endothelium and SMCs and vice versa. The endothelium is a 0.2-4 μm thick monolayer of cells that completely

covers the luminal surface of the blood vessel, which is composed entirely of endothelial cells (ECs). This is now considered to be one of the body's largest organs, composed of approximately 6 trillion cells and weighing roughly 1.5 kg (Vanhoutte, Perrault and Vilaine 2007).

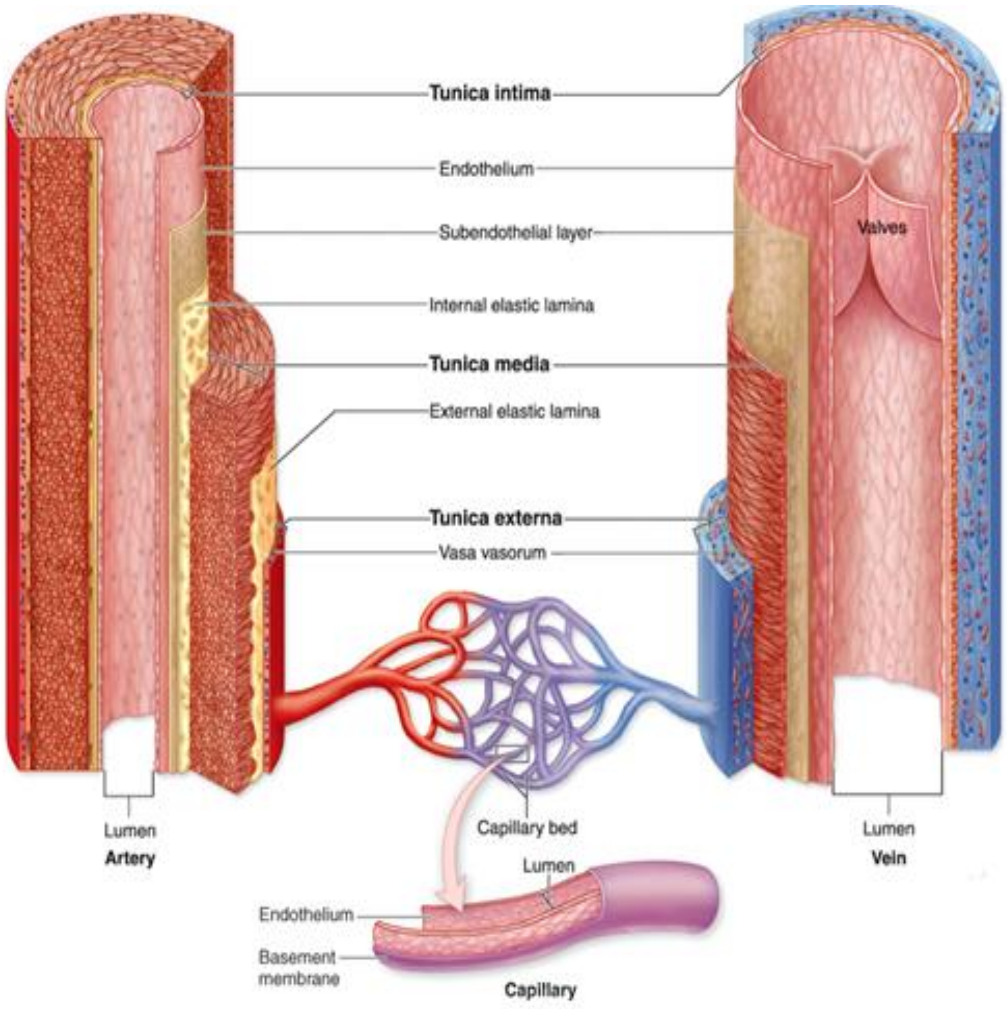

Figure 1.1: Anatomical structure of arteries and veins, showing the layers of blood vessels (McKinley and O'loughlin 2006).

1.2.1 The vascular endothelium

The ability of the vascular endothelium to sense and respond to the flow of blood was observed more than 150 years ago by the famous pathologist

Rudolf Virchow. Virchow pointed to the heterogeneous morphology of the endothelium along the arterial tree, which correlated with the patterns of flow to which the cells were exposed (Resnick, et al. 2003). Virchow also postulated a passive role of the endothelium in transferring nutrients from the bloodstream to tissues and functioning as an insulation barrier, separating platelets from the thrombogenic sub-endothelial connective tissue. It is now known that the vascular endothelium is not only a barrier between the blood and vessel wall or a metabolic exchanger, but because of its unique position it works as a receptor-effector organ which plays a critical role in vessel homesostasis and is implicated in the pathogenesis of CVD. The endothelium plays an important role in the control of vascular tone, blood pressure, hemostatic balance, permeability, proliferation, survival and innate and adaptive immunity. The endothelium is involved in most if not all vascular disease stages, either as a primary determinant of pathophysiology or as a victim of collateral damage (Aird 2008).

Under normal physiological conditions the endothelium expresses a vasodilatory, anti-coagulant and anti-adhesive phenotype which is referred to as ‘quiescent’ or ‘non-activated’ (Aird 2008). These terms have given the illusion of the endothelium as being just a static barrier. However, studies have indicated that ECs have several essential roles in vascular maintenance including: (i) vascular remodelling through the production of growth-promoting and growth-inhibiting substances; (ii) modulating hemostasis and thrombosis through the secretions of pro-coagulant, anti-coagulant and fibrinolytic agents; (iii) mediating inflammatory responses through the expression of chemotactic and adhesion molecules on their membrane surfaces and; (iv) regulating vascular smooth muscle cell contraction through the release of vasodilators and vasoconstrictors (Li, Haga and Chien 2005).

ECs have three surfaces: cohesive, adhesive and luminal. The “*cohesive*” surface adjoins neighbouring endothelial cells to one another and facilitates transport processes. This surface consists of specialised intercellular junctions: gap junctions, tight junctions and adherens junctions. The “*adhesive*” surface of endothelial cells adheres to the basal lumina. The “*luminal*” side of endothelial cells are composed of molecules and specific binding proteins that regulate trafficking of circulating blood cells (Galbraith, Skalak and Chien 1998).

ECs *in vivo* exhibit an elongated shape that is orientated in parallel to the direction of blood flow in relatively straight regions of the vasculature. This laminar shear-induced remodelling typically happens in three phases: (i) cell elongation, where actin stress fibre and microfilament formation, and intracellular junction disruption, are observed within the first three hours of shear; (ii) cell movement with the loss of peripheral bands, which together with the nucleus become located at the upstream side of the cell body after six hours of shear and; (iii) the cell becomes "adjusted" to the flow direction with the formation and alignment of thick stress fibres and dense microfilaments and the reestablishment of cell junctions after twelve hours of shearing (Li, Haga and Chien 2005). In contrast, cells near arterial bifurcations or areas of high curvature have a more polygonal shape and the cytoskeleton is more randomly organised. These regions of the vasculature correspond to locations of "complex flow dynamics" of oscillatory flow and up-regulation of pro-inflammatory processes that lead to increased risk of atherosclerotic plaque formation and CVD.

1.2.2 Endothelial dysfunction

Endothelial dysfunction occurs as a result of the 'activation' of the endothelium. This activation can be stimulated by the action of blood-borne constituents, injury, hypoxia, altered hemodynamics etc. If the activation is short lived normal physiological conditions prevail. If the activation of the endothelium is sustained, endothelial function is impaired and endothelial dysfunction ensues. Alterations in EC morphology and phenotype are considered as early and crucial steps in the development and progression of cardiovascular disease (Ross, 1999).

As a direct consequence of the dendritic morphology of the vascular system, certain areas are more prone to dysfunction than others, such as bifurcations and curves. As such, atherosclerotic plaques are not evenly distributed over the arterial system. There are three types of EC response to injury: (i) immediate transient response: this response begins immediately after a

mild injury and lasts 15-30 min, causing increased vascular permeability; (ii) the immediate-sustained response: this occurs after severe injury and is associated with necrosis of ECs. Leakage starts immediately after injury and may last for several days; (iii) the delayed-prolonged response: in this case, vascular leakage occurs after direct injury of ECs caused by mild-to-moderate thermal exposure, X-ray or UV radiation etc. Leakage is delayed and lasts for several hours to days (Pasyk and Jakobczak, 2004).

One of the earliest biomarkers of endothelial dysfunction is impaired nitric oxide (NO) production in conjunction with excessive oxidative stress (Taddei, et al. 2001).

1.2.3 Hemodynamic forces

Due to its location in the blood vessel, the endothelium is in constant contact with the circulating blood and all of its components. Due to the non-Newtonian and pulsate flow of blood it imparts frictional stresses onto the vessel in the form of the hemodynamic forces, cyclic strain and frictional shear stress (Figure 1.2). *The latter stimulus, shear, will form the basis of this PhD report.*

Cyclic strain is generated by the heart pumping and wall stretch in the circumferential and longitudinal directions. It is directly related to blood pressure and vessel diameter. The vessel wall thickens or thins so that force per unit of wall is consistent (Schiffrin 1992), this can be described by Laplace's Law (Laplace 1899).

$$T = \frac{\mathrm{Pr}}{h}$$

Where T = wall tension (or force per unit length of the vessel), P = blood pressure, r = radius and h = the thickness of the vessel wall. Arteries also

remodel in response to changes in fluid flow so that the vessel diameters are all matched to the volume of the blood (Schaper 2009).

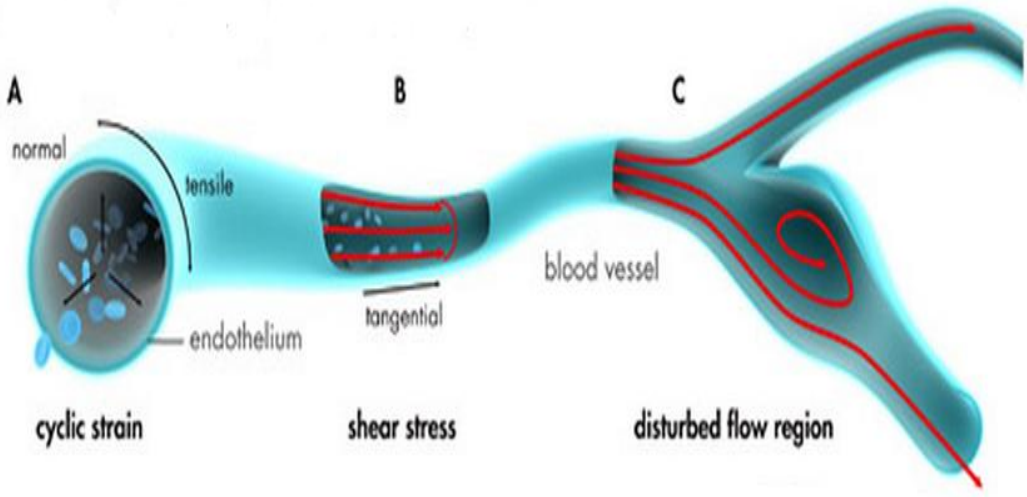

Figure 1.2: Forces affecting ECs in the vasculature. (A) Cyclic stain, which is felt predominantly in larger arterial vessels. (B) Laminar shear stress, which is sensed particularly in straight sections of the vasculature. (C) Disturbed shear, which is found in areas of high curvature or downstream of bifurcations (www.sabiosciences.com/pathwaymagazine/minireview/Adhesionmoleculesmechanotransduction.php)

Cyclic strain is predominant in larger arterial vessels such as the aorta, but is less influential in veins. Cyclic strain acts on both EC and SMCs and at physiological levels plays an important part in endothelial function such as permeability (Collins, et al. 2005) and migration (Von Offenberg Sweeney, et al. 2005). However, at pathophysiological levels cyclic strain can cause hemodynamic dysregulation leading to atherosclerosis (Frangos, Gahtan and Sumpio 1999) or intimal hyperplasia (Newby and Zaltsman 2000).

Any fluid moving along a solid boundary will incur a shear stress on that boundary. It is this principle that explains frictional shear stress on the endothelium. Shear stress is expressed in units of force / unit area (Newton per meter squared [N/m^2] or Pascal [Pa] or dynes/cm^2; 1 N/m^2 = 1 Pa = 10 dynes/cm^2). Under normal physiological conditions, the shear stress to which the

endothelium is exposed is in the range of 10-20 dyne/cm^2. In the case of laminar flow, vessel shear can be expressed as follows:

$$\tau = \frac{4\mu Q}{\pi r^3}$$

Where τ = shear stress, μ = blood viscosity, Q = flow rate and r = vessel radius. Physiologically, flow rate is highest at the centre of the blood vessel and decreases toward the endothelium.

Studies have shown that laminar shear stress (LSS) is an atheroprotective stimulus, causing a dose-related reduction of EC proliferation rate (Levesque, Nerem and Sprague 1990, Traub and Berk 1998). It has also been shown that ECs subjected to a long duration of laminar flow have a lower rate of DNA synthesis than ECs under static conditions and that laminar flow reduces the number of cells entering the cell cycle (Akimoto, et al. 2000). LSS has also been proven to: (i) suppress apoptosis by its up-regulation of NO production (Dimmeler, et al. 1997); (ii) to significantly enhance wound healing through its effect on focal adhesion remodelling (Li, et al. 1997) and; (iii) to decrease microvascular endothelium permeability due to its effect on tight junctions (Levesque, Nerem and Sprague 1990, Colgan, et al. 2007). Thus, the continuous exposure of the endothelium to a physiological range of LSS, particularly in straight sections of the vasculature, promotes the establishment of important physiologic characteristics (i.e. anti-inflammatory, anti-thrombotic, anti-coagulative, pro-fibrinolytic and anti-hypertensive properties).

Disturbed blood flow usually occurs at branching points and curvatures of the arterial tree. At such sites, flow separation leads to transient vortex formations and even flow reversal, leading to a variety of different flow patterns such as oscillatory flow, low flow velocities and multi-frequency/multi-directional secondary flows. Studies have shown that cells exposed to disturbed or oscillatory shear stress (OSS) have a higher proliferation rate than static cells (Levesque, Nerem and Sprague 1990). Also the rate of DNA synthesis is significantly higher in areas of disturbed shear than in areas of laminar shear

(Chiu 1998). Reactive oxygen species are up-regulated as a result of OSS, thus reducing the bioavailability of nitric oxide and inducing inflammatory gene expression, migration and dysregulated cell morphology (Helmlinger, et al. 1991), all of which are central mechanisms for initiation and progression of atherosclerosis (Taniyama and Griendling 2003).

Under these conditions, ECs lose their ability to maintain homeostasis and so become dysfunctional, leading to infiltration of lipids and leukocytes (monocytes and T-lymphocytes) into the sub-endothelial space. The resultant inflammatory response leads to fatty streak appearance, the first step in the formation of an atherosclerotic plaque. If the situation persists, fatty streaks progress and develop into vulnerable plaques that could potentially rupture leading to thrombosis and vascular occlusion (Figure 1.3).

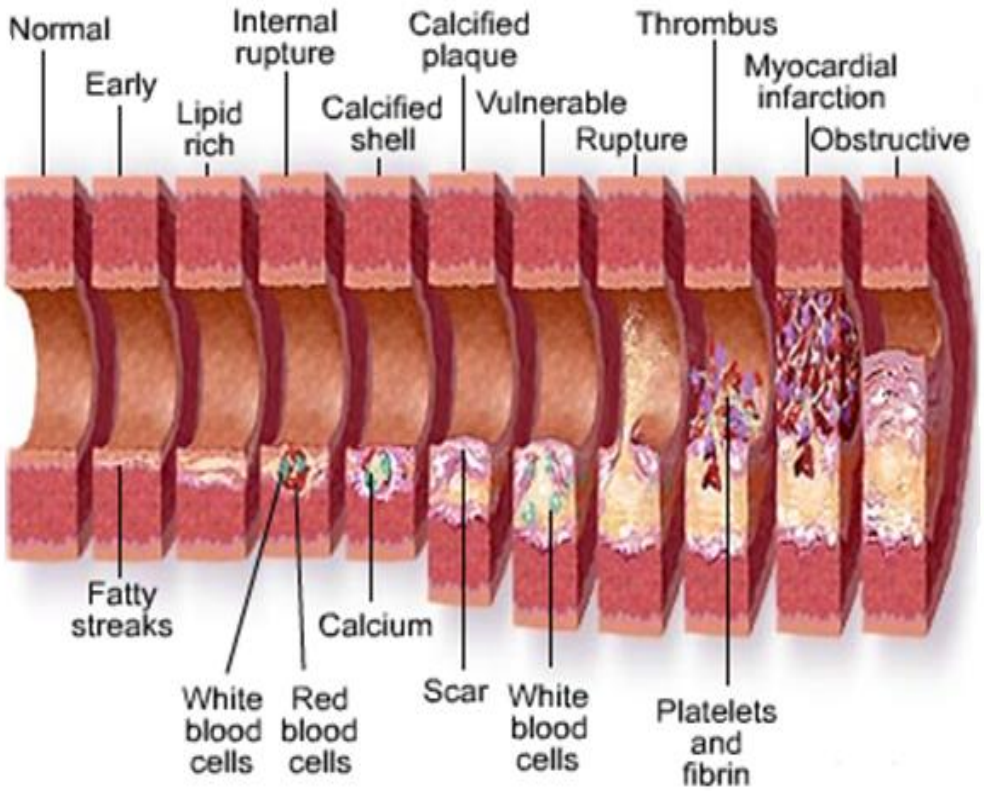

Figure 1.3: The progression of atherosclerotic plaque build-up and rupture (medmovie.com).

1.2.3 Mechanotransduction

Mechanotransduction is the process by which the cells of the endothelium convert these mechanical forces into biochemical signals, which will then lead to functional responses from the cells. As a result, shear stress modulates the expression of genes that encode for growth factors, adhesion molecules, vasoactive substances, oxygen scavengers, coagulation factors and chemoattractants. It also regulates activation of several transcription factors, which are capable of binding to positive or negative shear stress response elements (SSREs) at promoters of mechanosensitive genes, inducing or suppressing their expression with downstream consequences for cellular function and morphology (Pasyk and Jakobczak 2004, Masatsugu, et al. 2003).

Endothelial responses to flow occur in a coordinated sequence and exhibit time constants ranging from milliseconds to many hours. Many putative mechanotransducers have been proposed to function in sensing flow such as ion channels, integrins, receptor tyrosine kinases, the apical glycocalyx, primary cilia, heterotrimeric G proteins, platelet and endothelial cell-adhesion molecule-1 (PECAM-1) and vascular endothelial (VE)-cadherin (Hahn and Schwartz 2009) (Figure 1.4).

1.2.3.1 Luminal mechanosensors

1.2.3.1.1 Primary cilia

Primary cilia are specialised membrane-covered rod-like organelles that are several micrometers long, protruding from virtually all mammalian cells (D'Angelo and Franco 2009). Primary cilia can sense shear stress as low as 0.007 dynes/cm^2 (Goldsmith, Cokelet and Gaehtgens 1989) and function as flow sensors in kidney epithelium (Praetorius and Spring 2003), bile duct epithelium and vascular endothelium (Hierck, et al. 2008). The function of primary cilia in endothelial shear sensing appears to be biphasic. Fluid flow and the associated

ciliary deformation lead to a polycystin-mediated intracellular Ca^{2+} transient within seconds (Nauli, et al. 2008). Cilia-associated proteins polycystin 1 and 2 are expressed in ECs, with mutations or deletions of these genes in either humans or mice leading to vascular defects (Kim, et al. 2000). Also, the cilium is considered to amplify the cytoskeletal strain, resulting in prolonged effects on gene expression of shear-responsive genes (Hierck, et al. 2008).

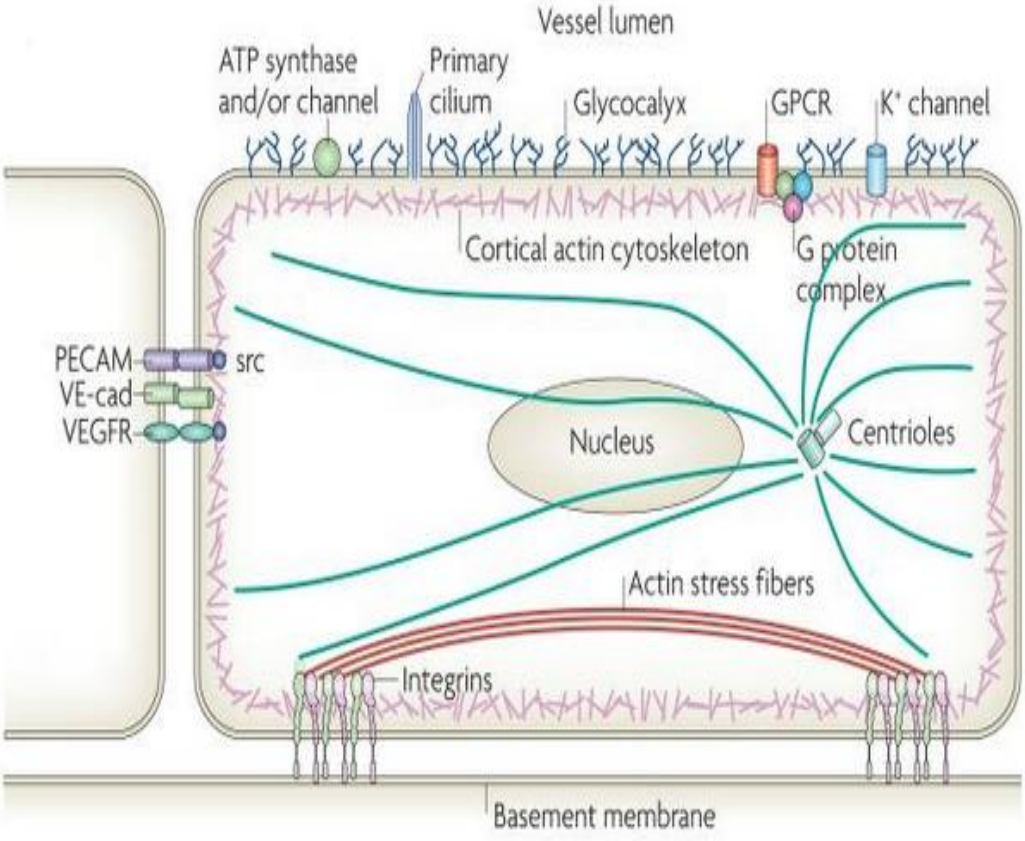

Figure 1.4: Endothelial mechanosensors**.** The figure shows the cellular localisation of the mechanosensors on the luminal, cohesive and adhesive surfaces of the EC. (Hahn and Schwartz, 2009).

The distribution of primary cilia has been described to be spatio-temporally linked to shear stress *in vivo*. In adult vasculature, primary cilia are located at atherosclerotic predilection sites where flow is low and oscillatory. Moreover, ECs in areas of high shear stress are devoid of cilia (Van der Heiden,

et al. 2008). Therefore, it is plausible that cilia could mediate mechanotransduction from these sites (Hahn and Schwartz 2009).

1.2.3.1.2 Endothelial glycocalyx

The endothelial glycocalyx (EG) was visualised over 40 years ago using electron microscopy (Luft 1966). However, until recently little was known of the composition and function of this layer. We now know that the EG consists of a negatively charged, organised mesh of membranous glycoproteins, proteoglycans, glycosaminoglycans and associated plasma proteins, which is situated at the luminal side of all blood vessels (Pries, Secomb and Gaehtgens 2000) (Figure 1.5)

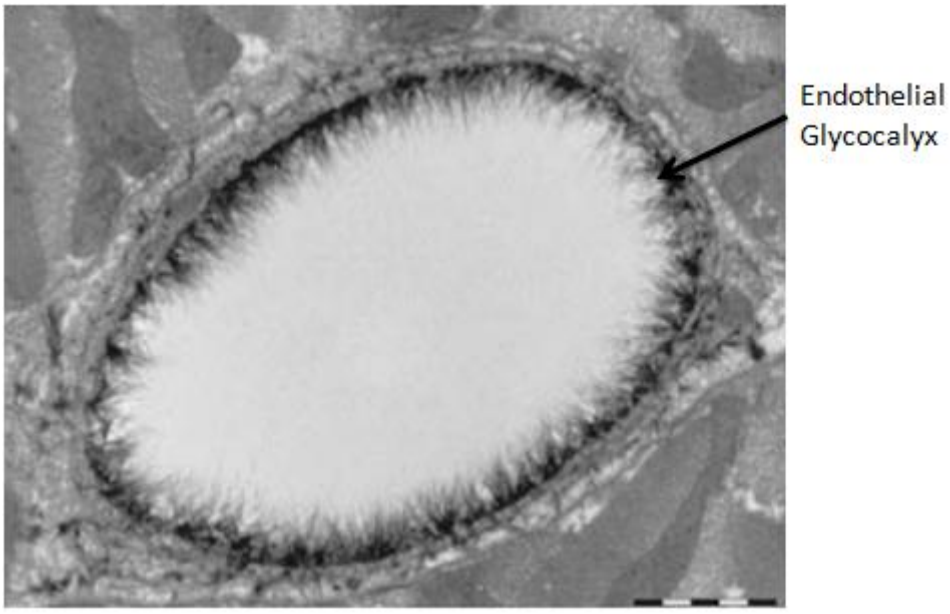

Figure 1.5: Visualisation of the endothelial glycocalyx. Figure shows the endothelial glycocalyx of a rat left ventricular myocardial capillary, visualised using electron microscopy. Bar represents 1 μm (Reitsma et al., 2007).

Its major constituents comprise hyaluronic acid and the negatively charged heparin sulphate proteoglycans. Historically, the EG was thought to be confined to a thickness of only several nanometers (~400 nm). Now thanks to advances in rapid freezing/freeze substitution transmission electron microscopy, BAEC EG has been measured at 11 μm (Ebong, et al. 2011).

There is increasing evidence that the EG plays a considerable physiological role in relation to vascular permeability, adhesion of leucocytes and platelets, mediation of vascular stress and modulation of inflammatory responses (Weinbaum, Tarbell and Damiano 2007, Levick 2004, Pries and Kuebler 2006, Parish 2006). Recent findings also demonstrate that damage to the EG plays a role in several pathologies such as diabetes, reperfusion injury and atherosclerosis (Nieuwdorp, et al. 2006, Mulivor and Lipowsky 2004, Nieuwdorp, et al. 2005).

1.2.3.1.3 G-proteins

G-proteins are heterotrimers composed of Gα and Gβγ subunits which are located at the inner surface of the plasma membrane, where they are associated with transmembrane G-protein coupled receptors (GPCRs). G-proteins regulate a variety of endothelial functions including migration, proliferation, differentiation, survival and tissue homeostasis (Hamm 1998, Wieland and Mittmann 2003, Andreeva, et al. 2006, Knezevic, et al. 2009). There are 16 genes encoding for 23 known Gα subunits, 5 genes for Gβ subunits and 12 genes for Gγ subunits (Hurowitz, et al. 2000). The Gβγ dimer anchors the G-protein to the cytoplasmic face of the plasma membrane, while the Gα chain exchanges GDP for GTP upon GPCR activation (Papadaki and Eskin 1997). This leads to dissociation of the α and βγ subunits, both of which are now free to act on specific downstream effectors (Wieland and Mittmann 2003). Gudi et al. have shown that G-protein activation occurs 1 sec after shear onset, while inhibition of G-proteins using antisense Gαq oligonucleotides blocked shear-induced Ras-GTPase activity (Gudi, Clark and Frangos 1996, Gudi, et al. 2003).

G-proteins associated with transmembrane receptors that are involved in signal transduction in ECs include: (i) G_q proteins, which activate phospolipase C (PLC); (ii) G_s proteins or stimulatory G-proteins, which activate Ca^{2+} channels and adenylate cyclase (AC), and; (iii) G_i proteins or inhibitory G-proteins, which inhibit AC and are thought to be involved in the stimulation of K^+ channels in endothelial cells (Simon, Strathmann and Gautam 1991).

Shear stress activation of G-proteins has also been shown to be involved in several flow-initiated endothelial responses that regulate vascular tone, including release of the vasodilators NO (Ohno, et al. 1993) and PGI_2 (Berthiaume and Frangos 1992) and vasoconstrictors such as endothelin (Kuchan and Frangos 1993). Through the use of a co-culture system, of ECs and vascular SMCs, Redmond et al. demonstrated that flow mediates selective changes in EC and SMC G-protein expression associated with changes in G-protein functionality and cellular signalling capacity. Moreover, flow-induced changes in SMC G-protein signalling capacity are endothelium dependent. This suggests that G-protein modulation may represent an important mechanism whereby hemodynamic forces regulate vessel wall function (Redmond, Cahill and Sitzmann 1998).

1.2.3.1.4 Ion channels

The lipid bilayer of cell membranes has high permeability for hydrophobic and small polar molecules while it is highly impermeable to ions, a function which is critical for the cell to maintain different concentrations of solutes from those in the extracellular fluid. Ion channels are responsible for the transfer of specific ions across the plasma membrane. One of the most rapid endothelial responses to flow is the activation of these flow-sensitive ion channels; therefore, these channels have been proposed for candidates as mechanotransduction (Davies 1995).

Inward-rectifying potassium (Kir) channels were the first type of flow-activated ion channel reported in ECs (Olesen, Claphamt and Davies 1988).

Activation of Kir channels is virtually immediate on flow onset and results in hyperpolarisation of the EC membrane.

A second type of flow-sensitive ion channel has also been identified as an outward-rectifying chloride (Cl^-) channel (Barakat, et al. 1999). The outward-rectifying Cl^- current is induced virtually instantaneously on flow onset, a response which is independent of Kir activation. The effect of activation of the flow-sensitive outward-rectifying Cl^- channels on EC membrane potential counteracts that of the Kir channels.

There is mounting evidence that flow-sensitive K^+ and Cl^- channels play a central role in regulating overall endothelial responsiveness to flow. By modulating flow-induced responses, ECs activation of flow-sensitive ion channels likely plays an important role in regulating aspects of normal vascular physiology. These include vasoregulation in response to acute changes in arterial blood flow and arterial well remodelling after chronic hemodynamic alterations (Barakat, Lieu and Gojova 2006).

Moreover, flow-sensitive ion channels may play a role in the endothelial dysfunction associated with the onset of atherosclerosis. Suvatne et al. have demonstrated that blocking flow-sensitive K^+ and Cl^- channels greatly attenuates flow-induced increases in endothelial Na-K-Cl co-transport protein (Suvatne, Barakat and O'Donnell 2001). It has also been shown that the blocking of these ion channels inhibits EC spreading during endothelial wound closure after mechanical injury (Gojova and Barakat 2005) and that blocking K^+ channels inhibits the induction of NO by shear stress (Shasby 2007).

1.2.3.2 Cohesive mechanosensors

1.2.3.2.1 PECAM-1

Platelet endothelial cell adhesion molecule-1 (PECAM-1) is a 130 kDa type I transmembrane glycoprotein that is expressed on the surface of platelets, monocytes, macrophages and endothelial cells, where it is localised to the border of adjacent cells at $1x10^6$ to $2x10^6$ copies/cell (Newman 1994) (Figure 1.6). PECAM-1 is a primary constituent of endothelial cell-cell junctions in confluent vascular beds. It is composed of 6 extracellular immunoglobulin domain-like loops which participate in homophilic interaction with the neighbouring cell, where it plays a role in the transendothelial migration of leukocytes (Vaporciyan, Delisser and Yan 1993, Wakelin, et al. 1996).

Given its abundant expression in ECs, PECAM-1 has been demonstrated to be involved in the initial formation and stabilisation of cell-cell contacts at lateral junctions of ECs, the maintenance of a vascular permeability barrier, modulation of cell migration, transendothelial migration and angiogenesis (Newman, et al. 1990, Albelda, et al. 1990, Albelda, et al. 1991, Ferrero, et al. 1995, Schimmenti, et al. 1992, DeLisser, et al. 1997). More recent results have indicated a role for PECAM-1 in mechanosensing, with tyrosine phosphorylation of PECAM-1 occurring within 30 sec of shear onset. Once activated, PECAM-1 activates ERK 1/2 through the Ras signalling pathway (Fujiwara, et al. 2001). Kano et al. demonstrated that this phosphorylation could also be induced by mechanical pulling applied to PECAM-1 via the twisting of magnetic beads coated in PECAM-1 antibodies (Kano, Katoh and Fujiwara 2000) thereby confirming the mechanosensitive nature of the molecule. Mechanical stimulation of PECAM-1 has been implicated in activating Src family tyrosine kinase, one of the earliest known intracellular signalling events in this pathway (Tzima, et al. 2005).

1.2.3.2.2 VE-cadherin

Vascular endothelial cadherin (VE-cadherin) is a 140 kDa type II classical cadherin (Figure 1.6). It is found exclusively in vascular ECs, where it is concentrated in adherens junctions (Breier, et al. 1996). Adherens junctions are a dynamic complex present at cell-cell borders between adjacent endothelial and epithelial cells.

VE-cadherin is a calcium-dependent cell-cell adhesion glycoprotein composed of 5 extracellular cadherin repeats, a transmembrane region and a highly conserved cytoplasmic tail. VE-cadherin's extracellular domain binds to the extracellular domain of another VE-cadherin expressed in the membrane of an adjacent EC. By forming a homotypic bond in this manner, VE-cadherin glues the neighbouring cells together (Rudini and Dejana 2008). Intracellularly, VE-cadherin is connected to the actin cytoskeleton via a family of catenins. Catenins not only serve as a structural linker, they also transduce biochemical signals for cell-cell communication. The stability of the VE-cadherin-catenin-cytoskeleton complex is essential to the maintenance of endothelial barrier function (Sallee, Wittchen and Burridge 2006, Vincent, et al. 2004).

VE-cadherin functions are crucially regulated by the shear stress of blood flow (Hahn and Schwartz 2009). Recently published work from our laboratory demonstrates a role for VE-cadherin in the transmission of physiological shear signals to tight junction occludin through a Tiam1/Rac1 signal mechanism, leading to up-regulation of brain microvascular EC barrier integrity (Walsh, et al. 2011). *In vivo* studies indicate that VE-cadherin expression at cell-cell junctions is weaker in atherosclerosis susceptible sites, such as bifurcations, with intermittent staining patterns under low net flow; however, total cellular VE-cadherin levels remained unaltered, indicating a redistribution within the membrane (Hahn and Schwartz 2009).

Gene deletion studies show that VE-cadherin is essential for embryonic angiogenesis, vascular maintenance and restoration of vascular integrity after injury (Gentil-dit-Maurin, et al. 2010, Gulino, et al. 1998). Mice deficient in VE-

cadherin die as a result of severe vascular defects, which are characterised by defective capacities in sprouting angiogenesis, suggesting a putative role for VE-cadherin in vascular morphogenesis (Gory-Faure, et al. 1999). VE-cadherin has been found to be an essential molecule in the contact inhibition of EC cell proliferation as a result of junctional stabilisation (Lampugnani, et al. 2003).

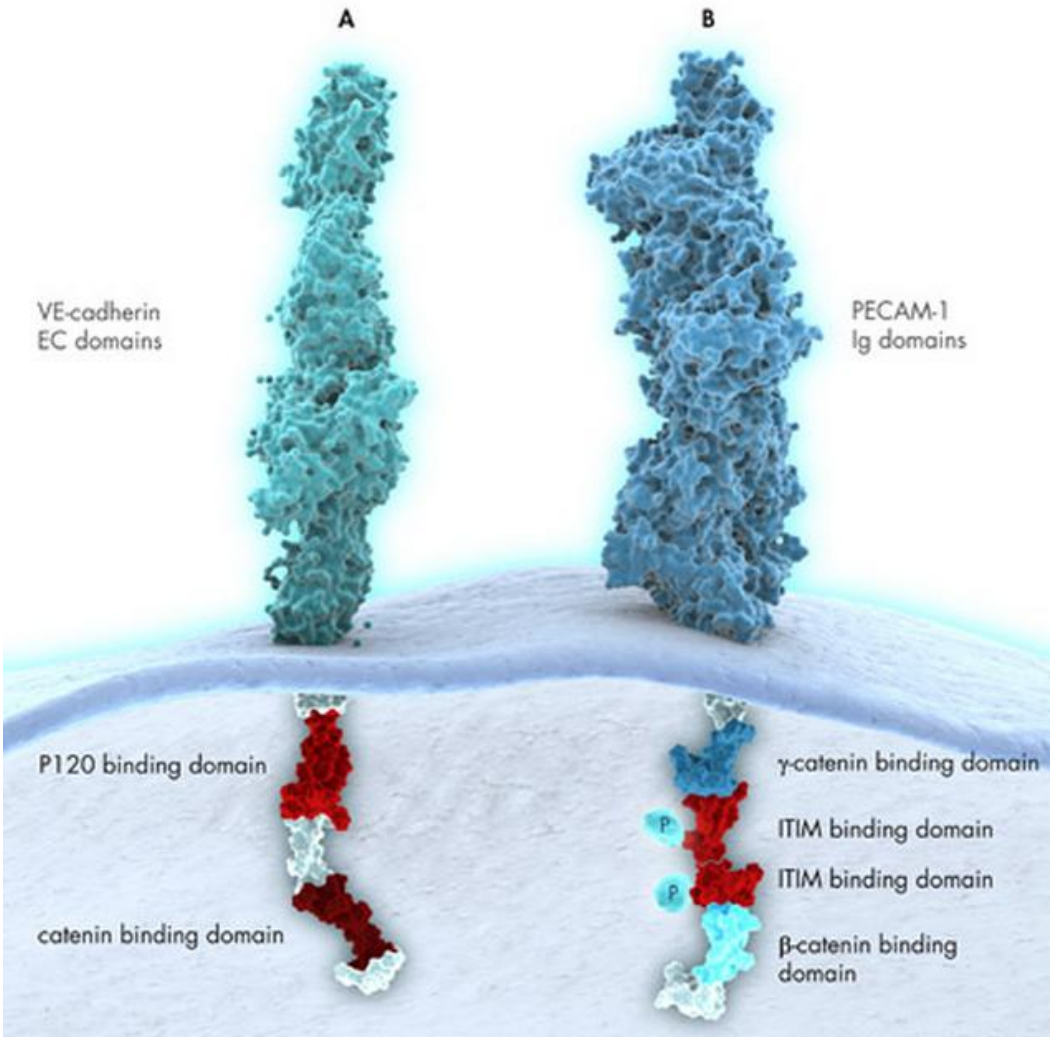

Figure 1.6: General structure of VE-cadherin (A) and PECAM-1 (B). Both transmembrane proteins contain an extracellular region responsible for forming trans homodimers with neighbouring cells. The intracellular cytoplasmic tails of each molecule can interact with the actin cytoskeleton (www.sabiosciences.com/pathwaymagazine/minireview/Adhesionmoleculesmechanotransduction.php).

1.2.3.2.3 Receptor tyrosine kinases

The kinase family is one of the largest effector families in the human genome, with over 500 members. The principal functions of the tyrosine kinase sub-family include cell/cell signalling, adhesion and motility (Sharma and Priyank 2011). Tyrosine kinases are enzymes that transfer a phosphate group from ATP to a target cellular protein, thereby acting as an on/off switch in many cellular functions.

Receptor tyrosine kinases (RTKs) are monomeric, transmembrane cell surface receptors with an extracellular N-terminal and an intracellular C-terminal region. To elicit signal transduction cascades, RTKs need to form dimers in the plasma membrane, these dimers being stabilised by ligands binding to the receptor. The interaction between the cytoplasmic domains stimulates the auto-phosphorylation of tyrosine within the domains of the RTKs, leading to tyrosine kinase activation. In turn, these docking phosphotyrosines recruit specific intracellular adaptor proteins (Src, Shc) and activate intracellular signal transduction pathways such as phosphatidylinosityl 3-kinase (PI3K)/Akt, mitogen-activated protein (MAP) kinases or protein kinase C (PKC) (Lemmon and Schlessinger 2010). PI3K and MAP kinases mediate the effect of RTKs on cell proliferation, survival, differentiation, migration and cytoskeletal reorganisation (Schlessinger 2000, Blume-Jensen and Hunter 2001, Cantley and Cantley 1995).

It has been reported almost all RTKs are activated by shear stress and that shear stress causes quick ligand-independent phosphorylation of RTKs (Jong Lee and Young Koh 2003). RTKs play a critical role in the regulation of endothelial cell proliferation and survival. Their expression, usually low in normal vessels, is increased in atherosclerotic lesions, in correlation with an increased expression of their ligands (Ross 1993). Mutations in RTKs and attenuated activation of their signalling pathways have been linked to numerous diseases including breast cancer (Boulay, et al. 2008) and venous malformation (Vikkula, et al. 1996).

1.2.3.2.4 VEGFR-2

Vascular endothelial growth factor receptor-2 (VEGFR-2) is a 230 kDa class V RTK. VEGFR-2 consists of an extracellular ligand-binding domain with seven immunoglobulin-like motifs, a single transmembrane and a cytoplasmic domain that contains a juxtamembrane region, a kinase domain and a carboxyl terminus.

VEGFR-2 appears to mediate all known cellular responses to VEGF (Holmes, et al. 2007). The critical role of VEGFR-2 in vascular development is demonstrated by the death of VEGFR-$2^{-/-}$ mice due to defective development of blood islands, ECs and haematopoietic cells (Shalaby, et al. 1995). During shear mechanotransduction, VEGFR-2 uses VE-cadherin as an adaptor which brings it into proximity with PECAM-1, thereby facilitating the activation of VEGFR-2 by Src, a ligand-independent transactivation in response to flow. VEGFR-2 is activated within 15 sec of the onset of flow and is localised to cell-cell junctions. Once activated, VEGFR-2 recruits and activates PI3K, which mediates crucial downstream signals (Shay-Salit, et al. 2002, Jin, et al. 2005). One such signal is the Akt-dependent phosphorylation of endothelial NO synthase, which contributes to the stimulation of NO release and vessel relaxation (Fleming, et al. 2005). This flow-induced activation of VEGFR-2 was shown to be absent in both PECAM-$1^{-/-}$ and VE-$cadherin^{-/-}$ ECs at all times between 15 sec and 5 min. This demonstrates that VEGFR-2 activation by shear stress is downstream of the junctional receptors (Tzima, et al. 2005).

1.2.3.3 Adhesive mechanosensors

1.2.3.3.1 Integrins

Integrins are membrane-associated glycoproteins found predominantly on the basolateral surface of ECs. These glycoproteins are heterodimers composed of an α and β subunit. In vertebrates, there are 18 α and 8 β subunits that can assemble into 24 different receptors with different binding properties and different tissue distributions (Hynes 2002, Barczyk, Carracedo and Gullberg 2010). The extracellular domain binds directly to extracellular matrix (ECM) proteins such as vitronectin, fibronectin, laminin and collagen. The cytoplasmic domain of both the α and β subunits interact with signalling molecules and cytoskeletal proteins to regulate cellular events such as signal transduction, cytoskeletal organisation and cell motility (Shyy and Chien 2002). Integrins have been shown to be highly sensitive to hemodynamic forces, and their subsequent activation has been shown to be essential to flow-mediated NO release (Muller, Chilian and Davis 1997), cellular realignment (Tzima, et al. 2005) and ERK 1/2 activation (Takahashi and Berk 1996).

The specific binding of integrins to extra cellular matrix (ECM) proteins or to counter-receptors on adjacent cells, supports cell adhesion and is crucial for embryonic development, tissue maintenance and repair, host defence and haemostasis (Harburger and Calderwood 2009). Integrins are unique structures due to their ability to regulate ‘inside-out’ signalling, where intracellular signals affect their binding affinity to ECM ligands (Shattil, Kim and Ginsberg 2010). Integrins also regulate ‘outside-in’ signalling where they transmit signals into the endothelial cells providing information on location, adhesive state and surrounding matrix (Hynes 2002).

1.2.3.3.2 Cytoskeleton

Endothelial mechanics are largely determined by the cytoskeleton, which is mainly composed of actin, intermediate filaments and microtubules. These components physically connect different regions of the EC to transmit forces from the apical domain, where shear is applied, to the basal or lateral domains, where mechanotransduction has been observed (Davies 1995).

The cytoskeleton is strong enough to build a scaffold which defines cell shape, but which is flexible enough to tolerate the hemodynamic forces acting upon it. However, the cytoskeleton is not a constant structure, as is shown through the dramatic realignment of actin fibres in the direction of shear (Oberleithner, et al. 2007). As such the cytoskeleton is involved in modulating hemodynamic forces, transmitting them through the cell and transducing the mechanical force into a biochemical signal which finally leads to a change in cellular function. Mechanical properties have an impact at each stage of the mechano-signalling cascade and as such it is plausible that disturbances in mechanical forces can disturb endothelial functions (Kliche, et al. 2011). Furthermore, disruption of the actin cytoskeleton has been found to be sufficient to negate the effect of shear stress-mediated signalling and changes in gene expression (Imberti, et al. 2000).

1.3 Zinc Metallopeptidases

Peptides are used by all cell types to elicit cellular functions. The use of peptides as messengers usually involves the following steps: (i) production and release of the peptide by a specific cell; (ii) interaction of the peptide with a receptor on the surface of the target cell and; (iii) degradation of the peptide to terminate action. The first and last steps of this scheme require the participation of proteases/peptidases. There is increasing evidence that both soluble and membrane-associated zinc-metallopeptidases play important roles in both of

these steps (Ghaddar, et al. 2000). Although activation of inactive pro-hormone precursors into bioactive peptides is generally performed by proteases of the subtilisin family located either in the trans-Golgi network or in secretary granules of the cell, a few peptides require a final processing step after secretion (Seidah, Chretien and Day 1994). Of particular importance within the blood vessels are the membrane-associated zinc metallopeptidases, which hydrolyse peptide bonds of less than 40 aa, the length of most bioactive hormones. In addition to their role in peptide activation, cell surface zinc-metallopeptidases are also known to terminate peptidergic signals by degrading the active peptides into inactive fragments. One of the best known of these peptidases is neprilysin (NEP), which is involved in the physiological degradation of several bioactive peptides (Kohne, et al. 1998) as discussed below.

Zinc-dependent proteases constitute one of four major types of proteases, the others being aspartate, serine and cysteine proteases. Members of the zinc-dependent class of metallopeptidases are characterised by a catalytic metal ion, which cleaves peptide bonds following a common mechanism with the participation of a solvent molecule and a polarising general base/acid, usually a glutamate (Gomis-Ruth 2008, Bayés, et al. 2007). Upon binding of the substrate, the metal simultaneously coordinates the scissile carboxyl oxygen and the solvent molecule, and the glutamate activates the latter by degradation of the peptide bond (Gomis-Ruth, Botelho and Bode 2011) (Figure 1.7).

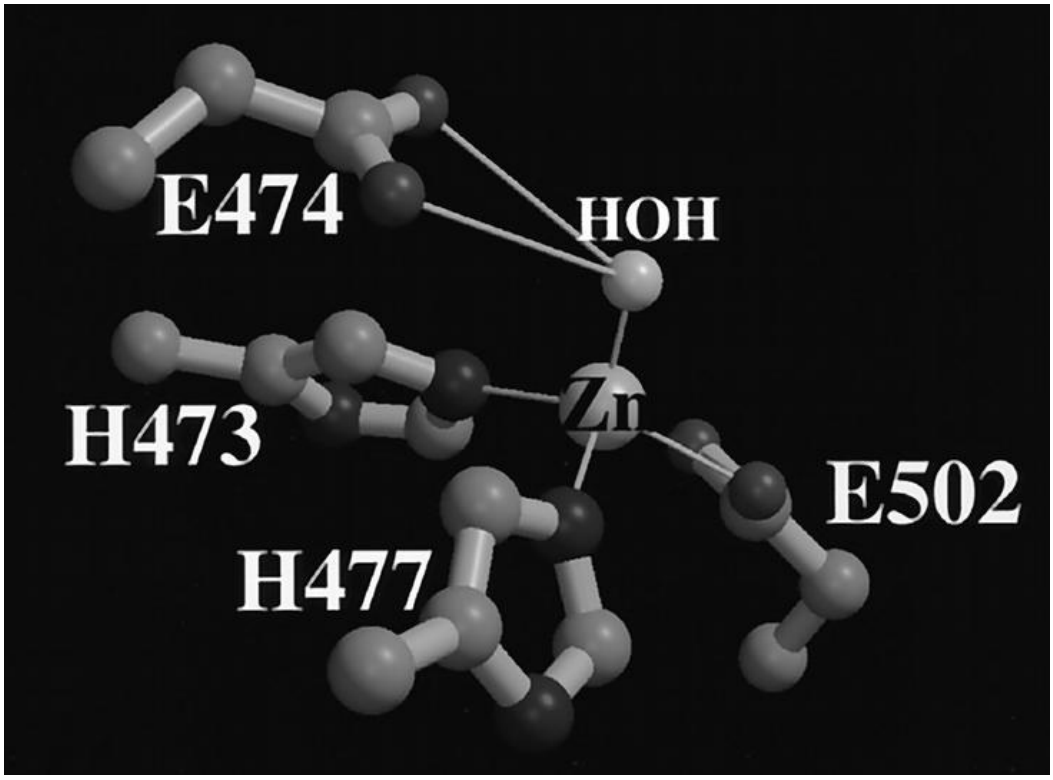

Figure 1.7: Model of zinc-coordinating residues within the TOP active site. A view of conserved residues involved in zinc coordination and substrate catalysis. For clarity, only the side chains and C-α′ carbons of the coordinating residues as well as the zinc atom and the activated water molecule are shown. Atoms proposed to coordinate with zinc are connected by a *thin white line*. The graphical representations were depicted with MOLSCRIPT with subsequent renderings using RASTER 3D (Shrimpton, Smith and Lew 2002).

There are several methods to classify metallopeptidases; one such method is classification based on the catalytic mechanism, the critical amino acid residue involved and amino acid sequence similarity within peptidase moieties. Rawlings and Barrett devised a classification system for dividing peptidases into clans and sub-clans; there is a constantly evolving classification system that can be accessed online (http://merops.sanger.ac.uk). Metallopeptidases are currently split into 62 families (M1-M85, with several unassigned numbers) (Rawlings and Barrett 1993).

One of the largest clans in this classification is the Clan MA. These are distinguished by the active site motif HE*XX*H, in which two histidine residues, together with a third distant residue (typically a glutamate/histidine residue), bind the zinc atom. This clan is again divided into two major sub-clans: MA (E), the

gluzincins, where the third ligand is a glutamate, and MA (M), the metzincins, where the third ligand is a histidine or an aspartate. The sub clan MA (M) is typified by the matrix metalloproteases and their relatives (Lew 2004).

The gluzincins are further subdivided into families based on homology. The families commonly relevant to mammalian signalling systems are M1 (e.g. aminopeptidases), M2 (e.g. angiotensin-converting enzyme (ACE)), M3 (e.g. thimet oligopeptidase (TOP) and neurolysin), and M13 (e.g. neprilysin (NEP) and endothelin-converting enzyme (ECE)).The following sections will discuss these metallopeptidases in greater detail. Moreover, of particular interest to this project are the peptidases in the family M3, specifically **TOP**, and in family M13, specifically **NEP**.

1.3.1 M2/M13 family members

1.3.1.1 Neprilysin

Neprilysin (neutral endopeptidase, NEP, EC3.4.24.11) is a member of the M13 family of zinc metallopeptidases. It is a type II membrane-bound zinc metallopeptidase that cleaves endogenous peptides at the amino side of hydrophilic residues. Its target substrates include a number of endogenous vasodilator peptides, including atrial natriuretic peptide (ANP), brain natriuretic peptide (BNP), C-type natriuretic peptide (CNP), substance P and bradykinin (BK), as well as vasoconstrictor peptides such as endothelin-1 (ET-1) and angiotensin II (Ang II) (Ferro, et al. 1998) (Figure 1.8). NEP is found in ECs, vascular SMCs, cardiac myocytes and renal epithelial cells as well as in fibroblasts. A pharmacologically induced NEP blockade typically leads to elevated natriuresis and vasodilation (Quaschning, Galle and Wanner 2003), and induces anti-proliferative effects on vascular SMCs (Barber, et al. 2005). This suggests a potentially important role for NEP in pathologies characterised by flow-dependent endothelial dysfunction and remodelling. As such, it is a

therapeutically relevant target in the treatment of endothelial dysfunction and CVD. In view of its importance to endothelial function (and dysfunction), the regulation of NEP by hemodynamic forces is highly relevant and will be studied in detail in this project.

NEP was originally identified as a major antigen of renal membranes over 30 years ago and was implicated in the metabolism of insulin; however, there is little evidence to support this. NEP is now linked to the metabolism of neuropeptides in the central nervous system, especially enkephalins and substance P (Skidgel, et al. 1984). NEP is also shown to be the principal enzyme responsible for inactivating the vasodilator, ANP (Turner 2003).

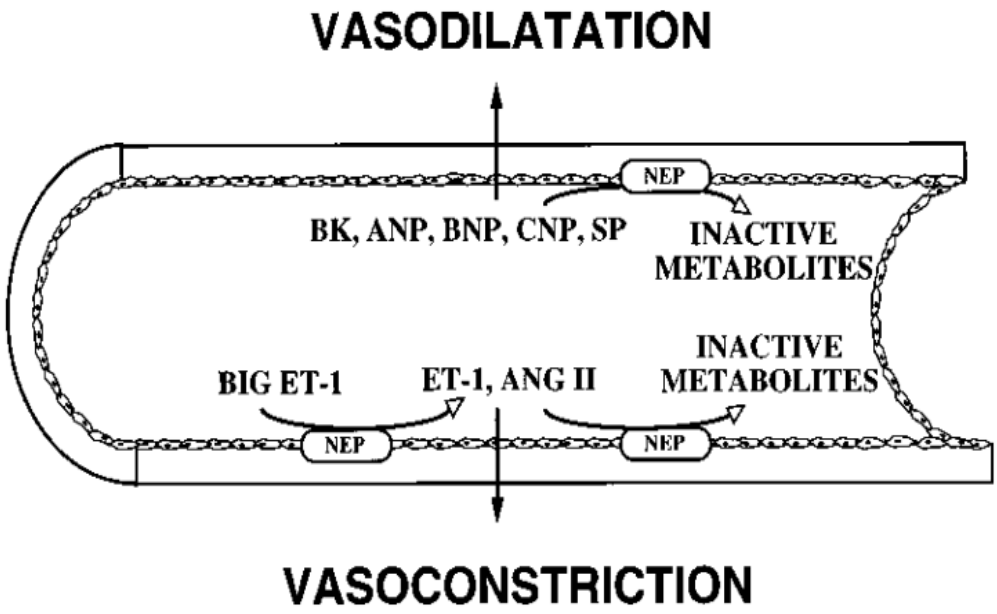

Figure 1.8: Metabolites of NEP in vasodilation and vasoconstriction. NEP catalyses the metabolism of the vasoconstrictor peptides ET-1 and Ang II, as well as the metabolism of several vasodilator peptides, including BK, ANP, BNP, CNP, and substance P. NEP is also involved in the enzymatic conversion of big ET-1 to its active form, the vasoconstrictor peptide ET-1. The balance of effects of NEP inhibition on vascular tone, therefore, will depend on whether the predominant substrate(s) degraded by NEP are vasodilators or vasoconstrictors and on the extent of NEP involvement in the processing of big ET-1 (Ferro et al., 1998).

Structurally, NEP consists of a short N-terminal cytoplasmic domain (25 aa), followed by a single hydrophobic transmembrane helix domain (24 aa), that functions as both a transmembrane domain and a signal peptide, and a large C-terminal extracellular domain that contains the catalytic site with a conserved HE*XX*H motif participating in zinc coordination (D'Adamio, et al. 1989). NEP also contains a shear stress response element (SSRE) in its promoter region and has been shown to be regulated by hemodynamic forces in a reactive oxygen species (ROS)-dependent manner (Fitzpatrick, et al. 2009). The crystal structure of human NEP has been resolved at 2.1Å (Figure 1.9). One of the most interesting things this has revealed is the restricted active site cleft preventing access of large peptides and proteins, thus explaining its oligopeptidase character (Carson and Turner 2002). Analysis of the N-terminal sequence of the cytosolic domain identified a myristoylation consensus site. Myristoylation is an important post-translational function in many cellular pathways, including signal transduction, apoptosis and extracellular transport of proteins. It has been shown that the second glycine in the NEP protein is myristoylated, and that myristoylation results in increased NEP protein at the cell membrane (Zheng, et al. 2010).

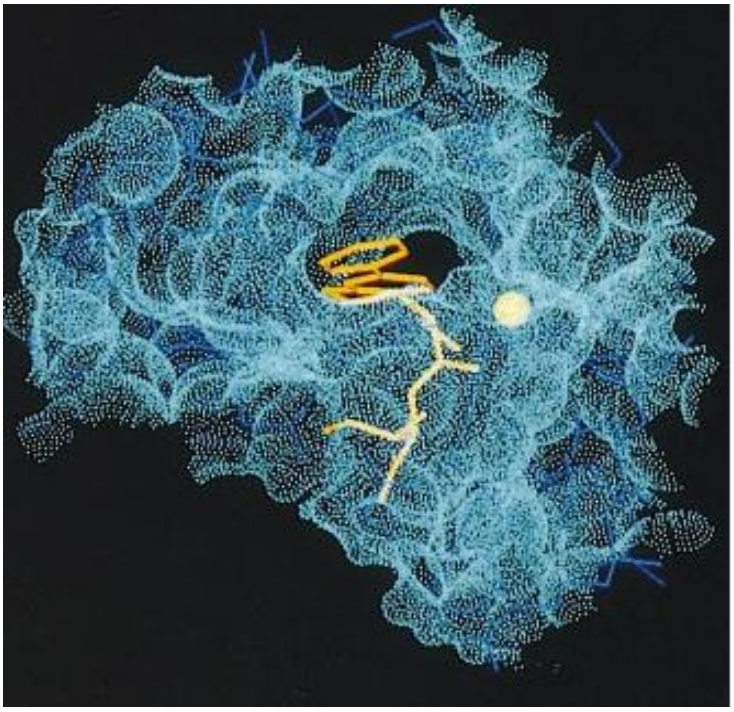

Figure 1.9: The structure of NEP. NEPs active site model is shown in the centre of the image, with its zinc atom in yellow (Tiraboschi et al., 1998).

In addition to roles in the vasculature, central nervous system and kidneys, NEP is also implicated in oncogenesis, most notably prostate cancer, in which NEP is dramatically down-regulated or indeed absent (Osman, et al. 2004). A measurement of NEP and ECE in a range or prostate cancers demonstrates that there is a balance between levels of NEP and ECE which determines the level of malignancy of the cells and that ECE expression in metastatic cells may be indicative of its role in metastatic progression (Usmani, et al. 2002). Likewise, NEP has been implicated in the removal of amyloid β-peptide (Aβ), a 4 kDa peptide considered to be a primary trigger for the development of Alzheimer's disease, whilst NEP loss during normal aging contributes to amyloid accumulation in brain tissue (Turner 2003). NEP has also been shown to degrade peptides involved in learning and memory such as oxytocin, NYP and CCK (Carvajal, et al. 2004, Heinrichs, et al. 2004, Hadjiivanova, Belcheva and Belcheva 2003). Recently, NEP knockout mice, which are characterised by lower blood pressure and an enhanced lethality to endotoxin shock, demonstrated a greater ability to sustain learning and memory in older subjects than wild type control subjects (Walther, et al. 2009).

In addition to its catalytic function, NEP can alter the function of other proteins via direct protein–protein interactions. NEP directly binds to Ezrin/Radixin/Moesin (ERM) proteins resulting in a decreased binding of ERM proteins to actin filaments and, as such, cells expressing NEP demonstrate decreased cell adhesion and cell migration (Iwase, et al. 2004).

Other related proteins to NEP of note include ECE (as discussed below), KELL, PEX and ECEL-1. KELL is a protein which constitutes a major antigen on human erythrocytes. As a result of its location, incompatibility to KELL antigens can cause severe haemolytic reactions to blood transfusions as well as erythroblastosis in newborn children. The human PEX protein was identified from studies of patients with X-linked hypophosphatamemic rickets (Francis, et al. 1995). It was found to encode an NEP-like protein and subsequent cloning of PEX revealed an ability to cleave parathyroid hormone-like peptides. ECEL-1 is devoid of enzymatic activity and has no proteolytic activity to Aβ, but can hydrolyse synthetic NEP substrates, whilst phosphoramidon has been shown to inhibit its activity. ECEL-1, has been shown to be essential to the control of

respiration (Schweizer, et al. 1999). Distinct chromosomal locations have been identified for the genes encoding the human NEP-like enzymes. NEP, KELL, PEX, DINE and ECE-1 are found at chromosomal positions 3q25, 7q33, Xp22, 2q36-q37 and 1p36, respectively, implying that the gene duplications are ancient (Turner, Isaac and Coates 2001).

NEP2, a homologue of NEP with 66% sequence identity, has been shown to be restricted mainly to developing and differentiated fields of the CNS and to the testis, where it has been shown to be involved in sperm function and oocyte fertilisation (Bonvouloir, et al. 2001). NEP2 appears to have a unique feature for a member of the M13 family, in that NEP2 appears to be synthesised as an inactive enzyme, needing post-translational modifications to be transported out of the ER and become active (Rose, et al. 2002). Unlike NEP and ECE, which are broadly expressed in the CNS and periphery, NEP2 is found exclusively in selected populations of neurons and in the spinal cord. The only peripheral areas where expression of NEP2 was detected were the pituitary and choroid plexus. NEP2 was also found capable of degrading Aβ and its distant localisation from NEP suggests that, together with ECE, it may be better poised to catabolise Aβ as it is more abundantly expressed in areas relevant to Alzheimer's disease pathology (Facchinetti, et al. 2003, Thomas, et al. 2005).

1.3.1.2 Angiotensin converting enzyme

Angiotensin converting enzyme (ACE or EC3.4.15.1) is a member of the M2 family of zinc metallopeptidases. ACE is a type I integral membrane zinc-dependent dipeptidase that is expressed on the surface of epithelial and endothelial cells. It is responsible for the conversion of angiotensin I (Ang I) to angiotensin II (Ang II), a potent vasoconstrictor, and for the inactivation of BK, a vasodilator (Yang, Erdos and Levin 1971). As such, ACE plays an important role in the regulation of hypertension and in the development of vascular pathology and endothelium remodelling in certain disease states.

Mammalian ACE exists in two distinct isoforms arising from the use of alternative promoters. The first is testicular ACE (tACE), which is essential for male fertility and which carries a single HE*XX*H zinc-binding active site as well as a catalytic domain. The second isoform is somatic ACE (sACE), which consists of two identical catalytic domains both containing a functional zinc-binding active site (Ehlers and Riordan 1989). Although ACE is primarily a membrane bound protein, a soluble form is found in many body fluids which is formed as a result of a post-translational proteolytic cleavage in the juxtamembrane stalk by a membrane protein secretase (Oppong and Hooper 1993).

ACE 2, a homologue of ACE, is also a type I integral membrane peptidase which is found in the kidneys, heart and lungs (Tipnis, et al. 2000). ACE 2 converts Ang II to angiotensin (1-7) (Ang (1-7)), which opposes the actions of Ang II. Ang II is a vasoconstrictor and also stimulates the secretion of aldosterone from the adrenal cortex. Aldosterone causes the tubules of the kidneys to increase the reabsorption of sodium and water into the blood. This increases the volume of fluid in the body, which also increases blood pressure. Ang (1-7) opposes the actions of Ang II. Therefore it is involved in vasodilation, vascular protection, cell growth inhibition and has anti-fibrinogenic, anti-thrombogenic and anti-arrythmogenic effects. Hence, ACE and ACE 2 act as counterbalances in metabolism in the renin-angiotensin system (RAS) (Crackower, et al. 2002). The RAS is a pivotal physiological regulator of cardiovascular homeostasis, potently impacting hydroelectrolyte balance, arterial tone, and blood pressure as well as modulating the growth and differentiation of vascular SMCs and cardiac myocytes. In contrast, dysregulation of the RAS is intrinsically associated with cardiovascular pathologies such as hypertension, myocardial infarction, and coronary heart disease (Ferrario 1990). The regulatory impact of shear stress on ACE has also been investigated, with ACE mRNA expression levels being suppressed under shear conditions, in a ROS-dependent manner (Rieder, et al. 1997). ACE is also known to contain two SSREs in its promoter region (Miyakawa, de Lourdes Junqueira and Krieger 2004). ACE inhibitors, beyond inhibiting the RAS, diminish the inactivation of bradykinin,

leading to an increase of NO release. Consequently pathological vasoconstriction is prevented and vasodilation occurs (Poredoš 2000).

Since 1981, inhibitors of ACE have been targeted as first-line therapy for a range of cardiovascular and renal diseases, including hypertension, congestive heart failure, myocardial infarction and diabetic nephropathy (Hooper and Turner 2003). Indeed, as recently as 2002, ACE inhibitors were the most commonly prescribed drugs for the treatment of hypertension in the USA (Ibrahim 2006).

1.3.1.3 Endothelin-converting enzyme

Endothelin-converting enzyme (ECE or EC3.4.24.71) is a type II integral membrane protein and a member of the M13 family of zinc metallopeptidases. ECE has two isoforms, ECE-1 and ECE-2, both of which are composed of a short cytoplasmic tail, followed by a membrane-spanning region and a large extracellular domain containing the zinc-binding motif essential for enzymatic activity. ECE is found predominantly in ECs but is also expressed by exocrine cells, smooth muscle cells, neurons and glia. ECE catalyses the final stage in post-translational modification of endothelin (ET), cleaving big ET to form ET (Khimji and Rockey 2010).

Endothelin is considered to be one of the most potent vasoconstrictors present in ECs. Four isoforms of ET have been discovered, ET-1, ET-2, ET-3 and ET-4. All are involved in the regulation of vascular tone and are required during embryonic development (Kurihara, et al. 1994). Each of the three peptides consists of 21 amino acid residues and is expressed, in different patterns, in various tissues and cells. The predominant ET produced in endothelial cells is ET-1. An important discovery during the early stage of ET research was the discovery of ET receptors. These receptors were designated the ET_A receptor and ET_B receptor. The ET_A receptor binds ET-1 and ET-2 with greater affinity than it does ET-3, while the ET_B receptor binds all three isoforms with equal affinity (Masaki 2004).

Analysis of the promoter region of ECE revealed the presence of four SSREs. Masatsugu et al. have also demonstrated that physiological shear stress down-regulates the mRNA expression of ECE-1 as well as ET-1, through an increase in oxidative stress in endothelial cells (Masatsugu, et al. 2003). Elevated levels of ECE and its product ET-1 have been shown to be involved in inflammatory conditions such as asthma (Zhang, Adner and Cardell 2004). Over-expression of ET-1 in the vasculature has also been noted in different models of hypertension (Iglarz and Schiffrin 2003) and atherosclerosis (Ihling, et al. 2001), suggesting a pathophysiological role for ET-1 in CVD. ECE is also involved in the hydrolysis of a number of active peptidases, such as BK, neurotensin, Ang I and amyloid peptide Aβ (Eckman, Reed and Eckman 2001, Johnson, Stevenson and Ahn 1999). As a result of its biological activity, ECE is a major target of therapeutic inhibitors. An excellent review by Cerdeira et al. covers all the major targets of ECE inhibitors and their effectiveness (Cerdeira, Bras-Silva and Leite-Moreira 2008).

1.3.2 M3 family members

1.3.2.1 Thimet oligopeptidase

Thimet oligopeptidase (TOP, EC3.4.24.15) is a member of the M3 family of zinc metallopeptidases. It is a predominantly soluble, 77 kDa, thiol-sensitive enzyme that preferentially cleaves peptide bonds on the carboxyl side of the hydrophobic amino acid residues in substrates of less than 20 aa. It has been implicated in the degradation of a range of bioactive peptides, including gonadotropin-releasing hormone (GnRH), Ang I, neurotensin and BK, both in the central nervous system and in the periphery. High levels of TOP activity have been localised, both catalytically and immunohistochemically, to the brain, pituitary and testis, with lower levels in tissues such as the lung, liver, kidney and spleen. Typically 80% of its activity in a tissue or cell line is cytosolic, with the

remainder being nuclear or membrane-associated (Chu and Orlowski 1985, Shrimpton, Smith and Lew 2002). It has been widely reported that ECs exhibit secreted and membrane-associated forms of TOP, thereby allowing it to putatively degrade peptides intracellularly and extracellularly (Crack, et al. 1999).

The structure of TOP has been resolved at 2.0 Å. The structure reveals TOP's active site to be located at the base of a deep channel that runs the length of the elongated molecule, limiting the size of peptides that can be degraded (Ray, et al. 2004) (Figure. 1.10). Moreover, like all peptidases in this family, TOP exhibits a HE*XX*H motif in its active site. It has also been shown to contain a SSRE (-GAGACC-) within its promoter region and to be regulated by hemodynamic forces such as cyclic strain. This study also concluded that cyclic strain modulates the release of TOP from bovine aortic endothelial cells (BAECs) and thus may have a significant influence on TOP's extracellular functions (Cotter, et al. 2004). Specific, site-directed inhibitors of TOP have been shown to potentiate bradykinin-induced vasodilation in rats (Smith, et al. 2000) and to decrease myocardial ischemia/reperfusion injury following 3 to 7 days reperfusion in rabbits (Schriefer, Broudy and Hassen 2001).

Although TOP was classified originally as a metabolising enzyme involved in the degradation of neuropeptides, a multiplicity of functions have since been ascribed to this enzyme. TOP is a true processing peptidase with the following properties. Firstly, the degrading/metabolising activity of TOP can terminate function by hydrolysing substrate, such that ligand binding to the cognate peptide receptor no longer occurs (Montiel, et al. 1997). Secondly, TOP can biotransform an inert precursor neuropeptide to an active moiety such as neo-endorphin to Leu-enkephalin (Acker, Molineaux and Orlowski 1987). Thirdly, as a convertase, TOP can convert a bioactive peptide agonist into a different bioactive peptide with agonist properties to another receptor. Lastly, TOP manifests a modulating activity, creating a peptide product with the opposite physiological effect as the original substrate. This is exemplified by the action of TOP cleaving Ang I to Ang (1-7), the latter peptide having a vasodilatory action unlike the vasoconstrictive action of the former (Chappell, et al. 1994).

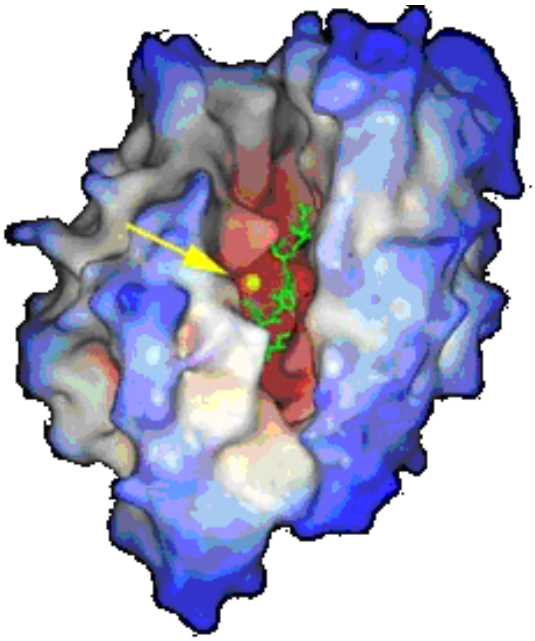

Figure 1.10: The structure of TOP. Its active site is indicated by the arrow (www.rosalindfranklin.edu/DNN/home/CMS/biochem/Faculty/Glucksman/tabid/1147/Default.aspx).

Interestingly, examination of TOP's protein sequence shows neither a readily identifiable secretory signal sequence nor a conventional hydrophobic, membrane-spanning domain, structural elements normally associated with extracellularly-acting peptidases. Its amino acid sequence also lacks the appropriate signals for myristoylation or glycosylphosphatidylinositol (GPI)-anchoring. However, it has been well documented that TOP has extracellular functions such as GnRH degradation and BK signalling (Jeske, et al. 2006, Lew, et al. 1997) and as such needs to be "released" from cells. This secretion is mediated though the so-called 'alternative' or 'non-classical' secretory mechanism (Nickel 2003). The various stages involved in protein secretion by this mechanism remain to be identified, and multiple pathways for unconventional protein secretion may exist (Nickel 2003, Carreno, et al. 2005). Other publications suggest that TOP secretion occurs by an unconventional pathway, but also utilises components of the conventional rough endoplasmic reticulum-Golgi apparatus (ER-Golgi) secretory pathway (Carreno, et al. 2005, Ferro, et al. 2004).

Russo et al. have demonstrated that TOP interacts with calmodulin (CaM) in a calcium-dependent manner to facilitate secretion (Russo, et al. 2009). CaM is a small, ubiquitously expressed acidic protein of approximately 148 aa that exists in at least two different configurations: (i) apo-calmodulin, which lacks calcium, and (ii) calcium-CaM, which can bind up to four calcium ions and undergo post-translational modifications, such as phosphorylation, acetylation, methylation and proteolytic cleavage, that modulate its action (Jurado, Chockalingam and Jarrett 1999). CaM mediates processes such as inflammation, metabolism, apoptosis, muscle contraction, intracellular movement, short-term and long-term memory, nerve growth and immune response (Colomer and Means 2008). Calcium-CaM is a positive regulator of exocytosis in neuroendocrine cells (Chen, et al. 1999), where it activates the opening of fusion pores at the plasma membrane (Bayer, et al. 2003) and the fusion of secretory granules (Cooperstein and Watkins 1995). Jeske et al. observed that TOP localises to lipid rafts (Jeske, Glucksman and Roberts 2004). Lipid rafts are stable yet dynamic structures that exist within the plasma membrane and can serve to centralise signal transduction across the membrane. Additionally, lipid rafts serve to anchor signalling molecules to the intra- and extracellular face of the plasma membrane (Galbiati, Razani and Lisanti 2001).

As evidenced above, the majority of work published on TOP has been on the functions of TOP as a neuropeptide-processing enzyme in the neural, endocrine and vascular systems. As neuropeptide substrates are found in the extracellular space, the activity of TOP has traditionally also been correspondingly localised to the extracellular milieu. Despite the focus on TOP activity in the extracellular space, subcellular fractionation experiments indicate that the majority (generally >80% (Crack, et al. 1999) of TOP is localised to the cytosol, where several recent studies have identified an important role for TOP in the immune system.

TOP is predominantly found in the brain, pituitary and testes, which are classically immune-privileged sites. Such immunoprivileged locations maintain low levels of major histocompatibility complex (MHC) class I expression relative to levels of MHC class I expression in lymphoid tissues, such as the spleen, lymph nodes or liver (Lampson 1995, Lidman, Olsson and Piehl 1999).

This implies that cytosolic TOP may have an important role in endogenous MHC class I regulation in tissues of elevated TOP expression and activity. As such TOP may have the potential to serve as a therapeutically significant protein, whose expression could be modulated to manipulate surface MHC class I expression to clinical advantage. Kim et al. demonstrated that cells over-expressing TOP are capable of inducing long-term repression of surface MHC class I. Conversely, they showed that the use of a TOP siRNA increased long-term surface expression of MHC class I. Another interesting result from the same study showed that the cells can overcome a small increase in TOP expression before MHC class I presentation is affected. After this threshold is crossed however, any compensatory cellular mechanisms were not able to overcome the quantitative decrease in the available pool of cytosolic peptides, and MHC class I surface expression falters (Kim, et al. 2003).

Recognition of antigens in the peptide-binding groove of surface-expressed MHC class I and class II molecules by specific T-cell receptors is central to T-cell activation. To fulfil their physiological function, MHC proteins must first acquire peptide antigens. The role of MHC class I molecules is to report on intracellular events (such as viral infection, the presence of intracellular bacteria or cellular transformation) to $CD8^+$ T cells (Jensen 2007). MHC class I molecules are composed of heavy chains and an invariant light chain, known as β_2-microglobulin. The temporal events in the biosynthesis of MHC class I molecules can be summarised in six steps: (i) acquisition of antigens from proteins with errors (for example, due to premature termination or mis-incorporation); (ii) misfolded proteins are tagged with ubiquitin for degradation; (iii) the proteasome degrades these ubiquitinated proteins into peptides; (iv) the peptides are delivered to the ER by the TAP complex; (v) the peptide is loaded onto nascent MHC class I molecules- this process is facilitated by members of the peptide-loading complex such as tapasin and two housekeeping ER proteins known as calreticulin and ERp57 and; (vi) the peptide-loaded MHC class I molecules are transported via the Golgi complex to the cell surface (Figure. 1.11).

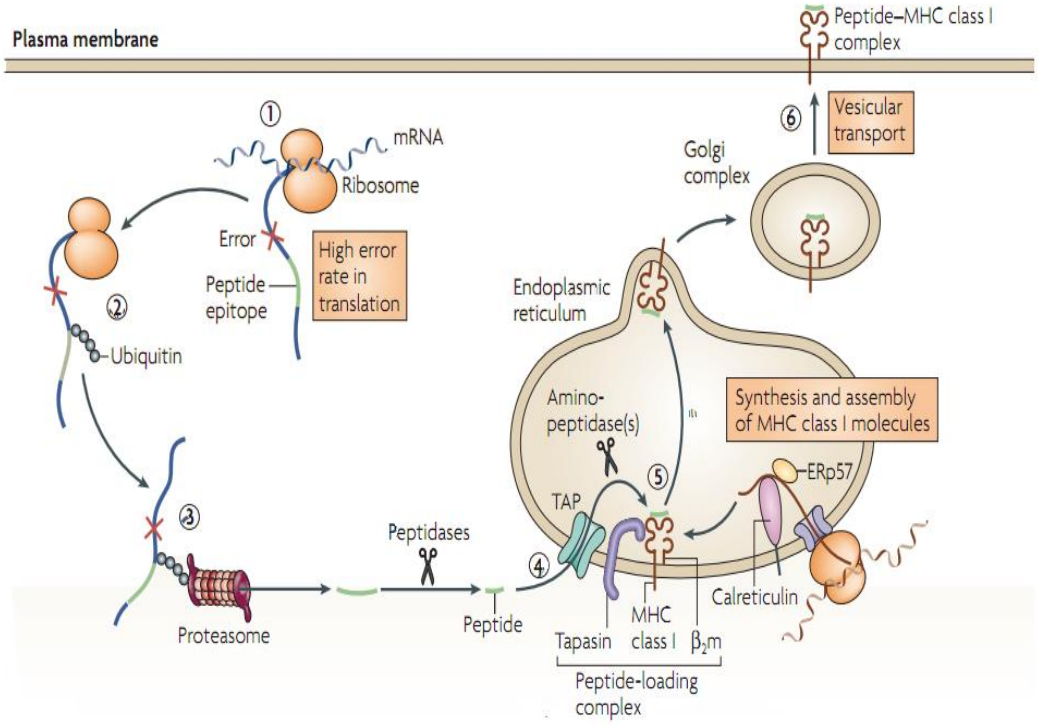

Figure 1.11: Six steps for loading and trafficking of MHC class I molecules to the cell surface. (1), Acquisition of antigenic peptides; (2) tagging of the antigenic peptide for destruction by ubiquitinylation; (3) proteolysis; (4) delivery of peptides to the ER; (5) binding of peptides to MHC class I molecules; and (6) display of peptide–MHC class I complexes on the cell surface. (Vyas et al., 2008).

Some publications have proposed that TOP may act as a chaperone-like molecule, binding to specific MHC class I peptides in the cytosol, thereby protecting them from degradation by other cytosolic peptidases (Portaro, et al. 1999). In a contrasting report, TOP was shown to efficiently degrade MHC class I peptides in cell extracts (Saric, et al. 2001). Recently Kessler et al. have shown that TOP-mediated processing both reduces the presentation of proteasomal products by MHC class I and also enlarges the MHC class I peptide repertoire by processing protein-degradation fragments that are not yet fit for antigenic presentation (Kessler, et al. 2011).

1.3.2.2 Neurolysin

Neurolysin (EC3.4.24.16) is a member of the M3 family of zinc metallopeptidases, which has 70% sequence homology with TOP (Kato, et al. 1997). It is found in the central nervous system and the gastrointestinal tract as well as the endothelium. Structurally, neurolysin is composed of two domains, with its HE*XX*H-containing active site located on domain 2, at the bottom of restricted cleft formed between domain 1 and 2 (Brown, et al. 2001). Neurolysin cleaves a number of peptides including BK and neurotensin. Both NEP and TOP also inactivate neurotensin, but at different sites to neurolysin (Kitabgi 2006).

Neurotensin is a 13 aa neuropeptide which is involved in modulation of dopaminergic and cholinergic circuits, thermoregulation, intestinal motility and blood pressure regulation (Goedert 1984). Dopamine receptors are divided into D1 and D2 sub-families, neurotensin causes antagonising dopamine effects at the D2 receptor. As such neurotensin may be involved in dopamine-related disorders such as Hungtinton's and Parkinson's disease. For this reason, modulating the concentration of neurotensin in the brain is of therapeutic interest and several neurotensin analogues have been developed (Boules, Fredrickson and Richelson 2006).

Much of neurolysin's activity is cytosolic, but it can be secreted or associated with the plasma membrane (Vincent, et al. 1996), or mitochondria (Kato, et al. 1997). Six splice variants of neurolysin were discovered by Kato et al., which are generated from a single gene as a result of alternative sites for the initiation of transcription. These six variants of mRNA are divided into two categories: (i) those containing an additional sequence that encodes a mitochondrial-targeting sequence and; (ii) those that lack the sequence (Kato, et al. 1997).

1.4 Vascular signalling

1.4.1 Reactive oxygen species

ROS are classically described as harmful by-products in aerobic metabolism (and indeed this is the case at pathologically high levels). ROS increase leukocyte adhesion molecule expression, stimulate SMC proliferation and migration, promote lipid oxidation, up-regulate matrix metalloproteinase activity and alter vasomotor activity. Endothelial ROS may also promote apoptosis and cellular injury e.g. during ischemia/reperfusion. Oxidative stress is also proposed to be involved in the aging process by inducing damage to mitochondrial DNA and by other mechanisms (Taniyama and Griendling 2003, Finkel and Holbrook 2000).

However, at physiologically minute levels, ROS serve as second messengers to activate multiple signalling pathways in vascular cells. Low-level ROS production can effectively and rapidly modulate the activity of several intracellular signalling pathways, affect the release/activity of paracrine factors and alter gene expression. Intracellular sources of ROS in endothelial cells include xanthine oxidase (XO), nitric oxide synthase (NOS), NADPH-dependent oxidase, cyclooxygenase, lipoxygenase and auto-oxidation of tissue metabolites (Bayraktutan, Blayney and Shah 2000). ROS produced by endothelial cells include superoxide (O_2^-), hydrogen peroxide (H_2O_2), hydroxyl radical ($^{\bullet}OH$) and other radicals (Dröge 2002).

ROS include a number of chemically reactive molecules derived from oxygen (Fridovich 1999) (Figure 1.12). One of the most important reactive oxygen species in the vasculature is O_2^-, which is formed by the univalent reduction of oxygen. Due to the fact O_2^- lacks the ability to penetrate lipid membranes, it is confined within the compartment in which it is produced (Nordberg and Arnér 2001). Accelerated degradation of NO by ROS accounts for a large portion of reduced NO bioavailability and endothelial dysfunction. The

major ROS responsible for this is O_2^-. NO is degraded very rapidly by O_2^- to form the vasoinactive peroxynitrite, a powerful and damaging oxidant more stable than either O_2^- or NO. In experimental models of vascular disease, increased O_2^- production participates critically in reduced NO bioavailability and endothelial dysfunction (Vanhoutte, Perrault and Vilaine 2007).

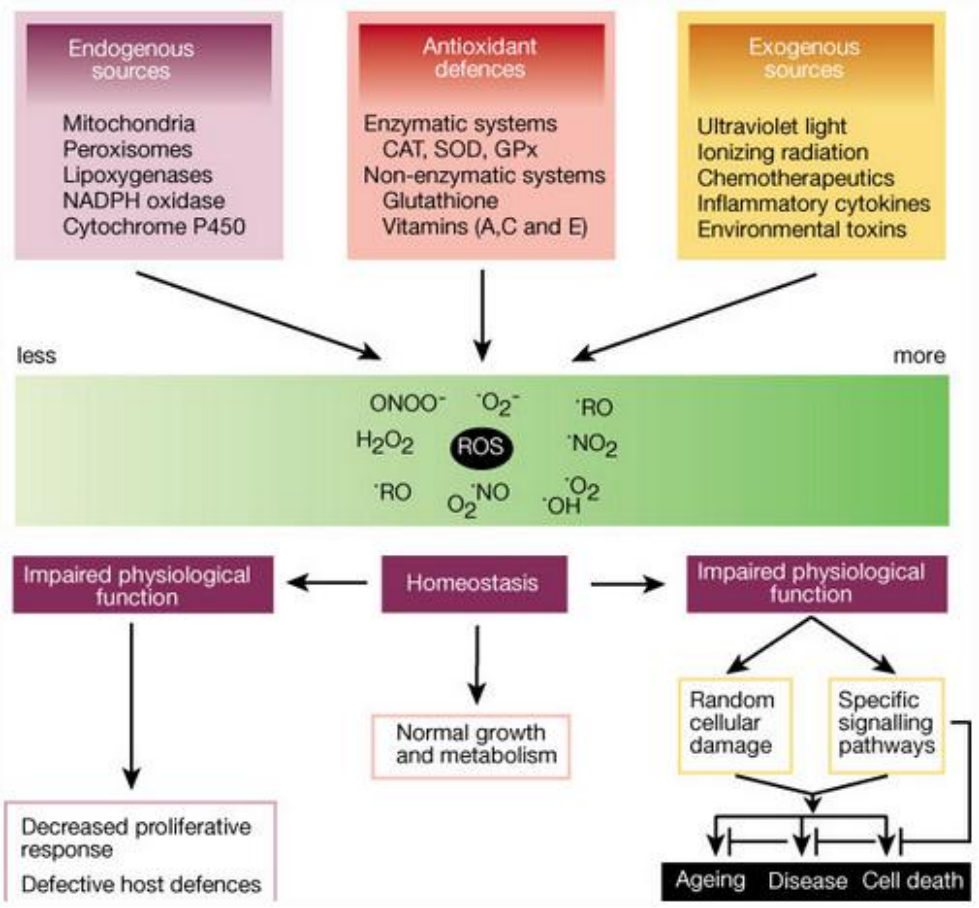

Figure 1.12: Sources of ROS and their effect on endothelial function (Finkel et al., 2000).

Under physiological conditions, super oxide dismutase (SOD), a major antioxidant, accelerates the removal of O_2^-. SOD produces the more stable ROS, H_2O_2, which is then converted enzymatically into H_2O by catalase and glutathione peroxidase (Taniyama and Griendling 2003). The cytosolic form of SOD permits the release of NO from the endothelium and NO-mediated vascular SMC relaxation. Extracellular SOD likely protects NO during its diffusion from

the endothelium to vascular SMCs. In patients with coronary artery disease, the activity of endothelial SOD diminishes substantially, contributing to coronary endothelial dysfunction (Landmesser, et al. 2000). Mitochondrial SOD (Mn-SOD) has been shown to be essential, as Mn-SOD$^{-/-}$ mice die soon after birth or suffer severe neurodegeneration (Melov, et al. 1998).

Hydroxyl radical ($^{\bullet}OH$), a short-lived ROS, is produced from H_2O_2 in a metal ion catalysed reaction. Due to its strong reactivity with biomolecules, $^{\bullet}OH$ is one of the most reactive ROS and has the potential to cause more damage to biological systems than any other ROS (Betteridge 2000). $^{\bullet}OH$ cannot be eliminated by enzymatic action; however, the antioxidant vitamin E can successfully scavenge $^{\bullet}OH$.

1.4.2 NADPH oxidase

There are at least five different enzyme systems known to contribute to the oxidation state of the vascular wall. These include: (i) lysyl oxidase (LOX), responsible for the covalent cross linking of collagen and elastin; (ii) xanthine oxidase (XO); (iii) monocyte-derived ROS; (iv) uncoupled eNOS and; (v) the NADPH family of oxidases, which are the primary contributors of ROS species in the vasculature (Cunningham and Gotlieb 2004).

NADPH oxidases are a major source of O_2^- in vascular cells (Robin and Ajay 2005). Vascular NADPH oxidase has been found to be essential in the physiological response of vascular cells, including growth, migration, and modification of the extracellular matrix. They have also been linked to hypertension and to pathological states associated with uncontrolled growth and inflammation, such as atherosclerosis (Griendling, Sorescu and Ushio-Fukai 2000). Results from this laboratory also indicate a role for NADPH oxidase in the regulation of the zinc metallopeptidase, NEP (Fitzpatrick, et al. 2009).

The NADPH oxidases of the cardiovascular system are membrane-associated enzymes that catalyse the one electron reduction of oxygen, using NADH or NADPH as the electron donor.

$$2O_2 + NADPH \rightarrow 2O_2^- + NADP^+ + H^+$$

Upon stimulation by various agents, O_2^- is produced within minutes to hours by both endothelial and smooth muscle cells. This contrasts with the release of O_2^- within seconds after stimulation by NADPH oxidase in neutrophils. One of the most important characteristics of the cardiovascular form of the oxidase is its response to vasoactive substances (e.g. Ang II, thrombin, platelet-derived growth factor etc.), flow-derived hemodynamic forces and local metabolic changes. NADPH oxidase activation can be mediated by a variety of intracellular second messengers (e.g. Ca^{2+}, PKC and lipoxygenase metabolites of arachidonic acid) (Meier 1996).

The core of the NADPH oxidase enzyme comprises five components: $p40^{PHOX}$,$p47^{PHOX}$, $p67^{PHOX}$, $p22^{PHOX}$ and $gp91^{PHOX}$ (Figure. 1.13). In the resting cell, $p40^{PHOX}$, $p47^{PHOX}$ and $p67^{PHOX}$ exist in the cytosol as a complex. $p22^{PHOX}$ and $gp91^{PHOX}$ are located in the membranes of secretory vesicles and specific granules, where they occur as a heterodimeric flavohemoprotein known as cytochrome $b_{558,}$ in a molar ratio of 1:1. Separating these two groups of components by distributing them between distinct subcellular compartments guarantees that the oxidase is inactive in the resting cell (Babior 1999).

When the resting cell is exposed to any of a wide variety of stimuli, the cytosolic component $p47^{PHOX}$ becomes heavily phosphorylated and the entire cytosolic complex migrates to the membrane, where it associates with cytochrome b_{558} to assemble the active oxidase. The assembled oxidase is now able to transfer electrons from the substrate to oxygen by means of its electron-carrying prosthetic groups, its flavin and then its heme group(s). Activation requires the participation, not only of the core subunits, but of two low-molecular-weight guanine nucleotide-binding proteins: Rac1 and Rap1A. During activation, Rac1 binds GTP and migrates to the membrane along with the core cytosolic complex. At the same time, cytochrome b_{558} and Rap1A are delivered to the cell surface by fusion of the secretory vesicle membranes and later the

specific granule membranes with the plasma membrane of the cell. This fusion event also releases the contents of the organelles to the exterior (Babior 1999).

The specific roles for the membrane subunits have been established. $gp91^{PHOX}$ is a highly glycosylated membrane-spanning protein. Its N-terminal contains six transmembrane α-helixes: the third and fifth each contain two invariant histidine residues that are positioned to coordinate two hemes, thereby placing one heme towards the inner face and one towards the outer face. The C-terminal half folds into a cytoplasmic domain containing the FAD- and NADPH-binding sites. Hence $gp91^{PHOX}$ contains the entire transmembrane redox machinery, in which electrons are transferred from NADPH on the cytoplasmic side via FAD and two non-equivalent hemes to molecular oxygen, the electron acceptor, thereby generating superoxide anion (Groemping and Rittinger 2005).

Although $gp91^{PHOX}$ is the catalytic component of flavocytochrome b_{558}, its partner, $p22^{PHOX}$, is essential for optimal activity. $p22^{PHOX}$ is a non-glycosylated integral membrane protein containing two transmembrane segments. Its C-terminal cytoplasmic tail contains a proline-rich region, which serves as an anchoring site for $p47^{PHOX}$ (Sumimoto, Miyano and Takeya 2005).

The specific roles for each of the cytosolic subunits have also been established. After extensive phosphorylation, $p47^{PHOX}$ is responsible for transporting the cytosolic complex from the cytosol to the membrane during oxidase activation. The effect of $p47^{PHOX}$ is to tighten, by nearly 100-fold, the binding between each of the other cytosolic proteins to the assembled oxidase. $p67^{PHOX}$ is an essential subunit; inactivation of this subunit will cause inhibition of the oxidase. Its activation domain stimulates electron transfer to the flavin of cytochrome b_{588}, which is the rate-determining step in superoxide generation. Less is known about $p40^{PHOX}$ than the other subunits. However, it is believed that during cell activation, $p40^{PHOX}$ facilitates membrane translocation of $p67^{PHOX}$ and $p47^{PHOX}$, leading to enhanced superoxide production by the NADPH oxidase. The N-terminal of $p40^{PHOX}$ is capable of specifically and strongly binding to phosphatidylinositol 3-phosphate, a lipid enriched in the phagosomal membrane, and thus considered to play a role in recruiting the protein complex correctly to the phagosome (Sumimoto, Miyano and Takeya 2005). It has also been shown

that interfering with $p40^{PHOX}$ binding to $p67^{PHOX}$ reduces O_2^- production by 50%, implying $p47^{PHOX}$ is a stimulatory subunit (Tsunawaki, et al. 1996).

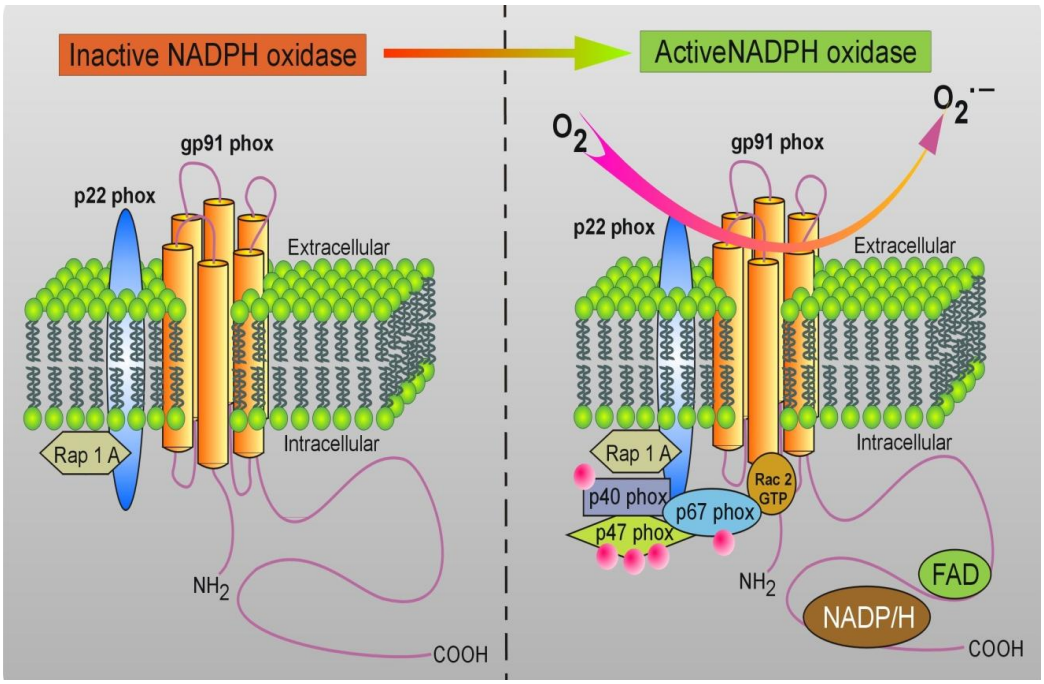

Figure 1.13: Activation of NADPH oxidase. In the resting cell, the subunits of the oxidase are distributed between the cytosol ($p40^{PHOX}$, $p47^{PHOX}$, $p67^{PHOX}$ and Rac1) and the membranes (Rap1A and cytochrome b_{558}, a $p22^{PHOX}$, $gp91^{PHOX}$ complex). When the cell is activated, $p47^{PHOX}$ becomes heavily phosphorylated and the cytosolic subunits migrate to the membrane, where they bind to cytochrome b_{558} to assemble the active oxidase (www.genkyotex.com).

1.4.3 Bradykinin

Bradykinin (BK) is a short (9 aa) vasoactive peptide that induces vasodilation. BK is produced mainly in plasma through the kinin-kallikrein system by the proteolytic cleavage of the plasma precursor kininogen (H-kininogen). BKs larger homologue, kallidin (KD), is produced predominantly in tissues from a low molecular mass variant of kininogen (L-kiningoen). In addition, KD can be converted to BK by the enzyme aminopeptidase-N (Sharma and Al-Sherif 2011).

The principle pharmacological action of BK in the regulation of blood pressure is through vasodilation in most areas of the circulation, a reduction of total peripheral vascular resistance and a regulation of sodium excretion from the kidney (Adetuyibi and Mills 1972). BK contributes to the maintenance of cardiovascular homeostasis by opposing the vasoconstrictor activity of Ang II (Madeddu, et al. 1998). Reduced local BK generation and blunted NO formation have been reported in microvessels of failing human hearts (Kichuk, et al. 1996).

BK exerts its action through the activation of two GPCR sub-types, B_1 and B_2. The B_1 receptor is poorly expressed in normal tissue and is activated by metabolic products of BK. B_1 expression is up-regulated in pathological states associated with inflammation and tissue injury (Marceau, Hess and Bachvarov 1998). B_1 receptors have been observed in sympathetic neurons, macrophages, fibroblasts, vascular SMCs and ECs. After stimulation B_1 receptors are not internalised, and after the up-regulation, receptor activity persists in damaged or inflamed tissues. The B_1 receptor is linked to chronic pain, vasodilation, plasma extravasation, neutrophil accumulation and further release of mediators such as IL-6, IL-1β and TNF-α, which sustain a positive feedback loop between B_1 receptor expression and inflammation (Abraham, Scuri and Farmer 2006, Mombouli and Vanhoutte 1999).

The B_2 receptor is constitutively expressed in many cell types and tissues of the central and peripheral nervous system, the vascular endothelium and inflammatory cells. The binding of BK activates the B_2 receptor, which is then rapidly desensitised and internalised. B_2 receptors mediate important physiological functions including blood pressure regulation, smooth muscle contraction and pain (Leeb-Lundberg, et al. 2005). Bartus et al. have previously demonstrated that BK permeabilises the blood brain barrier (BBB) in a dose-related fashion and that tachyphylaxis occurs with continuous administration of BK (Bartus, et al. 1996). Tachyphylaxis describes a decrease in the response to a drug due to previous exposure to that drug, and is related to depletion of receptors available for ligand binding.

Termination of BK signalling is controlled by zinc metallopeptidases (Rawlings and Barrett 1993, Turner 2003). It has been previously demonstrated

that degradation of BK in human plasma is dependent upon its concentration. At physiologically relevant levels of BK, ACE is the major source of BK hydrolysis. However, at higher concentrations, the major degrading enzyme is carboxypeptidase N (CPN), with ACE playing a minor role (Kuoppala, et al. 2000). CPN cleaves BK at the Phe^{8}-Arg^{9} bond, yielding a ligand for B_1 receptors and as such can be implicated in pathological states associated with inflammation and tissue injury. However, ACE can again cleave this ligand at the Phe^{5}-Ser^{6} bond to produce an active metabolite (BK 1-5) that has been implicated as a selective inhibitor of thrombin-induced platelet activation (Hasan, Amenta and Schmaier 1996). TOP and neurolysin cleave full-length BK at the Phe^{5}-Ser^{6} bond to produce the same metabolite. Jeske et al. have shown that TOP and neurolysin are co-localised with the B2 receptor on the exofacial leaflet of plasma membranes and in lipid rafts, indicating a potential physiologic role for TOP in modulating BK activation and sensitisation of nociceptors (Jeske, Glucksman and Roberts 2004).

The hydrolysis of BK by ECE is exclusively at the Pro^{7}-Phe^{8} bond (ACE and NEP also cleave BK at this site) whilst NEP can also hydrolyse BK at the Gly^{4}-Phe^{5} bond (Figure 1.14). NEP has also been shown to degrade KD, at the same bond sites as in BK. Hence NEP not only inactivates BK but can also inhibit BK production, again highlighting NEP as an important therapeutic target in cardiovascular research.

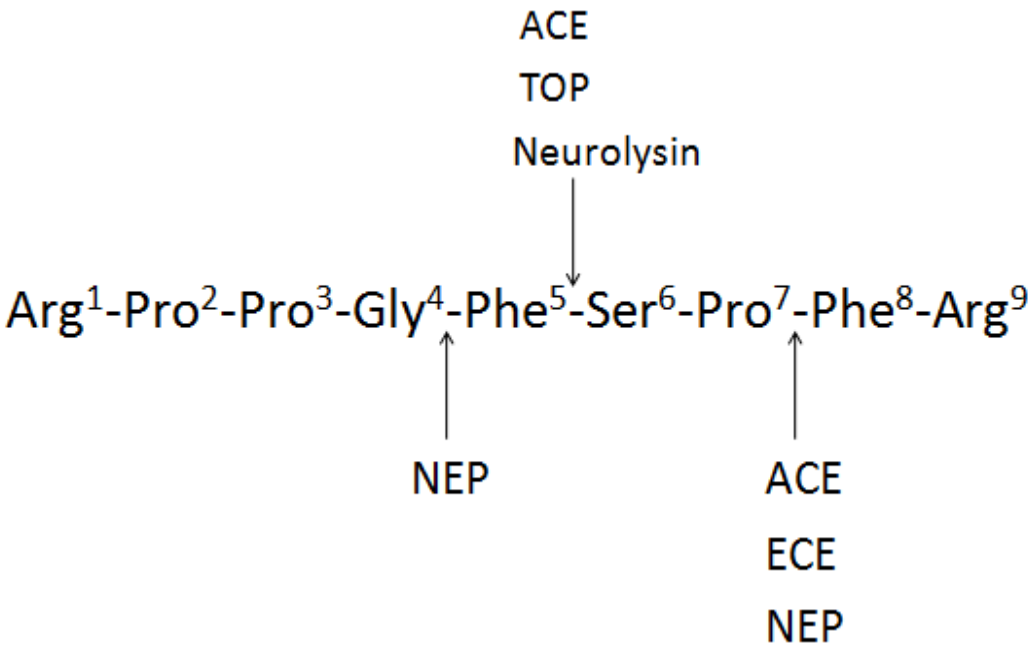

Figure 1.14: The amino acid structure of BK. The hydrolysis sites of zinc metallopeptidases within BK.

1.4.4 Nitric oxide

In the early 1980s Furchgott and Zawadzhi reported the production of an endothelium-derived relaxing factor (EDRF) (Furchgott and Zawadzki 1980), which was later identified as the gas NO. NO has since emerged as a ubiquitous signalling messenger molecule involved in diverse pathophysiologic processes such as neurotransmission, inflammatory and immune responses, and vascular homeostasis (Gong, et al. 2004). NO is a biatomic free radical gas that contains an unpaired electron and has a half-life of approximately 5-10 seconds. The best known stimulants of NO production include shear stress and cyclic circumferential strain. NO levels are also attenuated in response to hormones such as estrogens, autacoids such as bradykinin and histamine, and platelet-derived factors such as serotonin and adenosine diphosphate (ADP), as well as products of blood coagulation such as thrombin (Vanhoutte, Perrault and Vilaine 2007).

NO produced in endothelial cells permeates into the underlying SMCs and, by preventing calcium entering the SMCs, causes vascular relaxation. NO is also released into the bloodstream where, before inactivation by oxyhemoglobin, it can remain biologically active in close proximity to the endothelial surface and inhibit leukocyte adhesion, augment fibrinolysis and inhibit platelet adhesion and activation synergistically with prostaglandin I_2 (PGI_2) (Gryglewski 1995).

NO also undergoes a number of reactions, acting either as a weak oxidant or as a reducing compound. It is synthesised from the terminal guanidine nitrogen atom of the amino acid L-arginine and molecular oxygen, in an enzyme-catalysed reaction producing NO and the amino acid L-citrulline. The enzyme involved in the reaction is nitric oxide synthase (NOS) (Figure 1.15).

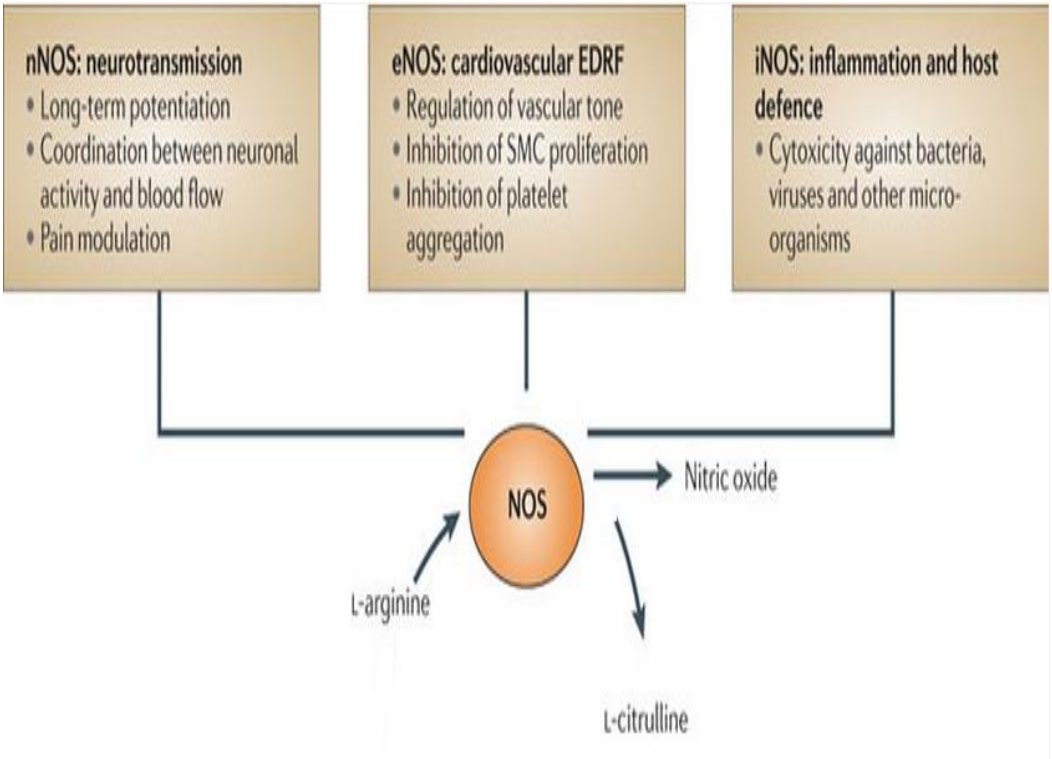

Figure 1.15: NO synthesis. Mammalian NO synthesis is catalysed by three isoforms of NOS that have different tissue distributions: neuronal NOS (nNOS), endothelial NOS (eNOS) and inducible NOS (iNOS). L-arginine is the substrate for all three isoforms of NOS in the production of NO (Leiper & Nandi, 2011).

Three major isoforms of NOS have been identified: NOS 1, NOS 2 and NOS 3, each being the product of a distinct gene. NOS 1 or neuronal-type NOS (nNOS) is found predominantly in central and peripheral nerves, platelets and in pancreatic islet cells. nNOS assists in vasoneuronal coupling and the regulation of cerebral blood flow, as well as in modulating the tone of peripheral vessels by nitrergic neurons. NOS 2 or inducible NOS (iNOS), is an inducible form of nitric oxide synthase, found in macrophages, neutrophils, and to a lesser degree in hepatocytes and SMCs. It is induced by bacterial lipopolysaccharides and cytokines, so that its levels are high during inflammatory states. iNOS-derived NO has been associated with several vascular disease states. iNOS-deficient mice have elevated cholesterol levels and an increased incidence of atherosclerotic plaques (Ihrig, Dangler and Fox 2001). Also, inhibition of iNOS in atherosclerotic plaques is associated with increased expression of matrix metalloproteinase-9 that may destabilise the lesion (Knipp, et al. 2004). NOS 3 or endothelium-type NOS (eNOS) is found predominantly in ECs and is also expressed to a lower extent in cardiac myocytes, renal mesangial cells, osteoblasts and osteoclasts. Through NO production, eNOS sustains the anti-coagulant, anti-adhesive, and anti-proliferative properties of vascular endothelium. A mitochondrial NOS has also been discovered (mtNOS), a calcium-dependent enzyme that appears to play a regulatory role in respiration, matrix pH and transmembrane potential in mitochondria (Napoli, et al. 2006).

In endothelial cells, eNOS is located close to the inner surface of the apical cell membrane and localises mainly in caveolae, small cholesterol-rich invaginations of the plasma membrane that contain the transmembrane protein caveolin and a number of signalling molecules such as GPCRs and protein kinases. The targeting of eNOS to caveolae depends on dual acylations of the protein by myristoylation and palmitoylation. Myristoylation of eNOS occurs at its N-terminus and is essential in transporting the protein to the caveolae, and its subsequent anchorage. Palmitoylation of eNOS is a reversible post-translational event that occurs at two cysteine residues near the N-terminus (Yeh, et al. 1999). eNOS binds caveolin or CaM in a mutually exclusive manner. In the resting condition, the caveolin binding suppresses eNOS activity. During activation, increased cytosolic calcium promotes a reversible dissociation of eNOS from

caveolin and induces CaM binding, which augments eNOS activity. Although eNOS depends primarily on calcium and CaM, evidence has shown a shear stress-dependent activation of eNOS (Vanhoutte, Perrault and Vilaine 2007).

The principal biological effect of NO within the endothelium is as a vasodilator, and as a result, NO is generally viewed as *atheroprotective* as it regulates the flow of blood to tissues. The effect of NO in the control of vascular tone is attenuated by the presence of ROS, in particular O_2^-, H_2O_2 and $^{\bullet}OH$. O_2^- is produced by phagocytes and other inflammatory cells in large quantities. It has also been shown that endothelial cells release O_2^- generated by enzymes including NADPH oxidase, xanthine oxidase and also NOS itself (NOS generates O_2^- in preference to NO in situations where either L-arginine or tetrahydrobiopterin (BH_4) are deficient or if low-density lipoprotein is present). O_2^- is converted to H_2O_2 in a reaction catalysed by the enzyme SOD. Moreover O_2^- reacts spontaneously and rapidly with NO, leading to the production of peroxynitrite ($ONOO^-$), a particularly powerful oxidant and cytotoxic agent (Jourd'heuil, et al. 2001).

The ability of laminar flow to up-regulate NOS expression has been widely studied. Indeed, NOS is so positively up-regulated by flow that nine repeats of the –GAGACC- SSRE have been identified in the 5' promoter region of the gene encoding eNOS (Loscalzo and Welch 1995). Production of eNOS as a result of shear is biphasic. Initially, there is a Ca^{2+}/CaM dependent disruption of eNOS interaction with caveolin-1, resulting in the production of NO. Then there is a more Ca^{2+}-independent, slow production of NO in response to sustained steady laminar flow (Cunningham and Gotlieb 2004).

Microparticles, membranous vesicles released from activated T lymphocytes with pro-coagulant and pro-inflammatory properties, induce endothelial dysfunction by decreasing eNOS expression and over-expressing cavelolin-1 in ECs activated during artherogenesis (Martin, et al. 2004). This observation shows that once the atheroprotective role of the endothelium, in part through its eNOS activity, has been compromised, a vicious cycle of vascular wall injury and remodelling, inducing plaque formation and subsequent disruption in blood flow, can facilitate atheroma progression and potentially

impart vulnerability onto atherosclerotic lesions. However, studies have shown that antioxidants may re-establish NO-dependent endothelial function (Keaney, et al. 1993, Keaney Jr, et al. 1995).

1.5 Study hypothesis

Blood flow-associated laminar shear stress (LSS) generally imparts an atheroprotective stimulus on vascular endothelial cells, which is essential to vessel wall health and remodelling. As such, flow dysregulation can lead to endothelial dysfunction and vascular diseases such as atherosclerosis, coronary artery disease, stroke, heart failure, and hypertension. The starting points for many of these diseases usually arise at sites of disturbed shear, such as at bifurcations and curvatures in large vessels.

TOP and NEP are essential to endothelial function and remodelling events and frequently manifest opposing effects in the vascular wall. Using vascular EC models, it has previously been shown in our laboratory that NEP expression is attenuated by laminar shear stress in a ROS-dependent manner (Fitzpatrick, et al. 2009) whilst TOP is up-regulated by physiologically relevant levels of cyclic strain (Cotter, et al. 2004). cDNA analysis has revealed the presence of a single copy SSRE in the promoter region of both enzymes, suggesting regulation by hemodynamic forces. It is therefore hypothesized that:

(i) Both NEP and TOP expression in vascular ECs are regulated by shear stress in a *divergent* manner.

(ii) Shear-dependent regulation of NEP and TOP expression is ROS-dependent (and specifically, on NADPH oxidase-generated superoxide).

(iii) The shear-induced changes in NEP/TOP expression have functional consequences on the endothelium.

1.6 Thesis Overview

The data presented in the following chapters examines the regulatory effect of laminar shear stress on zinc metallopeptidases, specifically TOP and NEP in cultured BAECs and HAECs. It also examines the role played by ROS produced by NADPH oxidase, with special emphasis on O_2^-, in the differential regulation of these peptides. Over-expression plasmids and siRNAs were used also to examine the functional consequences of the dysregulation of NEP and TOP. The research findings of this thesis are presented in the following chapters.

Chapter 3: Preliminary characterisation studies and investigation of shear-mediated regulation of neprilysin (NEP) expression.

Chapter 4: Investigation of the effects of shear stress on thimet oligopeptidase (TOP) expression.

Chapter 5: Functional consequence(s) of the shear-mediated regulation of NEP and TOP in vascular endothelial cells.

Chapter 2:

Materials and Methods

2.1 Materials

Abcam (MA, USA)

Mouse anti-TOP monoclonal IgG antibody, rabbit anti-vWF polyclonal IgG antibody.

Aktiengeselischaft and Company (Numbrecht, Germany)

T25 tissue culture flasks, T75 tissue culture flasks, T175 tissue culture flasks, 6-well tissue culture plates, 2 ml, 5 ml, 10 ml and 25 ml serological pipettes, 15 ml falcons, 50 ml flat-bottom falcons, cryovials, cell scrapers.

Amaxa Biosystems (Köln, Germany)

Basic nucleofector kit for primary mammalian endothelial cells, Primocin.

Applied Biosystems (CA, USA)

Fast optical 96-well reaction plates (with adhesive covers), high capacity cDNA reverse transcription kit, TOP siRNA (s14110), p47 siRNA (8087).

Barloworld-Scientific (London, UK)

White flat-bottomed 96-well plates.

BioLegend (CA, USA)

Mouse anti-MHC class I IgG antibody.

BioRad (CA, USA)

Coomassie stain, Precision Plus protein marker, thick mini trans-blot filter paper.

Calbiochem (San Diego, CA)

Apocynin, NSC23766 (Rac1 Inhibitor).

Carl Stuart Ltd. (Dublin, Ireland)

Agilent RNA 6000 NANO kit.

Cayman Chemical Company (MI ,USA)

Mouse anti-eNOS polyclonal IgG antibody.

Corriell Cell Repository (NJ, USA)

Bovine Aortic Endothelial Cells (BAECs).

Enzo Life Sciences (NY, USA)

Bradykinin ELISA kit.

Eurofins MWG Operon (Ebersberg, Germany)

Primer sets: NEP, GAPDH (human and bovine), TOP, p47, eNOS.

Fermentas (York, UK)

Green Taq, DNA ladder 100 bp and 1 Kb, dNTPs, 10X Buffer, $MgCl_2$.

GE-Healthcare (Bucks, UK)

Hyperfilm, ECL Secondary Ab (donkey anti-rabbit).

ibidi (Martinsried, Germany)

Mounting medium, µ-slide I, µ-slide y-shaped.

Invitrogen (Groningen, The Netherlands)

Alexa Fluor® 488 $F(ab')_2$ fragment of rabbit anti-goat IgG (H+L), CFSE kit, DH5α *E-coli* competent cells, Ultra Pure water, SyberSafe®, Trizol.

Labtech (East Sussex, UK)

ADAM™ Counter kit, Microporation kit, Microporator tubes, solution E buffer, solution R buffer, 10 and 100 µl gold tips.

Medical Supply Company (Dublin, Ireland)

0.2 and 0.5 ml PCR tubes.

Millipore (MA, USA)

Millicell hanging cell culture transwell inserts (6-well format, 0.4 µm pore size, 24 mm filter diameter).

Mirus (WI, USA)

Trans*IT*®*-2020* Reagent, Trans*IT-siQUEST*® Reagent.

PALL Corporation (Dun Laoghaire, Ireland)

Acrodisc 32 mm syringe filter with 0.2 µm super membrane, nitrocellulose membrane.

Pierce Chemicals (Cheshire, UK)

BCA protein assay kit, Supersignal West Pico chemilumescent substrate.

Promega (WI, USA)

Dual-Glo Luciferase assay.

PromoCell (Heidelberg, Germany)

Endothelial cell growth medium MV, Human Aortic Endothelial Cells (HAECs).

Qiagen (West Sussex, UK)

HiSpeed Midi-prep kit.

R&D Systems (MN, USA)

Goat anti-neprilysin polyclonal IgG antibody.

Roche Diagnostics (Basal, Switzerland)

E plate, FastStart universal SYBR green (ROX), protease and phosphatase inhibitor cocktail.

Sigma-Aldrich (Dorset, UK)

2,3-diaminonaphthalene, autoradiography developing and fixer solutions, acetone, agarose, ammonium persulfate, ampicillin sodium salt, bradykinin, bromophenol blue, DAPI, DMSO, DNAse kit, EDTA, fetal bovine serum, FITC-dextran (40 kDa), glucose, glycerol, HEPES, LB agar, LB broth, magnesium sulphate, monopotassium phosphate, PBS tablets, penicillin-streptomycin (100X), Ponceau S solution, phosphoramidon, RPMI-1640 medium, sodium bicarbonate, sodium chloride, sodium deoxicholate, sodium dodecyl sulphate, sodium fluoride, sodium phosphate, sucrose, TEMED, trypsin-EDTA solution (10X), Triton® X-100, trizma base, tryptone, Tween®20.

Terumo (NJ, USA)

10 ml syringe without needle.

Thermo Fisher Scientific (Leicestershire, UK)

BCA reagent kit, BSA, buffer solution pH4 (phthalate), buffer solution pH7 (phosphate), buffer solution pH10 (borate), glycine, isopropanol, trizmabase, weigh boats, RNase Away.

Tocris (MO, USA)

HOE140 (BK antagonist).

VWR International Ltd. (West Sussex, UK)

Methanol.

Whatman International Ltd. (Maidstone, England)

Whatman chromatography paper.

2.2 Cell culture methods

All cell culturing techniques were carried out in a clean and sterile environment using a Holten Lamin Air laminar flow cabinet. Cells were visualised using a Nikon Eclipse TS100 phase-contrast microscope.

2.2.1 Endothelial cells

2.2.1.1 Culture of bovine aortic endothelial cells (BAECs)

Differentiated BAECs were obtained from Coriell Cell Repository (New Jersey, USA). The cells were derived from a 1 yr old male Hereford cow post-mortem. Cells were maintained in RPMI-1640 medium supplemented with 10% (v/v) fetal bovine serum (FBS), 100 U/ml penicillin and 100 μg/ml streptomycin. Cells were cultured in T175 cm^2, T75 cm^2, T25 cm^2 and 6-well plates. Cells between passages 5-14 were used for experimental purposes, and were maintained in a humidified atmosphere of 5% CO_2/95% air at 37°C.

2.2.1.2 Culture of human aortic endothelial cells (HAECs)

Differentiated HAECs were obtained from PromoCell GmbH (Heidelberg, Germany). The cells were derived from the thoracic aorta of a 21 yr old human male post-mortem. Cells were maintained in Endothelial cell growth medium MV supplemented with a separate SupplementMix® of growth factors containing ECGS/H 0.4% (v/v), FBS 5.0% (v/v), EGF 10 ng/ml and hydrocortisone 1 μg/ml. 100 U/ml penicillin and 100 μg/ml streptomycin were

also added. Cells between passages 5-11 were used for experimental purposes and were maintained in a humidified atmosphere of 5% CO_2/95% air at 37°C.

2.2.2 Trypsinisation of cells

As all cell lines used were adherent, trypsinisation was required for the purposes of sub-culturing. Briefly, growth medium was removed from flasks and cells washed 2-3 times in sterile PBS to remove α-macroglobulin, a trypsin inhibitor present in FBS. An appropriate volume of trypsin-EDTA (10% (v/v) in PBS) was subsequently added to the cells and incubated at 37°C for 3 min (or until the cells began to detach from the flask surface). Growth medium containing FBS was added to prevent further trypsinisation and cells were collected from suspension by centrifugation at 100 x g for 5 min at room temperature. Cells were resuspended in growth medium (or freeze medium) and counted using either a Neubauer chamber haemocytometer or ADAM™ Counter. Cells were routinely split at a 1:5 ratio for BAECs or a 1:3 ratio for HAECs either for further sub-culturing or to be cryopreserved.

2.2.3 Cryogenic preservation and recovery of cells

For long term storage, cells were maintained in a liquid nitrogen cryo-freezer unit (Taylor-Wharton, USA). Following trypsinisation, cells to be stored were centrifuged at 100 x g for 5 min at room temperature and the resultant pellet was resuspended in the appropriate medium for the cell line, containing 20% (v/v) FBS, dimethylsulphoxide (DMSO) 10% (v/v) and 1% (v/v) penicillin/streptomycin. 1 ml aliquots were transferred to sterile cryovials and frozen in a –80°C freezer at a rate of –1°C/minute using a Mr Freeze® cryo-freezing container. Following overnight freezing at –80°C, the cryovials were transferred to the cryo-freezer unit.

For recovery of cells, cryovials were thawed rapidly in a 37°C water bath and added to a cell culture dish containing pre-warmed (37°C) growth medium to dilute the DMSO. After 24 hrs the medium was removed, the cells were washed in PBS and fresh growth medium added.

2.2.4 Cell counting

2.2.4.1 Haemocytometer

To aid in reproducibility of experiments, cells were seeded at precise numbers and densities. This was done using a Neubauer chamber haemocytometer following trypan blue staining for cell viability. 20 μl of trypan blue was added to 100 μl of cell suspension and the mixture left to incubate for 2 min. 20 μl of this mixture was loaded into the counting chamber of the haemocytometer and cells visualized by light microscopy (Figure 2.1). Viable cells excluded the dye, whilst dead cells stained blue due to compromise of the cell membrane. Cells that touch the top and right lines of a square were not counted, while cells on the bottom and left side were counted. The number of cells was calculated using the following equation:

Average Cell No. x Dilution Factor x $1x10^4$ (area under cover slip mm^3) = Viable cells/ml

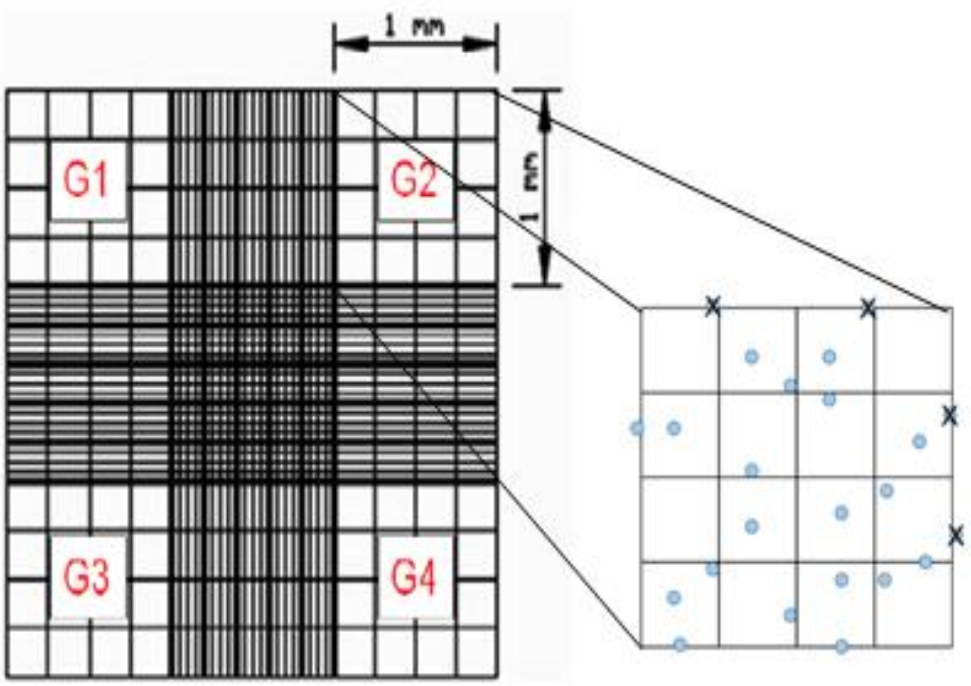

Figure 2.1: The haemocytometer, indicating the counting grid.

2.2.4.2 ADAM™ Counter

Cell counts were also made using an Advanced Detection and Accurate Measurement (ADAM™) cell counter (Digital Bio, Korea) which utilises fluorescent cell staining to determine total and viable cell count in a given sample. Cells are mixed with two solutions; Solution N, containing propidium iodide (PI), a fluorescent dye that will intercalate with DNA, but which cannot enter cells with intact membranes. Therefore, only non-viable cells will fluoresce with PI alone. The second, Solution T, contains PI and a detergent that will disrupt viable cell membranes allowing PI to stain both viable and non-viable cells. ADAM™ contains both laser optics and image analysis software that allows parallel determination of both total and viable cell numbers in a sample from these two staining methods.

Two 12 µl aliquots of a cell sample were taken; one aliquot was mixed with 12 µl of Solution N accustain and the second with 12

µl Solution T accustain. 20 µl of each cell mixture was then loaded into the appropriate labelled chamber in an AccuChip. The AccuChip was then loaded into the ADAM™ counter where 40-60 images were taken of the cell chambers and average cell number and viability calculated using the integrated image analysis software (Figure 2.2).

(A) (B)

Figure 2.2: (A) The ADAM™ counter and (B) loading of an AccuChip and reading.

2.2.5 Shear stress experiments

2.2.5.1 Orbital rotation

For laminar shear stress studies, orbital rotation was applied as in previous publications (Colgan, et al. 2007, Fitzpatrick, et al. 2009), BAECs and HAECs were seeded onto cell culture grade 6-well plates and allowed to adhere

for 24 hrs, then grown to 90% confluency. Culture medium was then removed, replenished with 4 ml of fresh medium and cells were exposed to laminar shear stress (0-10 dynes/cm^2, 0-24 hrs) using an orbital rotator (Stuart Scientific Mini Orbital Shaker, Staffordshire, UK) set to the appropriate speed as determined by the following equation (Hendrickson, et al. 1999) (Figure 2.3).

$$\text{Shear Stress} = \alpha\sqrt{\rho n(2\pi f)^3}$$

Where α = radius of rotation in cm

ρ = density of liquid in g/l

n = liquid viscosity 7.5 x 10^{-3} dynes/cm^2 @ 37°C

f = rotation per second

Control plates containing un-sheared "static" endothelial cells were cultured in the same incubator but on a different shelf to avoid vibrations caused by the orbital rotator. Studies were carried out for differing periods of time (0-48 hrs, 0–10 dynes/cm^2). Following shearing experiments, the cells were either: (i) harvested for Real-Time PCR measurement of mRNA expression levels; (ii) harvested for Western blotting to determine protein expression levels; (iii) fixed *in situ* for immunocytochemical staining; (iv) transplanted into Millicell hanging cell culture inserts for transendothelial permeability assays; (v) used in proliferation experiments; or (vi) BK experiments.

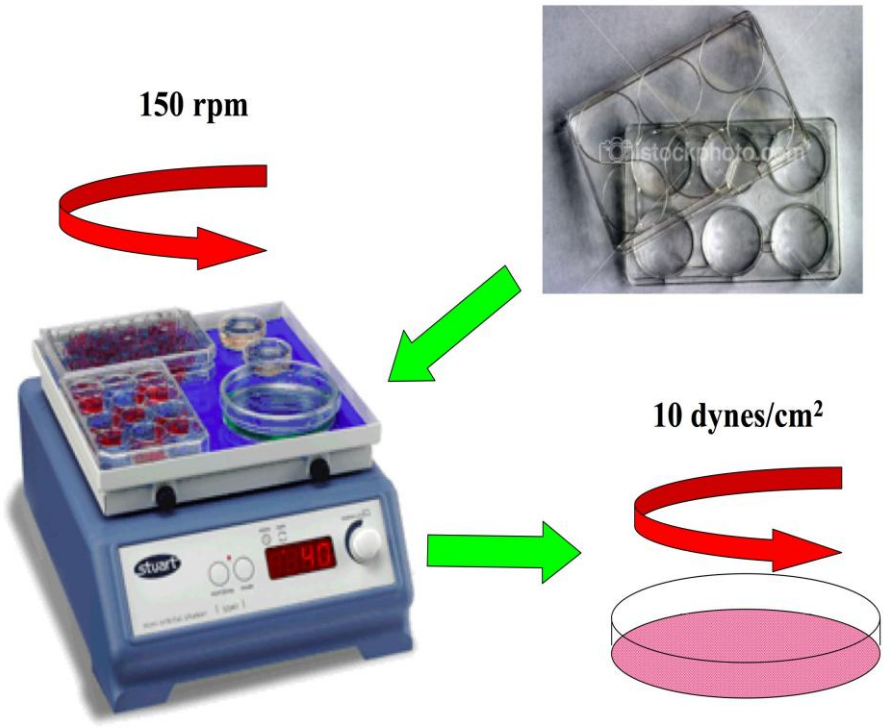

Figure 2.3: Orbital rotation model used in laminar shear stress studies.

2.2.5.2 Disturbed shear

For disturbed shear stress studies, BAECs and HAECs were seeded onto cell culture grade 6-well plates and allowed to adhere for 24 hrs, then grown to 90% confluency. Culture medium was then removed, replenished with 4 ml of fresh medium and cells were exposed to disturbed oscillatory shear stress (0-24 hrs) using a see-saw rocker (Stuart Scientific Rocker SSL4, Staffordshire, UK) set to 70 rpm (Figure 2.4).

Control plates containing un-sheared "static" endothelial cells were cultured in the same incubator but on a different shelf to avoid vibrations caused by the rocker. Following shearing experiments, the cells were either: (i) harvested for real-time PCR measurement of mRNA expression levels; (ii) transplanted into Millicell hanging cell culture inserts for transendothelial permeability assays; or (iii) fixed *in situ* for immunocytochemical staining.

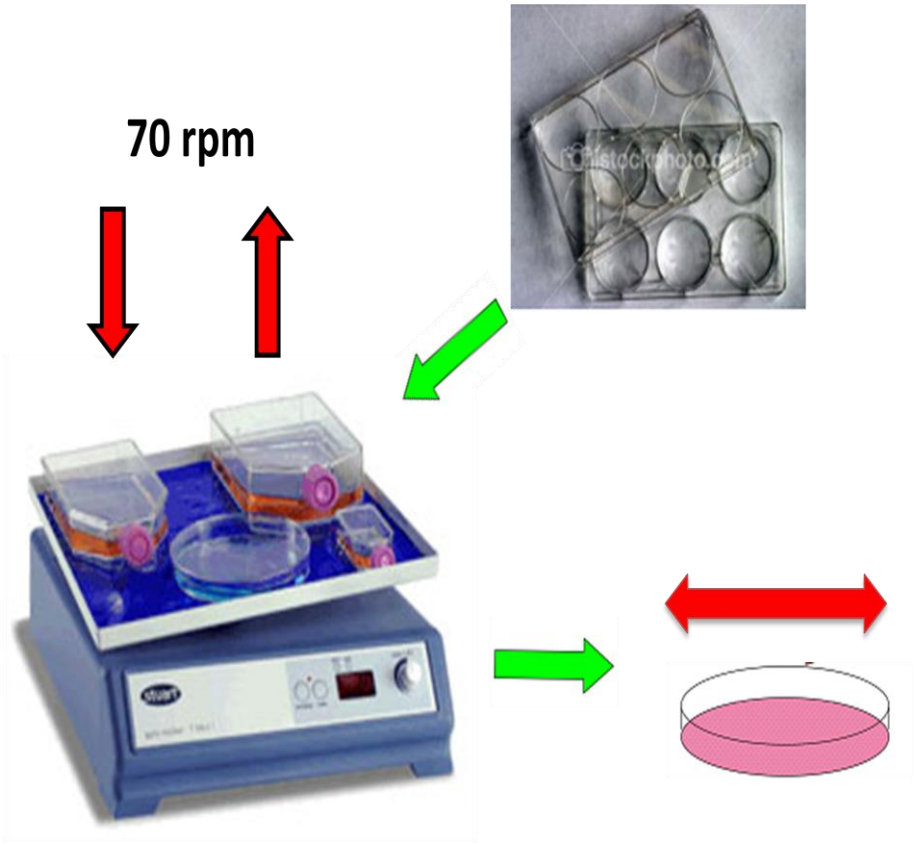

Figure 2.4: Disturbed shear model used in shear stress studies.

2.2.5.3 ibidi® (Integrated BioDiagnostics) flow system

The ibidi® pump system is a novel perfused flow system for exposing ECs to shear stress on ibidi® μ-slides (Figure 2.5). Prior to cell seeding, slides, tubing and medium were equilibrated overnight at 37°C in a tissue culture incubator. The following day, HAECs were seeded onto slides at a density of $1x10^6$ cells/ml and allowed to adhere. HAECs were allowed to grow to confluency at which point the μ-slides were connected to the pump system via its luer connectors in accordance with the manufacturer's instructions and previous publications (Walsh, et al. 2011), taking care not to introduce air bubbles. The cells were then exposed to either laminar or oscillatory shear stress at varying

doses. Following shear experiments, cells were fixed in situ for immunocytochemical staining and phase-contrast imaging.

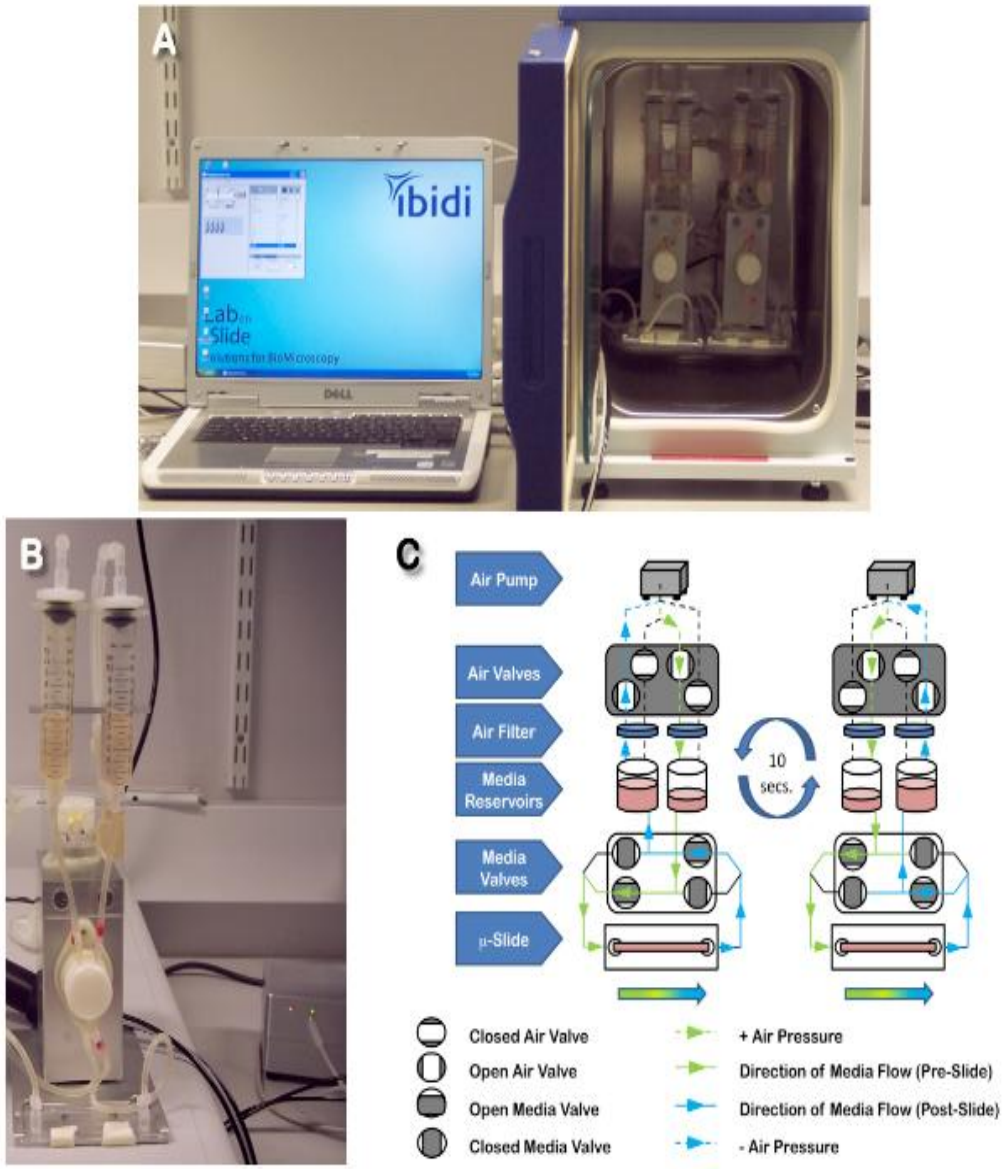

Figure 2.5: ibidi® µ-slide flow system. (A, B) Flow systems with custom CO_2 incubator in situ. (C) Schematic illustrating air and medium flow paths. Air pump operates on a 10 second reciprocation cycle to ensure steady forward flow of medium (Walsh, et al. 2011).

2.2.6 Transendothelial permeability assay

For analysis of permeability, following shear experiments, BAECs and HAECs were trypsinised and re-plated at high density ($1x10^5$ cells/well) into Millicell hanging cell culture inserts (6-well format, 0.4 μm pore size, 24 mm filter diameter). When cells had re-adhered to the surface of the membrane (24 hrs), transendothelial permeability was monitored as previously described (Collins, et al. 2005). In brief, fresh culture medium was added to the upper (abluminal) and lower (subluminal) chambers of the Millicell insert within the 6-well dish (2 ml: upper, 4 ml: lower). At time t=0, FITC-labelled dextran (40 kDa) was added to the abluminal chamber (giving a final concentration of 250 μg/ml) and transwell diffusion allowed to proceed (Figure 2.6). Medium samples (28 μl) were collected every 30 min from the subluminal compartment (for up to 3 hrs), diluted to a final volume of 400 μl with appropriate complete medium, and monitored for FITC-dextran fluorescence (as 3x100 μl replicates in a 96-well fluorescence microplate). Using a TECAN Safire 2 fluorospectrometer (Tecan Group, Switzerland), excitation and emission wavelengths of 490 and 520 nm, respectively, were selected. % transendothelial exchange (%TE) of FITC-dextran 40 kDa is expressed as the total subluminal fluorescence at a given time point (from 0-180 min) expressed as a percentage of total abluminal fluorescence at t=0 min.

2.2.7 Treatment with anti-oxidants and pharmacological inhibitors

Prior to treatment with anti-oxidants or pharmacological inhibitors, BAECs were grown until approximately 80% confluent, after which the growth medium was removed and cells washed in PBS. Inhibitors and anti-oxidants were reconstituted in a suitable diluent. Working concentrations were then made up in RPMI-1640 medium with FBS and antibiotics. For DMSO-soluble compounds, a

suitable stock concentration was prepared so that the final concentration of DMSO in working solutions was less than 0.5%.

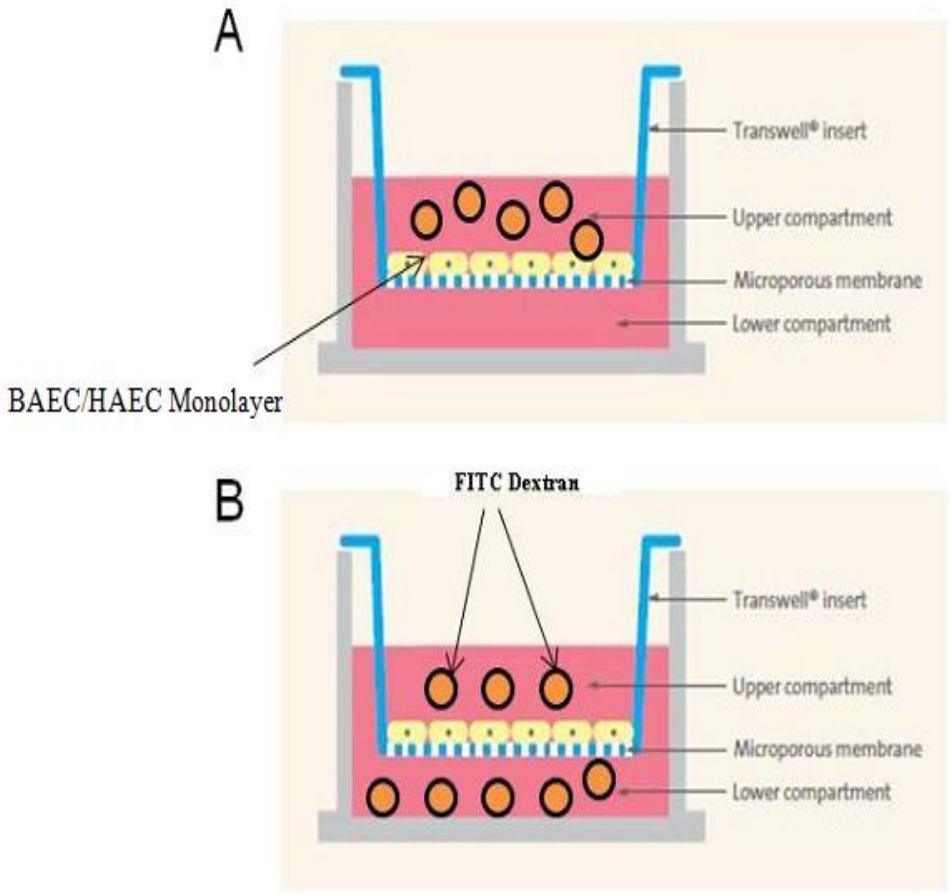

Figure 2.6: Transendothelial permeability assay. **(**A) Shows FITC-labelled dextran in the upper compartment (abluminal chamber) at t=0, which diffuses through the BAEC/HAEC monolayer and semi-permeable membrane, into the lower compartment (subluminal chamber) (B), from which samples (28 µl) are collected every 30 min over 3 hrs.

For anti-oxidant studies, working solutions were made up fresh and adjusted for pH immediately prior to incubation. N-Acetyl-L-cysteine (NAC), a broad spectrum anti-oxidant, was applied at a concentration of 5 mM. Anti-oxidants were applied to the cells for 1 hrs immediately prior to, or 4 hrs after, the commencement of shearing.

Studies to explore shear-dependent signal transduction pathways employed the following pharmacological inhibitors: apocynin (10 mM, NADPH oxidase), and NSC23766 (50 μM, Rac1). These studies mirrored those of the anti-oxidants, in that inhibitors were prepared in complete culture medium and applied to the cells for 1 hrs immediately prior to, or 4 hrs after, the commencement of shearing. Concentrations used were gained from both current literature and manufacturer's recommendations.

2.3 mRNA preparation and analysis

2.3.1 RNase-free environment

As RNA is easily degraded by ubiquitous RNases, standard procedures were employed to avoid this potential hazard (Sambrook, Fritsch and Maniatis 1989). Prior to working with RNA, any apparatus or surfaces to be used were treated with RNase AWAY spray (Thermo Fisher, Leicestershire, UK) to remove RNases. As hands are a major source of RNase contamination, gloves were used at all times and changed frequently.

2.3.2 RNA preperation

Trizol® is a ready-to-use reagent for the isolation of total RNA, DNA and/or protein from cells and tissues. RNA isolation was developed by Chomczynski and Sacchi (Chomczynski and Sacchi 1987). Trizol® reagent maintains the integrity of the RNA while disrupting the cells and dissolving the cell components.

Following shear experiments, cells were lysed directly in culture plates by the addition of 1 ml of Trizol® per 10 cm^2. A volume less than this can result

in contamination of the RNA with DNA. To ensure complete homogenization, cells were lysed by scraping the plate with a cell scraper. The samples were then incubated for 5 min at room temperature to allow complete dissociation of nucleoprotein complexes. 0.2 ml of chloroform was added per 1 ml of Trizol® reagent used, then mixed vigorously for 15 sec before being incubated for 10 min at room temperature. Samples were then centrifuged at 7,000 x g for 15 min at 4°C. The mixture separated into a lower red phenol-chloroform phase, an interphase and an upper colourless aqueous phase. RNA remains exclusively in the upper aqueous phase.

The aqueous phase was carefully removed and transferred to a fresh, sterile tube. The RNA was then precipitated out of solution by the addition of 0.5 ml of isopropanol per 1 ml of Trizol® used. Samples were inverted 5-8 times and incubated for 10 min at room temperature and then centrifuged at 7,000 x g for 10 min at 4°C. The RNA precipitate forms a gel-like pellet on the side of the tube. The supernatant was removed and the pellet washed in 1 ml of 75% ethanol per ml of Trizol® used followed by centrifugation at 7,000 x g for 5 min at 4°C. The resultant pellet was air-dried for 5-10 min before being re-suspended in DEPC-treated water. This was then incubated for 10 min at 60°C, to homogenize the sample prior to quantification. The concentration of total RNA was determined using a NanoDrop®, as outlined below. The sample was then stored at –80°C until used.

2.3.3 The NanoDrop® ND-1000 Spectrophotometer

The NanoDrop® ND-1000 Spectrophotometer was used to determine nucleic acid sample concentrations. An undiluted 1.2 µl sample was pipetted onto the end of a fibre optic cable (the receiving fibre). A second fibre optic cable (the source fibre) was then brought into contact with the liquid sample causing the liquid to bridge the gap between the fibre optic ends. (The gap is controlled to both 1 mm and 0.2 mm paths by the computer). A pulsed xenon flash lamp provided the light source and a spectrometer was used to analyse the light after

passing through the sample. The instrument was controlled by special software run from a PC, and the data were logged in an archive file on the PC.

The NanoDrop® automatically calculates the purity of the nucleic acid samples by reading the absorbance at 260 nm and the absorbance at 280 nm and then determining the ratio between the two (ABS_{260}/ABS_{280}) (Figure 2.7). Pure DNA which has no protein impurities has a ratio of 1.8 whereas pure RNA has a ratio of 2.0. Lower ratios indicate the presence of proteins, higher ratios imply the presence of organic reagents. Purification of RNA samples was achieved using a DNase treatment kit (Sigma-Aldrich, Dorset, UK) as described below.

2.3.4 DNase treatment of mRNA

The RNA sample for analysis was digested with 1 µl RNase-free DNase I along with 1 µl 10X DNase Buffer and incubated for 15 min at 37°C. 1 µl DNase stop solution was added to the reaction mixture and was incubated for a further 10 min at 70°C to denature the DNase enzyme. The RNA could then be synthesised to cDNA.

2.3.5 Reverse transcription

In this process, mRNA was transcribed into cDNA by the enzyme reverse transcriptase. A high capacity cDNA reverse transcription kit (Applied Biosystems, CA, USA) was used as described below.

20 µl reactions were made up as follows;

RT Buffer (10X)	2 µl
dNTP mix (100 mM)	0.8 µl

Random Primers (10X)	2 µl
MultiScribe Reverse Transcriptase	1 µl
Nuclease-free H_2O	4.2 µl

A

B **C**

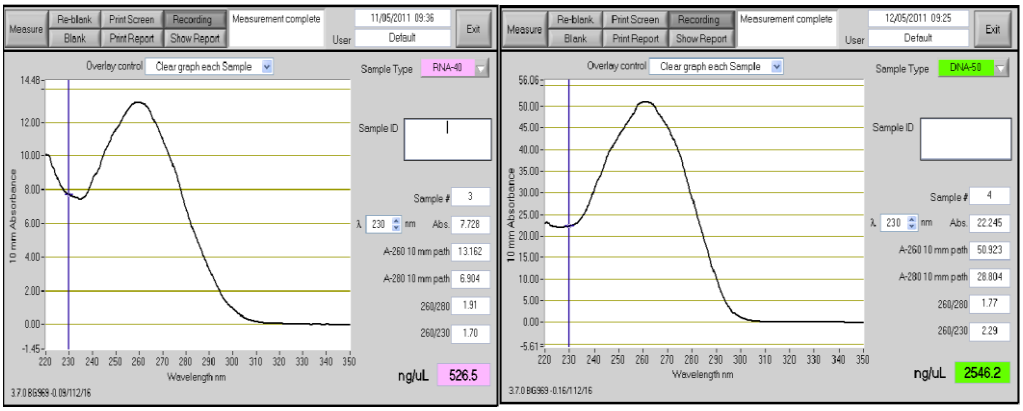

Figure. 2.7: Figure shows (A) the NanoDrop® machine and typical graph readouts for (B) RNA and (C) DNA.

This was added to a 0.2 ml PCR tube containing 1000 ng RNA diluted in nuclease-free water to 10 µl. Samples were spun down briefly in a centrifuge and then placed into a desktop PCR machine and run at 25°C for 10 min, 37°C for 120 min and finally 85°C for 5 min. cDNA products were then quantified on a NanoDrop® (Section 2.2.8.3) to check concentration and purity of samples.

2.3.6 Polymerase chain reaction (PCR)

Desktop PCR was used to optimize primer sets and to rule out primer dimerisation before their use in quantitative Real-Time PCR (qPCR). 25 μl PCR reaction mixtures were prepared as follows:

Forward primer (10 μM)	1 μl
Reverse primer (10 μM)	1 μl
cDNA sample	1 μl
Reaction buffer (10X)	2.5 μl
dNTP (10 mM)	2 μl
$MgCl_2$ (25 mM)	1.5 μl
Taq Polymerase	0.25 μl
RNase free water	15.75 μl

The solution was then placed into an MJ Mini thermal cycler with hot-lid (Bio-Rad, CA, USA). Samples were then subjected to the following cycling conditions:

Denature		95°C	5 min	
Cycling	Denature	95°C	15 sec	40 cycles
	Annealing	55-60°C	30 sec	
	Extension	72°C	15 sec	

Extension	72°C	5 min
Hold	4°C	Forever

Annealing temperatures varied as they were specific to primer sets (Table 2.1).

Target Gene	Primer Sequence	Product size	Annealing Temp °C
NEP For	5` caa agc caa aga aga aac ag 3`	290 bp	55
NEP Rev	5` cat ctc tta aaa tgt caa a 3`		
TOP For	5` tga agg tca ccc tca agt a 3`	401 bp	56
TOP Rev	5` tcc acc tgg ttc atg tag ta 3`		
Bovine GAPDH For	5’ agg tca tcc atg acc act tt 3`	337 bp	55
Bovine GAPDH Rev	5’ ttg aag tcg cag gag aca a 3`		
Human GAPDH For	5’ gag tca acg gat ttg gtc gt 3`	238 bp	56
Human GAPDH Rev	5’ ttg att ttg gag gga tct cg 3`		
eNOS For	5’ gct tga gac cct cag tca gg 3`	300 bp	59
eNOS Rev	5’ ggt ctc cag tct tga gct gg 3’		
p47 For	5’ acc cag cca gca cta tgt gt 3’	288 bp	58
p47 Rev	5’ agt agc ctg tga cgt cgt ct 3`		

Table 2.1: Table shows primer sequences, product size and annealing temperature used for PCR and qPCR. All primer sets, with the exception of bovine GAPDH, were produced from human sequences, with consensus overlap with bovine sequences.

2.3.7 Quantitative real-time polymerase chain reaction

After optimisation of primers by RT-PCR, they were used in qPCR. This technique follows the general principle of RT-PCR with amplified DNA quantified in real-time as it accumulates in the reaction. This quantification was facilitated using SYBR green, a dye that fluoresces only when bound to the minor groove of double stranded DNA. This fluorescence is then read by a laser at the end of every cycle and the amount of cDNA product formed during the PCR cycles can be quantified in real time and graphed. To normalise the optical system involved in real-time analysis, ROX, a passive dye, is incorporated into the SYBR mastermix. This is achieved by the signal of the reporter dye (SYBR) being measured against the passive reference dye (ROX) signal to normalise for non-PCR-related fluorescence fluctuations occurring from well to well. The threshold cycle represents the refraction cycle number at which a positive amplification reaction was measured and was set at 10 times the standard deviation of the mean baseline emission calculated for PCR cycles 3 to 15. The results were analysed according to the Comparative C_T method ($\Delta\Delta C_T$) as described by (Livak and Schmittgen 2001).

qPCR was carried out using an Applied Biosystems 7900HT Fast real-time PCR machine. Each reaction was set up in triplicate as follows:

Forward primer (10 μM)	1.0 μl
Reverse primer (10 μM)	1.0 μl
cDNA	2.0 μl
SYBR Green	11.5 μl
RNase free water	9.5 μl

Samples were then subjected to an initial denaturation step of 95°C for 10 min followed by 40 cycles of 95°C for 15 sec and a primer-specific temperature of between 55-60°C for 1 min. Data were collected during the annealing step. Quantification of cDNA target was normalised for differences across experiments/samples using an endogenous housekeeper control, GAPDH, as an active reference gene.

Routinely, melt curve analysis was carried out to ensure single product formation and to rule out possible contamination of product by non-specific binding and primer dimerisation. Samples from both RT-PCR and qPCR reactions were then visualized on 1% agarose gels as described below.

2.3.8 Agarose gel electrophoresis

Agarose gels were prepared by boiling 1 g of agarose in 100 ml of 1X TAE buffer (40 mM Tris-Acetate pH 8.2, 1 mM EDTA) to make a 1% gel. After sufficient cooling (~60°C) 10 µl SYBR Safe (Invitrogen, The Netherlands) was added to the gel, mixed by swirling and then poured into a casting rig. A comb was inserted for formation of wells. The gel was allowed to cool and polymerise before filling the chamber with 1X TAE and removing the comb.

As the 10X buffer in the RT-PCR reaction already contained a loading and tracking dye 15 µl of RT-PCR product was loaded directly to the gel. A 1 KB or 100 bp DNA ladder was also added to one well as a molecular weight marker for reference. The gel was run at constant voltage (5 V/cm, usually 100 V), for 1 to 2 hrs. Samples were then visualised using the transilluminator settings on a G:BOX (Syngene, UK). Images could then be saved for later densitometric analysis.

2.4 DNA preparation and analysis

2.4.1 Reconstituting plasmid DNA

Reconstitution of DNA-based plasmids on air dried filter paper was achieved by adding a 1 cm^2 area of filter paper containing the appropriate plasmid to a sterile micro-centrifuge tube. Approximately 100 µl of sterile, endotoxin-free TE-buffer was added to the micro-centrifuge tube. This mixture was vortexed for 10 sec and subsequently incubated at room temperature for 5 min. Following this incubation the mixture was again vortexed for 10 sec and the tube was then centrifuged for 15 sec at 100 x g. Approximately, 1-10 µl of supernatant was used in subsequent bacterial transformations.

2.4.2 Bacterial transformations

A 95 µl aliquot of competent DH5α *E. coli* were placed in a pre-chilled microfuge tube containing 5 µl DNA (~100 ng/10 µl). The contents of the tube were mixed gently by flicking and incubated on ice for 30 min, during which time an aliquot of SOC medium was pre-heated to 37°C. After 30 min on ice, the cells were heat-shocked in a water bath at 42°C for 50 sec, and were then removed immediately for incubation on ice for a further 2 min. A 900 µl aliquot of pre-heated SOC was added to the cells which were then incubated at 37°C in a shaking incubator for 1 hrs. The cells were then pelleted by centrifugation for 3 min at 3,420 x g. Following centrifugation, 900 µl of supernatant was removed and discarded. The cells were re-suspended in the remaining supernatant and plated out (with the controls) on LB plates containing 50 µg/ml ampicillin, and incubated overnight at 37°C. Plasmids carrying the antibiotic resistance gene confer this resistance to the transformed cells and thus only transformed cells

will yield colonies. These colonies were subsequently used to prepare broth cultures for DNA midi-preparations.

2.4.3 Midi-preparation of plasmid DNA

Successfully transformed colonies were picked from selective agar plates using a flame sterilised inoculating loop, and then grown overnight in sterilised baffled culture flasks containing 150 ml of LB broth supplemented with 50 µg/ml ampicillin at 37°C with 150 rpm agitation. Following bacterial culture, DNA purification was carried out using a Qiagen plasmid midi-prep kit as per the manufacturer's instructions.

Bacterial cells were pelleted at 3,000 x g for 15 min at 4°C. The supernatant was decanted and the cell pellet was suspended completely in 6 ml of Buffer P1 containing RNase A (100 µg/ml). The bacterial cells were then lysed by addition of 6 ml Buffer P2 and vigorous shaking for 30 sec followed by incubation at room temperature for 5 min. Following incubation, 6 ml of pre-chilled Buffer P3 was added (to precipitate genomic DNA, protein, cell debris and SDS), mixed thoroughly by inverting the tube 5-6 times and poured into a prepared filter cartridge and incubated for 10 min at room temperature, allowing the precipitant to rise.

The Qiagen-tip 100 column was equilibrated by applying 4 ml of QBT buffer and allowing the column to empty by gravity. The column does not dry out at this stage, as the flow of buffer will stop when the buffer reaches the upper filter. Following equilibration, the cell lysate was filtered into the column and allowed to flow through the resin where the plasmid binds. The Qiagen-tip was washed with 20 ml of Buffer QC, to flush out any bacterial cell proteins. DNA was then eluted with 5 ml of Buffer QF. DNA was precipitated by adding 3.5 ml of isopropanol. The DNA/isopropanol mixture was then filtered through a Qia-precipitator and the bound plasmid was subsequently washed with 2 ml of 70% (v/v) ethanol. The precipitator was then dried by flushing air through and the bound plasmid eluted into a sterile 1.5 ml micro-centrifuge tube by the addition

of 1 ml of sterile Buffer TE. The eluted DNA was flushed through the precipitator once more to remove any unbound DNA. DNA was then quantified on a NanoDrop® (Section 2.3.3), and quality of the DNA was checked by agarose gel electrophoresis (Section 2.3.8) (Adapted from the manufacturer's protocol Qiagen® Plasmid Purification Handbook, 2005).

2.4.4 Preparation of glycerol stocks

Glycerol enables long term storage of bacteria as glycerol prevents water in the broth from forming ice crystals that can puncture and kill bacterial cells. Glycerol stocks of bacterial cultures were prepared by adding 0.5 ml of a 50% (v/v) glycerol solution to 0.5 ml of the overnight bacterial culture of interest, mixing and storing at -80°C for future use.

2.5 Transfection methods

2.5.1 Amaxa™ nucleofection

Nucleofection is a novel transfection technique in which DNA/siRNA is transported directly into the nucleus to give high transfection efficiency and cell viability. The technique itself is a non-viral based method that is based on a combination of unique electrical parameters and cell specific solutions. For all nucleofector transfections the basic endothelial cell kit was used in accordance with the manufacturer's instructions.

Briefly, for each well of a 6-well plate to be transfected, 2.5 ml of pre-warmed culture medium was added and equilibrated in a tissue culture incubator. HAECs and BAECs were trypsinised, counted and pelleted. Residual medium

was removed by washing the cell pellets with PBS. Following this, cells were centrifuged at 100 x g for 5 min and residual PBS was removed by aspiration; finally, cells were re-suspended at a final concentration of 5 x 10^5 cells/100 µl, in nucleofection solution. Care was taken not to store the cell suspension in nucleofection solution longer than 15 min as this would result in a serious loss of cell viability. For each individual sample, 100 µl cell suspension (5 x 10^5 cells) was mixed with 1.5-3.0 µg DNA and the sample was transferred to a nucleofection cuvette. At this stage, any bubbles in the cuvette were carefully removed and the cuvette was closed. The cuvette was then inserted into the Amaxa™ nucleofector (Lonza, Cologne, Germany) (Figure 2.8). For BAECs and HAECs, the programme used to nucleofect the cells was M-003. Immediately following nucleofection, 500 µl of pre-warmed 37°C culture medium containing serum but no antibiotic was added. The nucleofected sample was then carefully transferred to the pre-incubated well of a 6-well plate and incubated overnight in a tissue culture incubator at 37°C. Culture medum was replaced the following day.

Figure 2.8: The Amaxa™ nucleofector for electroporation (www.amaxa.com).

2.5.2 Microporation

Microporation is a unique transfection technique that utilises a gold-plated pipette tip as an electroporation device. This allows for a more uniform electric field to be generated with minimal heat generation, metal ion dissolution, pH variation and oxide formation that are consistent difficulties in conventional electroporation protocols. Microporation was carried out using a microporation solution kit in accordance with the manufacturer's instructions.

Cells were trypsinised and centrifuged at 100 x g for 2 min at room temperature and the solution aspirated. The remaining pellet was washed using PBS. The cells were then counted, re-suspended and divided into aliquots containing a final density of 500,000 cells/100 µl. Aliquots of cell suspension were centrifuged at 100 x g for 5 min at room temperature. To each well of a 6-well plate to be transfected, 2 ml of pre-warmed culture medium containing serum (but without antibiotics), was added and equilibrated in a tissue culture incubator. Aliquoted cell pellets were re-suspended in 110 µl/transfection of Buffer R. Re-suspended cells were transferred to a 1.5 ml eppendorf tube and 3 µg plasmid DNA or 1-100 nM siRNA/500,000 cells was added. Upon addition of 3 ml Buffer E, the microporation tube was inserted into the pipette station to form the microporation unit (Labtech, East Sussex, UK) (Figure 2.9). The suspension was then pipetted into a 100 µl gold-tip using the microporator pipette. For BAECs, the desired pulse conditions were set; 1450 V, 20 pulse width (ms) and 2 pulse number. For HAECs, the desired pulse conditions were set; 1000 V, 30 pulse width (ms) and 3 pulse number. After microporation each 100 µl sample was transferred to a well of the 6-well plate, each well containing 2 ml pre-incubated culture medium. Cells were allowed to recover overnight, after which the culture medium was changed.

Figure 2.9: The microporator. (A) The microporation unit that generates the electrical parameters necessary for the transfection of DNA and siRNA into cells; (B) The microporation unit consisting of the microporation tube (containing the electroporation buffer) and the microporation pipette used to deliver the electroporation parameters to the cells suspended in the gold-plated pipette tip; (C) The microporation kit containing the necessary microporation solutions, tips and microporation tubes. (www.microporator.com)

2.5.3 *Trans*IT-siQUEST® transfection reagent

*Trans*IT-siQUEST® is a high efficiency, low toxicity, siRNA-specific transfection reagent for mammalian cells. Transfection was carried out in accordance with the manufacturer's instructions.

BAECs and HAECs were trypsinised and seeded to 6-well plates at the required concentration, allowed to adhere, and come to 80% confluency with regular medium changes. Prior to transfection, *Trans*IT-siQUEST® reagent was warmed to room temperature. 250 µl per transfection of pre warmed culture medium was added to a 1.5 ml micro-centrifuge tube. 7 µl of *Trans*IT-siQUEST® reagent and the required concentration of siRNA were added to the medium and left to form complexes at room temperature for 30 min. Fresh medium was added to the cells (2 ml per well) and the transfection suspension then added to each

well. Cells were placed into a 37°C incubator overnight and experiments carried out after this time.

2.5.4 *Trans*IT-2020® transfection reagent

*Trans*IT-2020® is a high-performance, animal-origin free, broad spectrum transfection reagent for mammalian cells. Transfection was carried out in accordance with the manufacturer's instructions.

BAECs and HAECs were trypsinised and seeded to 6-well plates at the required concentration, allowed to adhere, and come to 80% confluency with regular medium changes. Prior to transfection, *Trans*IT-2020® reagent was warmed to room temperature. 250 µl per transfection of pre warmed culture medium was added to a 1.5 ml micro-centrifuge tube. 7 µl of *Trans*IT-2020® reagent and the required concentration of plasmid DNA were added to the medium and left to form complexes at room temperature for 30 min. Fresh medium was added to the cells, 2 ml per well, and the transfection suspension then added to each well. Cells were placed into a 37°C incubator overnight and experiments carried out after this time.

2.6 Immunodetection techniques

2.6.1 Western blotting studies

2.6.1.1 Preparation of whole cell lysates

For the purposes of Western blotting, cells were harvested in the following manner. On ice or at 4°C, culture medium was removed and cells were

washed three times in PBS solution. Following complete aspiration of PBS, 1X radioimmunoprecipitation assay (RIPA) lysis buffer (20 mM Tris, 150 mM NaCl, 1 mM Na_2EDTA, 1 mM EGTA, 1% Triton X-100 (v/v), 2.5 mM sodium pyrophosphate, 1 mM β-glycerophosphate, 1 mM sodium orthovanadate, 1 μg/ml leupeptin) was added to the cells, which were then harvested using a cell scraper. The resultant lystaes were frozen and thawed three times followed by three cycles of ultrasonication for 5 sec on ice using a sonic dismembrator (Vibra Cell, Sonics and Materials Inc, CT, USA). Cell lysate samples were either stored at -80°C for later analysis or used immediately in a BCA assay or Western blot.

2.6.1.2 Bicinchoninic acid (BCA) protein microassay

The BCA assay is a biochemical assay for quantifying the total amount of protein in a solution. This is achieved by Cu^{2+} reacting with protein under alkaline conditions to produce Cu^{+}, which in turn reacts with bicinchoninic acid (green) to form a complex (purple) that strongly absorbs light at 562 nm.

Two separate reagents were supplied in this commercially available assay kit (Pierce Chemicals, Cheshire, UK); (A) an alkaline bicarbonate solution and (B) a copper sulphate solution. One part solution B is mixed with fifty parts solution A; 200 μl of this mixture is added to 10 μl of protein lysate or BSA standards (standard curve in the range 0-2 mg/ml) in a 96-well plate. Each protein lysate sample and BSA standard were assayed in triplicate. The plate was then incubated at 37°C for 30 min and the absorbance read at 560 nm using a EL*x*800 microplate reader (BioTek, VT, USA).

2.6.1.3 SDS-polyacrylamide gel electrophoresis of proteins

SDS-polyacrylamide gel electrophoresis (PAGE) resolves cellular proteins based solely on their electrophoretic mobility. During SDS-PAGE,

proteins are driven by an applied current through a mesh of cross-linked polyacrylamide gel. PAGE is carried out in the presence of the negatively charged detergent sodium dodecylsulphate (SDS), which binds to all types of protein molecules, denaturing the protein to its primary structure. Electrostatic repulsion between the bound SDS molecules causes the proteins to unfold into a similar rod-like shape, removing secondary and tertiary structure as a factor in separation. As the amount of SDS bound is proportional to the molecular weight of the polypeptide and is sequence independent, SDS-polypeptide complexes migrate through polyacrylamide gels in accordance with the size of the polypeptide (Laemmli 1970).

2.6.1.3.1 Preparation of SDS-polyacrylamide gels

Denaturing SDS-PAGE were performed using resolving gels 10% (v/v) and 5% (v/v) stacking polyacrylamide gels according to the method of (Laemmli 1970). The gels were prepared as follows:

Resolving Gel:	1.5 ml	Buffer A (1.5 M Tris pH 8.8)
	1.5 ml	40% (w/v) acrylamide stock
	3 ml	Distilled water
	60 µl	10% (w/v) SDS
	30 µl	10% (w/v) ammonium persulphate
	7 µl	TEMED
Stacking Gel:	0.75 ml	Buffer B (0.5 M Tris pH6.8)
	0.375 ml	40% (w/v) acrylamide stock
	1.85 ml	Distilled water

30 µl	10% (w/v) SDS
15 µl	10% (w/v) ammonium persulphate
7 µl	TEMED

Protein samples were prepared as follows; 4X loading buffer (8% SDS (w/v), 20% β-mercaptoethanol (v/v), 40% glycerol (v/v), Brilliant Blue R in 0.32 M Tris pH 6.8) was added to the protein samples, which were then boiled at 95°C for 5 min, and immediately placed on ice. Samples were then loaded into the appropriate lanes along with 3 µl of Precision Plus® protein molecular weight marker (BioRad). Both samples and protein markers were electrophoretically separated for 120 min at 100 V.

2.6.1.4 Wet transfer

The wet or tank transfer method of Towbin *et al.* was utilized for electrotransfer of proteins to membrane in all circumstances (Towbin, Staehelin and Gordon 1979). This was accomplished using a Mini PROTEAN® Trans Blot Module (BioRad, CA, USA) according to the manufacturer's instructions. Following SDS-PAGE electrophoresis, gels were removed from glass plates and the stacking gel was discarded. The resolved gel was then soaked for 10 min in transfer buffer (25 mM Tris, 192 mM Glycine, 20% methanol) to remove any SDS complexes bound to the gel that could affect successful protein transfer. At this time, the transfer cassette was assembled and nitrocellulose membrane (Millipore) was cut to the exact dimensions of the resolving gel and allowed to soak in transfer buffer for 5 min. Following the gel and membrane pre-soakings, the transfer cassette accompanying the Mini-PROTEAN® electrophoresis system (BioRad, CA, USA) was assembled as in Figure 2.10 below.

Once assembled, the cassette was checked to be free of air bubbles by rolling a 2 ml pipette over the cassette while submerged in transfer buffer to

remove any residual bubbles. The cassette was then placed in the Trans Blot Module with the correct orientation and subjected to 100 V for 2 hrs.

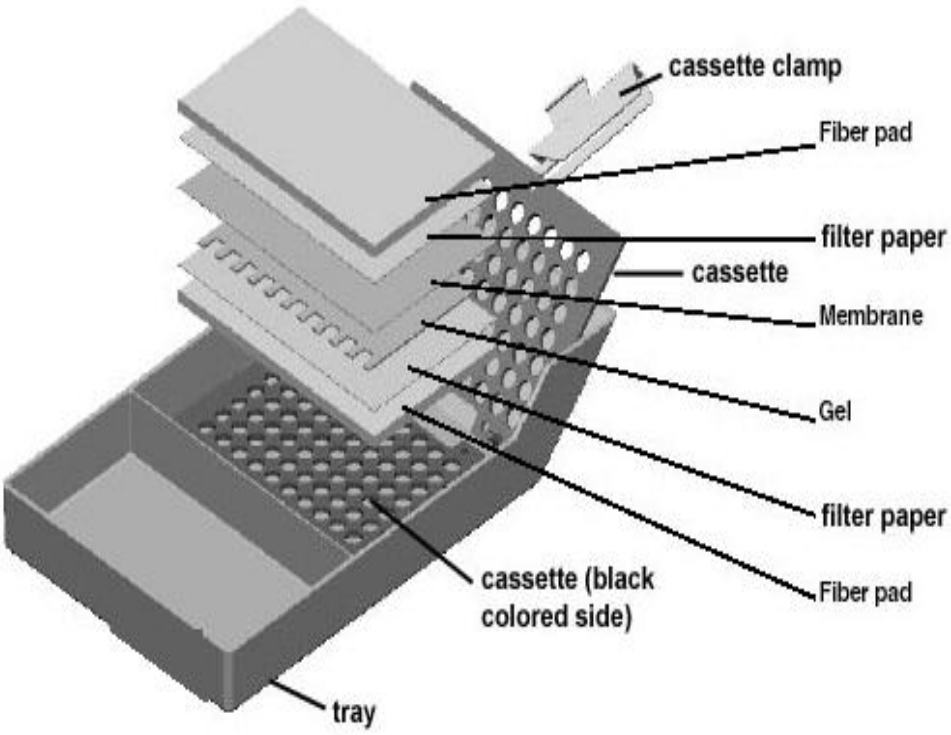

Figure 2.10: Figure shows the layout of the transfer cassette used to transfer electrophoresed proteins from an SDS-PAGE gel to nitrocellulose membrane. The black coloured side is assembled face down, overlaid with a fibre pad, filter paper, resolved gel, nitrocellulose membrane, filter paper, and fibre pad, and sealed using the cassette clamp.

2.6.1.5 Ponceau S staining

To visually confirm uniform transfer of protein to the nitrocellulose membrane, Ponceau S stain was applied. Ponceau S is a negative stain, which binds to positively charged amino acid groups of proteins. It also binds non-

covalently to non-polar regions of proteins. Transferred protein was detected as red bands on a white background. This staining technique is reversible to allow further immunological analysis. Following electrophoretic transfer, the nitrocellulose membrane was immersed in 20 ml Ponceau S solution (Sigma-Aldrich, Dorset, UK) and stained for 3 min with constant agitation. After proteins were visualised, the membrane was washed in several changes of dH_2O until all the stain had been washed away. The membrane was then used for immunological probing.

2.6.1.6 Immunoblotting and chemiluminescence band detection

Membranes were blocked for 90 min in blocking solution (5% (w/v) BSA in Tris Buffered Saline (TBS), 10 mM Tris pH 8.0, 150 mM NaCl). Membranes were then incubated overnight at 4°C with primary antibody (Table 2.2), with gentle agitation on a rocker (Stuart Scientific, Rocker SSL4, Staffordshire, UK).

Primary Antibody	Primary Dilution	Secondary Antibody	Secondary Dilution
vWF (Abcam)	8 µg/ml	Rabbit	1:2000
NEP (Alpha Diagnostics)	2 µg/ml	Goat	1:500
TOP (AbCam)	0.5 µg/ml	Mouse	1:2000
MHC I (BioLegend)	10 µg/ml	Mouse	1:1000
GAPDH (Santa Cruz)	0.4 µg/ml	Rabbit	1:3000

Table 2.2: Primary and secondary antibody dilutions. This table displays the optimised primary and secondary antibody dilutions for proteins monitored by Western blot, and the commercial sources of antibodies.

Following primary incubations, membranes were washed 3 times for 5 min in wash buffer (0.5% TBST). Membranes were subsequently incubated with the appropriate secondary antibody in TBST (5% BSA (w/v)) for 2 hrs with gentle agitation at room temperature. Membranes were then washed again using the same conditions described above.

Supersignal® West Pico (Pierce, Cheshire, UK) was the chemiluminescent substrate used for detection of horseradish peroxidise (HRP)-conjugated secondary antibodies. This was prepared according to the manufacturer's instructions and incubated with the membranes for 5 min, following which excess substrate was removed and the chemiluminescent signal was detected in a dark room by autoradiography (GE-Healthcare, Bucks, UK).

2.6.1.7 Coomassie gel staining

Coomassie gel staining is used to visualise protein bands on an SDS-PAGE gel. This is a useful technique to ensure that the transfer method worked as expected. In brief, the SDS-PAGE gel was overlaid with filtered (0.25 μm) coomassie solution whilst rocking for approximately 4 hrs. The gel was then de-stained, whilst rocking, in a methanol:acetic acid (50:50) solution until the protein bands appeared clear and distinct with no background staining, changing the de-stain solution regularly.

2.6.2 Immunocytochemistry

In order to visually monitor the expression and/or subcellular localization of proteins, cells were prepared for immunocytochemical analysis as previously described by Groarke *et al.* with some minor modifications (Groarke, et al. 2001). BAECs and HAECs were washed 3 times in PBS and fixed with 3% (v/v) formaldehyde for 15 min. Cells were subsequently washed in PBS 3 times; at this

point samples could be stored in PBS for up to 2 days at 4°C. Permeabilisation was achieved using 0.2% (v/v) Triton X-100 for 15 min, following which cells were again washed 3 times. Cells were then blocked for 30 min in PBS containing 5% (w/v) BSA solution. After blocking, cells were incubated with the appropriate primary antisera or stain (Table 2.3), followed by 3 washes in PBS and a 1 hrs incubation with 1:400 Alexa Fluor 488 anti-mouse (TOP) or anti-goat (NEP) antisera. Again cells were washed 3 times in PBS after which, nuclear DAPI staining was performed by incubating cells with 500 ng/ml DAPI for 3 min. Samples were then washed for a final time and mounting medium was added to the cells. Samples were visualised by standard fluorescent microscopy (Nikon Eclipse Ti, Tokyo, Japan).

Primary Antibody/Stain	Dilution
NEP (R&D Systems)	1:20 (1 hrs)
TOP (Abcam)	1:25 (1 hrs)
F-actin (Invitrogen)	1:50 (1 hrs)
DAPI	1:2000 (2 min)

Table 2.3: Immunocytochemistry primary antibody dilutions. Table displays the optimised incubations for all primary antibody and stain dilutions of proteins monitored by immunocytochemistry.

2.7 Luciferase assay

Following transfection of HAECs with pRL-CMV Renilla vector (normalising control) and either pGL3-TOP or pGL3-CONT firefly vector (TOP or empty vector) (Morrison and Pierotti 2003), cells were sheared and promoter activity was determined by means of a dual glow luciferase assay. Firefly luciferase from the firefly *Photinus pyralis*, a monomeric 61 kDa protein, and *Renilla* luciferase, a 36 kDa protein, both catalyse luciferin oxidation using ATP-

Mg^{++} as a co-substrate. In this luminescent reaction, light is produced by converting the chemical energy of luciferin oxidation through an electron transition to form oxyluciferin. In the conventional assay for luciferase, a flash of light is generated that decays rapidly after the enzyme and substrates are combined.

Luciferase assay reagent was prepared by reconstituting luciferase assay substrate with luciferase assay buffer (Promega, WI, USA) and stored in aliquots protected from light at -80°C. Sufficient time was allocated to allow the luciferase detection reagent to equilibrate to room temperature before use. A volume of 20 µl of cell lysate was dispensed into individual wells in a white 96-well plate, along with 20 µl of 1X lysis buffer to act as a blank. Subsequently, 100 µl of luciferase assay reagent was added to the lysate and mixed by repetitive pipetting ensuring no bubbles were produced. This was read on a luminometer (Labsystems, Luminoskan 391A, NJ, USA) to obtain Firefly luciferase activity results. 100 µl 'Stop and Glow' reagent was then added to each well; this quenches the luminescence from the firefly reaction by at least 10,000-fold and provides the substrate for *Renilla* luciferase. This latter activity was then read on the luminometer.

2.8 Flow cytometry

Flow cytometry may be defined as a technology to measure properties of cells as they move, or flow, in liquid suspension. Most flow cytometers can measure two kinds of light from cells, light scatter and fluorescence. Light scatter is the interaction of light and matter. All materials, including cells, will scatter light. In the flow cytometer, light scatter detectors are located opposite the laser (relative to the cell), and to one side of the laser, in-line with the fluid-flow/laser beam intersection. The measurements made by these detectors are called forward scatter and side scatter, respectively. Forward scatter provides information on the relative size of individual cells, whereas side scatter provides information on the relative granularity of individual cells. Fluorescence is the property of a molecule

to absorb light of a particular wavelength and re-emit light of a longer wavelength. The wavelength change relates to an energy loss that takes place during the process.

FACS analysis was performed for optimisation of transfection reagents and machines, using a GFP marker. FACS analysis was also carried out for cell proliferation studies (Section 2.8.1).

2.8.1 CFSE staining

Carboxyfluorescein diacetate succinimidyl ester (CFDA-SE) is a highly cell-permeable reagent. CFDA-SE is non-fluorescent; however, as it enters the cytoplasm of cells, intracellular esterases remove its acetate groups. This converts the molecule to the fluorescent ester, carboxyfluorescein succinimidyl ester (CFSE), which is retained within cells and covalently couples to intracellular molecules. Due to this covalent coupling reaction, fluorescent CFSE is retained within the cell, for extremely long periods. Also, due to this stable linkage, once incorporated within cells the dye is not transferred to adjacent cells. Thus, decreasing levels of CFSE in cells is a useful index of cellular proliferation.

Post-shear BAECs and HAECs were trypsinised and a cell count performed. Cells were then seeded to 6-well plates, 50,000 cells per well. After 4 hrs, samples were washed in 1X PBS and stained with CFSE, 5 µM/ml in 0.1% BSA/PBS, for 15 min at 37°C. Cells were then washed in PBS and fresh medium added. After 30 min, cells were trypsinised and analysed on the FACS Guava (Millipore, MA, USA) (Figure 2.11). Cells were then analysed every 24 hrs.

Figure 2.11: Figure shows the Millipore FACS Guava system, with analysis software and 96-well plate sample reading format.

2.9 Proliferation

2.9.1 xCELLigence®

The xCELLigence® system (Roche, Basal, Switzerland) monitors cellular events in real time without the incorporation of labels. The system measures electrical impedance across micro-electrodes integrated on the bottom of tissue culture E-Plates. The presence of the cells on top of the electrodes affects the local ionic environment at the electrode/solution interface, leading to an increase in the electrode impedance. The more cells that are attached on the electrodes, the larger the increases in electrode impedance (Figure 2.12). Thus making this

system ideal for the monitoring of adhesion and proliferation patterns in both BAECs and HAECs.

Following shear experiments, cells were trypsinised and a cell count performed (Section 2.2.4.2); 4,000 cells per condition were then added per well in a 16-well E-Plate. Initial adhesion of the cells was measured at 5 min intervals from 0-7 hrs. After this, measurements were extended to every 25 min for up to 6 days for the monitoring of cell proliferation. Feeding of cells occurred every 24 hrs just after a time point, to minimize the effect of the medium change on results. This was done by removing 100 µl of medium from each well and replacing it with 100 µl of fresh medium. Water levels were also maintained in reservoirs surrounding each well, to provide an efficient heat transfer to the medium.

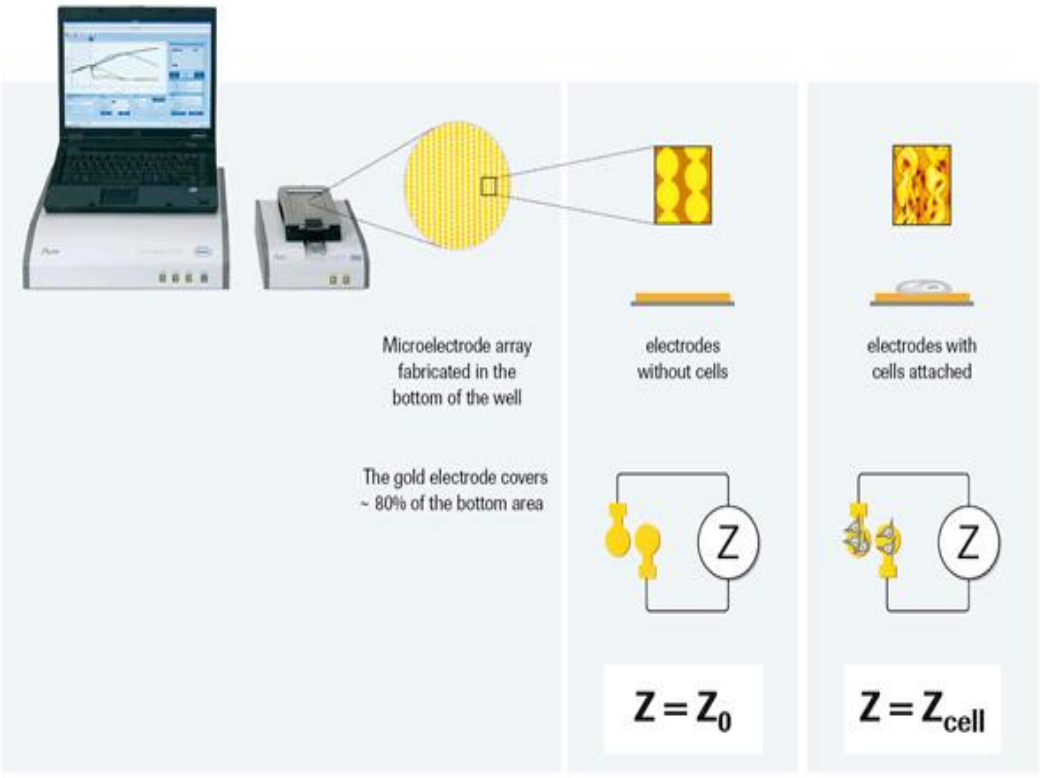

Figure 2.12: Figure shows the xCELLigence® system with E-plate attached. Figure also demonstrates how cell impedance is measured (www.roche-applied-science.com).

2.10 Bradykinin ELISA

HAECs were transfected with either TOP siRNA (1 µM) or a TOP over-expression plasmid (3 ng) and sheared for 24 hrs at 10 dynes/cm^2, after which they were washed in sterile 1X PBS. HEPES-Krebs buffer was then added to cells at 2 ml per well. Inhibitors were added to each well for blockade of ACE (Captopril 10 µM), ECE and NEP (Phosphoramidon 2 nM) activity. After 30 min, bradykinin was added (20 ng) per well and cells left to incubate for 12 hrs at 37°C. Following incubation, medium samples were collected for analysis, using a BK ELISA kit (Enzo Life Sciences, NY, USA), following the manufactures instructions.

Briefly, 150 µl of assay buffer was added to non-specific binding wells and 100 µl of assay buffer into the Bo wells (0 ng/ml standard). 100 µl of standards and samples were also added to the appropriate wells. 50 µl of BK conjugate and 50 µl of BK antibody were then added to the appropriate wells. The plate was then sealed and incubated on an orbital rotator for 2 hrs at 300 rpm at room temperature. The wells were then washed three times with 400 µl of wash buffer and the plate tapped dry onto lint-free paper. 200 µl of HRP conjugate was added to the appropriate wells and the plate sealed and incubated on an orbital rotator for 30 min at 300 rpm at room temperature. The wells were then washed again, as above. 200 µl tetramethylbenzidine (TMB) substrate was added to each well and the plate sealed and left for 30 min at room temperature, without shaking. 50 µl of stop solution was added to each well and the plate was read at 450 nm on an EL*x*800 microplate reader (BioTek, VT, USA) (Figure 2.13). (Note. Amount of signal is inversely proportional to the level of BK in the sample).

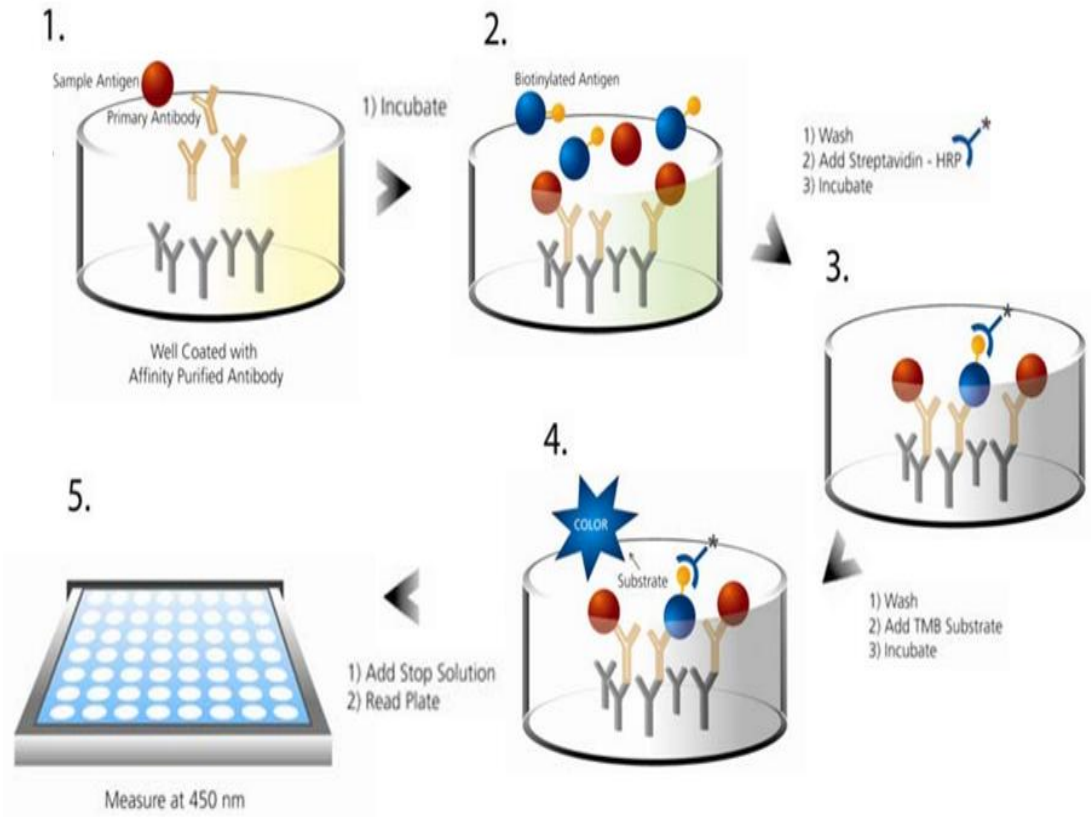

Figure 2.13: Figure shows the principle steps in the BK elisa. (1-2) Incubation of standards and samples in pre-coated wells of a 96-well plate; (2-3) after washing of the plate, HRP conjugate is added to the wells and incubated; (3-4) after further wash steps, TMB substrate is added to the wells and incubated again; (4-5) the reaction is quenched using a stopping buffer and results are obtained using plate reader at 450 nm (http://www.enzolifesciences.com).

2.12 Statistical analysis

Results are expressed as mean±sem. Experimental points were performed in triplicate with a minimum of three independent experiments (n=3). Statistical comparisons between controls versus treated groups were made by Student's unpaired *t*-test and Wilcoxon Signed-Ranked test (for non-parametric comparisons). A value of $*P \leq 0.05$ (or $\Phi P \leq 0.05$) was considered significant.

Chapter 3:

Preliminary characterisation studies and investigation of shear-mediated regulation of neprilysin (NEP) expression.

3.1 Introduction

As a consequence of its unique location, the ability of the endothelium to sense and respond to changes in the vascular environment is of paramount importance to vascular health. ECs utilise the presence of mechanosensors in their plasma membrane to convert the physical pressure of hemodynamic forces, such as cyclic strain and shear stress, into biochemical signals that can alter the cells gene expression profile. In addition to changes in gene expression, shear activates various signalling pathways which can modulate cell morphology, barrier function, proliferation and migration. Of direct relevance to this thesis is the shear-sensitive zinc metallopeptidase family. Various members of this family have been shown to possess vasoconstrictive (NEP) or vasodilatory (TOP) properties, and as a result are viable targets for therapeutic applications. In view of the relevance of flow to endothelial health and dysfunction, therefore, it is necessary to determine how these enzymes are regulated by flow in ECs and the signalling pathways involved.

Of specific interest to this chapter is the vasoconstrictor NEP, a pivotal regulator of natriuresis and vascular tone. It has previously been shown to be a shear-sensitive enzyme and to contain a SSRE in its promoter region (-GAGACC-), similar to that found in the ACE and ECE gene promoter regions (Kim, et al. 2003, Li, et al. 1995). Previous work from this laboratory has also confirmed NEP down-regulation under shear to be dependent on a Gβγ signalling pathway, with evidence also suggesting roles for NADPH oxidase and ROS (Fitzpatrick, et al. 2009).

The aims of this chapter are four fold: (i) to characterise the cell types studied as endothelial; (ii) to assess the effects of physiologically relevant levels of laminar and disturbed shear on the morphology and barrier function of both BAECs and HAECs; (iii) to assess the effects of physiologically relevant levels of laminar and disturbed shear on NEP expression (with relation to dose and time) using qPCR and immunocytochemistry; and (iv) to examine the role of NADPH oxidase and ROS in the shear-dependent regulation of NEP expression levels.

3.2 Results

3.2.1 Characterisation of endothelial cells

3.2.1.1 Endothelial cell markers

Endothelial cells contain specific markers that are easily characterised to ensure the validity of our commercially-sourced cell lines. These include Von Willebrand Factor (vWF) and endothelial nitric oxide synthase (eNOS). vWF protein was clearly expressed in both BAECs and HAECs (Figure 3.1 A). eNOS mRNA was detected in both BAECs and HAECs (Figure 3.1 B).

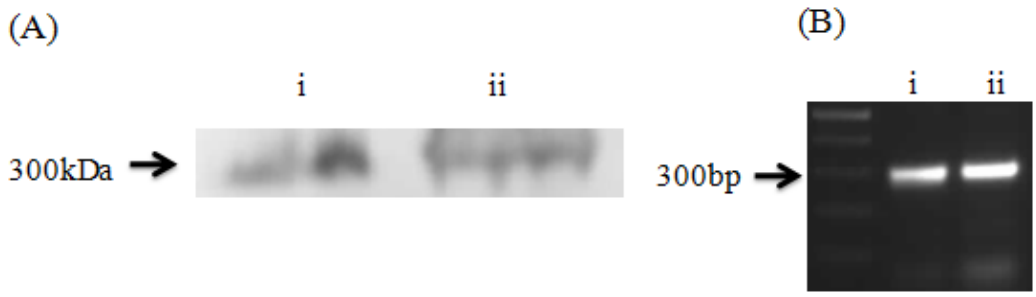

Figure 3.1: Characterisation of endothelial cells. (A) Shows the presence of the endothelial cell marker vWF as detected by Western blot in (i) BAECs and (ii) HAECs. (B) Shows the presence of endothelial cell marker eNOS as detected by RT-PCR in (i) BAECs and (ii) HAECs. Blots are representative.

3.2.1.2 Endothelial cell morphology

BAEC and HAECs were grown to confluency and monitored by phase-contrast microscopy for characteristic growth patterns and typical 'cobblestone' shaped morphology (Figure 3.2). Following application of LSS (10 dynes/cm^2, 24 hrs), cells realign in the direction of flow. The cells now have a more

streamlined shape to minimise the frictional force of shear, the tapered end of each cell pointing in the direction of flow.

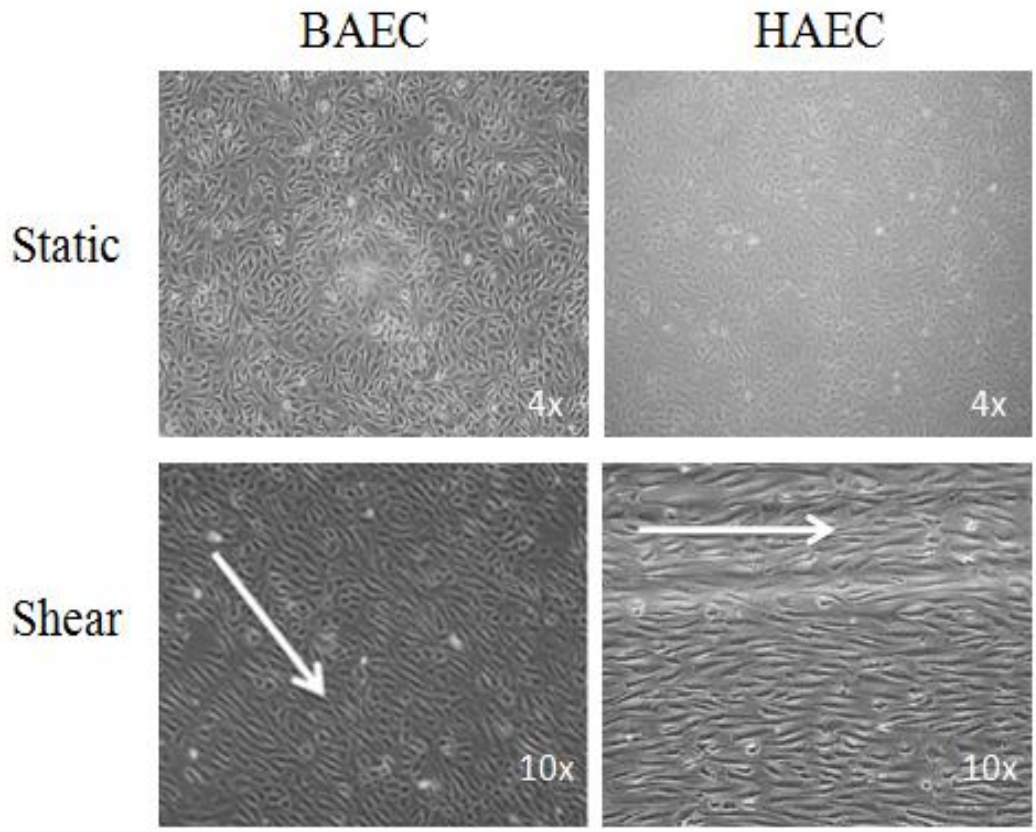

Figure 3.2: Endothelial cell morphological alterations in response to LSS compared to static control cells. BAECs were sheared by orbital rotation, while HAECs were sheared using the ibidi® system. White arrows indicate the direction of the flow. Images are representative.

3.2.1.3 Actin realignment in response to shear

BAECs and HAECs (Figure 3.3) were exposed to either LSS (10 dynes/cm^2) or disturbed shear stress (DSS) for 24 hrs. The realignment of the structural actin filaments becomes visible within 6 hrs of LSS onset and is fully evident after 24 hrs. However, as a result of the non-uniform and multi-directional flow of medium in the disturbed shear samples, the DSS-treated cells are not able to adjust their morphology in response to the shear stimulus and resemble static control cells. This was visualised using fluorescence microscopy with phalloidin stain for F-actin (Invitrogen, Groningen, The Netherlands).

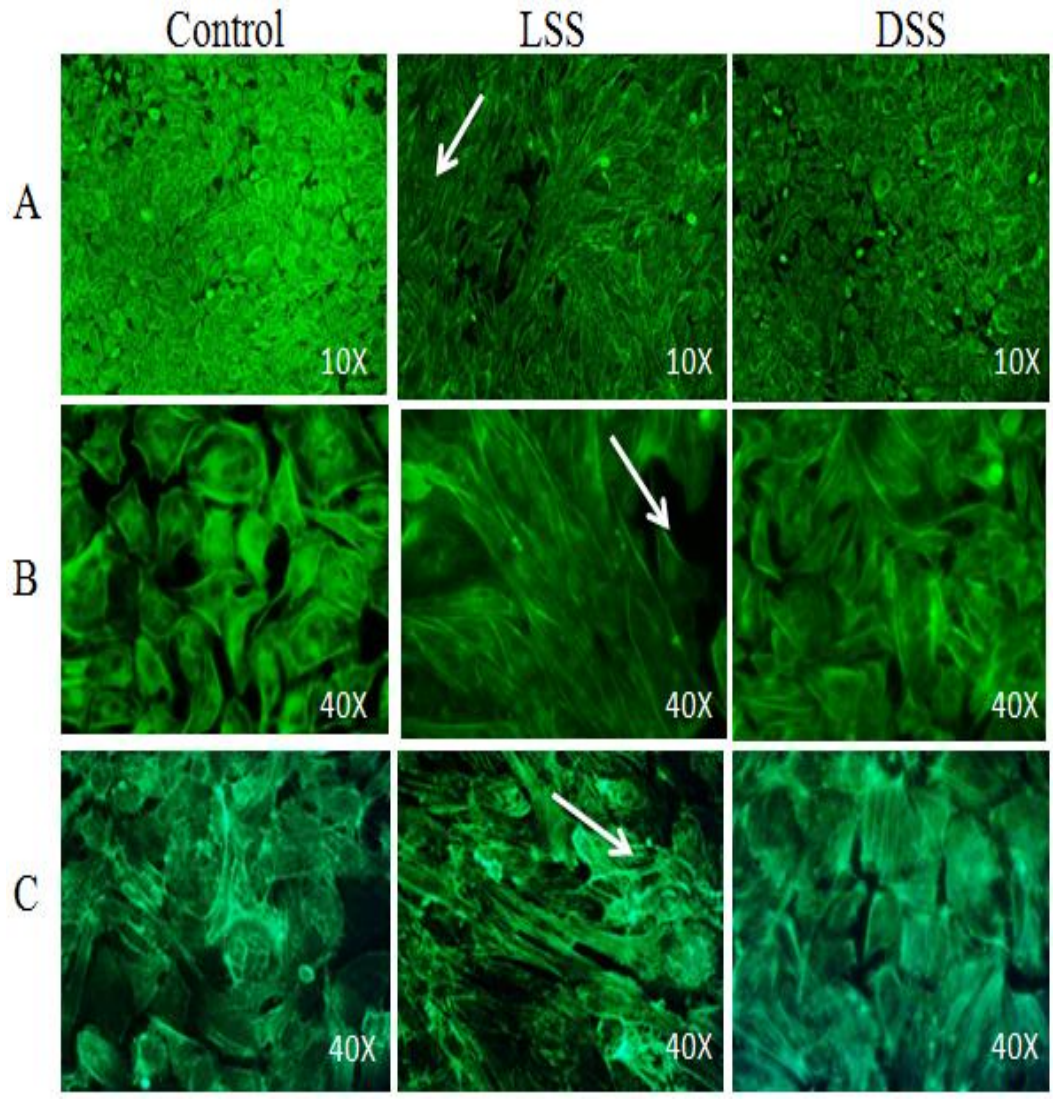

Figure 3.3: F-actin staining. Confluent BAECs (A,B) and HAECs (C) were exposed to LSS (10 dynes/cm^2, 24 hrs), and monitored for F-actin realignment using fluorescent microscopy (phalloidin stain for F-actin). BAEC and HAEC F-actin filaments realign in the direction of flow under LSS. No F-actin realignment is observed under DSS conditions, which instead closely resemble static control cells. Images are representative.

3.2.1.4 The effect of shear stress on EC barrier integrity

Under physiological levels of LSS, barrier function in ECs is increased, thus preventing unwanted solutes from crossing the endothelium and consistent with the 'atheroprotective' nature of LSS. This is most prominent in the blood-brain barrier of the microvasculature, but is an effect also seen throughout the

macrovasculature. A weakened barrier can be caused by disturbed shear and it is at these sites that endothelial dysfunction may occur and atherosclerotic plaques may be initiated.

Both BAECs and HAECs were grown to confluency and subjected to either LSS, 10 dynes/cm^2, (Figure 3.4) or DSS (Figure 3.5) for 24 hrs. Barrier integrity was then measured by transendothelial permeability assay as previously described (Walsh et al., 2011) using FITC-dextran (40 kDa). Higher levels of FITC-dextran in the basolaterally-harvested medium samples indicates a weakening of EC barrier integrity. As can be seen with both BAECs and HAECs (Figure 3.4), barrier integrity is significantly enhanced under LSS over a 24 hrs period. Conversely, with DSS of both BAECs and HAECs (Figure 3.5), barrier integrity is slightly weakened.

Blood flow in different areas of the vasculature can vary greatly, ranging from almost static in parts of the liver to 30 dynes/cm^2 in the aorta (Vanhoutte 1989). Blood flow can also fluctuate as a result of plaque build-ups and blockages in the vasculature. As a consequence, it was also decided to investigate the effect of *varying* levels of LSS on both BAEC and HAEC barrier integrity. Confluent BAECs and HAECs were exposed to low (1 dyne/cm^2, 24 hrs) or normal (10 dynes/cm^2, 24 hrs) LSS. Barrier integrity was then measured by transendothelial permeability assay. Results indicated that there was no significant change in barrier integrity under low LSS conditions when compared to static control cells. Data not shown.

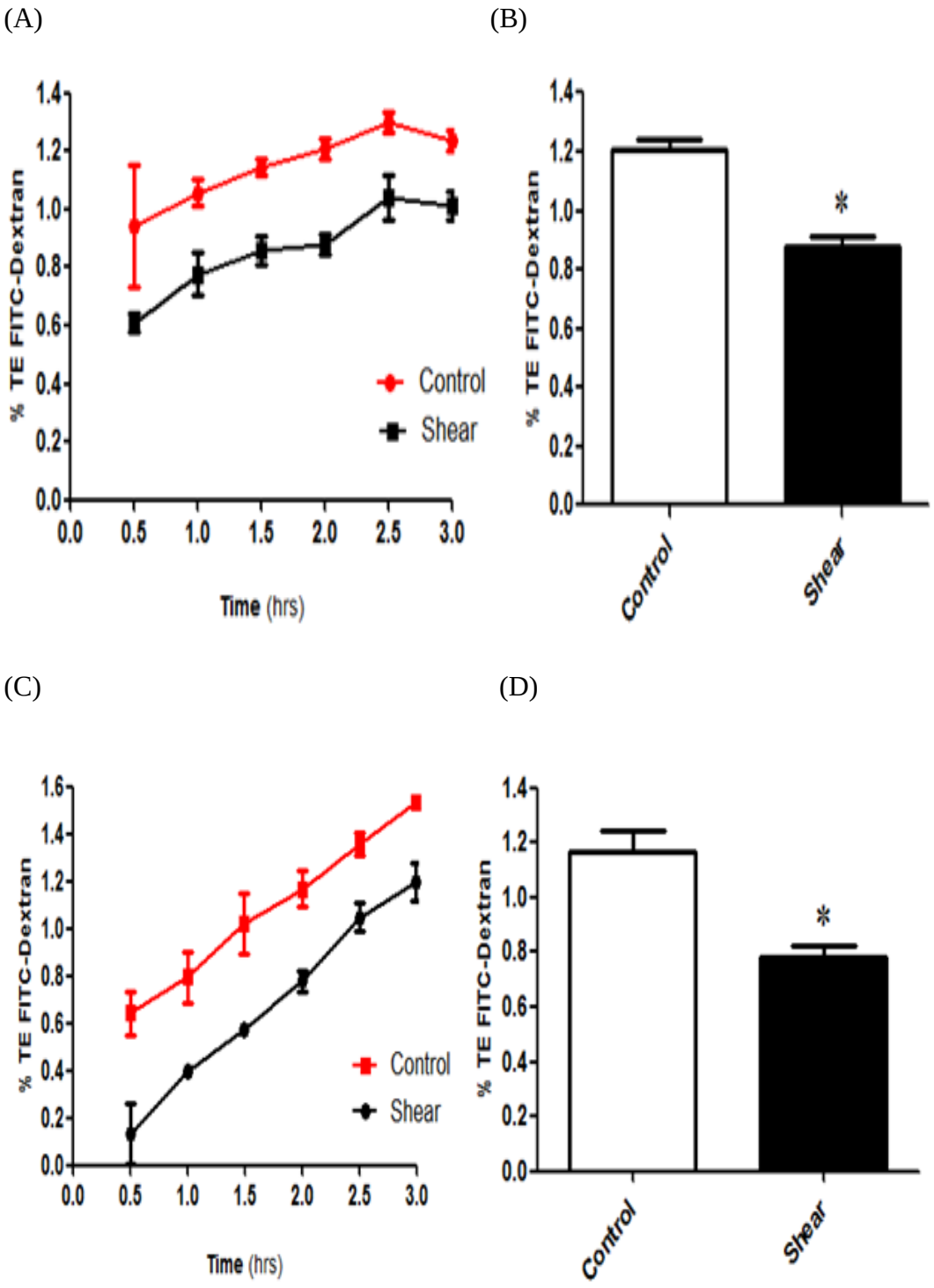

Figure 3.4: The effect of LSS on paracellular permeability in BAECs (A, B) and HAECs (C, D). Confluent BAECs and HAECs were subjected to LSS (10 dynes/cm^2, 24 hrs), harvested and replated in transwell inserts and monitored by transendothelial permeability assay, as described in methods. (A, C) Line graphs showing the % trans-endothelial exchange of FITC-Dextran over 3 hrs. (B, D) histograms showing the difference in permeability after 2 hrs of exchange. Results are averaged from three independent experiments ±SEM; *$P \leq 0.05$ vs static control cells.

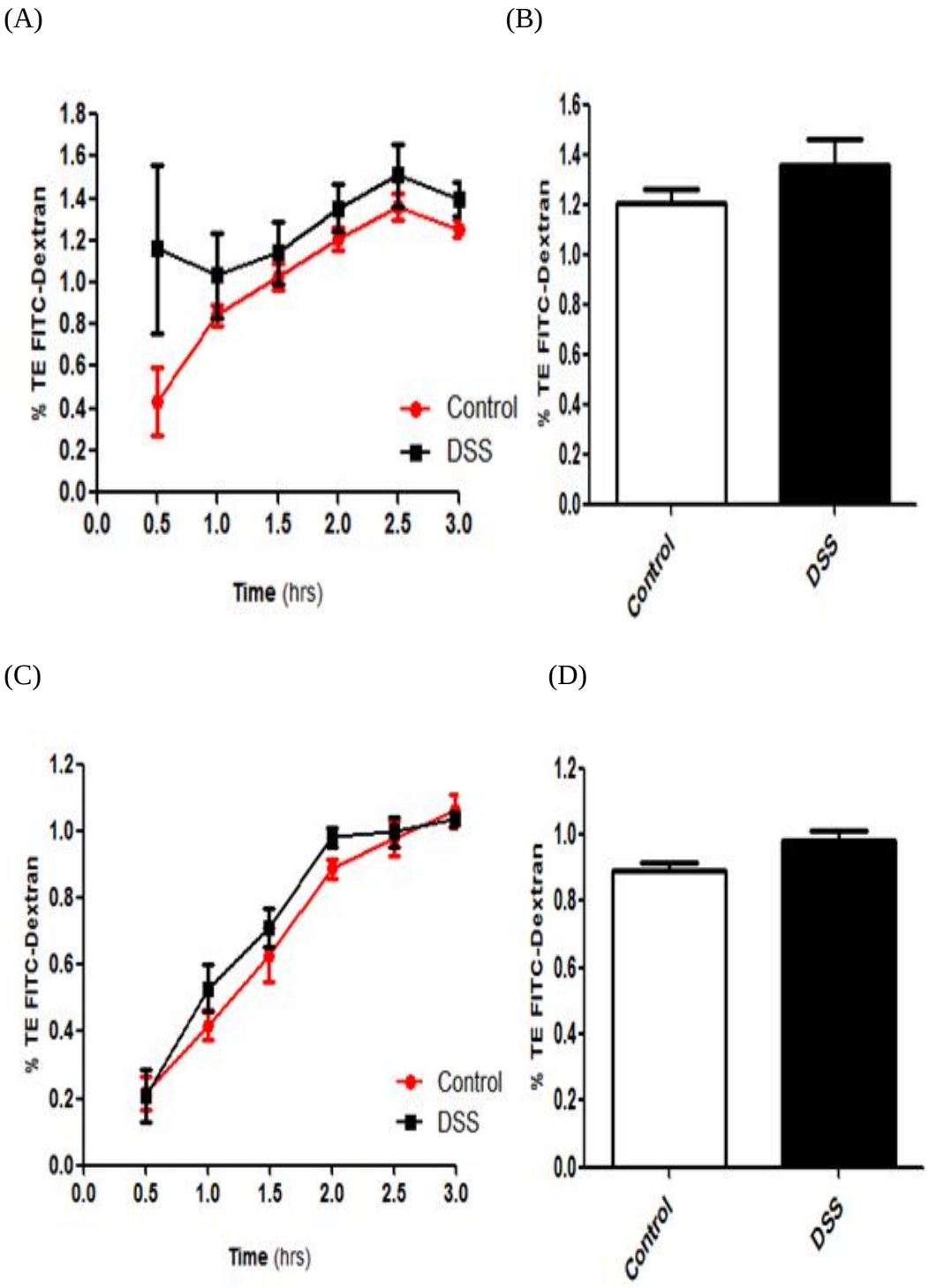

Figure 3.5: The effect of DSS on paracellular permeability in BAECs (A, B) and HAECs (C, D). Confluent BAECs and HAECs were subjected to DSS (10 dynes/cm^2, 24 hrs), harvested and replated in transwell inserts and monitored by transendothelial permeability assay, as described in methods. (A, C) Line graphs showing the % trans-endothelial exchange of FITC-Dextran over 3 hrs. (B, D) histograms showing the difference in permeability after 2 hrs of exchange. Results are averaged from three independent experiments ±SEM; *$P \leq 0.05$ vs static control cells.

3.2.2 The effect of shear on NEP expression

3.2.2.1 Primers and MIQE guidelines

The Minimum Information for publication of Quantitative real-time PCR Experiments (MIQE) guidelines set out to standardise the publication of qPCR results (Bustin, et al. 2009). All primers used for qPCR in this thesis fall within these new guidelines. NEP primers are calculated to be 90% efficient with an R^2 value of 0.9997. NEP primers were used on both bovine and human samples. The reference gene for all qPCR normalisation in this thesis is GAPDH. Bovine GAPDH primers were found not to amplify human samples and as a result human GAPDH primers were also designed. Bovine GAPDH primers were found to have an efficiency of 103% with an R^2 value of 0.9940, whilst human GAPDH primers were found to be 91% efficient with an R^2 value of 0.9993.

3.2.2.2 NEP primer validation

To confirm that NEP primers were specific to NEP and do not amplify non-specific targets, extensive bioinformatical analysis was carried out during the primer design stage. Standard RT-PCR was performed using these primers and the products were characterised on a 1% agarose gel. One clear band at the expected product size of 290 bp was visualised (Figure 3.6 A). All qPCR experiments performed in this study employed SYBR green detection. As SYBR green detects all amplification and is not sequence specific, dissociation, or melt curve analysis, was routinely carried out after qPCR to again ensure only NEP was being amplified (Figure 3.6 B). This involved a stepwise 1°C incremental increase in temperature over a set range, with fluorescence exhibited by the sample monitored during this time. SYBR green dye associates with double-stranded DNA. Therefore, at the temperature threshold at which the generated PCR product dissociates to yield a single-stranded product, there is a drop in the fluorescence activity. Thus, a sample with a single PCR product will demonstrate only one peak corresponding to the melting temperature of the product.

As a reference gene for all qPCR experiments, GAPDH was used to normalise results. Again RT-PCR and disassociation curves were used to ensure primers were specific to their target (Figure 3.6 C-F).

3.2.2.3 LSS down-regulates NEP expression in a time-dependent manner

It has previously been shown from work carried out in this laboratory that NEP mRNA/protein expression in BAECs is down-regulated by LSS (10 dynes/cm^2, 24 hrs) (Fitzpatrick, et al. 2009), however, neither dose- nor time-dependency studies were done for this paper. Results from the present study now demonstrate how this attenuation temporally progresses over a 24-48 hrs period.

BAECs were grown to confluency and subjected to LSS for 0-48 hrs at 10 dynes/cm^2. NEP mRNA levels were then monitored using qPCR. Results demonstrate that NEP mRNA expression is fully down-regulated (~42%) within 24 hrs and maintained at this reduced level thereafter compared to static control cells (Figure 3.7).

3.2.2.4 LSS down-regulates NEP expression in a dose-dependent manner

Areas of the vasculature which are experiencing atherosclerotic plaque build up are often associated with areas of low, high or disturbed blood flow. As such, altered expression levels of vasoactive zinc metallopeptidases might be expected in these areas. This makes the effect of low or disturbed shear on the expression profile of ECs highly important (e.g. as NEP is a vasoconstrictor, higher expression levels at low shear would lead to elevated blood pressure and related pathologies).

Both BAECs and HAECs were exposed to low (1 dyne/cm^2, 24 hrs) or normal (10 dyne/cm^2, 24 hrs) LSS levels. NEP mRNA expression was then monitored by qPCR. The trend of NEP down-regulation at 10 dynes/cm^2 (but *not* at 1 dyne/cm^2), is observed in both BAEC and HAEC (Figure 3.8).

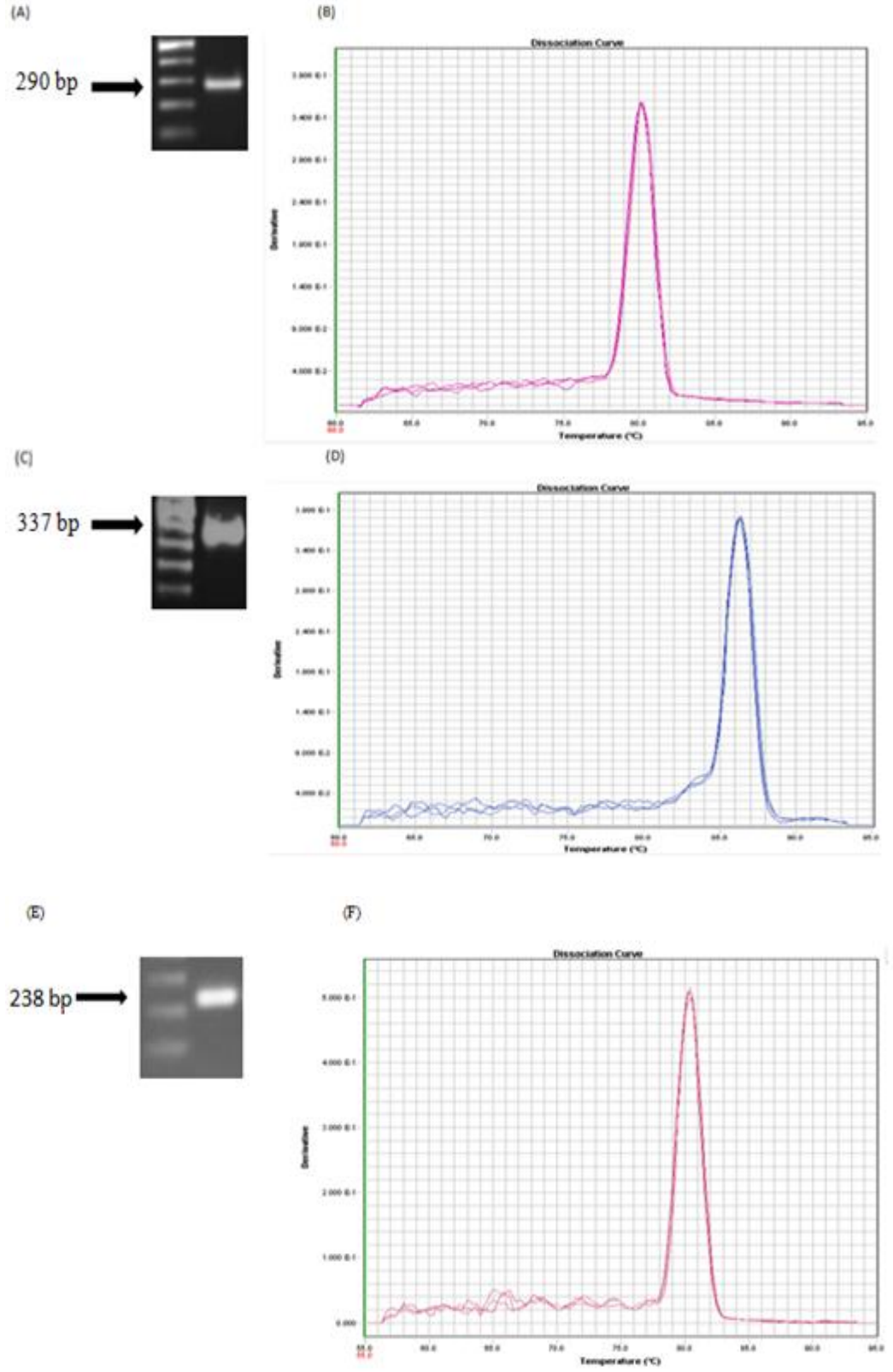

Figure 3.6: NEP, bovine GAPDH and human GAPDH primer validation. (A, C, E) Shows RT-PCR products run out on a 1% agarose gel, giving a single band at the expected product size for NEP, bovine GAPDH and human GAPDH. (B, D, F) Shows the corresponding dissociation curves. Blots and scans are representative.

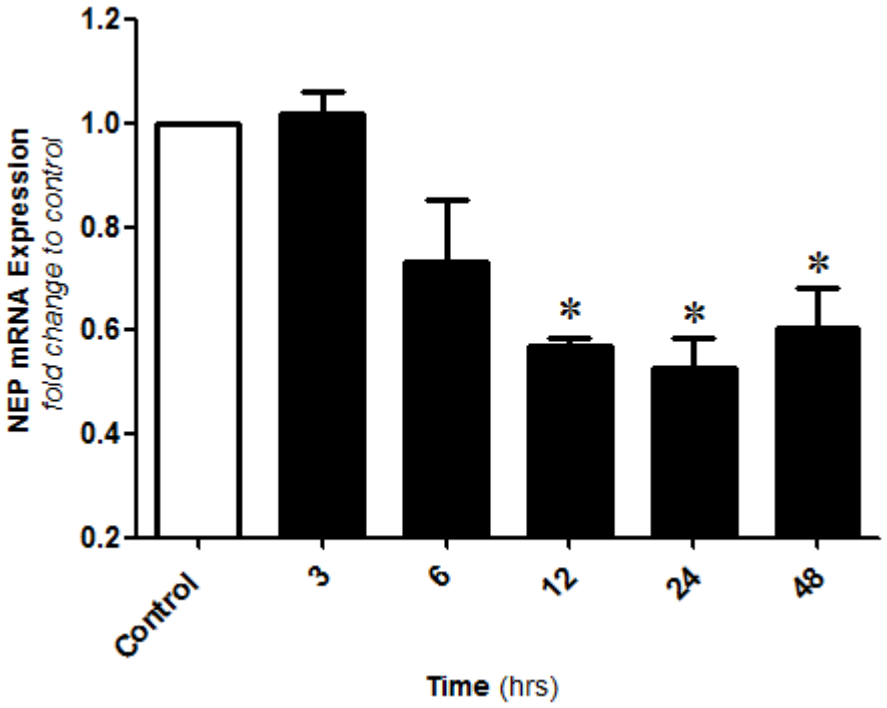

Figure 3.7: The time-dependent down-regulation of NEP mRNA in BAECs by LSS. BAECs were grown to confluency and subjected to LSS of 10 dynes/cm^2 for 3, 6, 12, 24 and 48 hrs. Cells were harvested and analysed by qPCR. Histogram shows the time-dependent attenuation of NEP expression levels. Results are averaged from three independent experiments ±SEM; *$P \leq 0.05$ vs control.

3.2.2.5 The effect of DSS on NEP expression levels

BAECs and HAECs were grown to confluency and subjected to DSS for 24 hrs. Cells were then harvested and analysed by qPCR. In direct contrast to NEP mRNA down-regulation observed under LSS conditions, DSS was not found to cause NEP mRNA attenuation in either BAECs or HAECs when compared to static control cells (Figure 3.9).

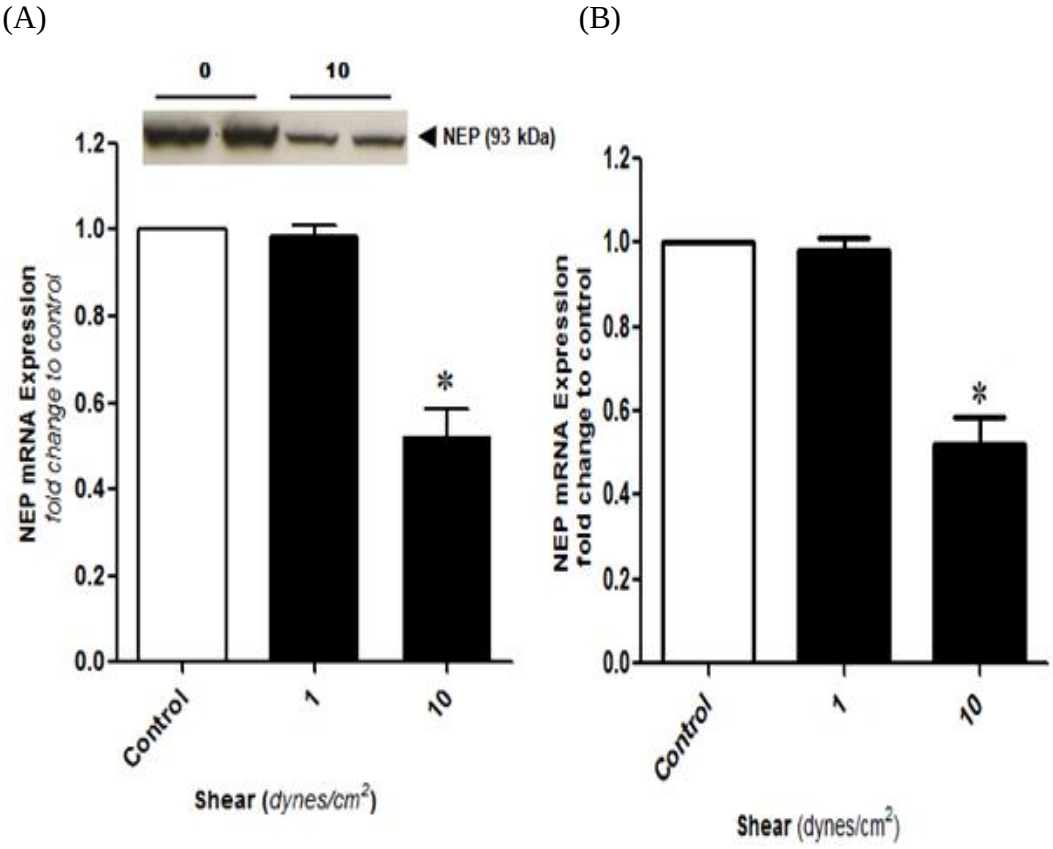

Figure 3.8: Magnitude-dependent effects of LSS on NEP mRNA expression. BAECs (A) and HAECs (B) were subjected to low (1 dyne/cm^2, 24 hrs) and normal (10 dynes/cm^2, 24 hrs) levels of LSS. Cells were harvested and analysed by qPCR. Results are averaged from three independent experiments ±SEM; *$P\leq$ 0.05 vs control. Western blot insert in (A) shows down-regulation of NEP protein at 10 dynes/cm^2 (Fitzpatrick et al., 2009). Blot is representative.

3.2.2.6 Immunocytochemical analysis of NEP expression under shear

To analyse the effect of shear variations on NEP levels, the ibidi® micro-fluidic slide-flow system was employed. Slide chambers simulate the vascular environment. HAECs were seeded onto ibidi® Y-slides and grown to confluency. Cells were then sheared using LSS (10 dynes/cm^2, 24 hrs) or oscillatory shear stress (OSS) (+/-10 dynes/cm^2, 24 hrs). Cells were then prepared for immunocytochemical staining for NEP as described in methods (Figure 3.10).

(A) (B)

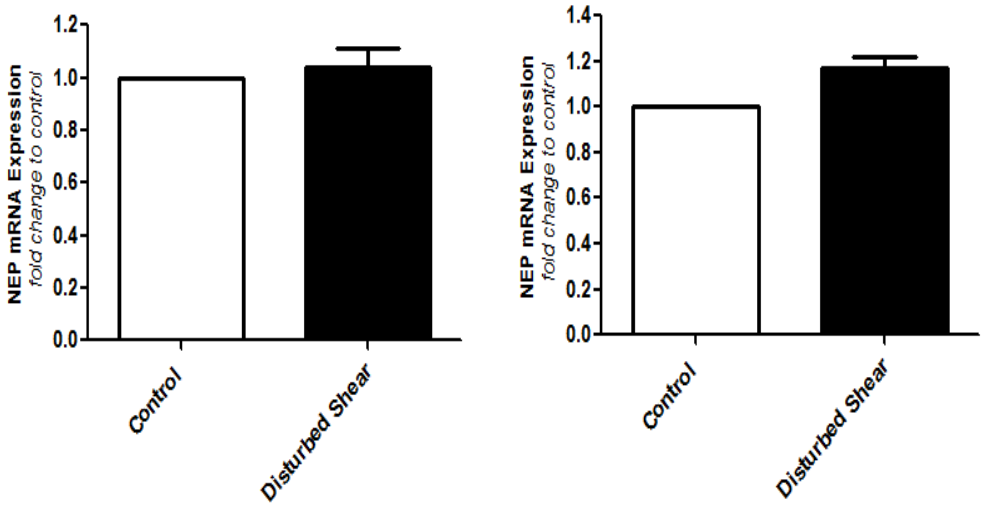

Figure 3.9: The effect of DSS on NEP mRNA expression levels. (A) BAECs and (B) HAECs were grown to confluency and exposed to DSS for 24 hrs. Cells were harvested and analysed by qPCR. Results are averaged from three independent experiments ±SEM.

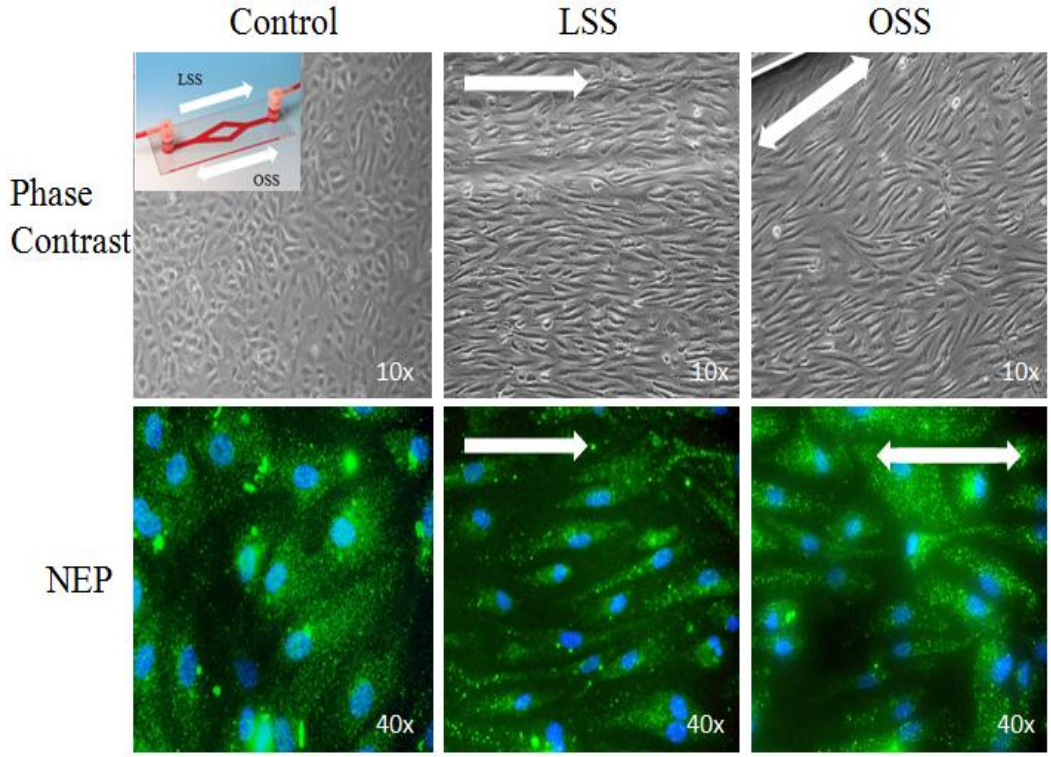

Figure 3.10: The regulation of NEP protein expression by LSS (10 dynes/cm^2) and OSS (+/- 10 dynes/cm^2). Top row shows HAECs under phase-contrast view. Bottom row shows HAEC IC images for NEP. HAECs can be seen to realign in the direction of flow under LSS. However in OSS image cells are less clearly aligned. White arrows indicate the direction of flow. Images are representative. Insert in top left-hand corner image illustrates ibidi® Y-slide format.

3.2.3 NEP signal transduction pathway

Previous work from our laboratory has demonstrated a role for ROS in the shear-dependent down-regulation of NEP (Fitzpatrick, et al. 2009). Moreover, as the major source of ROS (specifically O_2^-) in ECs is due to the activity of NADPH oxidase, it was decided to fully elucidate this by testing an siRNA directed towards the p47 subunit of the enzyme complex (the aforementioned paper only used apocynin as a test reagent). To expand on this work, it was also decided to examine the temporal relationship between shear-dependent ROS production and NEP down-regulation. Specifically, NAC was added 1 hrs before shear onset to allow sufficient time to scavenge its target, O_2^-. NAC was also added at the 4 hrs time point as it has previously been demonstrated that a ROS 'burst' occurs between 0-3 hrs after shear onset (Fitzpatrick et al., 2009; see paper in appendix); thus, addition of NAC at 4 hrs (i.e. after the surge) should indicate how significant this early ROS surge is in NEP regulation in response to shear onset.

3.2.3.1 p47 primer validation

To confirm that p47 primers were specific to p47 and not amplifying non-specific targets extensive bioinformatical analysis was carried out during the primer design stage. Standard RT-PCR was carried out using the primers and the products were characterised on a 1% agarose gel. One clear band at the expected product size of 288 bp was visualised (Figure 3.11 A). Dissociation curves were routinely carried out after qPCR to ensure only p47 was being amplified (Figure 3.11 B). As a reference gene for all qPCR experiments GAPDH was used to normalise results. As in section 3.2.2.1, p47 primers were subjected to the MIQE guidelines and found to be 102% efficient with an R^2 value of 0.9983.

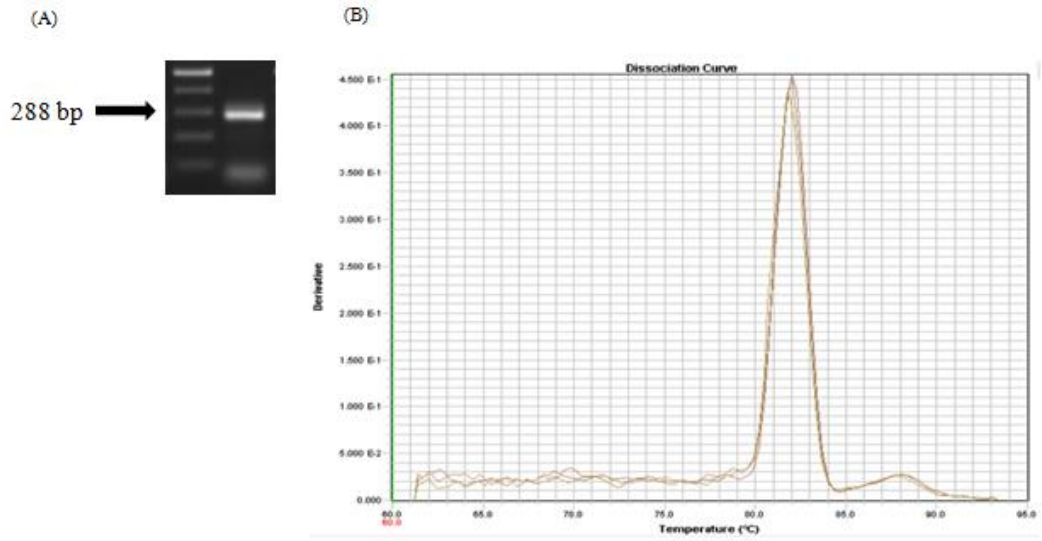

Figure 3.11: p47 primer validation. (A) Shows the product of a RT-PCR, run out on a 1% agarose gel, giving a single band at the expected product size for p47. (B) Shows the corresponding dissociation curve.

3.2.3.2 Effect of p47 siRNA

HAECs were transfected with p47 siRNA (15 nM), as determined by optimisation experiments (Figure 3.12). Controls included either mock transfection (use of transfection reagents without siRNA) or 15 nM scrambled siRNA, as both had negligible effects on NEP expression and so were used as controls. Post-transfection, cells were allowed overnight recovery before the application of LSS (10 dynes/cm^2, 24 hrs). Cells were then harvested for mRNA and analysed by qPCR. Results of this assay show that silencing of the NADPH oxidase subunit p47 leads to a negation of the expected down-regulatory effect of LSS on NEP mRNA expression (Figure 3.13).

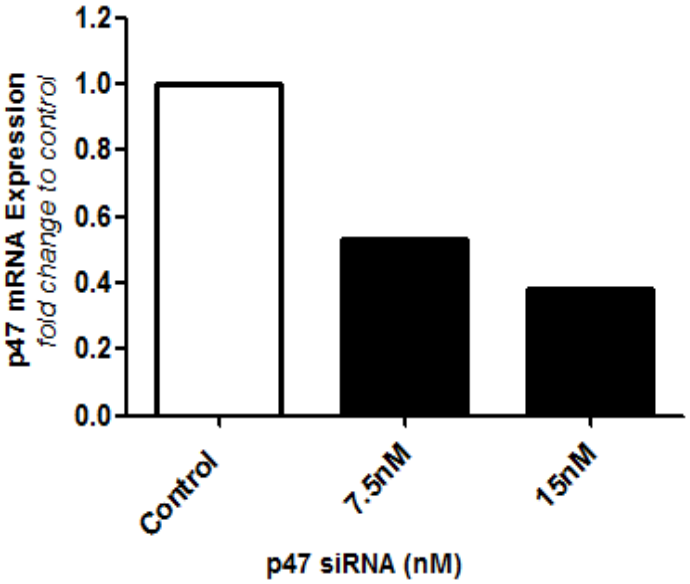

Figure 3.12: Optimisation of p47 siRNA concentrations in HAECs. Control study indicating how increasing concentrations of p47 siRNA (0, 7.5 and 15 nM) caused a marked decrease in p47 mRNA expression levels. N=1.

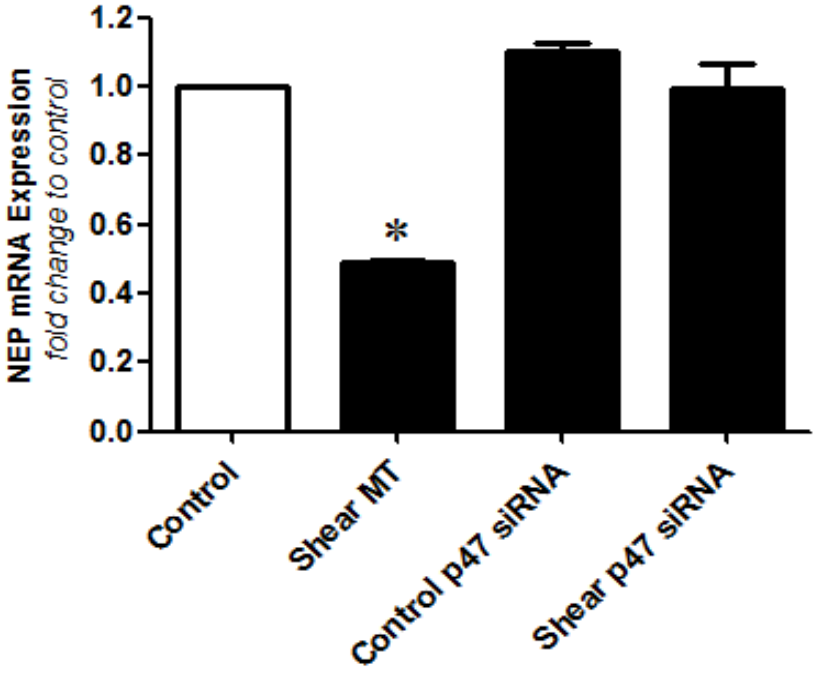

Figure 3.13: The role of NADPH oxidase in NEP mRNA expression. HAECs were transfected with p47 siRNA (15 nM) and subjected to LSS (10 dynes/cm^2, 24 hrs). Control cells demonstrated the expected NEP down-regulation in response to LSS. However, the introduction of p47 siRNA negates this effect, bringing NEP mRNA expression back to control levels. Results are averaged from three independent experiments ±SEM; *$P\leq$ 0.05 vs control. MT= mock transfection.

3.2.3.3 Effect of N-Acetyl-L-cysteine (NAC)

The antioxidant NAC (5 mM) was added to confluent BAECs 1 hrs before or 4 hrs after the onset of LSS (10 dynes/cm^2, 24 hrs). The results show that the LSS down-regulation of NEP is negated by the introduction of NAC 1 hrs prior to shear onset, but not 4 hrs post shear onset (i.e. after the ROS surge) (Figure 3.14).

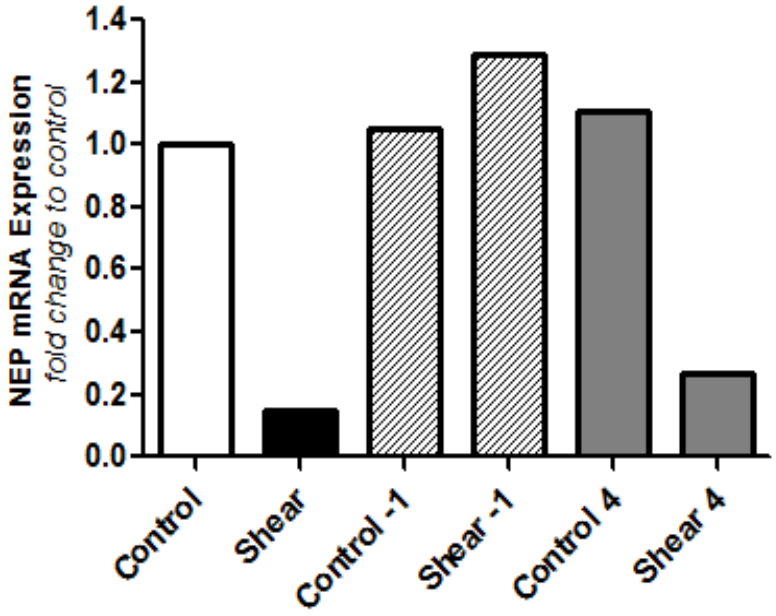

Figure 3.14: Temporal effect of NAC on shear-dependent modulation of NEP expression. BAECs were grown to confluency and NAC was added to samples 1 hrs before or 4 hrs after onset of LSS (10 dynes/cm^2, 24 hrs). N=1.

3.4 Discussion

Our initial investigation in this chapter consisted of control studies that were focused on the characterisation of our commercial cell lines through the detection of known endothelial markers. Both cell lines (BAEC and HAEC) were found to express vWF and eNOS, established endothelial markers (Jaffe, Hoyer and Nachman 1973). Moreover, characteristic endothelial cell morphological and actin filament realignment in response to physiological levels of LSS were also observed (Suciu, et al. 1997). There were various reasons behind the use of two different endothelial cell lines in this study. Earlier preliminary studies by Fitzpatrick et al. (2009) from this research group were performed in BAECs, thus serving as a platform for pursuit of further studies on NEP and TOP. HAECs were also introduced into studies because of their heightened suitability for transfection studies (particularly using the microporation system) and ultimately because of their greater translational relevance.

In further characterisation studies, the effect of physiological versus non-physiological levels of LSS on endothelial barrier integrity was compared, with significant levels of barrier strengthening (i.e. reduced permeability) noted at the higher physiological levels of shear (Krizanac-Bengez, et al. 2006, Walsh, et al. 2011). When compared with ECs that were subjected to disturbed shear (DSS), typical of curvatures and bifurcations in blood vessels, areas of high risk of developing atherosclerotic plaques, we can see that DSS results in a slight weakening of barrier integrity. This indicates a role for LSS in atheroprotection of the vasculature. It also demonstrates the role played by disturbed shear on the endothelium and the detrimental effect it may have if ECs are exposed to this pathological stimulus for long periods of time (Cunningham and Gotlieb 2004).

In subsequent investigations, we examined the regulation of the zinc metallopeptidase, NEP, by various patterns of shear stress. It can be seen from the results presented that NEP expression is attenuated in both a dose- and time-dependent manner by LSS. As NEP has been shown to act by degrading a number of vasodilatory peptides, such as those of the natriuretic peptide family for example, we can conclude that lower levels of NEP under LSS will result in

potentation of the vasodilatory effects of natriuretic peptides, with likely beneficial consequences for vascular tone and remodelling.

One can further speculate that high levels of NEP in the endothelium will invariably lead to a constriction of blood vessels through the elevated degradation of vasodilatory peptides. In this regard, results presented in this chapter have shown that under disturbed shear conditions, no NEP attenuation is observed. If DSS is applied for a prolonged period, therefore, this will likely induce higher levels of NEP production in conjunction with weakened EC barrier integrity. This will cause the affected area of the endothelium to become dysfunctional, with associated up-regulation of pro-atherogenic and pro-inflammatory genes, as well as altered migratory and proliferative profile of cells (Figure 3.15).

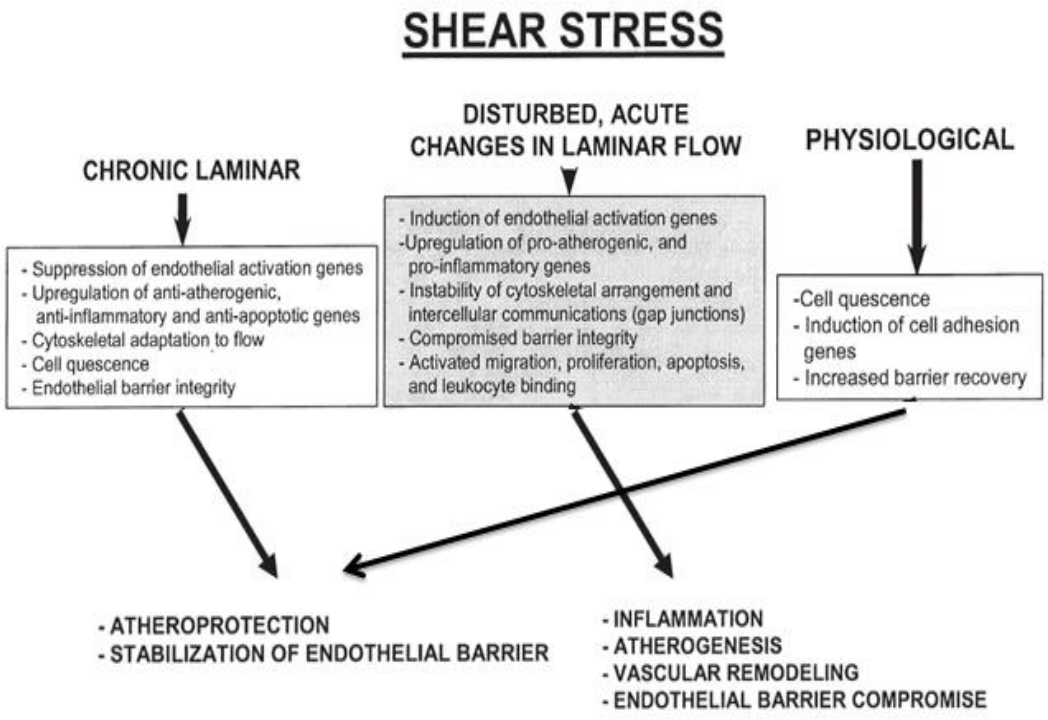

Figure 3.15: The differential responses of the endothelium to various patterns of shear stress. Physiologically relevant LSS promotes endothelial cell quiescence, induces the expression of anti-atherogenic and anti-inflammatory genes, and promotes endothelial barrier integrity. In contrast, disturbed flow induces endothelial activation, extracellular matrix production, and expression of pro-inflammatory and apoptotic genes, which may lead to vascular remodelling and propagate endothelial barrier dysfunction, atherogenesis, and inflammatory processes in the vasculature (Shepro 2006).

It has been previously published that members of the zinc metallopeptidase family are shear-sensitive, namely ECE and ACE. Studies have also demonstrated that regulation of these zinc metallopeptidases occurs in a ROS-dependent manner under LSS- ACE (Ackermann, et al. 1998), ECE (Masatsugu, et al. 2003). Therefore, the role of ROS in the shear-dependent regulation of NEP expression was also considered in this chapter, and specifically the role of NADPH oxidase, the major superoxide producer in ECs (Griendling, Sorescu and Ushio-Fukai 2000). In this respect, a p47 siRNA construct was employed to silence p47 subunit expression and effectively inhibit NADPH oxidase in endothelial cells. This subunit is known to interact with the p40 and p67 subunits to facilitate NADPH oxidase activation during a stimulus-induced temporal ROS surge (Sumimoto et al., 2005).

Our results indicate that the silencing of p47 expression (confirmed by qPCR) negates the down-regulatory effect of LSS on NEP mRNA expression levels, confirming a role for NADPH oxidase in the LSS-dependent regulation of NEP. This finding is consistent with the recent study of Fitzpatrick et al. (2009) who reported a similar result, albeit using apocynin (a pharmacological inhibitor of NADPH oxidase).

As NADPH oxidase was proven to be involved in the regulation of NEP and, as previously stated, it is also the major source of superoxide (O_2^-) in ECs, it was therefore decided to examine the role of ROS in NEPs regulation. Specifically, we were interested in the role of the early ROS surge following shear onset. Duerrschmidt et al. previously demonstrated that there is a transient activation of O_2^- formation by short term LSS (2-24 hrs) (Duerrschmidt, et al. 2006). A similar study in this laboratory showed that a ROS 'burst' occurs within 0-3 hrs post LSS onset (Fitzpatrick, unpublished data, figure 3.16 B). The levels of ROS eventually decrease to baseline levels (similar to cells under static conditions), most likely due to temporal activation of cellular anti-oxidant mechanisms, an observation consistent with the atheroprotective effects of laminar flow (Hahn and Schwartz 2009) (Figure 3.16 A).

A preliminary study was conducted whereby the antioxidant NAC was used to scavenge ROS 1 hrs prior to and 4 hrs post shear onset, bracketing the

reported ROS burst. Results indicate that the scavenging of ROS 1 hrs prior to, *but not 4 hrs post*, shear onset inhibits the effect of LSS on NEP attenuation. This clearly points to the importance of ROS production during the early phase of shear onset in the LSS-induced down-regulation of NEP expression.

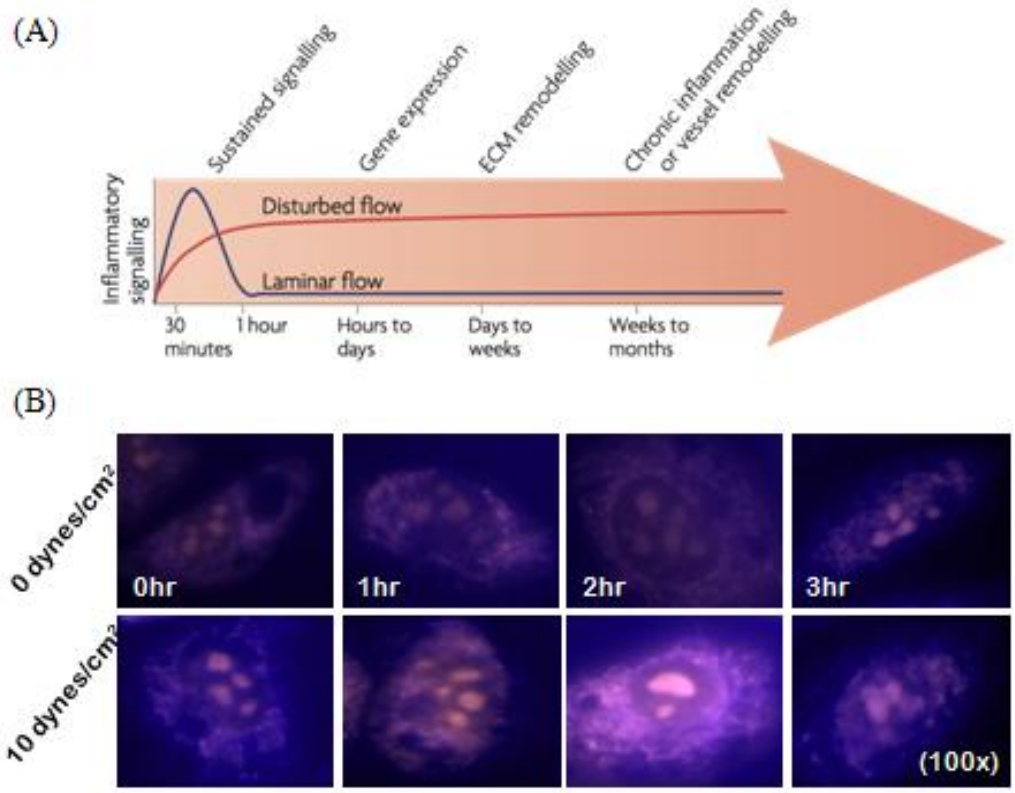

Figure 3.16: Early LSS-induced ROS production. (A) Cells under laminar flow (blue line) transiently activate various inflammatory signalling pathways, including production of ROS. Disturbed shear activates the same pathways in a sustained manner (Hahn and Schwartz, 2009). (B) Dihydroethidium staining to illustrate intracellular ROS induction (shown in pink) in BAECs under LSS (Fitzpatrick, unpublished result). Images are representative.

In conclusion, we have demonstrated the LSS-dependent increase in barrier function, which is absent under DSS conditions. Moreover, we have demonstrated the down-regulation of NEP in both a time- and dose-dependent manner under physiologically relevant levels of LSS, but not DSS. Finally, we have conclusively demonstrated the involvement of NADPH oxidase in this

signalling cascade, most likely via generation of an early ROS surge during shear onset (0-3 hrs), leading to activation of downstream signalling effectors. Downstream of oxidant production, signalling effectors mediating NEP regulation by LSS may include mitogen activated kinases (MAPKs), such as p38 and JNK (Go, et al. 1999, Huot, et al. 1997, Hashimoto, et al. 2001, Chen and Keaney Jr 2004).

Chapter 4:

Investigation of the effects of shear stress on thimet oligopeptidase (TOP) expression.

4.1 Introduction

In the previous chapter the regulation of NEP by shear stress was examined. In this chapter, the regulation of TOP will be investigated. Indeed, no published information on the shear-dependent nature of this latter enzyme currently exists, although a previous study by Cotter et al. (2004) has reported the up-regulation of TOP by cyclic circumferential strain. It should also be noted that, like NEP, TOP has a SSRE in its promoter region, suggesting likely regulation by shear stress in endothelial cells (Cummins, Cotter and Cahill 2004).

TOP has a number of alternative physiological functions. Firstly, it can transform an inert precursor neuropeptide into an active peptide (Acker, Molineaux and Orlowski 1987). Secondly, it acts as a convertase, changing one bioactive peptide into a different peptide that either binds to a different receptor or binds to the same receptor but conveys different downstream messages (Bourguignon, et al. 1994). Finally, TOP has a biomodulating action, forming a peptide product that opposes the action of its parent peptide (Chappell, et al. 1994). As a result, TOP serves to balance the action of several vasoactive peptides, both centrally and peripherally, with consequences for vascular tone. Thus, understanding TOP regulation by shear stress is of potentially high importance to cardiovascular research.

The aims of this chapter are three-fold; (i) confirm the role of TOPs SSRE with respect to its shear-dependent regulation; (ii) assess the effects of physiologically relevant levels of laminar and disturbed shear on TOP expression (with relation to dose and time) using qPCR and immunocytochemistry; (iii) examine the role of NADPH oxidase and ROS in the shear-dependent regulation of TOP expression.

4.2 Results

4.2.1 The effect of shear on TOP

4.2.1.1 The relevance of the -GAGACC- SSRE in the TOP promoter

HAECs were transfected with either pGL3-TOP (*Firefly* luciferase vector containing the full length rat TOP promoter -901/+120) or pGL3-CONT (empty vector, as mock control) (Morrison and Pierotti 2003). The pRL-CMV *Renilla* vector was also included in all transfections as a normalising control. Cells were then exposed to LSS (10 dynes/cm^2, 24 hrs) and promoter activity (*Firefly/Renilla*) was monitored using the Promega Dual-Glow^{TM} Luciferase assay, as described in methods. A statistically insignificant fold increase in baseline luciferase levels was observed under the non-sheared condition relative to mock transfections (1.31±0.15 fold). By contrast, we observed a substantial fold increase in luciferase levels relative to mock transfections under sheared conditions (5±0.21 fold) (Figure 4.1).

4.2.1.2 TOP primer validation

To confirm that TOP primers were specific to TOP and were not amplifying non-specific targets, extensive bioinformatical analysis was carried out during the primer design stage. Standard RT-PCR was carried out using the primers and the products were characterised on a 1% agarose gel. One clear band at the expected product size of 401 bp was visualised (Figure 4.2 A). Dissociation curves were routinely carried out after qPCR to ensure only TOP was being amplified (Figure 4.2 B). As a reference gene for all qPCR experiments, GAPDH was used to normalise results. As in section 3.2.2.1, TOP

primers were subjected to the MIQE guidelines and found to be 95% efficient with an R^2 value of 0.9961.

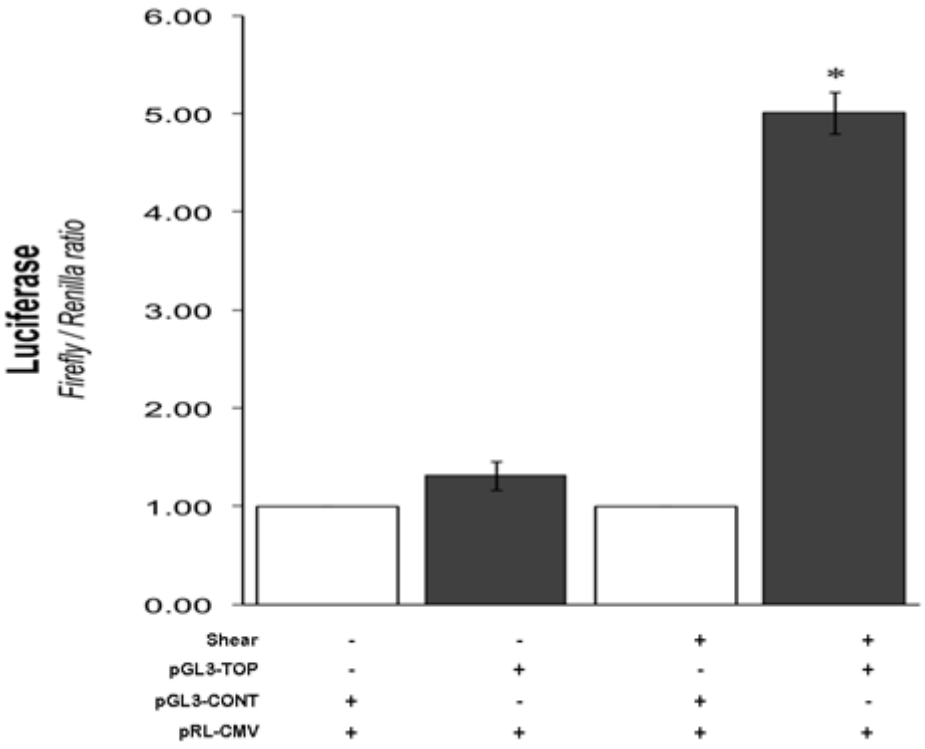

Figure 4.1: Effect of shear stress on TOP promoter activity. HAECs were transfected with either pGL3-TOP or pGL3-CONT and exposed to LSS (10 dynes/cm^2, 24 hrs). The pRL-CMV *Renilla* vector was also included in all transfections as a normalising control for the Promega Dual-Glo™ luciferase assay. *Firefly/Renilla* luciferase ratios under static and shear conditions are expressed as fold change to associated empty vector controls (each normalised to a value of 1). Results are averaged from three independent experiments ±SEM; *$P \leq 0.05$ vs control.

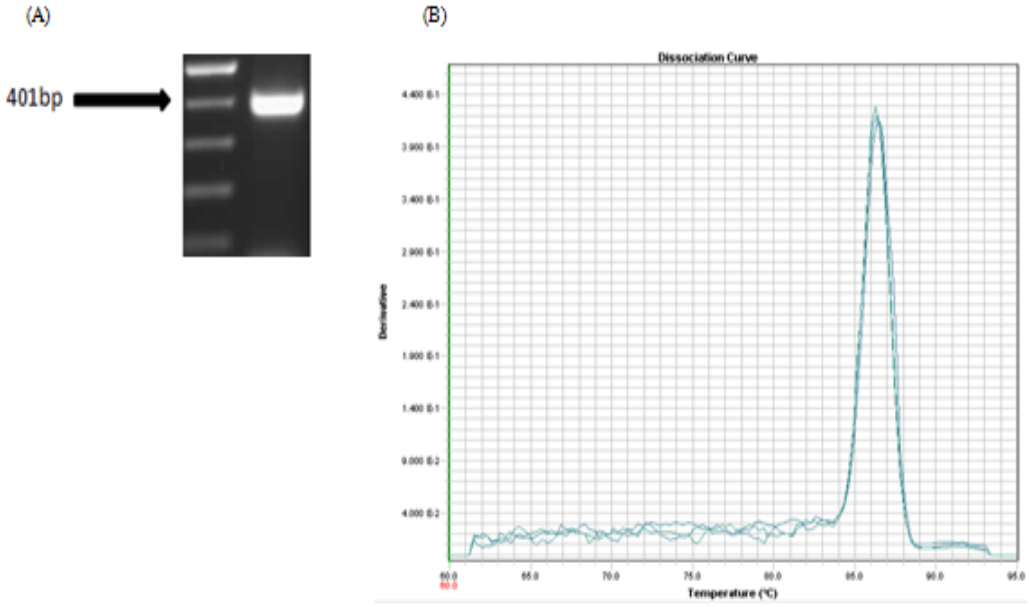

Figure 4.2: TOP primer validation. (A) Shows the product of a RT-PCR, run out on a 1% agarose gel, giving a single band at the expected product size for TOP. (B) Shows the corresponding disassociation curve.

4.2.1.3 LSS up-regulates TOP expression in a time-dependent manner

It has previously been shown from work carried out in this laboratory that TOP expression and activity in BAECs is up-regulated in response to physiological cyclic strain (Cotter, et al. 2004). In the present study we investigate if this up-regulation also occurs as a result of flow associated-LSS.

BAECs were grown to confluency and subjected to LSS for 0-48 hrs at 10 dynes/cm^2. TOP mRNA levels were then monitored using qPCR. Results demonstrate that TOP mRNA expression is up-regulated (~45%) by 24 hrs and maintained at this increased level thereafter compared to static control cells (Figure 4.3).

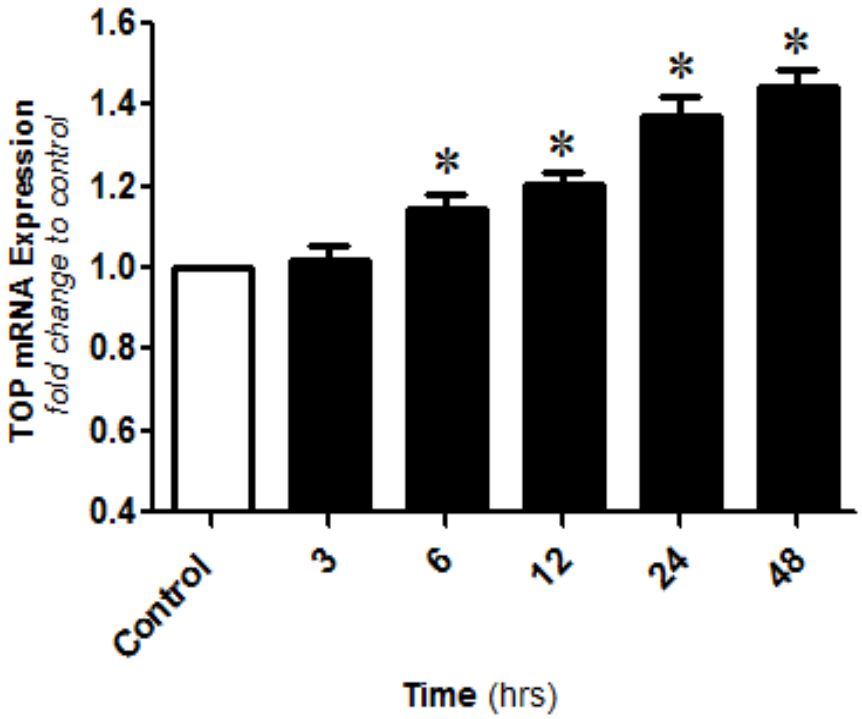

Figure 4.3: The time dependent up-regulation of TOP in BAECs by LSS. BAECs were grown to confluency and subjected to LSS of 10 dynes/cm^2 for 3, 6, 12, 24 and 48 hrs. Cells were harvested and analysed by qPCR. Histogram shows the time-dependent up-regulation of TOP expression levels. Results are averaged from three independent experiments ±SEM; *$P \leq 0.05$ vs control.

4.2.1.4 LSS up-regulates TOP expression in a dose-dependent manner

Both BAECs and HAECs were grown to confluency and exposed to low (1 dyne/cm^2, 24 hrs) or normal (10 dyne/cm^2, 24 hrs) LSS levels. TOP mRNA expression was then monitored by qPCR. The trend of TOP up-regulation at 10 dynes/cm^2 (but *not* at 1 dyne/cm^2) is observed in both BAECs and HAECs (Figure 4.4).

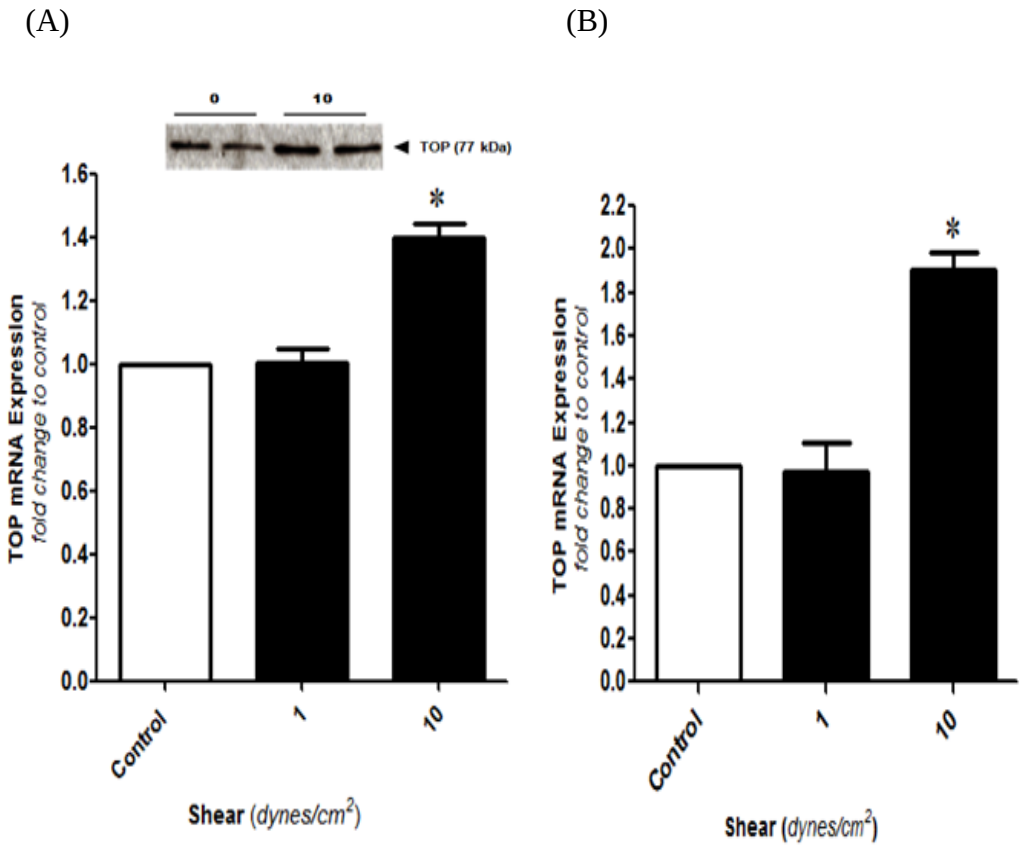

Figure 4.4: Magnitude-dependent effects of LSS on TOP mRNA expression. (A) BAECs and (B) HAECs were subjected to low (1 dyne/cm^2, 24 hrs) and normal (10 dynes/cm^2, 24 hrs) levels of LSS. Cells were harvested and analysed by qPCR. Results are averaged from three independent experiments ±SEM; *$P\leq$ 0.05 vs control. Western blot inset in (A) shows up-regulation of TOP protein at 10 dynes/cm^2 (Fitzpatrick, Endothelial Biology Group, unpublished data). Blot is representative.

4.2.1.5 The effect of DSS on TOP expression levels

BAECs and HAECs were grown to confluency and subjected to DSS for 24 hrs. Cells were then harvested and analysed by qPCR. In direct contrast to TOP mRNA up-regulation observed under LSS conditions, DSS was not found to cause TOP mRNA enhancement in BAECs. Results also indicate that in HAECs, TOP mRNA expression levels were actually down-regulated in a significant manner under DSS when compared to static control cells (Figure 4.5).

(A) (B)

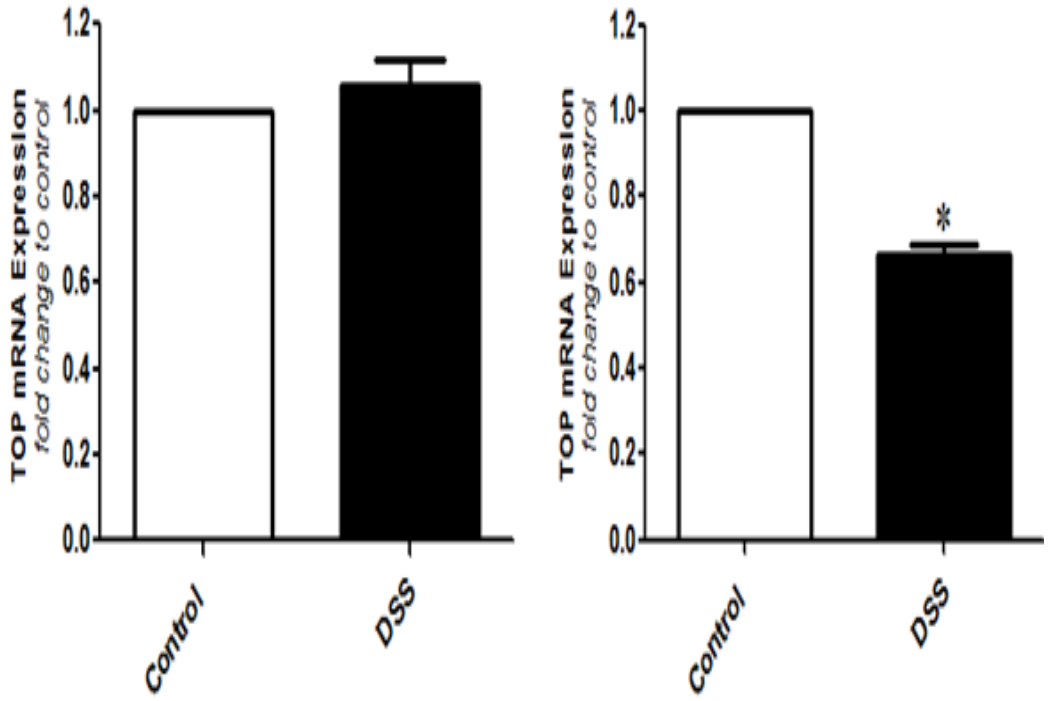

Figure 4.5: The effect of DSS on TOP mRNA expression levels. (A) BAECs and (B) HAECs were grown to confluency and exposed to DSS for 24 hrs. Cells were harvested and analysed by qPCR. Results are averaged from three independent experiments ±SEM; *$P \leq 0.05$ vs control.

4.2.1.6 Immunocytochemical analysis of TOP expression under shear

To analyse the effect of shear variations on TOP levels, the ibidi® micro-fluidic slide-flow system was employed. Slide chambers simulate the vascular environment. HAECs were seeded onto ibidi® Y-slides and grown to confluency. Cells were then sheared using LSS (10 dynes/cm^2, 24hrs) or oscillatory shear stress (OSS) (+/-10 dynes/cm^2, 24 hrs). Cells were then prepared for immunocytochemical staining for TOP as described in methods (Figure 4.6).

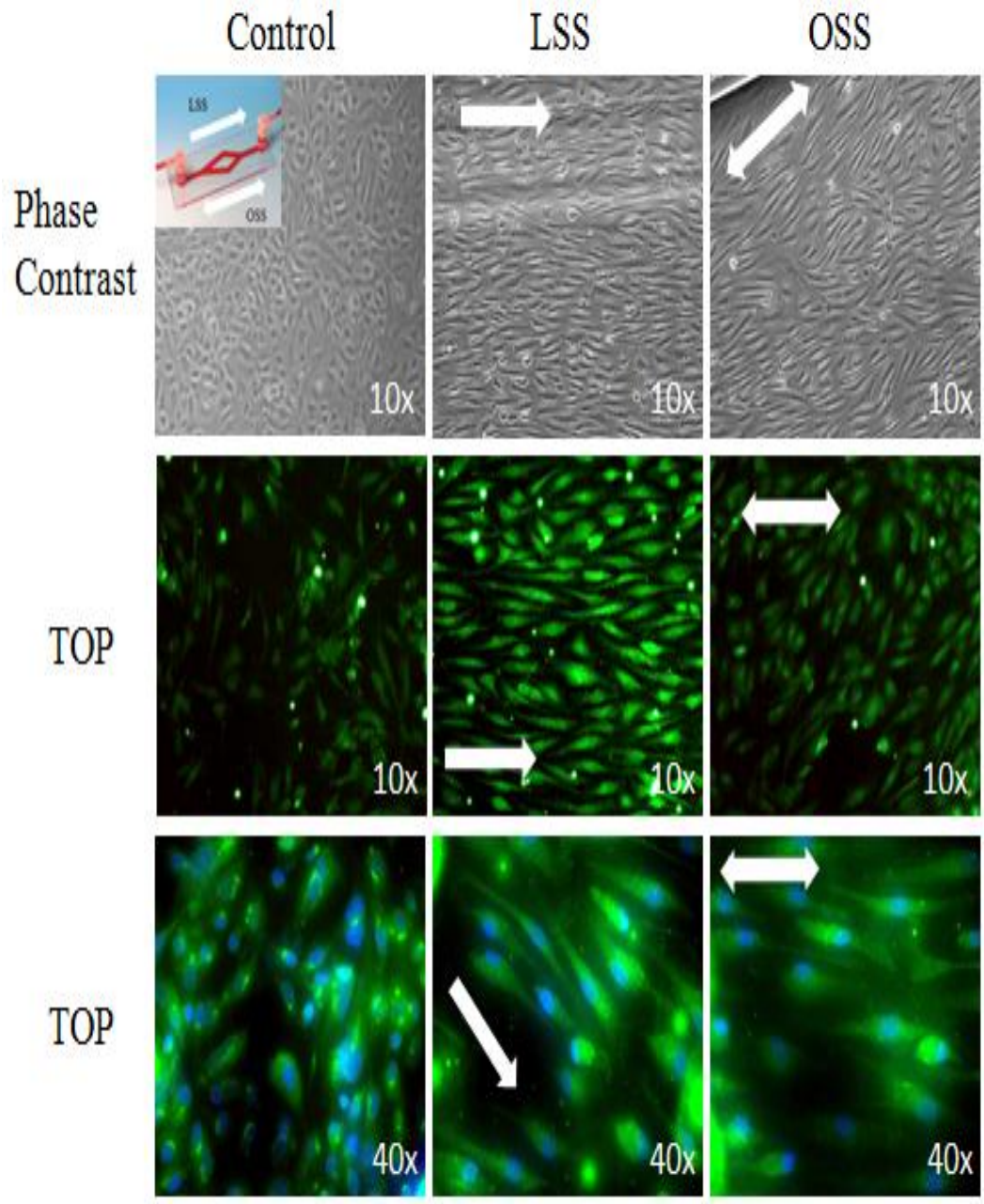

Figure 4.6: The regulation of TOP protein expression by LSS and OSS. Top row shows HAECs under phase-contrast view. Middle and bottom rows show HAEC IC images for TOP at 10x and 40x magnifications. HAECs can be seen to realign in the direction of flow under LSS. However, in OSS image cells are less clearly aligned. Images are representative. White arrows indicate the direction of flow. Insert in top left corner image illustrates ibidi® Y-slide format.

4.2.2 TOP signal transduction pathway

As with NEP, the shear signalling pathway for TOP is yet to be fully determined. It is logical however to speculate that it is regulated in a ROS-dependent manner, as we have shown for NEP, and as previously published work has shown for other shear-sensitive zinc metallopeptidases such as ACE (Ackermann, et al. 1998) and ECE (Masatsugu, et al. 2003).

It was therefore decided to examine the temporal relationship between shear-dependent ROS production and TOP up-regulation. A short preliminary study by Fitzpatrick et al. in this laboratory (unpublished data) has previously demonstrated the ROS-dependence of TOP up-regulation by shear stress (see Appendix). We decided to extend this work by confirming the involvement of NADPH oxidase in these events (using apocynin and p47 siRNA). Moreover, the temporal relationship between TOP up-regulation and the shear-induced ROS surge were determined. As with NEP, pharmacological reagents were added to BAECs 1 hrs before or 4 hrs after shear onset (essentially bracketing the ROS surge), and the effects on TOP expression subsequently monitored. Specifically agents included NAC, NSC23766 (Rac 1) and apocynin (NADPH oxidase).

4.2.2.1 Effect of N-Acetyl-L-cysteine (NAC)

The antioxidant NAC (5 mM) was added to confluent BAECs 1 hrs before or 4 hrs after the onset of LSS (10 dynes/cm^2, 24 hrs). The results show that the TOP LSS up-regulation is fully negated by the introduction of NAC 1 hrs prior to shear onset. This effect is lost when NAC is introduced 4 hrs post shear onset (Figure 4.7).

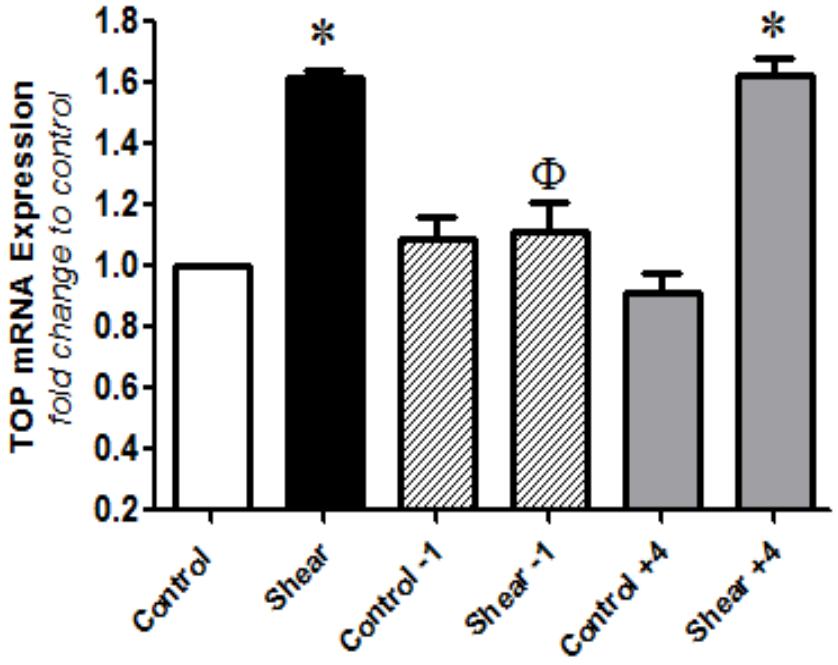

Figure 4.7: Temporal effect of NAC on shear-dependent modulation of TOP expression. BAECs were grown to confluency and NAC was added to samples 1 hrs before or 4 hrs after onset of LSS (10 dynes/cm^2, 24 hrs). Results are averaged from three independent experiments ±SEM; *$P\leq$ 0.05 vs control, Φ$P\leq$ 0.05 vs shear.

4.2.2.2 Effect of NSC23766

The Rac1-specific pharmacological inhibitor NSC23766 (50 µM) was introduced to BAECs 1 hrs before or 4 hrs after the onset of LSS (10 dynes/cm^2, 24 hrs). The results show that TOP LSS up-regulation is almost fully negated by the introduction of NSC23766 1 hrs prior to shear onset. This effect is lost when NSC23766 is introduced 4 hrs post shear onset (Figure 4.8).

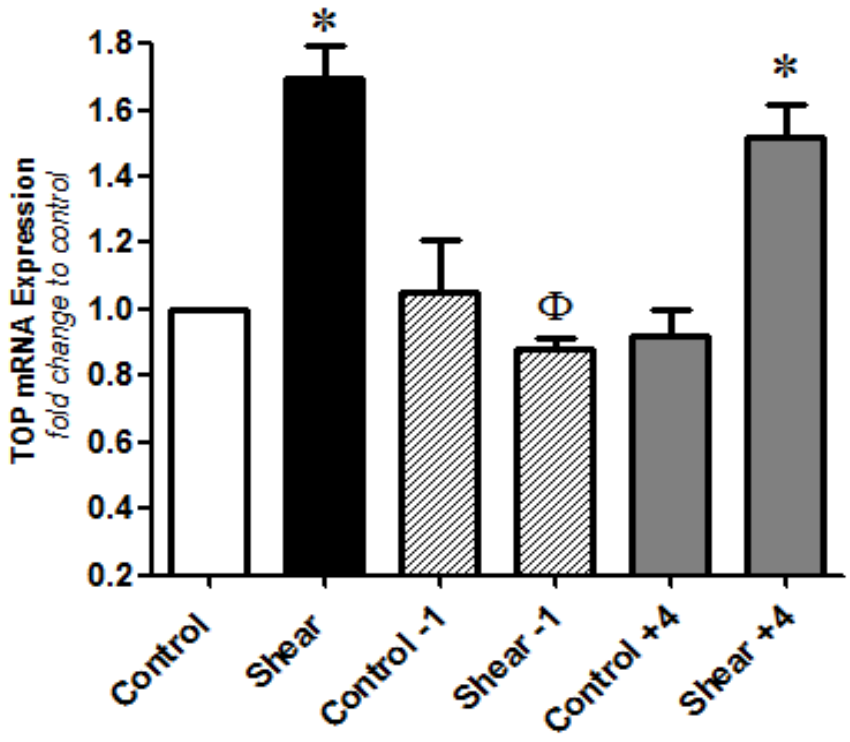

Figure 4.8: Temporal effect of NSC23766 on shear-dependent modulation of TOP expression. BAECs were grown to confluency and NSC23766 was added to samples 1 hrs before or 4 hrs after onset of LSS (10 dynes/cm^2, 24 hrs). Results are averaged from three independent experiments ±SEM; *$P\leq$ 0.05 vs control, Φ$P\leq$ 0.05 vs shear.

4.2.2.3 Effect of apocynin

The NAPDH oxidase inhibitor apocynin (50 μM) was introduced to BAECs 1 hrs before or 4 hrs after the onset of LSS (10 dynes/cm^2, 24 hrs). The results show that the TOP LSS up-regulation is substantially negated by the introduction of apocynin 1 hrs prior to shear onset. This effect is lost when apocynin is introduced 4 hrs post shear onset (Figure 4.9).

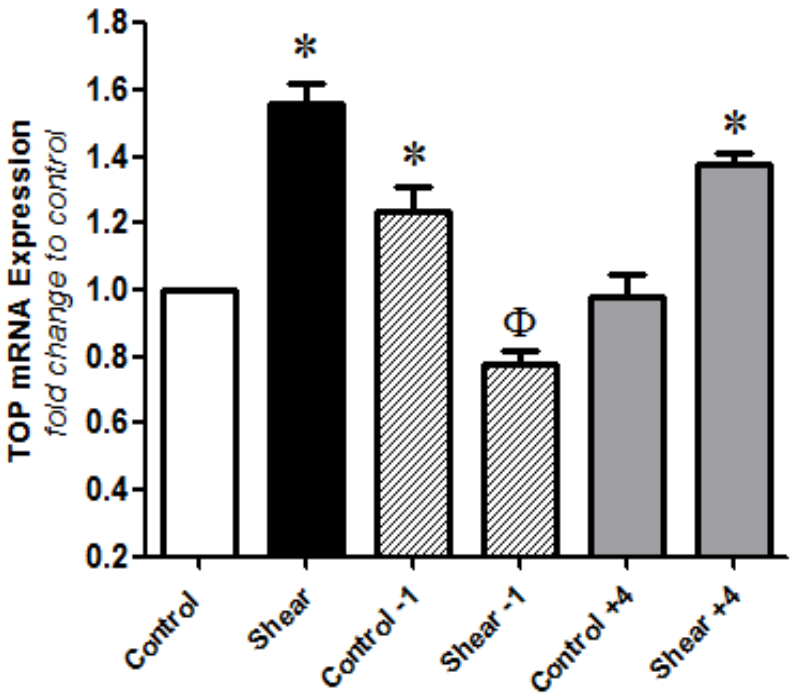

Figure 4.9: Temporal effect of apocynin on shear-dependent modulation of TOP expression. BAECs were grown to confluency and apocynin was added to samples 1 hrs before or 4 hrs after onset of LSS (10 dynes/cm^2, 24 hrs). Results are averaged from three independent experiments ±SEM; *$P\leq$ 0.05 vs control, Φ$P\leq$ 0.05 vs shear.

4.2.2.4 Effect of p47 siRNA

HAECs were transfected with p47 siRNA (15 nM). Either mock transfection (use of transfection reagents without siRNA) or 15 nM scrambled siRNA demonstrated negligible effects on TOP expression and so were used as controls. Post-transfection, cells were allowed overnight recovery before the application of LSS (10 dynes/cm^2, 24 hrs). Cells were then harvested for mRNA and analysed by qPCR. Results of this study show that silencing of the NADPH oxidase p47 subunit leads to a negation of the expected up-regulatory effect of LSS on TOP mRNA expression (Figure 4.10).

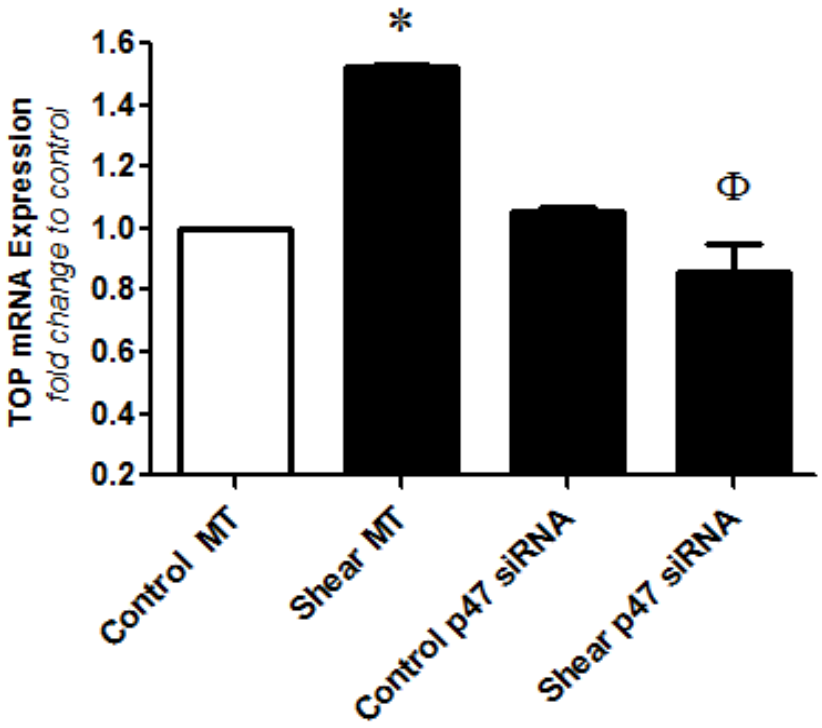

Figure 4.10: The role of NADPH oxidase in TOP mRNA expression. HAECs were transfected with p47 siRNA (15 nM) and subjected to LSS (10 dynes/cm^2, 24 hrs). Control cells demonstrated the expected TOP up-regulation in response to LSS. However, the introduction of p47 siRNA negates this effect, bringing TOP mRNA expression back to control levels. Results are averaged from three independent experiments ±SEM; *$P\leq 0.05$ vs control, Φ$P\leq 0.05$ vs shear MT. MT= mock transfection.

4.3 Discussion

It has been widely reported that ECs exhibit secreted and membrane-associated forms of TOP, thereby allowing it to putatively degrade peptides intracellularly and extracellularly (Crack, et al. 1999). Cotter et al. (2004) demonstrated for the first time the role of cyclic strain in regulating the expression and enzymatic activity of TOP, and its closely related zinc-metallopeptidase family member neurolysin, in BAECs. Their findings demonstrated that strain significantly increased TOP's soluble activity in a force- and time-dependent manner, with a 2.3 fold increase after 24 hours at 10% strain, in addition to up-regulating TOPs mRNA levels by 42%. That study also concluded that cyclic strain modulates the release of TOP from BAECs and thus may have a significant influence on TOP's extracellular functions (Cotter, et al. 2004). Interestingly, examination of TOP's protein sequence shows neither a readily identifiable secretory signal sequence nor a conventional hydrophobic, membrane-spanning domain, structural elements normally associated with extracellularly-acting peptidases. However, TOP is now believed to be secreted through non-classical pathways, e.g. lipid rafts (Jeske, et al. 2006).

In view of the multitude of studies demonstrating roles of TOP (EP24.15) in vasoactive peptide metabolism peripheral and cerebral vascular beds (Chappell, et al. 1994, Norman, et al. 2003b, Norman, et al. 2003a, Rioli, et al. 2003, Santos, et al. 1992) , and the up-regulation of TOP activity seen in response to cyclic strain (Cotter, et al. 2004), w*e hypothesised that TOP levels would be regulated in vascular endothelium by shear stress.* This chapter comprehensively examined, for the first time, the regulatory relationship between shear stress and TOP in macrovascular endothelial cells, and sheds light on the mechanotransduction pathway mediating any observed regulatory events.

It has previously been shown that TOP contains a -GAGACC- SSRE in its promoter sequence, and as such is believed to be shear-sensitive (McCool and Pierotti 1998). The initial investigation focused on the transfection of a pGL3 vector containing TOP's full length promoter sequence (pGL3-TOP) into HAECs and subsequently monitoring shear-dependent TOP promoter activation

via luciferase reporter assay. The results show that in the absence of shear, little or no luciferase activity is present in cells transfected with pGL3-TOP (i.e. versus empty vector pGL3-CONT). When HAECs are sheared, however, significantly elevated levels of luciferase activity are observed in pGL3-TOP transfected cells, clearly pointing to the mechao-sensitive nature of the TOP promoter.

We next examined how TOP may be regulated by LSS in a time- and magnitude-dependent manner. It can be seen from the results presented that TOP mRNA expression levels in both BAECs and HAECs are significantly up-regulated by normal LSS (10 dynes/cm^2) over a 24 hrs period and are maintained at this level even up to 48 hrs. Data also shows a relationship between shear magnitude and TOP regulation with normal LSS (10 dynes/cm^2), but *not* low (1 dyne/cm^2) or static (0 dynes/cm^2), causing significant up-regulation of TOP mRNA expression. These findings are in line with those of Cotter et al. (2004) who reported a similar increase in BAEC TOP mRNA expression levels, albeit under an alternative hemodynamic force, cyclic strain. Interestingly, results presented in this chapter have also shown that under DSS, no significant up-regulation of TOP is observed in BAECs, whilst in HAECs a significant decrease in TOP mRNA expression occurs. Collectively, these data suggest that TOP is up-regulated under atheroprotective conditions, and vice versa. As such, its dysregulation under conditions of compromised shear may contribute to a net alteration in local peptide balance, leading to endothelial dysfunction.

Immunocytochemical staining of TOP was also performed in HAECs exposed to laminar and oscillatory shear stress using an ibidi® micro fluidic slide flow system. An up-regulation of TOP immunostaining is clearly visible in HAECs under LSS (10 dynes/cm^2), when compared to static control cells. Interestingly, this up-regulation is not visible when HAECs were exposed to OSS (+/- 10 dynes/cm^2, 24 hrs). There also appears to be a visible subcellular relocation of TOP immunoreactivity, with TOP being located close to the nucleus in static control cells, whilst having a more ubiquitous expression pattern under LSS and OSS conditions (Figure 4.6). Importantly, these IC findings are consistent with observations for LSS and DSS effects on TOP mRNA/protein levels.

As with NEP, we next attempted to determine the role played by NADPH oxidase and ROS in the mechanotransduction pathway involved in TOP's shear-dependent regulation. In this respect, preliminary studies within the Endothelium Biology Group at DCU (unpublished data) have demonstrated that shear-dependent up-regulation of TOP can be blocked by ROS-sequestering agents. Moreover, treatment of *static* endothelial cells with either H_2O_2 or ROS-inducing Ang-II was found to up-regulate TOP expression (Appendix).

We therefore began by identifying a role for NADPH oxidase in these events. It has previously been published that p47 is responsible for transporting the cytosolic subunits of NADPH oxidase from the cytosol to the membrane during oxidase activation. The effect of p47 is to tighten the binding between each of the other cytosolic proteins to the assembled oxidase (Sumimoto, Miyano and Takeya 2005). Our results indicate that the silencing of p47 expression using an siRNA completely attenuates the effect of LSS up-regulation on TOP mRNA expression levels, strongly implicating a role for NADPH oxidase.

As in Chapter 3, the temporal ROS burst that occurs 0-3 hrs after the onset of shear was the main focus of the next set of experiments. Therefore, we utilised pharmacological inhibitors, NSC23766 (Rac1) and apocynin (p47), to disrupt NADPH oxidase and monitor the effect on the regulation of TOP under LSS conditions. A key step in the NADPH oxidase activation cascade occurs when Rac1 binds to the p67 subunit and migrates to the membrane along with the core cytosolic complex (Koga, et al. 1999). Zimmerman et al. (2004) demonstrated for the first time that a Rac1-dependent NADPH oxidase is a key source of O_2^- production in neurons. Apocynin is also known to inhibit the production of ROS by NADPH oxidase, by blocking migration of p47 to the membrane (Stolk, et al. 1994).

The results of the inhibition of Rac1 by NSC23766 indicate that disruption of the NADPH oxidase subunit leads to a attenuation of the effect of LSS on TOP when introduced to samples 1 hrs before shear onset. However, when NSC23766 is introduced 4 hrs after shear onset this effect is lost, implying a role for Rac1 in the early stages of shear activation of TOP. When BAECs were incubated with the NADPH oxidase inhibitor, apocynin, the same trend is again

seen, with the LSS shear-dependent up-regulation of TOP inhibited by addition of apocynin to BAECs 1 hrs before, but not 4 hrs after, shear onset. These results indicate that NADPH oxidase is essential in the regulation of TOP under LSS conditions during early shear onset phase.

As the zinc metallopeptidases ACE and ECE were previously shown to be regulated by shear stress in a ROS-dependent manner, the role of ROS in regulating TOP was next investigated. Again the temporal ROS burst that occurs 0-3 hrs after the onset of shear was the main focus of this experiment. Therefore, NAC was used to scavenge O_2^- in BAECs 1 hrs prior to and 4 hrs post shear onset. The results of this experiment indicate that the scavenging of O_2^- 1 hrs prior to, but not 4 hrs post, shear onset inhibits the effect of LSS on TOP attenuation, again confirming the role of this early ROS burst in the regulation of TOP under LSS conditions.

In conclusion, through the use of our shear stress model, we have shown that the LSS-induced up-regulation of TOP is likely due to the presence of an SSRE in its promoter region. This up-regulation was also shown to be both time- and dose-dependent under physiologically relevant levels of laminar shear, with opposite effects observed under conditions of disturbed or oscillatory shear. Finally this chapter demonstrates the role played by NADPH oxidase and ROS in the up-regulation of TOP by shear stress during the early phase of shear onset.

Chapter 5:

Functional consequence(s) of the shear-mediated regulation of NEP and TOP in vascular endothelial cells.

5.1 Introduction

In the previous chapters, the shear-dependent regulation of the zinc metallopeptidases, NEP and TOP, have been investigated. Numerous *in vivo* and *in vitro* studies have already ascribed roles to these enzymes in the regulation of net vasopeptide balance within the vasculature, with consequences for vascular tone. Moreover, studies in the previous two chapters clearly indicate that the expression of these enzymes is regulated in an opposing or divergent manner. The putative functional consequence(s) of their regulation by shear will therefore be examined in this chapter.

NEP is capable of efficiently degrading a number of bioactive peptides and cytokines including endothelin-1 (ET-1), enkephalins, *atrial natriuretic peptide* (ANP) and bombesin-like peptides (Turner and Tanzawa 1997). Inhibition of NEP increases levels of ANP and C *natriuretic peptide* (CNP), as well as bradykinin (BK). By simultaneously inhibiting the renin-angiotensin system and potentiating the natriuretic peptide and kinin systems, vasopeptidase inhibitors (i.e. towards ACE, ECE and NEP) reduce vasoconstriction, enhance vasodilation, improve sodium/ water balance and, as a result, decrease peripheral vascular resistance and blood pressure and improve local blood flow. Within the blood vessel wall, this leads to a reduction of vasoconstrictor and proliferative mediators such as angiotensin II and increased local levels of BK (and, in turn, nitric oxide) and natriuretic peptides (Corti, et al. 2001). Thus, the regulation (and dysregulation) of NEP within the endothelium is clearly of major importance to vascular health and vessel homeostasis.

Much of the work published on TOP has focused on its activity within the extracellular space, despite subcellular fractionation experiments indicating that the majority (generally >80%) of TOP is localised to the cytosol (Crack, et al. 1999). BK, a common substrate of zinc metallopeptidases, is a potent inflammatory mediator which produces vascular leakage and endothelium dependent vasodilation (Bhoola, Figueroa and Worthy 1992). A small proportion of total cellular TOP has been shown to be localised with the bradykinin B2

receptor on the exofacial leaflet of plasma membranes and in lipid rafts, indicating a potential physiologic role for TOP in modulating BK activation and sensitisation of nociceptors (Gomez, et al. 2011, Jeske, Glucksman and Roberts 2004, Norman, et al. 2003, Sandén, et al. 2008). Very importantly, exciting new studies have also identified an important hydrolytic role for cytosolic TOP in the immune system, where it participates in the degradation of proteosomal peptide fragments typically used by the cell in MHC class I antigen presentation (Kessler, et al. 2011, Kim, et al. 2003, Demasi, et al. 2008).

By employing strategies to selectively over-express and/or inhibit NEP and TOP under both static and shear conditions, the following preliminary functional analyses have been performed.

NEP: Barrier function, proliferation.

TOP: Proliferation, BK hydrolysis, MHC I presentation.

5.2 Results

5.2.1 NEP blockade and over-expression studies

5.2.1.1 NEP and barrier function

As shown in Chapter 3, endothelial permeability and NEP expression are both decreased in response to LSS. To investigate if there is a link between these events the effect of NEP inhibition and over-expression on barrier function was examined in static and sheared cells, respectively.

HAECs were first treated with phosphoramidon, an NEP (and ECE) inhibitor, to investigate if NEP blockade may further potentiate the shear-induced reduction in endothelial permeability. HAECs were grown to confluency and phosphoramidon (1 μM) added to cells before they were subjected to LSS (10 dynes/cm^2, 24 hrs). Barrier integrity was measured by transendothelial permeability assay as previously described (Walsh et al., 2011). Results indicate that barrier integrity is significantly enhanced under LSS, with no additional tightening of barrier witnessed under shear following the addition of phosphoramidon (Figure 5.1).

HAECs were next transfected with an NEP over-expression vector (NEP^{++}, the generous gift of Dr. Nanus at Cornell University, New York) to investigate if NEP over-expression can reverse the shear-induced reduction in EC permeability. Following transfection and recovery, cells were subjected to LSS (10 dynes/cm^2, 24 hrs). Barrier integrity was again measured by transendothelial permeability assay as previously described (Walsh et al., 2011). Results indicate that barrier integrity was enhanced under laminar shear (i.e. manifested as reduced permeability). Results also show that in ECs, NEP over-expression significantly weakened the endothelial barrier by increasing monolayer permeability to FITC-dextran (40 kDa) (Figure 5.2). A similar result was seen in BAECs transfected with NEP^{++} (data not shown).

(A) (B)

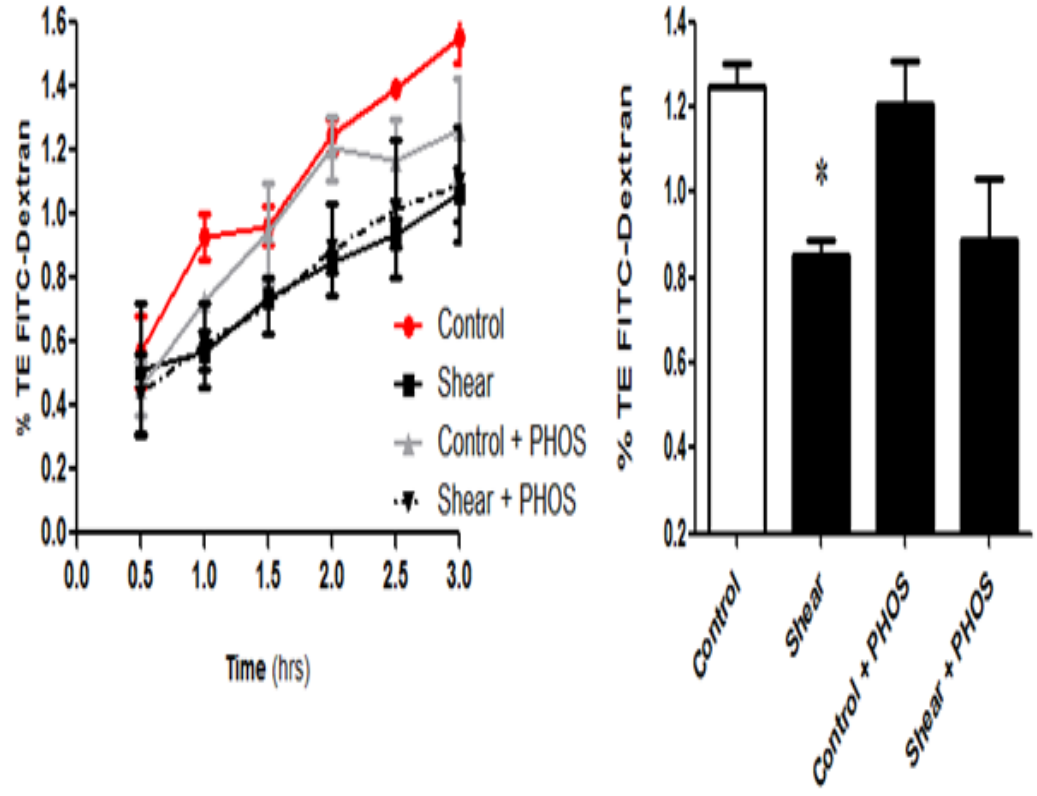

Figure 5.1: The effect of phosphoramidon on paracellular permeability in HAECs. Phosphoramidon (1 µM) was incubated with HAECs for 24 hrs on both control and LSS cells (10 dynes/cm^2, 24 hrs). Cells were then harvested and re-plated in transwell inserts and monitored by transendothelial permeability assay. (A) Line graphs showing the % trans-endothelial exchange of FITC-Dextran over 3 hrs. (B) histograms showing the difference in permeability after 2 hrs of exchange. Results are averaged from three independent experiments ±SEM; *$P \leq 0.05$ vs static control cells. PHOS= phosphoramidon.

(A) (B)

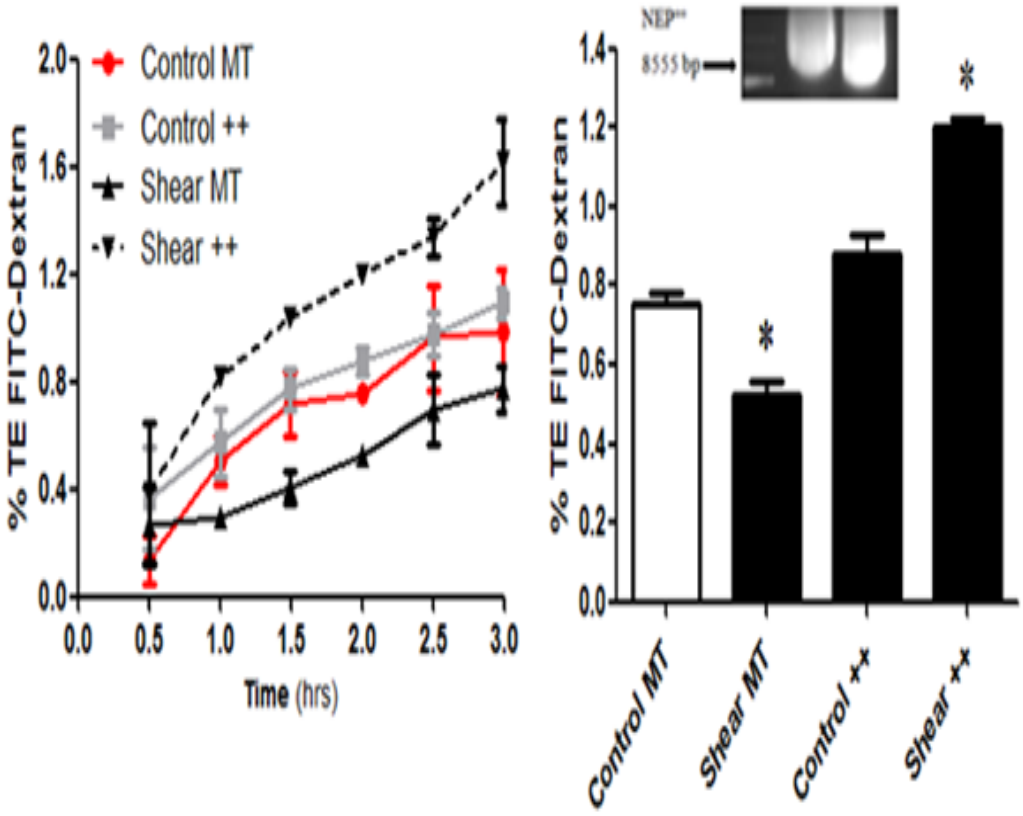

Figure 5.2: The effect of NEP over-expression on paracellular permeability in HAECs. HAECs were transfected with NEP^{++} and subjected to LSS (10 dynes/cm^2, 24 hrs). Cells were then harvested and re-plated in transwell inserts and monitored by transendothelial permeability assay as described in methods. (A) Line graph showing the % trans-endothelial exchange of FITC-Dextran over 3 hrs. (B) Histogram showing the difference in permeability after 2 hrs of exchange. N=2. Inset (B) shows NEP^{++} plasmid (prepared as described in methods) run out on a 1% agarose gel, giving a single band at the expected product size of (8.55 kb).

5.2.1.2 HAEC proliferation

It has previously been published that LSS has an anti-proliferative effect on ECs (White, et al. 2001). As a control study, HAECs were therefore grown to confluency and subjected to LSS (10 dynes/cm^2, 24 hrs). Cells were then harvested and a cell count performed. Cells were then re-plated at 4000 cells/well of a 16-well xCELLigence® plate (Roche). Proliferation was measured over 6

days by impedance (Figure 5.3 A), as described in methods. In a parallel control experiment, 50,000 cells/well (post-shear) were re-plated into a 6-well plate and stained with CFSE for proliferation analysis by FACS after 4 days (Figure 5.3 B), as described in methods. Results with both methods indicate that LSS increases cell doubling times and so decreases the rate of EC proliferation.

5.2.1.3 NEP and proliferation

To investigate if there is a link between shear-dependent decreases in NEP expression and proliferation rate, it was decided to examine the effects of NEP over-expression on shear-induced reduction in EC proliferation rate. HAECs were transfected with an NEP^{++} (3 ng) and left to recover for 24 hrs. Cells were then sheared under LSS (10 dynes/cm^2, 24 hrs). Cells were harvested and a cell count performed. Following this, cells were re-plated at 4,000 cells/well of a 16-well xCELLigence® plate. Proliferation was measured by impedance over 6 days (Figure 5.4 A), as described in methods. In a parallel experiment, 50,000 cells/well (post-shear) were re-plated into a 6-well plate and monitored for proliferation by CFSE FACS analysis (Figure 5.4 B), as described in methods. Results would indicate that the over-expression of NEP has no effect on the shear induced reduction of EC proliferation rate.

(A)

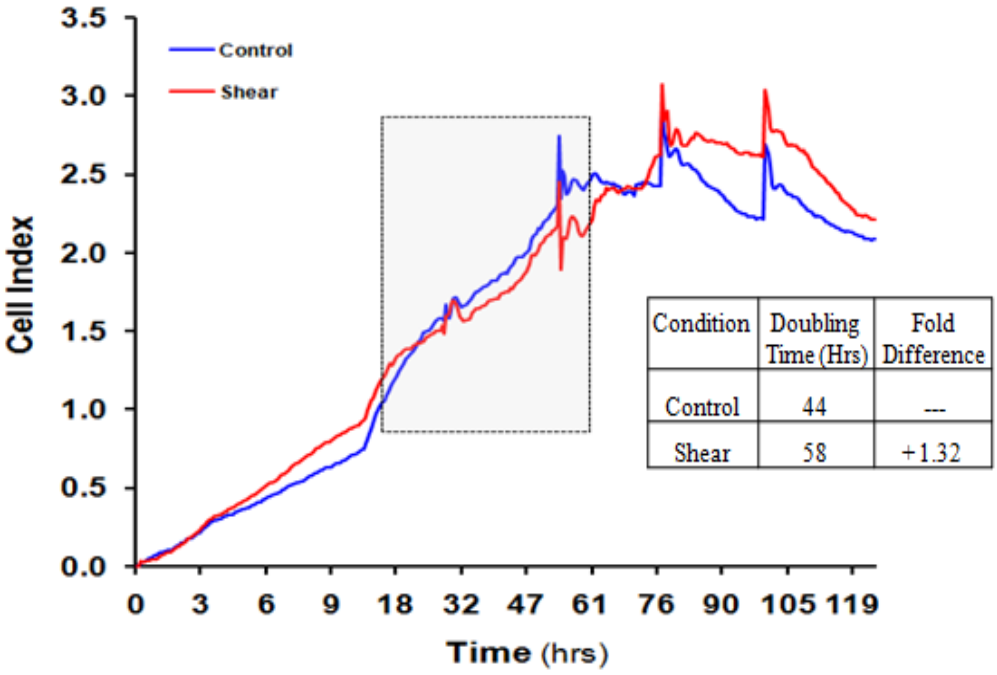

Condition	Doubling Time (Hrs)	Fold Difference
Control	44	---
Shear	58	+1.32

(B)

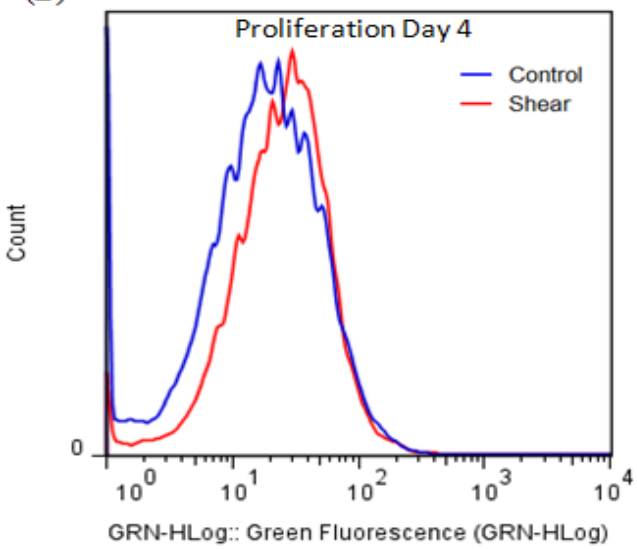

Figure 5.3: The effect of LSS on HAEC proliferation. HAECs were grown to confluency and subjected to LSS (10 dynes/cm^2, 24 hrs). Cells were then harvested, counted and re-plated in xCELLigence® E-Plates or regular 6-well plates and monitored for proliferation by (A) impedance or (B) CFSE staining, respectively, as described in methods. Table in (A) shows change in HAEC doubling time (hrs) across the indicated time window (shaded box) using the xCELLigence® E-plate method. (B) shows the result of CFSE staining on day 4 post staining. Curve shift to the left indicates higher proliferation rate due to cellular 'dilution' of CFSE dye, and vice-versa.

(A)

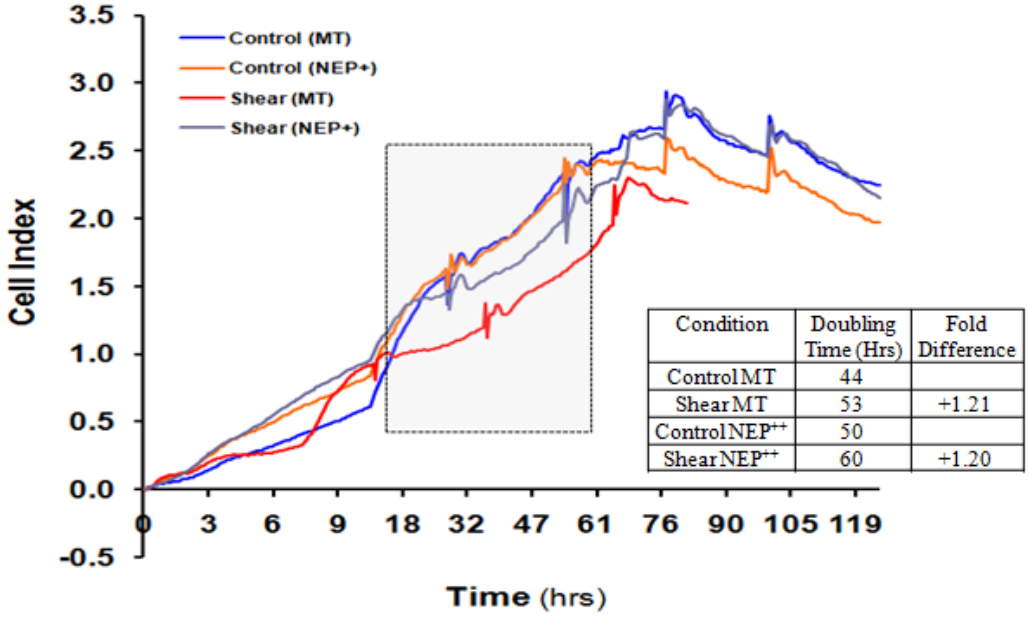

Condition	Doubling Time (Hrs)	Fold Difference
Control MT	44	
Shear MT	53	+1.21
Control NEP^{++}	50	
Shear NEP^{++}	60	+1.20

(B)

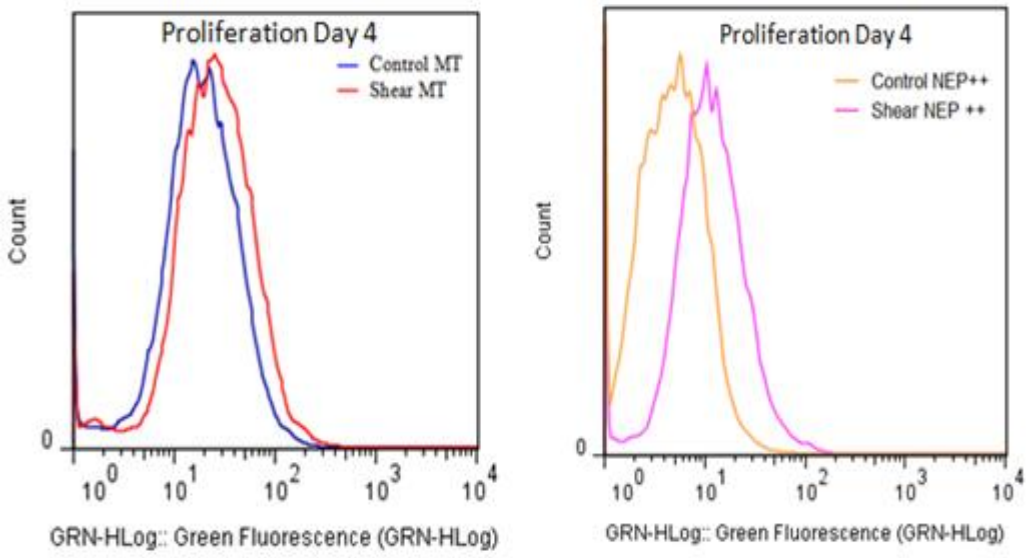

Figure 5.4: The effect of NEP over-expression on rate of HAEC proliferation. HAECs were transfected with NEP^{++} (3 ng) and subjected to LSS (10 dynes/cm^2, 24 hrs). Cells were harvested, re-plated in xCELLigence® E-Plates or regular 6-well plates and monitored for proliferation by (A) impedance or (B) CFSE staining, as described in methods. Table in (A) shows change in HAEC doubling time (hrs) across the indicated time window (shaded box) using the xCELLigence® E-plate method. (B) shows the result of CFSE staining on day 4 post staining. Curve shift to the left indicates higher proliferation rate due to cellular 'dilution' of CFSE dye, and vice-versa.

5.2.2 TOP blockade and over-expression studies

5.2.2.1 TOP siRNA optimisation

Following optimisation experiments to identify a working concentration of TOP siRNA (Figure 5.5) HAECs were transfected with TOP siRNA (1 µM) to monitor TOP knock-down under shear conditions. For control purposes, both mock transfection (use of transfection reagents without siRNA) and scrambled siRNA (1 µM) were employed (both found to have negligible effects on TOP expression). Post-transfection, cells were allowed overnight recovery before the application of LSS (10 dynes/cm^2, 24 hrs). Cells were then harvested for mRNA and analysed by qPCR (Figure 5.6). Results indicate that TOP siRNA significantly negates the expected up-regulation of TOP mRNA expression levels under LSS.

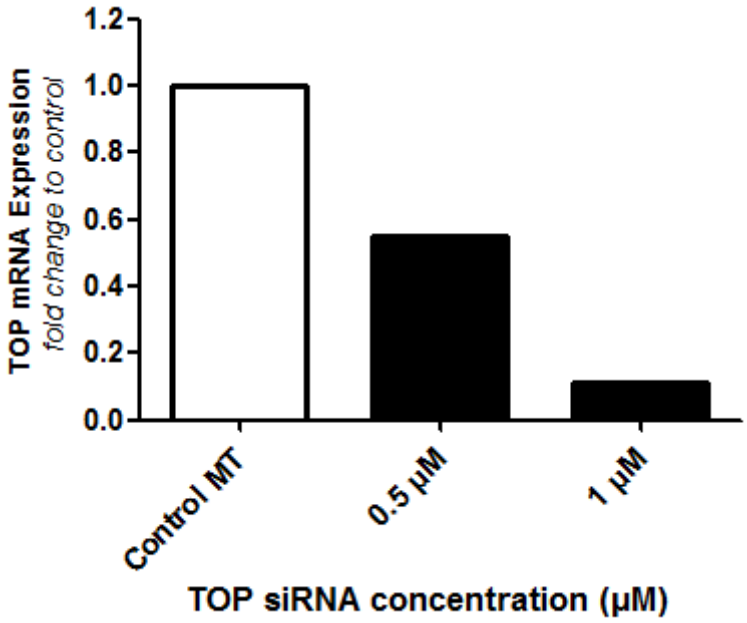

Figure 5.5: Optimisation of TOP siRNA concentrations. Control study demonstrates that increasing concentrations of TOP siRNA (0-1 µM) caused a marked decrease in TOP mRNA expression levels in static HAECs.

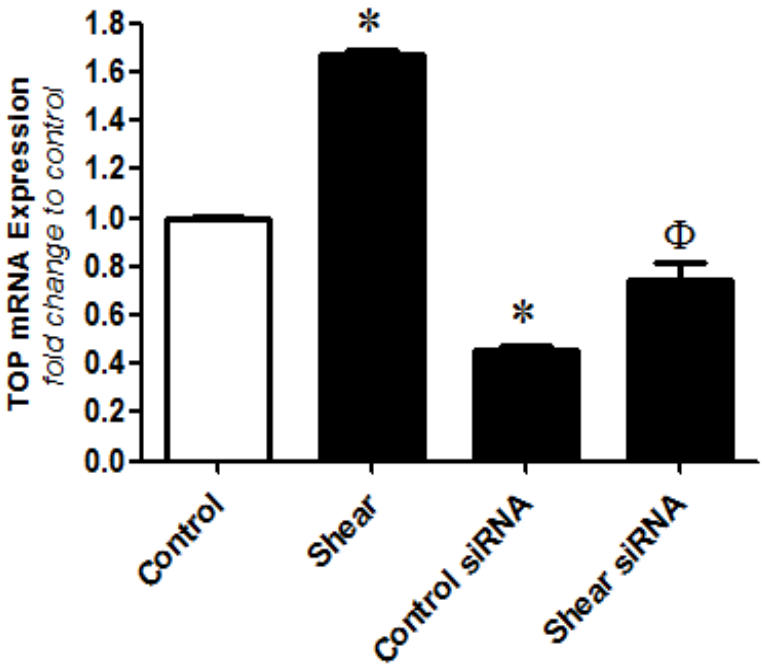

Figure 5.6: The effect of TOP siRNA on TOP mRNA expression under LSS. HAECs were transfected with TOP siRNA (1 μM) and subjected to LSS (10 dynes/cm^2, 24 hrs). Cells were harvested and analysed by qPCR. Results are averaged from three independent experiments ±SEM; *$P \leq 0.05$ vs control, Φ$P \leq 0.05$ vs shear.

5.2.2.2 TOP siRNA and proliferation

In similar experiments, HAECs were transfected with TOP siRNA (1 μM) and left to recover overnight. Cells were then exposed to LSS (10 dynes/cm^2, 24 hrs). Post-shear, cells were harvested and a cell count performed. Cells were then plated at 4,000 cells/well in a 16-well xCELLigence® plate and proliferation monitored via impedance over 120 hrs (Figure 5.7), as described in methods. Results indicate that siRNA silencing of TOP appears to modestly decrease the anti-proliferative effects of shear (~28%).

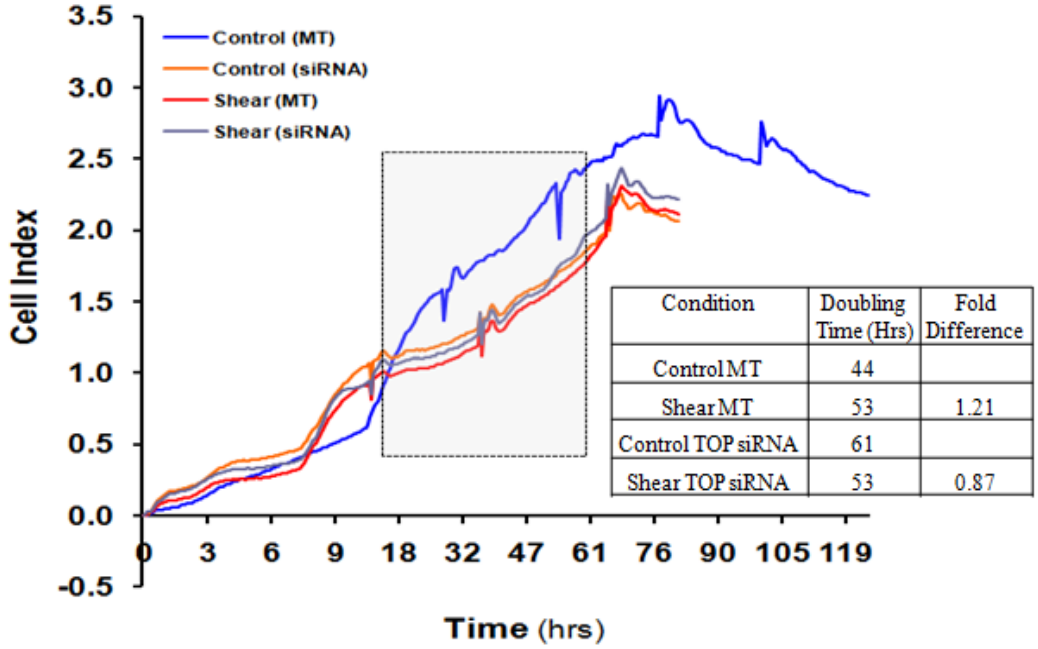

Condition	Doubling Time (Hrs)	Fold Difference
Control MT	44	
Shear MT	53	1.21
Control TOP siRNA	61	
Shear TOP siRNA	53	0.87

Figure 5.7: The effect of TOP silencing on rate of HAEC proliferation. HAECs were transfected with TOP siRNA (1 µM) and subjected to LSS (10 dynes/cm^2, 24 hrs). Cells were harvested, re-plated in E-Plates and monitored for proliferation by impedance, as described in methods. Table shows change in HAEC doubling time (hrs) across the indicated time window (shaded box) using the xCELLigence® E-plate method.

5.2.2.3 TOP and MHC I expression

It has previously been published that MHC I expression is attenuated in ECs under LSS (Martin-Mondiere, et al. 1989). Moreover, an early study by Kim et al. (2003) demonstrated that TOP (i.e. EP24.15) can reduce MHC I expression in cytotoxic T-lymphocytes. We therefore decided to investigate a possible relationship between shear-dependent MHC I reduction and TOP induction. To this end, a preliminary investigation was conducted whereby the effect of a TOP siRNA on shear-induced reduction of MHC I levels was examined.

HAECs were transfected with TOP siRNA (1 µM) and left to recover for 24 hrs. Cells were then subjected to LSS (10 dynes/cm^2, 24 hrs) and harvested for immunoblot analysis of MHC I, as in methods. Results show a decrease in

MHC I expression under LSS conditions, an effect which is reversed upon addition of TOP siRNA (Figure 5.8).

5.2.2.4 TOP and bradykinin (ELISA)

It has been previously published that extracellular termination of BK signalling is controlled by zinc metallopeptidases (Rawlings and Barrett 1993). Crack at al. demonstrated that TOP has an extracellular association with the plasma membrane and has an ecto-enzymatic activity (Crack, et al. 1999). Moreover, Cotter et al. showed that cyclic strain modulates the release of TOP from BAECs and thus may have a significant influence on TOP's extracellular functions (Cotter, et al. 2004). Therefore, it was decided to investigate a putative contribution of TOP induction in the extracellular hydrolysis of BK under LSS conditions. In this regard, we hypothesised that shear-induced TOP up-regulaton may putatively enhance extracellular degradation of BK. To test this hypothesis, it was necessary to inhibit a range of zinc metallopeptidases also known to hydrolyse BK using pharmacological inhibitors (in order to narrow hydrolysis down to TOP). These included the ACE inhibitor, captopril, and a dual ECE/NEP inhibitor, phosphoramidon.

HAECs were transfected with either TOP siRNA (1 µM) and allowed to recover overnight. Cells were then subjected to LSS (10 dynes/cm^2, 24 hrs), after which they were washed in sterile 1X PBS. HEPES-Krebs buffer was then added to cells at 2 ml per well. Inhibitors were added to each well for blockade of ACE (captopril, 10 µM), and ECE/NEP (phosphoramidon, 2 nM) activity. After 30 min, bradykinin was added (20 ng/per well) and cells left to incubate for either 3 or 12 hrs at 37°C. Following incubation, medium samples were collected for BK analysis by ELISA kit (Enzo Life Sciences, USA) (Figure 5.9), as in methods. (Assay based on a modification of the method of Norman et al. 2003)

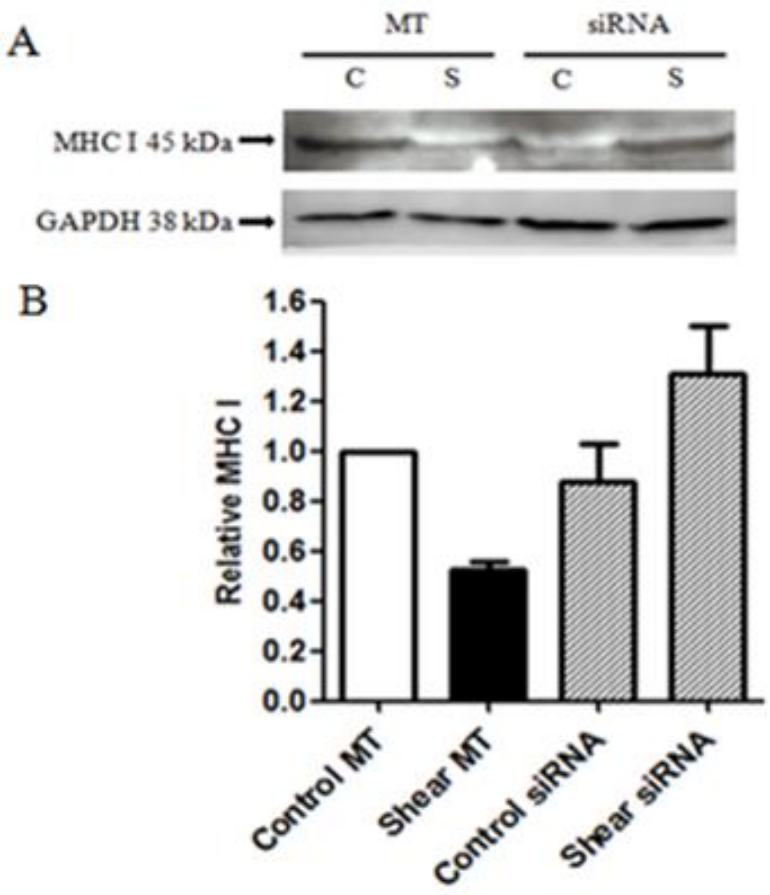

Figure 5.8: Impact of TOP siRNA on shear-induced MHC I reduction. HAECs were transfected with TOP siRNA and left to recover for 24 hrs. Cells were then subjected to LSS (10 dynes/cm^2, 24 hrs) and harvested for immunoblot analysis. (A) Immunoblots showing both MHC I and GAPDH. (B) Histogram of relative MHC I expression (i.e. MHC I/GAPDH) derived by scanning densitometry. N=2. MT= mock transfection.

Results clearly indicate significant depletion in BK medium levels between 3-12 hrs. Surprisingly, there is only marginal difference in levels of extracellular BK peptide hydrolysis between static control cells and sheared cells, with the latter conditions showing slightly lower levels of hydrolysis (i.e. higher BK levels found in medium) at both 3 and 12 hrs. In control cells at t=12 hrs, TOP blockade by siRNA appears to significantly slow extracellular BK peptide hydrolysis. In sheared cells at 12 hr, no significant difference is observed between conditions.

(A)

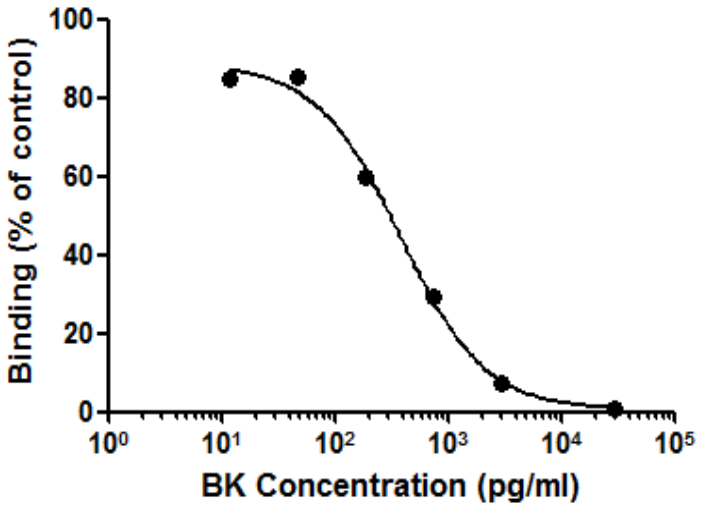

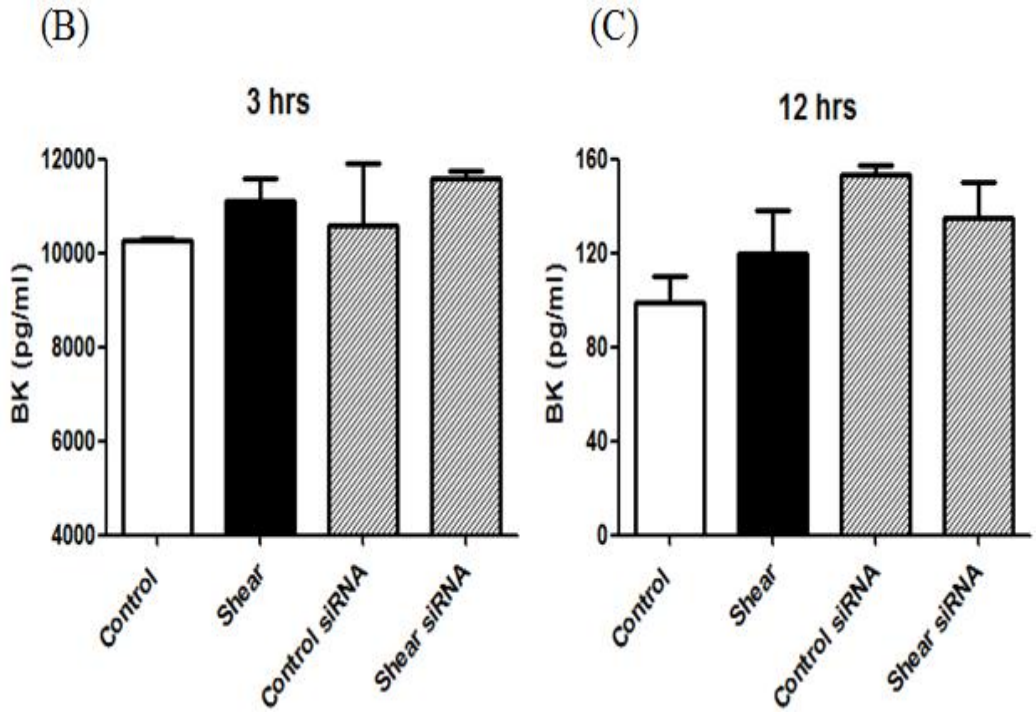

Figure 5.9: Extracellular BK hydrolysis by TOP. HAECs were transfected with TOP siRNA (1 µM) and allowed to recover for 24 hrs. Cells were then subjected to LSS (10 dynes/cm^2, 24 hrs), after which HEPES-Krebs buffer containing captopril (10 µM) and phosphoramidon (2 nM) was added to cells 30 min before the addition of BK (20 ng). Samples were harvested after 3 and 12 hrs and analysed by ELISA. (A) Graph shows BK standard curve used to calculate BK concentration from ELISA results. Histogram of BK (pg/ml) remaining per well after (B) 3 hrs and (C) 12 hrs of incubation with BAECs. Results are averaged from three independent experiments ±SEM; *$P \leq 0.05$ vs untreated control.

5.3 Discussion

This chapter's initial studies were focused on the putative relationship between shear-induced changes in both NEP and EC barrier function. It was shown in Chapter 3 that LSS increases EC barrier integrity whilst down-regulating NEP expression, observations that were seen to be reversed/absent under DSS conditions. In this chapter, we demonstrate that NEP over-expression (using NEP^{++}) significantly reverses the reductions in permeability induced by shear stress (LSS) on HAECs. Thus by preventing the down-regulation of NEP expression by shear (i.e. by adding NEP^{++}), enhancement of barrier function appears to have been blocked, suggesting a possible link between these two shear-dependent phenomena. The lack of effect of phosphoramidon (an NEP inhibitor) on shear-induced permeability reduction (i.e. we anticipated an even further reduction or 'additive' effect) may reflect an artefact/limitation of the permeability assay or may point to a possible non-enzymatic role for NEP in these events. In this respect, 'signalling' roles for NEP have previously been identified (Osman, et al. 2004). In summary therefore, the present data suggest a possible link between NEP down-regulation and permeability under LSS. Whilst the nature of this link is as yet unidentified, a possible mechanism may include focal adhesion kinase (FAK). FAK is a ubiquitously expressed cytoplasmic protein tyrosine kinase involved in the regulation of numerous endothelial cell functions (Grinnell and Harrington 2011). By transiently over-expressing various forms of FAK, previous publications have demonstrated cross-talk between FAK and adherens junctions in the regulation of endothelial barrier function (Usatyuk and Natarajan 2005, Quadri and Bhattacharya 2007). Indeed loss of FAK not only augments barrier deterioration, but it also delays barrier recovery in endothelial monolayers (Patterson 2005). Importantly Sumitomo et al. have previously reported that NEP enzymatic activity inhibits FAK phosphorylation and cell migration by affecting neuropeptide-induced interaction of FAK with cSrc (Sumitomo, et al. 2000).

Another main topic of this chapter concerns the effect of LSS on the rate of EC proliferation. At the cellular level, LSS is known to promote endothelial

quiescence (White, et al. 2001, Traub and Berk 1998) an observation confirmed in this chapter using both impedance analysis and CFSE FACs analysis. Conversely, the effects of DSS are significantly different from those of LSS and are typically characterised by increased proliferation, increased apoptosis, and a lack of alignment to flow (Kudo, et al. 2005). NEP is known to play important roles in neoplastic transformation and tumour progression in certain human malignancies through the enzymatic inactivation of bioactive peptides such as endothelin-1 (ET-1), angiotensin-II, and bombesin. Indeed, previously published data indicate that a loss of NEP in cultured prostate cancer cells results in stimulation of cell proliferation and migration (Osman, et al. 2004). Whilst, Barber et al. report that the inhibition of NEP promotes an anti-proliferative effect on vascular smooth muscle cells (Barber et al., 1995). In this chapter, we therefore undertook to investigate if the shear-induced reduction in NEP is putatively linked to the anti-proliferative effects of shear. For this purpose, we investigate HAEC proliferation in the presence of NEP^{++} under static and shear conditions. Data appear to indicate that the over-expression of NEP (effectively reversing the shear-induced reduction of NEP) does not affect the anti-proliferative effects of LSS when compared to mock transfected controls, suggesting no role for NEP in this context.

In the second half of this chapter the functional impact of TOP up-regulation by shear was assessed with respect to proliferation, MHC I presentation and BK hydrolysis. Beginning with proliferation, we investigated the effects of TOP up-regulation using the same experimental model as that used for NEP. Results demonstrated that silencing of TOP (using TOP siRNA) increases the rate of EC proliferation under shear stress (i.e. manifested as an decrease in doubling time). These results suggest a putative role for TOP in these shear-dependent events. Noteworthy, Cleverly et al. have previously shown that TOP could have a role in cellular proliferation of reproductive tissues through its regulation of luteinising hormone-releasing hormone (LHRH) levels (Cleverly and Wu 2010). Indeed, endothelial cells stimulate LHRH release via NO secretion.

The regulation of extracellular BK levels in ECs by TOP was also investigated in this chapter. The principle pharmacological action of BK in the

regulation of blood pressure is through vasodilatation in most areas of the circulation, a reduction of total peripheral vascular resistance, and a regulation of sodium excretion from the kidneys (Adetuyibi and Mills 1972). Reduced local BK generation and blunted NO formation have been reported in microvessels of failing human hearts (Kichuk, et al. 1996). It is well known that zinc metallopeptidases are capable of hydrolysing BK, with ACE, ECE and NEP being the main sources of BK hydrolysis. Importantly, Jeske et al. have shown that TOP is localised with the B2 receptor on the exofacial leaflet of plasma membranes and in lipid rafts, indicating a potential physiologic role for TOP in modulating BK activation and sensitisation of nociceptors (Jeske, Glucksman and Roberts 2004). Moreover, Cotter et al. showed that cyclic strain modulates the release of TOP from BAECs and thus may have a significant influence on TOP's extracellular functions (Cotter, et al. 2004). Our results subsequently showed that under shear conditions, blockade of TOP (siRNA) exhibited little or no difference to untreated HAECs with respect to BK hydrolysis levels. This would suggest that TOP induction by shear does not influence extracellular BK levels. Whilst non-specific BK hydrolysis has been controlled for with respect to ACE/ECE/NEP through the inclusion of inhibitors in the assay buffer, the possible complication of other peptideass (neurolysin, aminopeptidase N) (Kuoppala, et al. 2000) cannot be ruled out in this particular assay model.

We next turned our attention to a putative intracellular role for TOP: that of MHC I specific antigen presentation. Recognition of antigens in the peptide-binding groove of surface-expressed MHC I and II molecules by specific T-cell receptors, for example, is central to T-cell activation. Recently Kessler et al. have shown that TOP-mediated processing of intracellular peptides both reduces the presentation of proteasomal products by MHC I and also enlarges the MHC I peptide repertoire by processing protein-degradation fragments that are not yet fit for antigenic presentation (Kessler, et al. 2011). In an earlier study, Kim et al. showed that cells over-expressing TOP demonstrated a *marked decrease* in cell surface MHC I staining (Kim et al., 2003). Several human cancers also show down-regulation of MHC I, giving transformed cells the same survival advantage of being able to avoid normal immune surveillance designed to destroy any infected or transformed cells (Wang, et al. 2008). It has also previously been

published that MHC I expression is attenuated in ECs under LSS (Martin-Mondiere, et al. 1989). In the present study, we investigated therefore if shear-induced TOP expression impacted MHC I levels in HAECs. In this regard a preliminary study has demonstrated that LSS attenuates MHC I expression in HAECs and that this effect appears to be blocked by TOP siRNA. This is consistent with the aforementioned studies and suggests a role for TOP in MHC I-dependent antigen presentation in endothelial cells with shear stress being a regulatory factor. Further work will shed light on this increasingly important phenomenon.

In conclusion, results presented in this chapter have shown that NEP is putatively involved in the regulation of barrier integrity but not in EC proliferation under LSS. Our results also suggest that TOP putatively is involved in shear-dependent regulation of EC proliferation and MHC I antigen presentation, but not in modulation of extracellular BK levels.

Chapter 6:

Final Summary

6.1 Final Summary

Cardiovascular disease (CVD) refers to any abnormal condition characterised by the dysfunction of the heart or blood vessels, and includes coronary heart disease, cerebrovascular disease, hypertension, rheumatic and congenital heart disease and heart failure. CVD is the number one cause of death globally. The World Health Organisation estimates that 16.7 million people around the world die from the disease annually, or 29% of all annual deaths worldwide. They also predict a projected increase of this figure to 40% of all deaths by 2020, if the current trends continue. Moreover, it is estimated to have cost the EU economy €192 billion in 2008 (Allender, et al. 2008). As a result, expanding the knowledge base with respect to the underlying causes of CVD has become crucial, and is the focus of much study.

There are nine easily measurable and potentially modifiable risk factors that account for over 90% of the initial acute myocardial infarction. These nine factors are cigarette smoking, abnormal blood lipid levels, hypertension, diabetes, abnormal obesity, a lack of physical activity, low daily fruit and vegetable consumption, alcohol over-consumption and psychosocial index. Other uncontrollable factors that place subjects into a risk category for developing CVD are age, gender, family history and ethnicity.

The health of blood vessels can fundamentally be linked to the endothelium. The endothelium forms the inner lining of all blood vessels and is in direct contact with the blood as it flows through the lumen of the vessel. The unique position of this cell monolayer confers on it the ability to sense and respond to a variety of blood-borne stimuli. These include neurotransmitters, peptide hormones and growth factors (and their associated peptidases), as well as blood-flow associated mechanical forces such as shear stress and cyclic strain. These stimuli continuously elicit biophysical and biochemical changes within the endothelium which influence vessel homeostasis and remodelling on an ongoing basis (Traub and Berk 1998, Kakisis, Liapis and Sumpio 2004). In this context, the endothelium plays an important role in the control of vascular tone, blood

pressure, permeability, proliferation, survival and innate and adaptive immunity. Endothelial dysfunction arising from flow anomalies and other risk factors is therefore involved in many vascular diseases, either as a primary determinant of pathophysiology or as a victim of collateral damage (Aird 2008).

As mentioned previously, blood flow itself imparts a strong biomechanical influence on the vessel wall. Of particular importance are the mechanical forces of cyclic strain and shear stress with the latter stimulus being a central focus of this thesis. A characteristic response of cultured ECs to LSS is to undergo a transition from a cobble stone morphology with no preferred orientation (found under static conditions), to a more elongated stream-lined morphology aligned in the direction of LSS flow. This adaption to flow helps to reduce the effect of shear gradients on the cell surface.

Controlled transport of nutrients across the endothelium is an essential function of the vasculature. *In vivo* therefore, the endothelium monolayer forms a tight junction-dependent barrier between the blood and underlying SMCs. LSS is known to elicit a tightening of these junctions and, as a result, ECs can regulate the size of molecules that cross this barrier (Figure 6.1). Indeed loss of barrier integrity is a prominent feature of vascular diseases. Control studies clearly confirm that the regulation of EC barrier function is force-dependent, with increasing levels of 'atheroprotective' LSS inducing a tighter barrier (manifested as reduced permeability). As most atherosclerotic plaques form at areas of bifurcation or curvature within the macrovasculature, areas that are known to be sites of disturbed blood flow, the relationship between shear type and barrier integrity was also examined. Results of these studies confirm that, unlike LSS, DSS does not impart a tightening of EC barrier function nor a morphological realignment of endothelial cells.

The functional (and transcriptional) impact of shear stress derives from the fact that it acts directly on the cellular membrane leading to *mechano*transduction, the rapid conversion of mechanical signals into biochemical signals with the subsequent induction of appropriate cellular responses. Of primary importance among these responses is the ability of the endothelium to alter expression of vasoactive molecules (and their associated

regulatory enzymes) (Cummins, Cotter and Cahill 2004). In this regard, it has been previously published that members of the zinc metallopeptidases family are shear-sensitive, namely ECE and ACE (Masatsugu, et al. 2003, Ackermann, et al. 1998). Indeed, the promoter region of the ECE gene contains four SSRE sequences, whilst the promoter region of ACE contains two SSRE sequences. Moreover, shear stress was found to down-regulate both enzymes. More recently preliminary studies from our laboratory have demonstrated that NEP and TOP, also members of the zinc metallopeptidase family, are subject to shear regulation in endothelial cells (NEP:(Fitzpatrick, et al. 2009); TOP: unpublished observation), although details are extremely limited. It should also be noted that both NEP and TOP have an SSRE (-GAGACC-) within their promoter region.

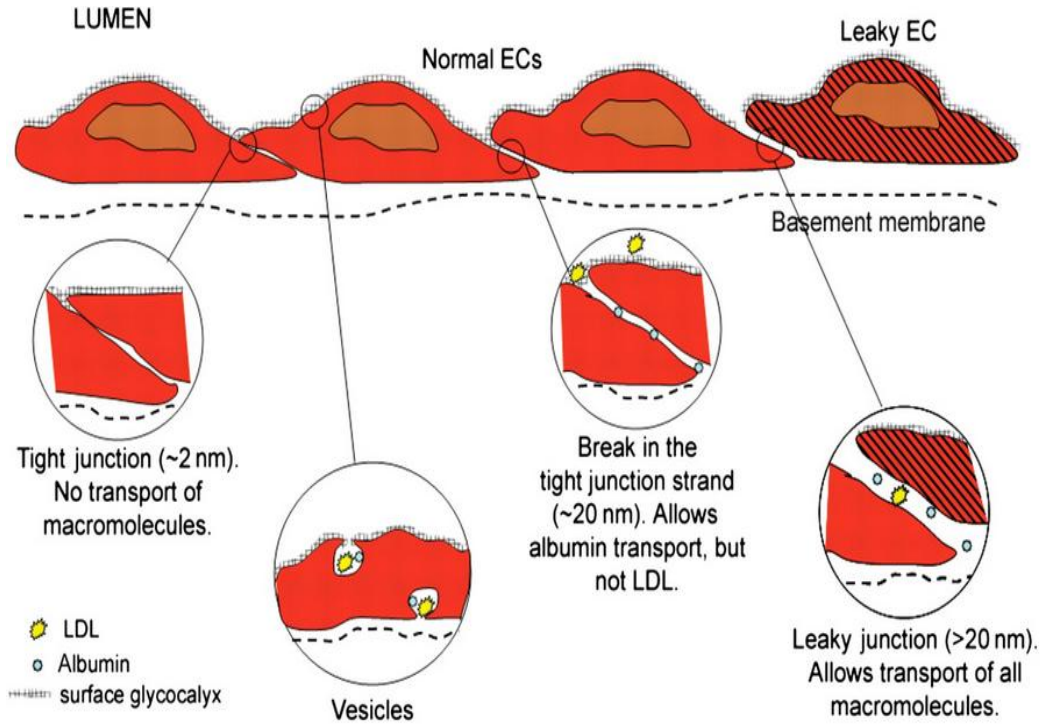

Figure 6.1: Transport pathways across the endothelium. The major transport pathways are: tight junctions, breaks in the tight junctions, vesicles and leaky junctions. The endothelial glycocalyx covers the entrance to all but the leaky junctions (Tarbell, 2010).

In this thesis we have decided to shed further light on the regulation of both NEP and TOP by shear stress in endothelial cells. Consistent with previous publications, our results demonstrate a regulatory role for LSS in NEP expression with respect to magnitude and duration of shear. NEP expression was also shown to be sensitive to the type of shear the cells were exposed to, with LSS but not DSS inducing NEP down-regulation. Using the same experimental paradigm we next investigated the regulation of TOP. TOP expression was shown to be up-regulated by LSS in a time- and magnitude-dependent manner, whilst DSS induced a down-regulation of TOP mRNA levels. To summarise, therefore, LSS appears to regulate NEP and TOP expression levels (mRNA and protein) in a divergent or opposing manner.

Investigation next focused on determining the signal transduction mechanisms through which shear stress altered endothelial NEP and TOP expression. Previous studies have shown that shear-dependent expression of various zinc metallopeptidases, namely ACE, ECE and NEP, are regulated through ROS production (Masatsugu, et al. 2003, Ackermann, et al. 1998, Fitzpatrick, et al. 2009). As NADPH oxidase has previously been shown to be the major source of superoxide in ECs (Griendling, Sorescu and Ushio-Fukai 2000), it was decided to confirm the involvement of this enzyme through the application of an siRNA targeted to the p47 subunit of the NADPH-oxidase complex, thereby neutralising its ROS-producing capability. Results of this study clearly indicated that selective blockade of NADPH oxidase attenuated the effects of LSS on the down- and up-regulation of both NEP and TOP, respectively. This confirms NADPH oxidase as an upstream signalling component in the mechanoregulation of NEP and TOP in vascular cells.

As NADPH oxidase is only ‘transiently’ activated by laminar shear stress, the result is typically a ‘temporal’ ROS surge in endothelial cells within 0-3 hrs of shear onset (Hahn and Schwartz 2009), that declines to baseline levels thereafter. Consistent with this, our experiments have clearly demonstrated that blockade of the ROS surge (using apocynin, NSC23766 and NAC) in advance of shear onset (-1 hrs), but not after shear onset (+4 hrs), prevents shear-dependent changes in NEP and TOP expression.

The functional consequences of shear-induced regulation of both NEP and TOP were also investigated. In initial studies HAECs over-expressing NEP were seen to exhibit a weakened barrier under both control and shear conditions when compared to untreated cells (manifested as increased permeability). Interestingly however, the use of an NEP inhibitor (phosphoramidon) did not show an additive effect towards shear-induced barrier up-regulation. These results suggest a possible link between the shear-dependent down-regulation of NEP and enhanced barrier function.

The link between the shear-induced regulation of NEP/TOP and endothelial cell proliferation was also investigated. This entailed shearing studies involving over-expression of NEP and TOP, and the silencing of TOP. Results presented point to a putative role for TOP, but not NEP, in the regulation of the anti-proliferative effects of shear on endothelial cells.

It has previously been published that MHC I expression is attenuated in ECs under LSS (Martin-Mondiere, et al. 1989), whilst Kim et al. demonstrated that over-expression of TOP is capable of inducing long-term repression of surface MHC I in CTLs. Conversely, the latter author also showed that the use of a TOP siRNA increased long-term surface expression of MHC I (Kim, et al. 2003). It was therefore decided to investigate if TOP plays a role in the intracellular shear-dependent regulation of MHC I expression, through the use of a TOP siRNA under LSS conditions. Preliminary results of this study suggest that TOP is involved in the regulation of MHC I, as the introduction of TOP siRNA under shear conditions reversed the down-regulatory effect of LSS on MHC I protein expression.

Within the vasculature, termination of BK signalling is controlled by zinc metallopeptidases (Rawlings and Barrett 1993, Turner 2003). As such, we examined the functional role that the shear-induced up-regulation of TOP plays in the extracellular hydrolysis of BK. This was achieved by over-expressing and silencing TOP under both static and shear conditions. However, our results indicate that TOP induction by shear does not appear to influence extracellular BK levels.

Notwithstanding further repeats of some studies to improve statistical significance, new areas for investigation could include (i) determining the role of junctional proteins such as VE-cadherin and PECAM-1 in the mechano regulation of NEP and TOP; (ii) investigation of the NEP and TOP signalling pathways downstream of ROS production, in which MAP kinases could be a primary focus; (iii) investigation of the putative roles of NEP and TOP in endothelial wound healing under LSS; (iv) use of apo-$E^{-/-}$ knockout mouse models to monitor NEP and TOP levels *in vivo* at sites of flow reduction and/or turbulence (e.g. aortic arch).

In conclusion this thesis has demonstrated that expression of both NEP and TOP are regulated by LSS in a time- and dose-dependent manner, with LSS displaying opposite effects on either enzyme. This study has also confirmed that this regulation is mediated by NADPH oxidase-dependent ROS production during the early shear phase. Moreover, functional studies have implicated roles for NEP in the regulation of endothelial barrier function under shear, whilst findings suggest that TOP is involved in the regulation of endothelial proliferation and MHC I antigen presentation under shear. These findings significantly contribute to our knowledge of vascular physiology and pathology by showing how shear regulates therapeutically relevant zinc metallopeptidases within the macrovascular endothelium.

Bibliography

Abraham, W., Scuri, M. and Farmer, S. 2006. Peptide and non-peptide bradykinin receptor antagonists: role in allergic airway disease. *European Journal of Pharmacology,* 533(1-3), pp.215-221.

Acker, G., Molineaux, C. and Orlowski, M. 1987. Synaptosomal membrane-bound form of endopeptidase-24.15 generates Leu-Enkephalin from Dynorphin 1-8, α- and β-Neoendorphin, and Met-Enkephalin from Met-Enkephalin-Arg6-Gly7-Leu. *Journal of Neurochemistry,* 48(1), pp.284-292.

Ackermann, A., Fernández-Alfonso, M., Sanchez de Rojas, R., Ortega, T., Paul, M. and Gonzalez, C. 1998. Modulation of angiotensin converting enzyme by nitric oxide. *British Journal of Pharmacology,* 124(2), pp.291-298.

Adetuyibi, A. and Mills, I. 1972. Relation between urinary kallikrein and renal function, hypertension, and excretion of sodium and water in man. *The Lancet,* 300(7770), pp.203-207.

Aird, W.C. 2008. Endothelium in health and disease. *Pharmacological Reports,* 60(1), pp.139-143.

Akimoto, S., Mitsumata, M., Sasaguri, T. and Yoshida, Y. 2000. Laminar shear stress inhibits vascular endothelial cell proliferation by inducing cyclin-dependent kinase inhibitor p21Sdi1/Cip1/Waf1. *Circulation Research,* 86(2), pp.185-192.

Albelda, S., Muller, W., Buck, C. and Newman, P. 1991. Molecular and cellular properties of PECAM-1 (endoCAM/CD31): a novel vascular cell-cell adhesion molecule. *The Journal of Cell Biology,* 114(5), pp.1059-1068.

Albelda, S., Oliver, P., Romer, L. and Buck, C. 1990. EndoCAM: a novel endothelial cell-cell adhesion molecule. *The Journal of Cell Biology,* 110(4), pp.1227-1237.

Allender, S., Scarborough, P., Peto, V., Rayner, M., Leal, J., Luengo-Fernandez, R. and Gray, A. 2008. European cardiovascular disease statistics. *Brussels: European Heart Network,*

Andreeva, A., Vaiskunaite, R., Kutuzov, M., Profirovic, J., Skidgel, R. and Voyno-Yasenetskaya, T. 2006. Novel mechanisms of G protein-dependent regulation of endothelial nitric-oxide synthase. *Molecular Pharmacology,* 69(3), pp.975-982.

Babior, B. 1999. NADPH oxidase: an update. *Blood,* 93(5), pp.1464-1476.

Barakat, A., Leaver, E., Pappone, P. and Davies, P. 1999. A flow-activated chloride-selective membrane current in vascular endothelial cells. *Circulation Research,* 85(9), pp.820-828.

Barakat, A., Lieu, D. and Gojova, A. 2006. Secrets of the code: Do vascular endothelial cells use ion channels to decipher complex flow signals? *Biomaterials,* 27(5), pp.671-678.

Barber, M., Gaspari, T., Kairuz, E., Dusting, G. and Woods, R. 2005. Atrial natriuretic peptide preserves endothelial function during intimal hyperplasia. *Journal of Vascular Research,* 42(2), pp.101-110.

Barczyk, M., Carracedo, S. and Gullberg, D. 2010. Integrins. *Cell and Tissue Research,* 339(1), pp.269-280.

Bartus, R., Elliott, P., Hayward, N., Dean, R., McEwen, E. and Fisher, S. 1996. Permeability of the blood brain barrier by the bradykinin agonist, RMP-7: evidence for a sensitive, auto-regulated, receptor-mediated system. *Immunopharmacology,* 33(1-3), pp.270-278.

Bayer, M., Reese, C., Bühler, S., Peters, C. and Mayer, A. 2003. Vacuole membrane fusion. *The Journal of Cell Biology,* 162(2), pp.211-222.

Bayés, À., Fernández, D., Sola, M., Marrero, A., García-Piqué, S., Avilés, F., Vendrell, J. and Xavier, F. 2007. Caught after the Act: A human A-type metallocarboxypeptidase in a product complex with a cleaved hexapeptide. *Biochemistry,* 46(23), pp.6921-6930.

Bayraktutan, U., Blayney, L. and Shah, A. 2000. Molecular characterization and localization of the NAD (P) H oxidase components gp91-phox and p22-phox in endothelial cells. *Arteriosclerosis, Thrombosis, and Vascular Biology*, 20(8), pp.1903-1911.

Berthiaume, F. and Frangos, J. 1992. Flow-induced prostacyclin production is mediated by a pertussis toxin-sensitive G protein. *FEBS Letters*, 308(3), pp.277-279.

Betteridge, D. 2000. What is oxidative stress? *Metabolism*, 49(2), pp.3-8.

Bhoola, K., Figueroa, C. and Worthy, K. 1992. Bioregulation of kinins: kallikreins, kininogens, and kininases. *Pharmacological Reviews*, 44(1), pp.1-80.

Blume-Jensen, P. and Hunter, T. 2001. Oncogenic kinase signalling. *Nature*, 411(6835), pp.355-365.

Bonvouloir, N., Lemieux, N., Crine, P., Boileau, G. and DesGroseillers, L. 2001. Molecular cloning, tissue distribution, and chromosomal localization of MMEL2, a gene coding for a novel human member of the neutral endopeptidase-24.11 family. *DNA and Cell Biology*, 20(8), pp.493-498.

Boulay, A., Breuleux, M., Stephan, C., Fux, C., Brisken, C., Fiche, M., Wartmann, M., Stumm, M., Lane, H. and Hynes, N. 2008. The Ret receptor tyrosine kinase pathway functionally interacts with the ERα pathway in breast cancer. *Cancer Research*, 68(10), pp.3743-3751.

Boules, M., Fredrickson, P. and Richelson, E. 2006. Bioactive analogs of neurotensin: focus on CNS effects. *Peptides*, 27(10), pp.2523-2533.

Bourguignon, J., Alvarez Gonzalez, M., Gerard, A. and Franchimont, P. 1994. Gonadotropin releasing hormone inhibitory autofeedback by subproducts antagonist at N-methyl-D-aspartate receptors: a model of autocrine regulation of peptide secretion. *Endocrinology*, 134(3), pp.1589-1592.

Breier, G., Breviario, F., Caveda, L., Berthier, R., Schnurch, H., Gotsch, U., Vestweber, D., Risau, W. and Dejana, E. 1996. Molecular cloning and expression of murine vascular endothelial-cadherin in early stage development of cardiovascular system. *Blood,* 87(2), pp.630-641.

Brown, C., Madauss, K., Lian, W., Beck, M., Tolbert, W. and Rodgers, D. 2001. Structure of neurolysin reveals a deep channel that limits substrate access. *Proceedings of the National Academy of Sciences U.S.A.,* 98(6), pp.3127-3132.

Bustin, S., Benes, V., Garson, J., Hellemans, J., Huggett, J., Kubista, M., Mueller, R., Nolan, T., Pfaffl, M. and Shipley, G. 2009. The MIQE guidelines: minimum information for publication of quantitative real-time PCR experiments. *Clinical Chemistry,* 55(4), pp.611-622.

Cantley, L. and Cantley, L. 1995. Signal transduction by the hepatocyte growth factor receptor, c-met. Activation of the phosphatidylinositol 3-kinase. *Journal of the American Society of Nephrology,* 5(11), pp.1872-1881.

Carreno, F., Goni, C., Castro, L. and Ferro, E. 2005. 14-3-3 epsilon modulates the stimulated secretion of endopeptidase 24.15. *Journal of Neurochemistry,* 93(1), pp.10-25.

Carson, J. and Turner, A. 2002. β-Amyloid catabolism: roles for neprilysin (NEP) and other metallopeptidases? *Journal of Neurochemistry,* 81(1), pp.1-8.

Carvajal, C., Vercauteren, F., Dumont, Y., Michalkiewicz, M. and Quirion, R. 2004. Aged neuropeptide Y transgenic rats are resistant to acute stress but maintain spatial and non-spatial learning. *Behavioural Brain Research,* 153(2), pp.471-480.

Cerdeira, A., Bras-Silva, C. and Leite-Moreira, A. 2008. Endothelin-converting enzyme inhibitors: their application in cardiovascular diseases. *Revista Portuguesa De Cardiologia : Orgao Oficial Da Sociedade Portuguesa De Cardiologia = Portuguese Journal of Cardiology : An Official Journal of the Portuguese Society of Cardiology,* 27(3), pp.385-408.

Chappell, M., Tallant, E., Brosnihan, K. and Ferrario, C. 1994. Conversion of angiotensin I to angiotensin-(1-7) by thimet oligopeptidase (EC 3.4.24.15) in vascular smooth muscle cells. *Journal of Vascular Medicine and Biology,* 5pp.129-137.

Chen, K. and Keaney Jr, J. 2004. Reactive oxygen species-mediated signal transduction in the endothelium. *Endothelium,* 11(2), pp.109-121.

Chen, Y., Duvvuri, V., Schulman, H. and Scheller, R. 1999. Calmodulin and protein kinase C increase Ca2+-stimulated secretion by modulating membrane-attached exocytic machinery. *Journal of Biological Chemistry,* 274(37), pp.26469-26476.

Chiu. 1998. Effects of disturbed flow on endothelial cells. *Journal of Biomechanical Engineering,* (120), pp.2-8.

Chomczynski, P. and Sacchi, N. 1987. Single-step method of RNA isolation by acid guanidinium thiocyanate-phenol-chloroform extraction. *Analytical Biochemistry,* 162(1), pp.156-159.

Chu, T. and Orlowski, M. 1985. Soluble metalloendopeptidase from rat brain: action on enkephalin-containing peptides and other bioactive peptides. *Endocrinology,* 116(4), pp.1418-1425.

Cleverly, K. and Wu, T. 2010. Is the metalloendopeptidase EC 3.4.24.15 (EP24. 15), the enzyme that cleaves luteinizing hormone-releasing hormone (LHRH), an activating enzyme? *Reproduction,* 139(2), pp.319-330.

Colgan, O., Ferguson, G., Collins, N., Murphy, R., Meade, G., Cahill, P. and Cummins, P. 2007. Regulation of bovine brain microvascular endothelial tight junction assembly and barrier function by laminar shear stress. *American Journal of Physiology- Heart and Circulatory Physiology,* 292(6), pp.H3190-H3197.

Collins, N., Cummins, P., Colgan, O., Ferguson, G., Birney, Y., Murphy, R., Meade, G. and Cahill, P. 2005. Cyclic strain-mediated regulation of vascular

endothelial occludin and ZO-1: Influence on intercellular tight junction assembly and function. *Arteriosclerosis, Thrombosis, and Vascular Biology*, 26pp.62-68.

Colomer, J. and Means, A. 2008. Physiological roles of the Ca 2 /CaM-dependent protein kinase cascade in health and disease. *Calcium Signalling and Disease*, 45pp.169-214.

Cooperstein, S. and Watkins, D. 1995. Ca2+-calmodulin-dependent phosphorylation and dephosphorylation of rat parotid secretion granules. *Biochemical and Biophysical Research Communications*, 215(1), pp.75-81.

Corti, R., Burnett Jr, J.C., Rouleau, J.L., Ruschitzka, F. and Lüscher, T.F. 2001. Vasopeptidase Inhibitors. *Circulation*, 104(15), pp.1856-1862.

Cotter, E., Sweeney, N., Coen, P., Birney, Y., Glucksman, M., Cahill, P. and Cummins, P. 2004. Regulation of endopeptidases EC3.4.24.15 and EC3.4.24.16 in vascular endothelial cells by cyclic strain: Role of Gi protein signaling. *Arteriosclerosis, Thrombosis, and Vascular Biology*, 24(3), pp.457-463.

Crack, P., Wu, T., Cummins, P., Ferro, E., Tullai, J., Glucksman, M. and Roberts, J. 1999. The association of metalloendopeptidase EC 3.4. 24.15 at the extracellular surface of the AtT-20 cell plasma membrane. *Brain Research*, 835(2), pp.113-124.

Crackower, M., Sarao, R., Oudit, G., Yagil, C., Kozieradzki, I., Scanga, S., Oliveira-dos-Santos, A., da Costa, J., Zhang, L. and Pei, Y. 2002. Angiotensin-converting enzyme 2 is an essential regulator of heart function. *Nature*, 417(6891), pp.822-828.

Cummins, P., Cotter, E. and Cahill, P. 2004. Hemodynamic regulation of metallopeptidases within the vasculature. *Protein and Peptide Letters*, 11(5), pp.433-442.

Cunningham, K. and Gotlieb, A. 2004. The role of shear stress in the pathogenesis of atherosclerosis. *Laboratory Investigation*, 85(1), pp.9-23.

D'Adamio, L., Shipp, M., Masteller, E. and Reinherz, E. 1989. Organization of the gene encoding common acute lymphoblastic leukemia antigen (neutral endopeptidase 24.11): multiple miniexons and separate 5' untranslated regions. *Proceedings of the National Academy of Sciences U.S.A.,* 86(18), pp.7103-7107.

D'Angelo, A. and Franco, B. 2009. The dynamic cilium in human diseases. *Pathogenetics,* 2(1), pp.3-18.

Davies, P. 1995. Flow-mediated endothelial mechanotransduction. *Physiological Reviews,* 75(3), pp.519-560.

DeLisser, H., Christofidou-Solomidou, M., Strieter, R., Burdick, M., Robinson, C., Wexler, R., Kerr, J., Garlanda, C., Merwin, J. and Madri, J. 1997. Involvement of endothelial PECAM-1/CD31 in angiogenesis. *The American Journal of Pathology,* 151(3), pp.671-677.

Demasi, M., Piassa Filho, G., Castro, L., Ferreira, J., Rioli, V. and Ferro, E. 2008. Oligomerization of the cysteinyl-rich oligopeptidase EP24.15 is triggered by S-glutathionylation. *Free Radical Biology and Medicine,* 44(6), pp.1180-1190.

Dimmeler, S., Haendeler, J., Nehls, M. and Zeiher, A. 1997. Suppression of apoptosis by nitric oxide via inhibition of interleukin-1beta-converting enzyme (ICE)-like and cysteine protease protein (CPP)-32-like proteases. *Journal of Experimental Medicine,* (185), pp.601-607.

Dröge, W. 2002. Free radicals in the physiological control of cell function. *Physiological Reviews,* 82(1), pp.47-95.

Duerrschmidt, N., Stielow, C., Muller, G., Pagano, P. and Morawietz, H. 2006. NO-mediated regulation of NADPH oxidase by laminar shear stress in human endothelial cells. *The Journal of Physiology,* 576(2), pp.557-567.

Ebong, E., Macaluso, F., Spray, D. and Tarbell, J. 2011. Imaging the endothelial glycocalyx in vitro by rapid freezing/freeze substitution transmission electron

microscopy. *Arteriosclerosis, Thrombosis, and Vascular Biology*, pp.[Epub ahead of print] PMID: 21474821.

Eckman, E., Reed, D. and Eckman, C. 2001. Degradation of the Alzheimer's amyloid β peptide by endothelin-converting enzyme. *Journal of Biological Chemistry*, 276(27), pp.24540-24548.

Ehlers, M. and Riordan, J. 1989. Angiotensin-converting enzyme: new concepts concerning its biological role. *Biochemistry*, 28(13), pp.5311-5318.

Facchinetti, P., Rose, C., Schwartz, J.C. and Ouimet, T. 2003. Ontogeny, regional and cellular distribution of the novel metalloprotease neprilysin 2 in the rat: a comparison with neprilysin and endothelin-converting enzyme-1. *Neuroscience*, 118(3), pp.627-639.

Ferrario, C. 1990. The renin-angiotensin system: importance in physiology and pathology. *Journal of Cardiovascular Pharmacology*, 15pp.S1-S5.

Ferrero, E., Ferrero, M., Pardi, R. and Zocchi, M. 1995. The platelet endothelial cell adhesion molecule-1 (PECAM1) contributes to endothelial barrier function. *FEBS Letters*, 374(3), pp.323-326.

Ferro, C., Spratt, J., Haynes, W. and Webb, D. 1998. Inhibition of neutral endopeptidase causes vasoconstriction of human resistance vessels in vivo. *Circulation*, 97(23), pp.2323-2330.

Ferro, E., Carreno, F., Goni, C., Garrido, P., Guimaraes, A., Castro, L., Oliveira, V., Araujo, M., Rioli, V. and Gomes, M. 2004. The intracellular distribution and secretion of endopeptidases 24.15 (EC 3.4. 24.15) and 24.16 (EC 3.4. 24.16). *Protein and Peptide Letters*, 11(5), pp.415-421.

Finkel, T. and Holbrook, N.J. 2000. Oxidants, oxidative stress and the biology of ageing. *Nature London*, 408pp.239-247.

Fitzpatrick, P., Guinan, A., Walsh, T., Murphy, R., Killeen, M., Tobin, N., Pierotti, A. and Cummins, P. 2009. Down-regulation of neprilysin (EC3.4.24.11)

expression in vascular endothelial cells by laminar shear stress involves NADPH oxidase-dependent ROS production. *The International Journal of Biochemistry & Cell Biology,* 41(11), pp.2287-2294.

Fleming, I., Fisslthaler, B., Dixit, M. and Busse, R. 2005. Role of PECAM-1 in the shear-stress-induced activation of Akt and the endothelial nitric oxide synthase (eNOS) in endothelial cells. *Journal of Cell Science,* 118(18), pp.4103-4111.

Francis, F., Hennig, S., Korn, B., Reinhardt, R., De Jong, P., Poustka, A., Lehrach, H., Rowe, P., Goulding, J. and Summerfield, T. 1995. A gene (PEX) with homologies to endopeptidases is mutated in patients with X–linked hypophosphatemic rickets. *Nature Genetics,* 11(2), pp.130-136.

Frangos, S., Gahtan, V. and Sumpio, B. 1999. Localization of atherosclerosis: role of hemodynamics. *Archives of Surgery,* 134(10), pp.1142-1149.

Fridovich, I. 1999. Fundamental aspects of reactive oxygen species, or what's the matter with oxygen? *Annals of the New York Academy of Sciences*, 893(1), pp.13-18.

Fujiwara, K., Masuda, M., Osawa, M., Kano, Y. and Katoh, K. 2001. Is PECAM-1 a mechanoresponsive molecule? *Cell Structure and Function,* 26(1), pp.11-17.

Furchgott, R.F. and Zawadzki, J.V. 1980. The obligatory role of endothelial cells in the relaxation of arterial smooth muscle by acetylcholine. *Nature*, 288(5789), pp.373-376.

Galbiati, F., Razani, B. and Lisanti, M. 2001. Emerging themes in lipid rafts and caveolae. *Cell,* 106(4), pp.403-411.

Galbraith, C., Skalak, R. and Chien, S. 1998. Shear stress induces spatial reorganization of the endothelial cell cytoskeleton. *Cell Motility and the Cytoskeleton,* 40(4), pp.317-330.

Gentil-dit-Maurin, A., Oun, S., Almagro, S., Bouillot, S., Courçon, M., Linnepe, R., Vestweber, D. and Huber, P. 2010. Unraveling the distinct distributions of VE-and N-cadherins in endothelial cells: A key role for p120-catenin. *Experimental Cell Research,* 316(16), pp.2587-2599.

Ghaddar, G., Ruchon, A., Carpentier, M., Marcinkiewicz, M., Seidah, N., Crine, P., Desgroseillers, L. and Boileau, G. 2000. Molecular cloning and biochemical characterization of a new mouse testis soluble-zinc-metallopeptidase of the neprilysin family. *Biochemical Journal,* 347(Pt 2), pp.419.

Go, Y., Patel, R., Maland, M., Park, H., Beckman, J., Darley-Usmar, V. and Jo, H. 1999. Evidence for peroxynitrite as a signaling molecule in flow-dependent activation of c-Jun NH2-terminal kinase. *American Journal of Physiology-Heart and Circulatory Physiology,* 277(4), pp.H1647-H1653.

Goedert, M. 1984. Neurotensin--a status report. *Trends in Neurosciences,* 7(1), pp.3-5.

Gojova, A. and Barakat, A. 2005. Vascular endothelial wound closure under shear stress: role of membrane fluidity and flow-sensitive ion channels. *Journal of Applied Physiology,* 98(6), pp.2355-2362.

Goldsmith, H., Cokelet, G. and Gaehtgens, P. 1989. Robin Fahraeus: evolution of his concepts in cardiovascular physiology. *American Journal of Physiology-Heart and Circulatory Physiology,* 257(3), pp.H1005-H1015.

Gomez, R., Por, E., Berg, K., Clarke, W., Glucksman, M. and Jeske, N. 2011. Metallopeptidase inhibition potentiates bradykinin-induced hyperalgesia. *Pain,* 152pp.1548-1554.

Gomis-Ruth, F. 2008. Structure and mechanism of metallocarboxypeptidases. *Critical Reviews in Biochemistry and Molecular Biology,* 43(5), pp.319-345.

Gomis-Ruth, F., Botelho, T. and Bode, W. 2011. A standard orientation for metallopeptidases. *Biochimica Et Biophysica Acta (BBA)-Proteins & Proteomics,* pp.[Epub ahead of print] PMID: 21558023.

Gong, L., Pitari, G., Schulz, S. and Waldman, S. 2004. Nitric oxide signaling: systems integration of oxygen balance in defense of cell integrity. *Current Opinion in Hematology,* 11(1), pp.7-14.

Gory-Faure, S., Prandini, M.H., Pointu, H., Roullot, V., Pignot-Paintrand, I., Vernet, M. and Huber, P. 1999. Role of vascular endothelial-cadherin in vascular morphogenesis. *Development,* 126(10), pp.2093-2102.

Griendling, K., Sorescu, D. and Ushio-Fukai, M. 2000. NADPH oxidase: role in cardiovascular biology and disease. *Circulation Research,* 86(5), pp.494-501.

Grinnell, K. and Harrington, E. 2011. Interplay between FAK, PKC [delta], and p190RhoGAP in the Regulation of Endothelial Barrier Function. *Microvascular Research,* pp.[Epub ahead of print] PMID: 21549132.

Groarke, D.A., Drmota, T., Bahia, D.S., Evans, N.A., Wilson, S. and Milligan, G. 2001. Analysis of the C-terminal tail of the rat thyrotropin-releasing hormone receptor-1 in interactions and co-internalization with β-arrestin 1-green fluorescent protein. *Molecular Pharmacology,* 59(2), pp.375-385.

Groemping, Y. and Rittinger, K. 2005. Activation and assembly of the NADPH oxidase: a structural perspective. *Biochemical Journal,* 386(Pt 3), pp.401-416.

Gryglewski, R. 1995. Interactions between endothelial mediators. *Pharmacology & Toxicology,* 77(1), pp.1-9.

Gudi, S., Clark, C. and Frangos, J. 1996. Fluid flow rapidly activates G proteins in human endothelial cells: involvement of G proteins in mechanochemical signal transduction. *Circulation Research,* 79(4), pp.834-839.

Gudi, S., Huvar, I., White, C., McKnight, N., Dusserre, N., Boss, G. and Frangos, J. 2003. Rapid activation of ras by fluid flow is mediated by G {alpha} q and G {beta}{gamma} subunits of heterotrimeric G proteins in human endothelial cells. *Arteriosclerosis, Thrombosis, and Vascular Biology,* 23(6), pp.994-1000.

Gulino, D., Delachanal, E., Concord, E., Genoux, Y., Morand, B., Valiron, M., Sulpice, E., Scaife, R., Alemany, M. and Vernet, T. 1998. Alteration of endothelial cell monolayer integrity triggers resynthesis of vascular endothelium cadherin. *Journal of Biological Chemistry*, 273(45), pp.29786-29793.

Hadjiivanova, C., Belcheva, S. and Belcheva, I. 2003. Cholecystokinin and learning and memory processes. *Acta Physiologica Et Pharmacologica Bulgarica*, 27(2-3), pp.83-88.

Hahn, C. and Schwartz, M.A. 2009. Mechanotransduction in vascular physiology and atherogenesis. *Nature Reviews Molecular Cell Biology*, 10(1), pp.53-62.

Hamm, H. 1998. The many faces of G protein signaling. *Journal of Biological Chemistry*, 273(2), pp.669-672.

Harburger, D. and Calderwood, D. 2009. Integrin signalling at a glance. *Journal of Cell Science*, 122(2), pp.159-193.

Hasan, A., Amenta, S. and Schmaier, A. 1996. Bradykinin and its metabolite, Arg-Pro-Pro-Gly-Phe, are selective inhibitors of {alpha}-thrombin–induced platelet activation. *Circulation*, 94(3), pp.517-528.

Hashimoto, S., Gon, Y., Matsumoto, K., Takeshita, I. and Horie, T. 2001. N-acetylcysteine attenuates TNF-α-induced p38 MAP kinase activation and p38 MAP kinase-mediated IL-8 production by human pulmonary vascular endothelial cells. *British Journal of Pharmacology*, 132(1), pp.270-276.

Heinrichs, M., Meinlschmidt, G., Wippich, W., Ehlert, U. and Hellhammer, D.H. 2004. Selective amnesic effects of oxytocin on human memory. *Physiology & Behavior*, 83(1), pp.31-38.

Helmlinger, G., Geiger, R.V., Schreck, S. and Nerem, R.M. 1991. Effects of pulsatile flow on cultured vascular endothelial cell morphology. *Journal of Biomechanical Engineering*, 113pp.123-131.

Hendrickson, R., Cahill, P., Sitzmann, J. and Redmond, E. 1999. Ethanol enhances basal and flow-stimulated nitric oxide synthase activity *in vitro* by activating an inhibitory guanine nucleotide-binding protein. *Journal of Pharmacology and Experimental Therapeutics,* 289(3), pp.1293-1300.

Hierck, B., Van der Heiden, K., Alkemade, F., Van de Pas, S., Van Thienen, J., Groenendijk, B., Bax, W., Van der Laarse, A., DeRuiter, M. and Horrevoets, A. 2008. Primary cilia sensitize endothelial cells for fluid shear stress. *Developmental Dynamics,* 237(3), pp.725-735.

Holmes, K., Roberts, O., Thomas, A. and Cross, M. 2007. Vascular endothelial growth factor receptor-2: structure, function, intracellular signalling and therapeutic inhibition. *Cellular Signalling,* 19(10), pp.2003-2012.

Hooper, N. and Turner, A. 2003. An ACE structure. *Nature Structural & Molecular Biology,* 10(3), pp.155-157.

Huot, J., Houle, F., Marceau, F. and Landry, J. 1997. Oxidative stress–induced actin reorganization mediated by the p38 mitogen-activated protein kinase/heat shock protein 27 pathway in vascular endothelial cells. *Circulation Research,* 80(3), pp.383-392.

Hurowitz, E., Melnyk, J., Chen, Y., Kouros-Mehr, H., Simon, M. and Shizuya, H. 2000. Genomic characterization of the human heterotrimeric G protein α, β, and γ subunit genes. *DNA Research,* 7(2), pp.111-120.

Hynes, R. 2002. Integrins: bidirectional, allosteric signaling machines. *Cell,* 110(6), pp.673-687.

Ibrahim, M. 2006. RAS inhibition in hypertension. *Journal of Human Hypertension,* 20(2), pp.101-108.

Iglarz, M. and Schiffrin, E.L. 2003. Role of endothelin-1 in hypertension. *Current Hypertension Reports,* 5(2), pp.144-148.

Ihling, C., Szombathy, T., Bohrmann, B., Brockhaus, M., Schaefer, H.E. and Loeffler, B.M. 2001. Co-expression of endothelin-converting enzyme-1 and endothelin-1 in different stages of human atherosclerosis. *Circulation,* 104(8), pp.864-869.

Ihrig, M., Dangler, C. and Fox, J. 2001. Mice lacking inducible nitric oxide synthase develop spontaneous hypercholesterolaemia and aortic atheromas. *Atherosclerosis,* 156(1), pp.103-107.

Imberti, B., Morigi, M., Zoja, C., Angioletti, S., Abbate, M., Remuzzi, A. and Remuzzi, G. 2000. Shear stress-induced cytoskeleton rearrangement mediates NF-kappaB-dependent endothelial expression of ICAM-1. *Microvascular Research,* 60(2), pp.182-188.

Iwase, A., Shen, R., Navarro, D. and Nanus, D.M. 2004. Direct binding of neutral endopeptidase 24.11 to ezrin/radixin/moesin (ERM) proteins competes with the interaction of CD44 with ERM proteins. *Journal of Biological Chemistry,* 279(12), pp.11898-11905.

Jaffe, E., Hoyer, L. and Nachman, R. 1973. Synthesis of antihemophilic factor antigen by cultured human endothelial cells. *Journal of Clinical Investigation,* 52(11), pp.2757-2764.

Jensen, P. 2007. Recent advances in antigen processing and presentation. *Nature Immunology,* 8(10), pp.1041-1048.

Jeske, N., Berg, K., Cousins, J., Ferro, E., Clarke, W., Glucksman, M. and Roberts, J. 2006. Modulation of bradykinin signaling by EP24.15 and EP24.16 in cultured trigeminal ganglia. *Journal of Neurochemistry,* 97(1), pp.13-21.

Jeske, N., Glucksman, M. and Roberts, J. 2004. Metalloendopeptidase EC3.4.24.15 is constitutively released from the exofacial leaflet of lipid rafts in GT1-7 cells. *Journal of Neurochemistry,* 90(4), pp.819-828.

Jin, Z., Wong, C., Wu, J. and Berk, B. 2005. Flow shear stress stimulates Gab1 tyrosine phosphorylation to mediate protein kinase B and endothelial nitric-oxide

synthase activation in endothelial cells. *Journal of Biological Chemistry*, 280(13), pp.12305-12309.

Johnson, G., Stevenson, T. and Ahn, K. 1999. Hydrolysis of peptide hormones by endothelin-converting enzyme-1. *Journal of Biological Chemistry*, 274(7), pp.4053-4058.

Jong Lee, H. and Young Koh, G. 2003. Shear stress activates Tie2 receptor tyrosine kinase in human endothelial cells. *Biochemical and Biophysical Research Communications*, 304(2), pp.399-404.

Jourd'heuil, D., Jourd'heuil, F.L., Kutchukian, P.S., Musah, R.A., Wink, D.A. and Grisham, M.B. 2001. Reaction of superoxide and nitric oxide with peroxynitrite. *Journal of Biological Chemistry*, 276(31), pp.28799-28805.

Jurado, L., Chockalingam, P. and Jarrett, H. 1999. Apocalmodulin. *Physiological Reviews*, 79(3), pp.661-682.

Kakisis, J., Liapis, C. and Sumpio, B. 2004. Effects of cyclic strain on vascular cells. *Endothelium*, 11(1), pp.17-28.

Kano, Y., Katoh, K. and Fujiwara, K. 2000. Lateral zone of cell-cell adhesion as the major fluid shear stress-related signal transduction site. *Circulation Research*, 86(4), pp.425-433.

Kato, A., Sugiura, N., Saruta, Y., Hosoiri, T., Yasue, H. and Hirose, S. 1997. Targeting of endopeptidase 24.16 to different subcellular compartments by alternative promoter usage. *Journal of Biological Chemistry*, 272(24), pp.15313-15322.

Keaney Jr, J.F., Xu, A., Cunningham, D., Jackson, T., Frei, B. and Vita, J.A. 1995. Dietary probucol preserves endothelial function in cholesterol-fed rabbits by limiting vascular oxidative stress and superoxide generation. *Journal of Clinical Investigation*, 95(6), pp.2520-2529.

Keaney, J.F., Gaziano, J.M., Xu, A., Frei, B., Curran-Celentano, J., Shwaery, G.T., Loscalzo, J. and Vita, J.A. 1993. Dietary antioxidants preserve endothelium-dependent vessel relaxation in cholesterol-fed rabbits. *Proceedings of the National Academy of Sciences U.S.A.,* 90(24), pp.11880-11884.

Kessler, J., Khan, S., Seifert, U., Le Gall, S., Chow, K., Paschen, A., Bres-Vloemans, S., de Ru, A., van Montfoort, N. and Franken, K. 2011. Antigen processing by nardilysin and thimet oligopeptidase generates cytotoxic T cell epitopes. *Nature Immunology,* 12pp.45-53.

Khimji, A. and Rockey, D.C. 2010. Endothelin--Biology and disease. *Cellular Signalling,* 22(11), pp.1615-1625.

Kichuk, M., Seyedi, N., Zhang, X., Marboe, C., Michler, R., Addonizio, L., Kaley, G., Nasjletti, A. and Hintze, T. 1996. Regulation of nitric oxide production in human coronary microvessels and the contribution of local kinin formation. *Circulation,* 94(1), pp.44-51.

Kim, K., Drummond, I., Ibraghimov-Beskrovnaya, O., Klinger, K. and Arnaout, M.A. 2000. Polycystin 1 is required for the structural integrity of blood vessels. *Proceedings of the National Academy of Sciences U.S.A.,* 97(4), pp.1731-1736.

Kim, S., Grum-Tokars, V., Swanson, T., Cotter, E., Cahill, P., Roberts, J., Cummins, P. and Glucksman, M. 2003a. Novel roles of neuropeptide processing enzymes: EC3.4.24.15 in the neurome. *Journal of Neuroscience Research,* 74(3), pp.456-467.

Kim, S., Pabon, A., Swanson, T. and Glucksman, M. 2003b. Regulation of cell-surface major histocompatibility complex class I expression by the endopeptidase EC3.4.24.15 (thimet oligopeptidase). *Biochemical Journal,* 375(Pt 1), pp.111-120.

Kim, S.I., Grum-Tokars, V., Swanson, T.A., Cotter, E.J., Cahill, P.A., Roberts, J.L., Cummins, P.M. and Glucksman, M.J. 2003c. Novel roles of neuropeptide processing enzymes: EC3.4.24.15 in the neurome. *Journal of Neuroscience Research,* 74(3), pp.456-467.

Kitabgi, P. 2006. Inactivation of neurotensin and neuromedin N by Zn metallopeptidases. *Peptides*, 27(10), pp.2515-2522.

Kliche, K., Jeggle, P., Pavenstädt, H. and Oberleithner, H. 2011. Role of cellular mechanics in the function and life span of vascular endothelium. *Pflügers Archiv European Journal of Physiology,* 462(2), pp.209-217.

Knezevic, N., Tauseef, M., Thennes, T. and Mehta, D. 2009. The G protein βγ subunit mediates reannealing of adherens junctions to reverse endothelial permeability increase by thrombin. *The Journal of Experimental Medicine*, 206(12), pp.2761-2777.

Knipp, B., Ailawadi, G., Ford, J., Peterson, D., Eagleton, M., Roelofs, K., Hannawa, K., Deogracias, M., Ji, B. and Logsdon, C. 2004. Increased MMP-9 expression and activity by aortic smooth muscle cells after nitric oxide synthase inhibition is associated with increased nuclear factor-kappaB and activator protein-1 activity. *The Journal of Surgical Research,* 116(1), pp.70-80.

Koga, H., Terasawa, H., Nunoi, H., Takeshige, K., Inagaki, F. and Sumimoto, H. 1999. Tetratricopeptide repeat (TPR) motifs of p67 phox participate in interaction with the small GTPase Rac and activation of the phagocyte NADPH oxidase. *Journal of Biological Chemistry,* 274(35), pp.25051-25060.

Kohne, C.H., Schoffski, P., Wilke, H., Kaufer, C., Andreesen, R., Ohl, U., Klaasen, U., Westerhausen, M., Hiddemann, W. and Schott, G. 1998. Effective biomodulation by leucovorin of high-dose infusion fluorouracil given as a weekly 24-hour infusion: results of a randomized trial in patients with advanced colorectal cancer. *Journal of Clinical Oncology,* 16(2), pp.418-426.

Krizanac-Bengez, L., Hossain, M., Fazio, V., Mayberg, M. and Janigro, D. 2006. Loss of flow induces leukocyte-mediated MMP/TIMP imbalance in dynamic in vitro blood-brain barrier model: role of pro-inflammatory cytokines. *American Journal of Physiology-Cell Physiology,* 291(4), pp.C740-C749.

Kuchan, M. and Frangos, J. 1993. Shear stress regulates endothelin-1 release via protein kinase C and cGMP in cultured endothelial cells. *American Journal of Physiology-Heart and Circulatory Physiology*, 264(1), pp.H150-H156.

Kudo, F., Warycha, B., Juran, P., Asada, H., Teso, D., Aziz, F., Frattini, J., Sumpio, B., Nishibe, T. and Cha, C. 2005. Differential responsiveness of early- and late-passage endothelial cells to shear stress. *The American Journal of Surgery*, 190(5), pp.763-769.

Kuoppala, A., Lindstedt, K.A., Saarinen, J., Kovanen, P.T. and Kokkonen, J.O. 2000. Inactivation of bradykinin by angiotensin-converting enzyme and by carboxypeptidase N in human plasma. *American Journal of Physiology-Heart and Circulatory Physiology*, 278(4), pp.H1069-H1074.

Kurihara, Y., Kurihara, H., Suzuki, H., Kodama, T., Maemura, K., Nagai, R., Oda, H., Kuwaki, T., Cao, W.H. and Kamada, N. 1994. Elevated blood pressure and craniofaclal abnormalities in mice deficient in endothelin-1. *Nature*, 368(6473), pp.703-710.

Laemmli, U.K. 1970. Cleavage of structural proteins during the assembly of the head of bacteriophage T4. *Nature*, 227(5259), pp.680-685.

Lampson, L. 1995. Interpreting MHC class I expression and class I/class II reciprocity in the CNS: reconciling divergent findings. *Microscopy Research and Technique*, 32(4), pp.267-285.

Lampugnani, M., Zanetti, A., Corada, M., Takahashi, T., Balconi, G., Breviario, F., Orsenigo, F., Cattelino, A., Kemler, R. and Daniel, T. 2003. Contact inhibition of VEGF-induced proliferation requires vascular endothelial cadherin, beta-catenin, and the phosphatase DEP-1/CD148. *The Journal of Cell Biology*, 161(4), pp.793-804.

Landmesser, U., Merten, R., Spiekermann, S., Buttner, K., Drexler, H. and Hornig, B. 2000. Vascular extracellular superoxide dismutase activity in patients with coronary artery disease: relation to endothelium-dependent vasodilation. *Circulation*, 101(19), pp.2264-2270.

Laplace, E. 1899. A new forceps for intestinal anastomosis. *Annals of Surgery*, 29(3), pp.297-305.

Leal, J., Luengo-Fernandez, R., Gray, A., Petersen, S. and Rayner, M. 2006. Economic burden of cardiovascular diseases in the enlarged European Union. *European Heart Journal*, 27(13), pp.1610-1619.

Leeb-Lundberg, L., Marceau, F., Müller-Esterl, W., Pettibone, D. and Zuraw, B. 2005. International union of pharmacology. XLV. Classification of the kinin receptor family: from molecular mechanisms to pathophysiological consequences. *Pharmacological Reviews*, 57(1), pp.27-77.

Leiper, J. and Nandi, M. 2011. The therapeutic potential of targeting endogenous inhibitors of nitric oxide synthesis. *Nature Reviews Drug Discovery*, 10(4), pp.277-291.

Lemmon, M. and Schlessinger, J. 2010. Cell signaling by receptor tyrosine kinases. *Cell*, 141(7), pp.1117-1134.

Levesque, M., Nerem, R. and Sprague, E. 1990. Vascular endothelial cell proliferation in culture and the influence of flow. *Biomaterials*, 11(9), pp.702-707.

Levick, J. 2004. Revision of the Starling principle: new views of tissue fluid balance. *The Journal of Physiology*, 557(3), pp.704-704.

Lew, R. 2004. The zinc metallopeptidase family: new faces, new functions. *Protein and Peptide Letters*, 11(5), pp.407-414.

Lew, R., Cowley, M., Clarke, I. and Smith, A. 1997. Peptidases that degrade gonadotropin-releasing hormone: influence on LH secretion in the ewe. *Journal of Neuroendocrinology*, 9(9), pp.707-712.

Li, C., Chen, G., Gerard, N.P., Gerard, C., Bozic, C.R. and Hersh, L.B. 1995. Comparison of the structure and expression of the human and rat neprilysin (endopeptidase 24.11)-encoding genes. *Gene*, 164(2), pp.363-366.

Li, S., Kim, M., Hu, Y., Jalali, S., Schlaepfer, D., Hunter, T., Chien, S. and Shyy, J. 1997. Fluid shear stress activation of focal adhesion kinase. Linking to mitogen-activated protein kinases. *Journal of Biological Chemistry,* (272), pp.30455-30462.

Li, Y., Haga, J.H. and Chien, S. 2005. Molecular basis of the effects of shear stress on vascular endothelial cells. *Journal of Biomechanics,* 38(10), pp.1949-1971.

Lidman, O., Olsson, T. and Piehl, F. 1999. Expression of nonclassical MHC class I (RT1-U) in certain neuronal populations of the central nervous system. *European Journal of Neuroscience,* 11(12), pp.4468-4472.

Livak, K.J. and Schmittgen, T.D. 2001. Analysis of relative gene expression data using real-time quantitative PCR and the 2-[Delta][Delta] CT method. *Methods,* 25(4), pp.402-408.

Loscalzo, J. and Welch, G. 1995. Nitric oxide and its role in the cardiovascular system. *Progress in Cardiovascular Diseases,* 38(2), pp.87-104.

Luft, J. 1966. Fine structures of capillary and endocapillary layer as revealed by ruthenium red. *Federation Proceedings,* 25(6), pp.1773-1783.

Madeddu, P., Milia, A., Salis, M., Gaspa, L., Gross, W., Lippoldt, A. and Emanueli, C. 1998. Renovascular hypertension in bradykinin B2-receptor knockout mice. *Hypertension,* 32(3), pp.503-509.

Marceau, F., Hess, J.F. and Bachvarov, D.R. 1998. The B1 receptors for kinins. *Pharmacological Reviews,* 50(3), pp.357-386.

Martin, S., Tesse, A., Hugel, B., Martinez, M.C., Morel, O., Freyssinet, J.M. and Andriantsitohaina, R. 2004. Shed membrane particles from T lymphocytes impair endothelial function and regulate endothelial protein expression. *Circulation,* 109(13), pp.1653.

Martin-Mondiere, C.F., Caprani, A., Desgrances, P.C., Loisance, D.Y. and Charrion, D.J. 1989. Shear stress affects expression of major histocompatibility complex antigens on human endothelial cells. *American Society of Artificial Internal Organs,* 35(3), pp.288-290.

Masaki, T. 2004. Historical review: endothelin. *Trends in Pharmacological Sciences,* 25(4), pp.219-224.

Masatsugu, K., Itoh, H., Chun, T.H., Saito, T., Yamashita, J., Doi, K., Inoue, M., Sawada, N., Fukunaga, Y. and Sakaguchi, S. 2003. Shear stress attenuates endothelin and endothelin-converting enzyme expression through oxidative stress. *Regulatory Peptides,* 111(1-3), pp.13-20.

McCool, S. and Pierotti, A.R. 1998. Promoter sequence of rat thimet oligopeptidase. *Biochemical Society Transactions,* 26(S15),

McKinley, M.P. and O'loughlin, V.D. 2006. *Human anatomy.* McGraw-Hill Higher Education.

Meier, B. 1996. Regulation of the superoxide releasing system in human fibroblasts. *Advances in Experimental Medicine and Biology,* 387pp.113-116.

Melov, S., Schneider, J.A., Day, B.J., Hinerfeld, D., Coskun, P., Mirra, S.S., Crapo, J.D. and Wallace, D.C. 1998. A novel neurological phenotype in mice lacking mitochondrial manganese superoxide dismutase. *Nature Genetics,* 18(2), pp.159-163.

Miyakawa, A., de Lourdes Junqueira, M. and Krieger, J. 2004. Identification of two novel shear stress responsive elements in rat angiotensin I converting enzyme promoter. *Physiological Genomics,* 17(2), pp.107-113.

Mombouli, J. and Vanhoutte, P. 1999. Endothelial dysfunction: from physiology to therapy. *Journal of Molecular and Cellular Cardiology,* 31(1), pp.61-74.

Montiel, J., Cornille, F., Roques, B. and Noble, F. 1997. Nociceptin/orphanin FQ metabolism: role of aminopeptidase and endopeptidase 24.15. *Journal of Neurochemistry,* 68(1), pp.354-361.

Morrison, L.S. and Pierotti, A.R. 2003. Thimet oligopeptidase expression is differentially regulated in neuroendocrine and spermatid cell lines by transcription factor binding to SRY (sex-determining region Y), CAAT and CREB (cAMP-response-element-binding protein) promoter consensus sequences. *Biochemical Journal,* 376(Pt 1), pp.189-197.

Mulivor, A. and Lipowsky, H. 2004. Inflammation-and ischemia-induced shedding of venular glycocalyx. *American Journal of Physiology-Heart and Circulatory Physiology,* 286(5), pp.H1672-H1680.

Muller, J., Chilian, W. and Davis, M. 1997. Integrin signaling transduces shear stress–dependent vasodilation of coronary arterioles. *Circulation Research,* 80(3), pp.320-326.

Napoli, C., de Nigris, F., Williams-Ignarro, S., Pignalosa, O., Sica, V. and Ignarro, L.J. 2006. Nitric oxide and atherosclerosis: an update. *Nitric Oxide,* 15(4), pp.265-279.

Nauli, S., Kawanabe, Y., Kaminski, J., Pearce, W., Ingber, D. and Zhou, J. 2008. Endothelial cilia are fluid shear sensors that regulate calcium signaling and nitric oxide production through polycystin-1. *Circulation,* 117(9), pp.1161-1171.

Newby, A. and Zaltsman, A. 2000. Molecular mechanisms in intimal hyperplasia. *The Journal of Pathology,* 190(3), pp.300-309.

Newman, P. 1994. The role of PECAM-1 in vascular cell biology. *Annals of the New York Academy of Sciences,* 714(1), pp.165-174.

Newman, P., Berndt, M., Gorski, J., White, G., Lyman, S., Paddock, C. and Muller, W. 1990. PECAM-1 (CD31) cloning and relation to adhesion molecules of the immunoglobulin gene superfamily. *Science,* 247(4947), pp.1219-1222.

Nickel, W. 2003. The mystery of non-classical protein secretion. *European Journal of Biochemistry,* 270(10), pp.2109-2119.

Nieuwdorp, M., Meuwese, M.C., Vink, H., Hoekstra, J.B.L., Kastelein, J.J.P. and Stroes, E.S.G. 2005. The endothelial glycocalyx: a potential barrier between health and vascular disease. *Current Opinion in Lipidology,* 16(5), pp.507-511.

Nieuwdorp, M., Mooij, H.L., Kroon, J., Atasever, B., Spaan, J.A.E., Ince, C., Holleman, F., Diamant, M., Heine, R.J. and Hoekstra, J.B.L. 2006. Endothelial glycocalyx damage coincides with microalbuminuria in type 1 diabetes. *Diabetes,* 55(4), pp.1127-1132.

Nordberg, J. and Arnér, E.S.J. 2001. Reactive oxygen species, antioxidants, and the mammalian thioredoxin system. *Free Radical Biology and Medicine,* 31(11), pp.1287-1312.

Norman, M., Lew, R., Smith, A. and Hickey, M. 2003a. Metalloendopeptidases EC 3.4.24.15/16 regulate bradykinin activity in the cerebral microvasculature. *American Journal of Physiology-Heart and Circulatory Physiology,* 284(6), pp.H1942-H1948.

Norman, M., Reeve, S., Dive, V., Smith, A. and Lew, R. 2003b. Endopeptidases 3.4.24.15 and 24.16 in endothelial cells: potential role in vasoactive peptide metabolism. *American Journal of Physiology-Heart and Circulatory Physiology,* 284(6), pp.H1978-H1984.

Oberleithner, H., Riethmüller, C., Schillers, H., MacGregor, G., De Wardener, H. and Hausberg, M. 2007. Plasma sodium stiffens vascular endothelium and reduces nitric oxide release. *Proceedings of the National Academy of Sciences U.S.A.,* 104(41), pp.16281-16286.

Ohno, M., Gibbons, G., Dzau, V. and Cooke, J. 1993. Shear stress elevates endothelial cGMP. Role of a potassium channel and G protein coupling. *Circulation,* 88(1), pp.193-197.

Olesen, S., Claphamt, D. and Davies, P. 1988. Haemodynamic shear stress activates a K+ current in vascular endothelial cells. *Nature,* 331(6152), pp.168-170.

Oppong, S. and Hooper, N. 1993. Characterization of a secretase activity which releases angiotensin-converting enzyme from the membrane. *Biochemical Journal,* 292(Pt 2), pp.597-603.

Osman, I., Yee, H., Taneja, S.S., Levinson, B., Zeleniuch-Jacquotte, A., Chang, C., Nobert, C. and Nanus, D.M. 2004. Neutral endopeptidase protein expression and prognosis in localized prostate cancer. *Clinical Cancer Research,* 10(12), pp.4096-4100.

Papadaki, M. and Eskin, S. 1997. Effects of fluid shear stress on gene regulation of vascular cells. *Biotechnology Progress,* 13(3), pp.209-221.

Parish, C. 2006. The role of heparan sulphate in inflammation. *Nature Reviews Immunology,* 6(9), pp.633-643.

Pasyk, K. and Jakobczak, B. 2004. Vascular endothelium: recent advances. *European Journal of Dermatology,* 14pp.209-213.

Patterson, C. 2005. *Perspectives on lung endothelial barrier function.* Elsevier Science.

Poredoš, P. 2000. Endothelial dysfunction and cardiovascular disease. *Pathophysiology of Haemostasis and Thrombosis,* 32(5-6), pp.274-277.

Portaro, F., Gomes, M., Cabrera, A., Fernandes, B., Silva, C., Ferro, E., Juliano, L. and De Camargo, A. 1999. Thimet oligopeptidase and the stability of MHC class I epitopes in macrophage cytosol. *Biochemical and Biophysical Research Communications,* 255(3), pp.596-601.

Praetorius, H. and Spring, K. 2003. Removal of the MDCK cell primary cilium abolishes flow sensing. *Journal of Membrane Biology,* 191(1), pp.69-76.

Pries, A. and Kuebler, W. 2006. Normal endothelium. *The Vascular Endothelium I,* pp.1-40.

Pries, A., Secomb, T. and Gaehtgens, P. 2000. The endothelial surface layer. *Pflügers Archiv European Journal of Physiology,* 440(5), pp.653-666.

Quadri, S. and Bhattacharya, J. 2007. Resealing of endothelial junctions by focal adhesion kinase. *American Journal of Physiology-Lung Cellular and Molecular Physiology*, 292(1), pp.L334-L342.

Quaschning, T., Galle, J. and Wanner, C. 2003. Vasopeptidase inhibition: a new treatment approach for endothelial dysfunction. *Kidney International*, 63pp.S54-S57.

Rawlings, N. and Barrett, A. 1993. Evolutionary families of peptidases. *Biochemical Journal*, 290(Pt 1), pp.205-218.

Barrett, A., Rawlings, N. and O'Brien, E. 2001. The MEROPS database as a protease information system. *Journal of Structural Biology*, 134(2-3), pp.95-102.

Ray, K., Hines, C.S., Coll-Rodriguez, J. and Rodgers, D.W. 2004. Crystal structure of human thimet oligopeptidase provides insight into substrate recognition, regulation, and localization. *Journal of Biological Chemistry*, 279(19), pp.20480-20489.

Redmond, E., Cahill, P. and Sitzmann, J. 1998. Flow-mediated regulation of G-protein expression in cocultured vascular smooth muscle and endothelial cells. *Arteriosclerosis, Thrombosis, and Vascular Biology*, 18(1), pp.75-83.

Resnick, N., Yahav, H., Shay-Salit, A., Shushy, M., Schubert, S., Zilberman, L. and Wofovitz, E. 2003. Fluid shear stress and the vascular endothelium: for better and for worse. *Progress in Biophysics and Molecular Biology*, 81(3), pp.177-199.

Rieder, M., Carmona, R., Krieger, J., Pritchard Jr, K. and Greene, A. 1997. Suppression of angiotensin-converting enzyme expression and activity by shear stress. *Circulation Research*, 80(3), pp.312-319.

Rioli, V., Gozzo, F., Heimann, A., Linardi, A., Krieger, J., Shida, C., Almeida, P., Hyslop, S., Eberlin, M. and Ferro, E. 2003. Novel natural peptide substrates for endopeptidase 24.15, neurolysin, and angiotensin-converting enzyme. *Journal of Biological Chemistry*, 278(10), pp.8547-8555.

Robin, R. and Ajay, M. 2005. NADPH oxidase and endothelial cell function. *Clinical Science,* 109pp.217-226.

Rose, C., Voisin, S., Gros, C., Schwartz, J.C. and Ouimet, T. 2002. Cell-specific activity of neprilysin 2 isoforms and enzymic specificity compared with neprilysin. *Biochemical Journal,* 363(Pt 3), pp.697-705.

Ross, R. 1999. Atherosclerosis is an inflammatory disease. *American Heart Journal,* 138pp.419-420.

Ross, R. 1993. The pathogenesis of atherosclerosis: a perspective for the 1990s. *Nature,* 362(6423), pp.801-809.

Rudini, N. and Dejana, E. 2008. Adherens junctions. *Current Biology,* 18(23), pp.R1080-R1082.

Russo, L., Goñi, C., Castro, L., Asega, A., Camargo, A., Trujillo, C., Ulrich, H., Glucksman, M., Scavone, C. and Ferro, E. 2009. Interaction with calmodulin is important for the secretion of thimet oligopeptidase following stimulation. *FEBS Journal,* 276(16), pp.4358-4371.

Sallee, J., Wittchen, E. and Burridge, K. 2006. Regulation of Cell Adhesion by Protein-tyrosine Phosphatases. *Journal of Biological Chemistry,* 281(24), pp.16189-16192.

Sambrook, J., Fritsch, E. and Maniatis, T. 1989. *Molecular cloning: a laboratory manual.* New York: Cold Spring Harbor Laboratory Press.

Sandén, C., Enquist, J., Bengtson, S., Herwald, H. and Leeb-Lundberg, L. 2008. Kinin B2 receptor-mediated bradykinin internalization and metalloendopeptidase EP24.15-dependent intracellular bradykinin degradation. *Journal of Pharmacology and Experimental Therapeutics,* 326(1), pp.24-32.

Santos, R., Brosnihan, K., Jacobsen, D., DiCorleto, P. and Ferrario, C. 1992. Production of angiotensin-(1-7) by human vascular endothelium. *Hypertension,* 19(2 Suppl), pp.I156-I161.

Saric, T., Beninga, J., Graef, C.I., Akopian, T.N., Rock, K.L. and Goldberg, A.L. 2001. Major histocompatibility complex class I-presented antigenic peptides are degraded in cytosolic extracts primarily by thimet oligopeptidase. *Journal of Biological Chemistry,* 276(39), pp.36474-36481.

Schaper, W. 2009. Collateral circulation: past and present. *Basic Research in Cardiology,* 104(1), pp.5-21.

Schiffrin, E. 1992. Reactivity of small blood vessels in hypertension: relation with structural changes. State of the art lecture. *Hypertension,* 19(2 Suppl), pp.1-9.

Schimmenti, L., Yan, H., Madri, J. and Albelda, S. 1992. Platelet endothelial cell adhesion molecule, PECAM-1, modulates cell migration. *Journal of Cellular Physiology,* 153(2), pp.417-428.

Schlessinger, J. 2000. Cell signaling by receptor tyrosine kinases. *Cell,* 103(2), pp.211-225.

Schriefer, J., Broudy, E. and Hassen, A. 2001. Inhibitors of bradykinin-inactivating enzymes decrease myocardial ischemia/reperfusion injury following 3 and 7 days of reperfusion. *Journal of Pharmacology and Experimental Therapeutics,* 298(3), pp.970-975.

Schweizer, A., Valdenaire, O., Köster, A., Lang, Y., Schmitt, G., Lenz, B., Bluethmann, H. and Rohrer, J. 1999. Neonatal lethality in mice deficient in XCE, a novel member of the endothelin-converting enzyme and neutral endopeptidase family. *Journal of Biological Chemistry,* 274(29), pp.20450-20456.

Seidah, N.G., Chretien, M. and Day, R. 1994. The family of subtilisin/kexin like pro-protein and pro-hormone convertases: divergent or shared functions. *Biochimie,* 76(3-4), pp.197-209.

Shalaby, F., Rossant, J., Yamaguchi, T., Gertsenstein, M., Wu, X., Breitman, M. and Schuh, A. 1995. Failure of blood-island formation and vasculogenesis in Flk-1-deficient mice. *Nature,* 376(6535), pp.62-66.

Sharma, J. and AL-Sherif, G. 2011. The Kinin System: Present and Future Pharmacological Targets. *Am.J.Biomed.Sci,* 3(2), pp.156-169.

Sharma, N. and Priyank, K. 2011. Tyrosine kinases: novel targets for cancer therapy. *Journal of Advanced Scientific Research,* 2pp.1-7.

Shasby, D. 2007. Cell-cell adhesion in lung endothelium. *American Journal of Physiology-Lung Cellular and Molecular Physiology,* 292(3), pp.L593-L607.

Shattil, S., Kim, C. and Ginsberg, M. 2010. The final steps of integrin activation: the end game. *Nature Reviews Molecular Cell Biology,* 11(4), pp.288-300.

Shay-Salit, A., Shushy, M., Wolfovitz, E., Yahav, H., Breviario, F., Dejana, E. and Resnick, N. 2002. VEGF receptor 2 and the adherens junction as a mechanical transducer in vascular endothelial cells. *Proceedings of the National Academy of Sciences U.S.A.,* 99(14), pp.9462-9467.

Shepro, D. 2006. *Microvascular Research.*

Shrimpton , C., Smith, A. and Lew , R. 2002. Soluble metalloendopeptidases and neuroendocrine signaling. *Endocrine Reviews,* 23(5), pp.647-664.

Shyy, J. and Chien, S. 2002. Role of integrins in endothelial mechanosensing of shear stress. *Circulation Research,* 91(9), pp.769-775.

Simon, M., Strathmann, M. and Gautam, N. 1991. Diversity of G proteins in signal transduction. *Science,* 252(5007), pp.802-808.

Skidgel, R., Engelbrecht, S., Johnson, A. and Erdos, E. 1984. Hydrolysis of substance P and neurotensin by converting enzyme and neutral endopeptidase. *Peptides,* 5(4), pp.769-776.

Smith, A., Lew, R., Shrimpton, C., Evans, R. and Abbenante, G. 2000. A novel stable inhibitor of endopeptidases EC 3.4.24.15 and 3.4.24.16 potentiates bradykinin-induced hypotension. *Hypertension,* 35(2), pp.626-630.

Stolk, J., Hiltermann, T., Dijkman, J. and Verhoeven , A. 1994. Characteristics of the inhibition of NADPH oxidase activation in neutrophils by apocynin, a methoxy-substituted catechol. *American Journal of Respiratory Cell and Molecular Biology*, 11(1), pp.95-102.

Suciu, A., Civelekoglu, G., Tardy, Y. and Meister, J. 1997. Model for the alignment of actin filaments in endothelial cells subjected to fluid shear stress. *Bulletin of Mathematical Biology*, 59(6), pp.1029-1046.

Sumimoto, H., Miyano, K. and Takeya, R. 2005. Molecular composition and regulation of the Nox family NAD(P)H oxidases. *Biochemical and Biophysical Research Communications*, 338(1), pp.677-686.

Sumitomo, M., Shen, R., Walburg, M., Dai, J., Geng, Y., Navarro, D., Boileau, G., Papandreou, C., Giancotti, F. and Knudsen, B. 2000. Neutral endopeptidase inhibits prostate cancer cell migration by blocking focal adhesion kinase signaling. *Journal of Clinical Investigation*, 106(11), pp.1399-1407.

Suvatne, J., Barakat, A. and O'Donnell, M. 2001. Flow-induced expression of endothelial Na-K-Cl co-transport: dependence on K+ and Cl− channels. *American Journal of Physiology-Cell Physiology*, 280(1), pp.C216-C227.

Taddei, S., Virdis, A., Ghiadoni, L., Salvetti, G., Bernini, G., Magagna, A. and Salvetti, A. 2001. Age-related reduction of NO availability and oxidative stress in humans. *Hypertension*, 38(2), pp.274-279.

Takahashi, M. and Berk, B.C. 1996. Mitogen-activated protein kinase (ERK1/2) activation by shear stress and adhesion in endothelial cells. Essential role for a herbimycin-sensitive kinase. *Journal of Clinical Investigation*, 98(11), pp.2623-2631.

Taniyama, Y. and Griendling, K. 2003. Reactive oxygen species in the vasculature: molecular and cellular mechanisms. *Hypertension*, 42(6), pp.1075-1081.

Tarbell, J.M. 2010. Shear stress and the endothelial transport barrier. *Cardiovascular Research*, 87(2), pp.320.

Thomas, J., Rylett, C., Carhan, A., Bland, N., Bingham, R., Shirras, A., Turner, A. and Isaac, R. 2005. Drosophila melanogaster NEP2 is a new soluble member of the neprilysin family of endopeptidases with implications for reproduction and renal function. *Biochemical Journal*, 386(Pt 2), pp.357-366.

Tipnis, S., Hooper, N., Hyde, R., Karran, E., Christie, G. and Turner, A. 2000. A human homolog of angiotensin-converting enzyme. *Journal of Biological Chemistry*, 275(43), pp.33238-33234.

Tiraboschi, G., Jullian, N., Thery, V., Antonczak, S., Fournie-Zaluski, M.C. and Roques, B.P. 1999. A three-dimensional construction of the active site (region 507–749) of human neutral endopeptidase (EC. 3.4. 24.11). *Protein Engineering*, 12(2), pp.141-149.

Towbin, H., Staehelin, T. and Gordon, J. 1979. Electrophoretic transfer of proteins from polyacrylamide gels to nitrocellulose sheets: procedure and some applications. *Proceedings of the National Academy of Sciences U.S.A.*, 76(9), pp.4350-4354.

Traub, O. and Berk, B.C. 1998. Laminar shear stress: mechanisms by which endothelial cells transduce an atheroprotective force. *Arteriosclerosis, Thrombosis, and Vascular Biology*, 18(5), pp.677-685.

Tsunawaki, S., Kagara, S., Yoshikawa, K., Yoshida, L.S., Kuratsuji, T. and Namiki, H. 1996. Involvement of p40phox in activation of phagocyte NADPH oxidase through association of its carboxyl-terminal, but not its amino-terminal, with p67phox. *Journal of Experimental Medicine*, 184(3), pp.893-902.

Turner, A. 2003. Exploring the structure and function of zinc metallopeptidases: old enzymes and new discoveries. *Biochemical Society Transactions*, 31pp.723-727.

Turner, A., Isaac, R. and Coates, D. 2001. The neprilysin (NEP) family of zinc metalloendopeptidases: genomics and function. *Bioessays,* 23(3), pp.261-269.

Turner, A. and Tanzawa, K. 1997. Mammalian membrane metallopeptidases: NEP, ECE, Kell, and PEX. *The FASEB Journal,* 11(5), pp.355-364.

Tzima, E., Irani-Tehrani, M., Kiosses, W.B., Dejana, E., Schultz, D.A., Engelhardt, B., Cao, G., DeLisser, H. and Schwartz, M.A. 2005. A mechanosensory complex that mediates the endothelial cell response to fluid shear stress. *Nature,* 437(7057), pp.426-431.

Usatyuk, P. and Natarajan, V. 2005. Regulation of reactive oxygen species-induced endothelial cell-cell and cell-matrix contacts by focal adhesion kinase and adherens junction proteins. *American Journal of Physiology-Lung Cellular and Molecular Physiology,* 289(6), pp.L999-L1010.

Usmani, B., Harden, B., Maitland, N. and Turner, A. 2002. Differential expression of neutral endopeptidase-24.11 (neprilysin) and endothelin-converting enzyme in human prostate cancer cell lines. *Clinical Science,* 103(48), pp.314-317.

Van der Heiden, K., Hierck, B., Krams, R., de Crom, R., Cheng, C., Baiker, M., Pourquie, M., Alkemade, F., DeRuiter, M. and Gittenberger-de Groot, A. 2008. Endothelial primary cilia in areas of disturbed flow are at the base of atherosclerosis. *Atherosclerosis,* 196(2), pp.542-550.

Vanhoutte, P. 1989. Endothelium and control of vascular function. State of the Art lecture. *Hypertension,* 13(6), pp.658-667.

Vanhoutte, P., Perrault, L. and Vilaine, J. 2007. *Endothelial dysfunction and vascular disease.*

Vaporciyan, A., Delisser, H. and Yan, H. 1993. Involvement of platelet-endothelial cell adhesion molecule-1 in neutrophil recruitment in vivo. *Science,* 262(5139), pp.1580-1582.

Vikkula, M., Boon, L., Iii, K., Calvert, J., Diamonti, A., Goumnerov, B., Pasyk, K., Marchuk, D., Warman, M. and Cantley, L. 1996. Vascular dysmorphogenesis caused by an activating mutation in the receptor tyrosine kinase TIE2. *Cell*, 87(7), pp.1181-1190.

Vincent, B., Beaudet, A., Dauch, P., Vincent, J. and Checler, F. 1996. Distinct properties of neuronal and astrocytic endopeptidase 3.4.24.16: a study on differentiation, subcellular distribution, and secretion processes. *The Journal of Neuroscience,* 16(16), pp.5049-5059.

Vincent, P., Xiao, K., Buckley, K. and Kowalczyk, A. 2004. VE-cadherin: adhesion at arm's length. *American Journal of Physiology-Cell Physiology*, 286(5), pp.C987-C997.

Von Offenberg Sweeney, N., Cummins, P., Cotter, E., Fitzpatrick, P., Birney, Y., Redmond, E. and Cahill, P. 2005. Cyclic strain-mediated regulation of vascular endothelial cell migration and tube formation. *Biochemical and Biophysical Research Communications,* 329(2), pp.573-582.

Vyas, J.M., Van der Veen, A.G. and Ploegh, H.L. 2008. The known unknowns of antigen processing and presentation. *Nature Reviews Immunology*, 8(8), pp.607-618.

Wakelin, M., Sanz, M., Dewar, A., Albelda, S., Larkin, S., Boughton-Smith, N., Williams, T. and Nourshargh, S. 1996. An anti-platelet-endothelial cell adhesion molecule-1 antibody inhibits leukocyte extravasation from mesenteric microvessels in vivo by blocking the passage through the basement membrane. *The Journal of Experimental Medicine,* 184(1), pp.229-239.

Walsh, T., Murphy, R., Fitzpatrick, P., Rochfort, K., Guinan, A., Murphy, A. and Cummins, P. 2011. Stabilization of brain microvascular endothelial barrier function by shear stress involves VE-cadherin signaling leading to modulation of pTyr-occludin levels. *Journal of Cellular Physiology*, 226(11), pp.3053-3063.

Walther, T., Albrecht, D., Becker, M., Schubert, M., Kouznetsova, E., Wiesner, B., Maul, B., Schliebs, R., Grecksch, G. and Furkert, J. 2009. Improved learning

and memory in aged mice deficient in amyloid β-degrading neutral endopeptidase. *PLoS One,* 4(2), pp.e4590-e4601.

Wang, Z., Zhang, L., Qiao, A., Watson, K., Zhang, J. and Fan, G. 2008. Activation of CXCR4 triggers ubiquitination and down-regulation of major histocompatibility complex class I (MHC-I) on epithelioid carcinoma HeLa cells. *Journal of Biological Chemistry,* 283(7), pp.3951-3959.

Weinbaum, S., Tarbell, J.M. and Damiano, E.R. 2007. The structure and function of the endothelial glycocalyx layer. *Annu.Rev.Biomed.Eng.*, 9pp.121-167.

White, C.R., Haidekker, M., Bao, X. and Frangos, J.A. 2001. Temporal gradients in shear, but not spatial gradients, stimulate endothelial cell proliferation. *Circulation,* 103(20), pp.2508-2513.

Wieland, T. and Mittmann, C. 2003. Regulators of G-protein signalling: multifunctional proteins with impact on signalling in the cardiovascular system. *Pharmacology & Therapeutics*, 97(2), pp.95-115.

Yang, H., Erdos, E. and Levin, Y. 1971. Characterization of a dipeptide hydrolase (kininase II: angiotensin I converting enzyme). *Journal of Pharmacology and Experimental Therapeutics,* 177(1), pp.291-300.

Yeh, D., Duncan, J., Yamashita, S. and Michel, T. 1999. Depalmitoylation of endothelial nitric-oxide synthase by acyl-protein thioesterase 1 is potentiated by Ca2+ -calmodulin. *Journal of Biological Chemistry*, 274(46), pp.33148-33145.

Zhang, Y., Adner, M. and Cardell, L.O. 2004. Interleukin-1β attenuates endothelin B receptor-mediated airway contractions in a murine in vitro model of asthma: roles of endothelin converting enzyme and mitogen-activated protein kinase pathways. *Clinical & Experimental Allergy*, 34(9), pp.1480-1487.

Zheng, R., Horiguchi, A., Iida, K., Lee, J., Shen, R., Goodman, O.B. and Nanus, D.M. 2010. Neutral endopeptidase is a myristoylated protein. *Molecular and Cellular Biochemistry*, 335(1), pp.173-180.

Zimmerman, M., Dunlay, R., Lazartigues, E., Zhang, Y., Sharma, R., Engelhardt, J. and Davisson, R. 2004. Requirement for Rac1-dependent NADPH oxidase in the cardiovascular and dipsogenic actions of angiotensin II in the brain. *Circulation Research,* 95(5), pp.532-539.

Appendix

BCA assay standard curve

The BCA assay is a biochemical assay for quantifying the total amount of protein in a solution. This is achieved by Cu^{2+} reacting with protein under alkaline conditions to produce Cu^{+}, which in turn reacts with bicinchoninic acid (green) to form a complex (purple) that strongly absorbs light at 562 nm. Results of standards and unknown samples are then graphed to obtain protein concentrations (Figure A).

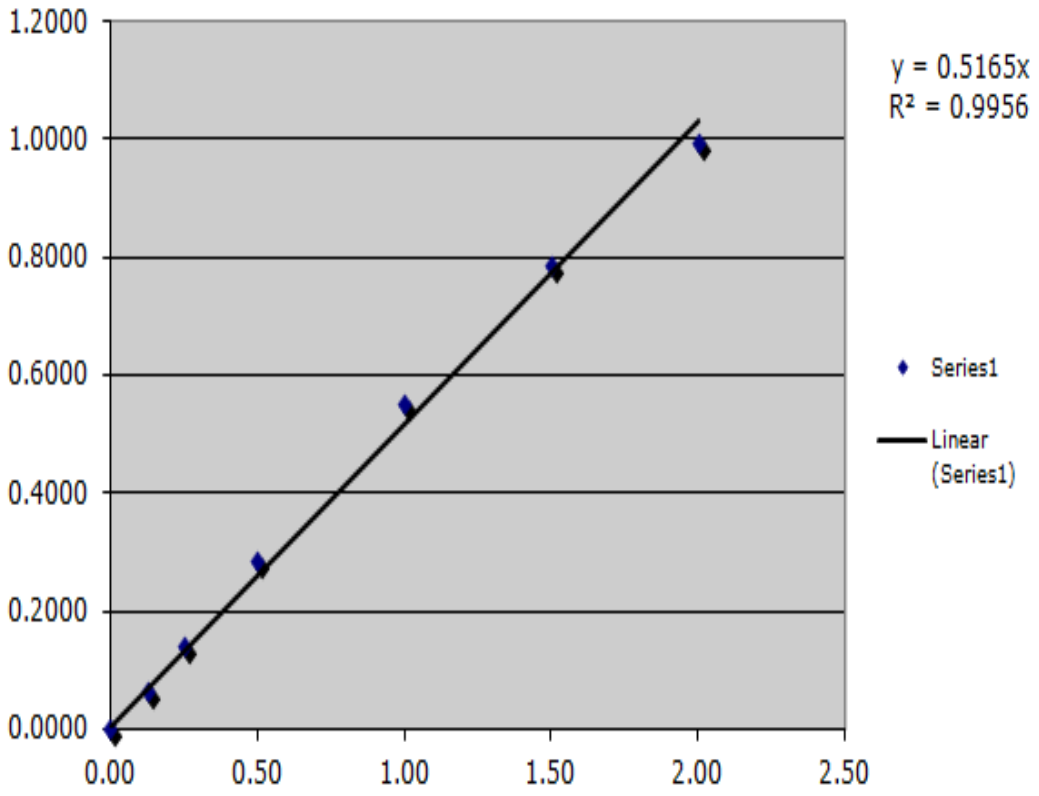

Figure A: Typical standard curve for a BCA assay, with absorbance on the Y-axis and concentration on the X-axis.

Unpublished results

Antioxidants

A short preliminary study carried out in this laboratory (unpublished data) has previously demonstrated the ROS-dependence of TOP up-regulation by shear stress. This was determined through the addition of antioxidants NAC, SOD and catalyse (CAT) to cells 1 hrs before the onset of LSS (10 dynes/cm^2, 24 hrs).

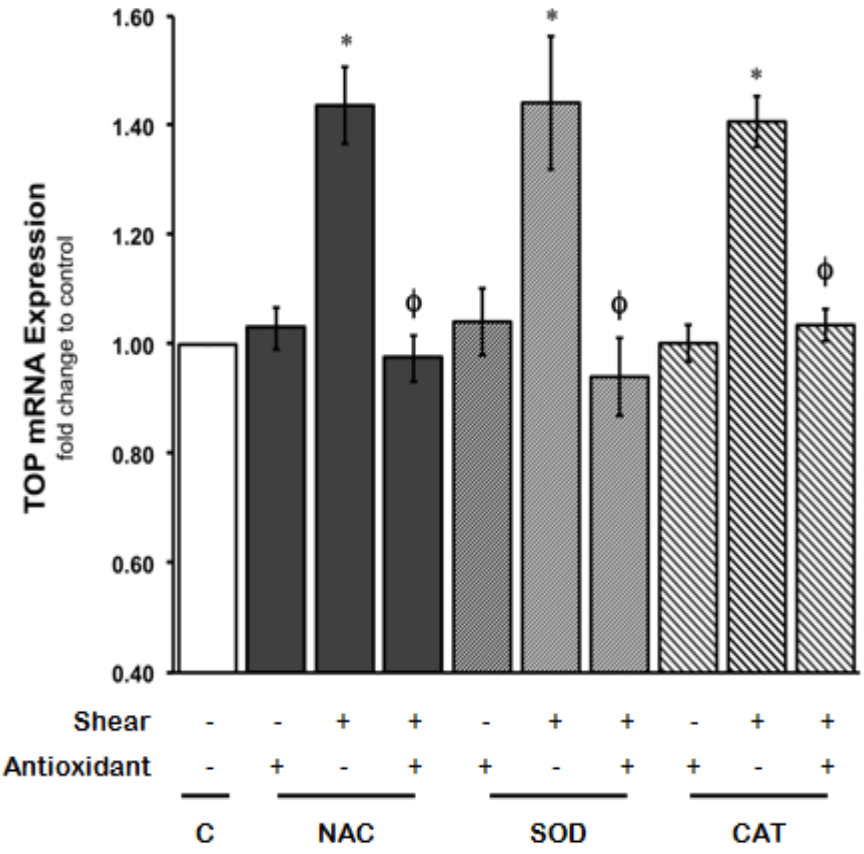

Figure B: Effect of antioxidants (NAC, SOD and catalyse (CAT)) in the regulation of TOP mRNA levels under both static and LSS (10 dynes/cm^2, 24 hrs) conditions. Results are averaged from three independent experiments ±SEM; *P≤0.05 vs static/untreated control cells, ΦP≤ 0.05 vs sheared/treated cells.

Oxidants

A short preliminary study carried out in this laboratory (unpublished data) has previously demonstrated the ROS-dependence of TOP up-regulation by shear stress. This was determined through the addition of oxidants H_2O_2 and Ang-II to static cells for 24 hrs and 8 hrs, respectively.

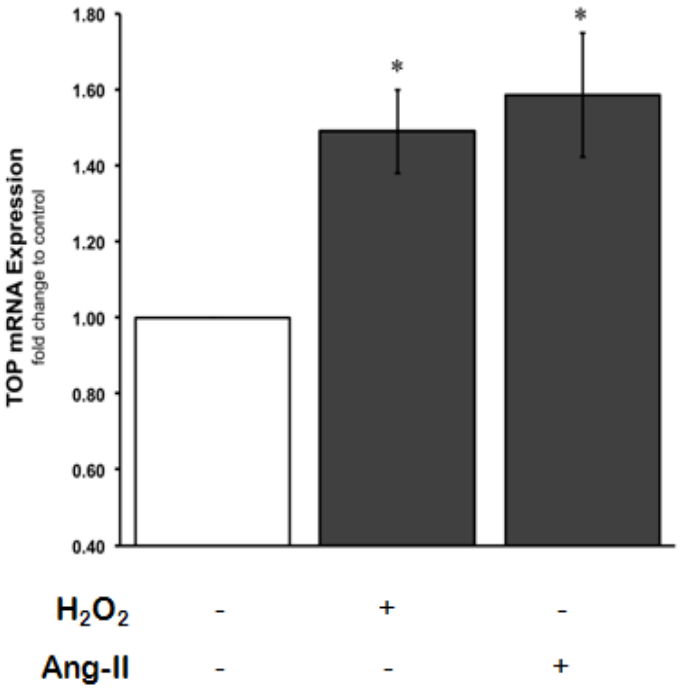

Figure C: Effect of oxidants (H_2O_2 and Ang-II) in the regulation of TOP mRNA expression levels under static conditions. Results are averaged from three independent experiments ±SEM; *$P \leq 0.05$ vs static/untreated control cells.

Recipes

Ampicillin stock solution

A stock solution of ampicillin was made up to a concentration of 100 mg/ml in dH_2O.

The stock solution was filter sterilised and stored at -20°C.

Coomassie stain

Coomassie Brilliant Blue R250 0.25g

Methanol:dH_2O (1:1 v/v) 90ml

Glacial Acetic acid 10ml

Filter the Coomassie stain using a 0.25μm filter

Coomassie destain solution

Methanol:Acetic acid mixed in a 50:50 ratio

HEPES-Krebs buffer

20 mM HEPES

103 mM NaCl

4.77 mM KCl

0.5 mM $CaCl_2$

1.2 mM $MgSO_4$

1.2 mM KH_2PO_4

25 mM $NaHCO_3$

15 mM Glucose

0.25% (w/v) BSA

pH to 7.4 and stored at 4°C.

LB agar

5 g Tryptone

2.5 g Yeast extract

5 g NaCl

7.5 g Agar

The volume was adjusted to 500 ml with dH_2O, followed by autoclaving and agar plates were stored at 4°C.

LB agar with antibiotics

Antibiotics were added to autoclaved LB broth to a final concentration of 100µg/ml (ampicillin), after cooling the LB agar to ~50°C. Plates were stored at 4°C.

LB broth

5 g Tryptone

2.5 g Yeast extract

5 g NaCl

The volume was adjusted to 500ml, followed by autoclaving for 20 minutes at

15 lb/sq. and storage at 4°C.

LB broth with ampicllin

Ampicillin was added to autoclaved LB broth to a final concentration of 100 µg/ml and stored at 4°C.

Phosphate buffered saline (PBS)

2 tablets were dissolved in 400 ml dH_2O to give a 1X working concentration of PBS, and the solution was sterilised by autoclaving.

SOB medium

10 g Tryptone

2.5 g Yeast extract

0.025 g NaCl

5 ml KCl (250 mM)

The pH was adjusted to 7.0 with 5M NaOH.

The volume was adjusted to 500 ml with dH_2O and the medium autoclaved.

2.5 ml of 2M MgCl2 was added after cooling the broth to 5°C and the medium was stored at 4°C.

SOC medium

98 ml SOB medium

2 ml 1M glucose (filter sterilised)

Stored at 4°C.

Stripping Buffer

Tris-HCl, pH6.8 62.5 mM

SDS 2% (w/v)

B-Mercaptoethanol 100 mM

1X Tris buffered saline (TBS)

6.1g Tris base

8.8g NaCl

800ml dH_2O

The pH was adjusted to 7.5 with HCl and the volume adjusted to 1 L. Stored at room temperature.

TBS-T

1L 1X TBS

1ml Tween 20

Stored at room temperature.

Papers

Fitzpatrick, P., **Guinan, A**., Walsh, T., Murphy, R., Killeen, M., Tobin, N., Pierotti, A. and Cummins, P. 2009. Down-regulation of neprilysin (EC3.4.24.11) expression in vascular endothelial cells by laminar shear stress involves NADPH oxidase-dependent ROS production. *The International Journal of Biochemistry & Cell Biology*, 41(11), pp.2287-2294.
www.ncbi.nlm.nih.gov/pubmed/19464387

Tobin NP, Henehan GT, Murphy RP, Atherton JC, **Guinan AF**, Kerrigan S, Cox D, Cahill PA, Cummins PM. *Helicobacter pylori*-induced inhibition of endothelial cell functions: a role for VacA-dependent nitric oxide reduction. American Journal of Physiology Heart Circulatory Physiology 2008; 295:H1403-H1413.
www.ncbi.nlm.nih.gov/pubmed/18660451

Walsh, T., Murphy, R., Fitzpatrick, P., Rochfort, K., **Guinan, A.**, Murphy, A. and Cummins, P. 2011. Stabilization of brain microvascular endothelial barrier function by shear stress involves VE-cadherin signaling leading to modulation of pTyr-occludin levels. *Journal of Cellular Physiology*, 226(11), pp.3053-3063.
www.ncbi.nlm.nih.gov/pubmed/21302304